Characterization of virulence factors of *Corynebacterium diphtheriae* and *Corynebacterium ulcerans*

Charakterisierung der Virulenzfaktoren von *Corynebacterium diphtheriae* und *Corynebacterium ulcerans*

Der Naturwissenschaftlichen Fakultät

der Friedrich-Alexander-Universität Erlangen-Nürnberg

zur

Erlangung des Doktorgrades Dr. rer. nat.

vorgelegt von

Dulanthi Weerasekera

aus Anuradhapura

Als Dissertation genehmigt von der Naturwissenschaftlichen Fakultät

der

Friedrich-Alexander-Universität Erlangen-Nürnberg

Tag der mündlichen Prüfung: 22.08.2019

Vorsitzender des Promotionsorgans: Prof. Dr. Georg Kreimer

Gutachter: Prof. Dr. Andreas Burkovski

Prof. Dr. Paul Hoskisson

Acknowledgements

Pursuing a Ph.D. is a life-changing experience in many ways. One must be patient and determined to take every opportunity as a blessing and work hard towards achieving the goal. The key to make it through towards the goal is to get up one more time than you fall. It is a great pleasure to thank those people who have guided and supported me throughout this journey, making this dissertation possible.

First and foremost, it is with immense gratitude that I thank Prof. Dr. Andreas Burkovski for giving me the opportunity to join his team to work on interesting and challenging projects in a very motivational, inspiring and a pleasant working atmosphere. I am grateful to him for the vivid scientific discussions, his unwavering support and patience. I appreciate the freedom and trust he has placed in me to manage my projects, allowing me to realize my ideas, believing in my scientific potential and all his contributions to make my Ph.D. experience productive and invigorating. His radiating knowledge, passion and enthusiasm for research was contagious and inspired me, even during tough times in the Ph.D. pursuit. I could not have imagined having a better supervisor and without whom, this thesis would never have been possible.

I would like to express my sincere gratitude to Prof. Dr. Martin Herrmann for introducing me to live-cell imaging experiments through our collaboration which helped to broaden my research perspectives. I am immensely grateful for the fruitful scientific discussions, technical guidance and also for being an examiner. The cell death studies discussed in this dissertation would not have been possible without his valuable inputs.

A debt of gratitude also goes to Prof. Dr. Paul Hoskisson for kindly accepting to review my thesis and Prof. Georg Kreimer for being an examiner in my Ph.D. defense. Many thanks also to PD. Dr. Anja Lührmann for mentoring in my first year in the context of SFB796 and for extending many helpful scientific suggestions for my work.

I would like to thank Dr. Lisa Bäumer for her invaluable support, advice and guidance in the lab. She introduced me to the world of cell culture studies and her excellent skills and knowledge in the field inspired me. I also thank her for helping me with the German language whenever the need arose. She provided an excellent example of a successful woman scientist and a good friend. I consider it as a privilege to have been working with her.

I am thankful to Dr. Camila Azevedo Antunes for contributing immensely to my personal and professional life at FAU. I greatly value the friendship as well as the advice given especially during the difficult times. I am glad we could share some interesting findings in DIP0733 world.

I gratefully acknowledge the funding sources that made my Ph.D. work possible. I was funded by the Deutscher Akademischer Austauschdienst (DAAD) and by the Deutsche Forschungsgemeinschaft in the frame of SFB796 (MGK) for my first three years. The final year of my Ph.D. was supported by the Förderung von Frauen in Forschung und Lehre (FFL) of the Friedrich-Alexander-Universität Erlangen-Nürnberg.

Due appreciation goes to all the former and current employees who performed the organizational work related to the scientific work. In this context, I wish to thank the former secretary Mrs. Donata Wehr for assisting me with all the necessary support to accommodate myself in Germany. I truly miss her warm and friendly demeanor and entertaining stories over lunch time that often lit up the dreary days. I am grateful to the current secretary Mrs. Kristin Jones for always being so helpful and providing me with assistance in numerous ways. I would also like to extend my gratitude to Dr. Gerald Seidel for his diligent attention on safety in the laboratory at all times and for his tremendous contribution to ensure that everything runs smoothly. I will never forget the funny stories which was always good for a laugh. Furthermore, a big thank you also goes to Manuela Hanuschik, Markus Müller and Susanne Gastiger for providing an excellent technical assistance.

I enjoyed my time at FAU, Germany largely due to my lab family that became a part of my life. I am grateful for the time spent with the members of AG Burkovski who provided me with constant support, motivation, perseverance, hospitality, beer, hot chilies, laughter and a feeling of belonging. Thank you, Dr. Renata Peixoto, for receiving me at the lab, the awesome caipirinhas, delicious brigadeiros and most importantly for becoming a good friend. I would also like to thank Dr. Elena Hacker, Dr. Christian Schwab, Jens Möller, Laura Grebenstein, Meng Xiangjun, Tamara Fastner, Maria Glatter, Cornelius Roth, Jennifer Patitz, Sebastian Winterl and Tom Unterleiter for their support and making the atmosphere at the working place both friendly and constructive. Thank you also for the enjoyable long scientific and non-scientific discussions.

I wish to say a heartfelt thank you to my family for their love and unfaltering support. For my parents who raised me with the love for science, always believing in me and encouraging me to pursue my dreams. My brother for supporting me in every possible way, especially during this challenging phase living far away from home. Thank you to all my relatives and friends who supported me throughout the duration of my doctoral studies, despite me having very little time for them. Finally, I owe a huge debt of gratitude to Ubaya, my husband who has been by my side throughout the phase of the Ph.D., living every single minute of it and without whom, I would not have had the courage to embark on this journey in the first place. Your love, passion, caring manner, and warm words are amazing and have gotten me through hard times in life.

TABLE OF CONTENTS

TABLE OF FIGURES

1. SUMMARY/ZUSAMMENFASSUNG

1.1. SUMMARY

Corynebacterium diphtheriae is the causative agent of respiratory diphtheria, a major cause of infant mortality until the 1930s (Hadfield et al., 2000; Burkovski, 2014). Although the incidence of diphtheria has declined due to vaccination with diphtheria toxoid, the disease has not been completely eradicated. Moreover, the occurrence of non-toxigenic strains which are associated with invasive infections have been increasingly reported. Recently, diphtheria-like infections caused by the emerging pathogen *Corynebacterium ulcerans* have become more numerous in the Western Europe. The zoonotic transmission of *C. ulcerans* has become a cause of concern. Despite the medical and veterinary importance of these pathogenic microorganisms, only a few virulence factors have been characterized in detail including pili structures and a few other adhesion factors which play a pivotal role in the intracellular communication and host-pathogen interactions. In the frame of my dissertation, important findings were obtained which contributed to the elucidation of virulence properties of pathogenic corynebacteria:

In studies from Peixoto et al., an invasive, non-toxigenic *C. diphtheriae* strain was characterized with respect to its ability to cause colonization and killing of *Caenorhabditis elegans*, adhesion to and invasion of epithelial cells, survival within human macrophages as well as induction of osteomyelitis in mice (Peixoto et al., 2016).

Furthermore, the DIP0733 protein a multifunctional pathogenicity determinant of *C. diphtheriae*, was studied in respect to its role in the interaction with biotic surfaces, nematodes, human epithelial and macrophage cell lines. Bioinformatic analyses revealed the presence of several short linear motifs and structural elements of DIP0733. Among those motifs, we were interested in the C-terminal coiled-coil domain of DIP0733 as it was only identified in pathogenic corynebacteria. By demonstrating the binding properties to extracellular matrix proteins, adhesion to and invasion of epithelial cells, detrimental effects on epithelial cells and

killing of nematodes, we were able to show that the mutants lacking the coiled-coil domain were less virulent, while the fusion of the coiled-coil domain to DIP0733 of a non-pathogenic strain enhanced its pathogenicity. Therefore, this study indicated the crucial role of the coiled-coil domain of DIP0733 in virulence of corynebacteria (Weerasekera et al., 2018).

Pathogenicity of corynebacteria seems to be a multifactorial process and sometimes corynebacteria acquire new virulence factors by horizontal gene transfer. The recent identification of the putative ribosome-binding protein of *C. ulcerans* 809, which showed a striking structural similarity to the A chain of Shiga-like toxins from *Escherichia coli* (Trost et al., 2011), indicated a higher pathogenic risk of these species. In this study, the first functional characterization of this putative toxin in *C. ulcerans* strain 809 was analyzed together with a homologous protein identified in *C. diphtheriae* strain HC04 which has not been reported before. We were able to show that the overexpression of the corresponding *rbp* genes led to severe detrimental effects in invertebrate model systems as well as in epithelial and macrophage cell lines, while the *rbp* disrupted mutant showed a reduced cytotoxic effect (Weerasekera et al., 2019b). Further, FACS analyses revealed that both *C. ulcerans* 809 and *C. diphtheriae* HC04 caused necrosis in human THP-1 cells (Weerasekera et al., in preparation).

Since the interaction of corynebacteria with macrophages is not well understood, we explored the activation of pattern recognition receptors expressed on different immune cells upon *C. diphtheriae* contact by utilizing murine and human phagocytes. Our study revealed that the absence of Mincle resulted in reduced G-CSF production while the uptake of the bacteria was not influenced. In contrast, both the uptake of the bacteria and the production of cytokines were blocked when Myd88 was absent. Hence, we propose that the phagocytosis of corynebacteria occur only when TLR/Myd88 pathway is functional. In addition, strain specific differences were observed in the internalization of the bacteria, indicating although all *Corynebacterium* strains in our study were recognized by TLR2, some strains had unknown mechanisms to avoid uptake by the host cells irrespective of the presence of the diphtheria toxin (Weerasekera et al., 2019a).

1.2. ZUSAMMENFASSUNG

Corynebacterium diphtheriae ist der Erreger der respiratorischen Diphtherie, eine der Hauptursachen für eine hohe Kindersterblichkeit bis in die 1930er Jahre (Hadfield et al., 2000; Burkovski, 2014). Obwohl die Inzidenz von Diphtherie aufgrund der Impfung mit Diphtherie-Toxoid zurückgegangen ist, wurde die Krankheit nicht vollständig ausgerottet. Darüber hinaus wurde zunehmend über das Auftreten nicht-toxigener Stämme berichtet, die mit invasiven Infektionen in Verbindung gebracht werden. Zudem haben Diphtherie-ähnliche Infektionen, die durch den Erreger *Corynebacterium ulcerans* verursacht werden, in Westeuropa zugenommen. Die zoonotische Übertragung von *C. ulcerans* gibt Anlass zur Sorge. Trotz der medizinischen und veterinärmedizinischen Bedeutung dieser pathogenen Mikroorganismen wurden nur wenige Virulenzfaktoren im Detail charakterisiert, darunter Pili-Strukturen und einige andere Adhäsionsfaktoren, die eine zentrale Rolle bei der intrazellulären Kommunikation und den Wechselwirkungen zwischen Wirt und Pathogen spielen. Im Rahmen meiner Dissertation wurden wichtige Erkenntnisse erzielt, die zur Aufklärung der Virulenz pathogener Corynebakterien beitrugen:

In einer Studie von Peixoto et al. wurde ein invasiver, nicht-toxigener *C. diphtheriae*-Stamm in Bezug auf seine Fähigkeit charakterisiert, eine Besiedlung und Abtötung von *Caenorhabditis elegans*, die Adhäsion an und Invasion von Epithelzellen, das Überleben in menschlichen Makrophagen sowie die Induktion von Osteomyelitis bei Mäusen zu bewirken (Peixoto et al., 2016).

Darüber hinaus wurde das DIP0733-Protein, ein multifunktionaler Pathogenitätsfaktor von *C. diphtheriae*, hinsichtlich seiner Rolle bei der Wechselwirkung mit biotischen Oberflächen, Nematoden, humanen Epithel- und Makrophagen-Zelllinien untersucht. Bioinformatische Analysen zeigten das Vorhandensein mehrerer kurzer linearer Motive und Strukturelemente von DIP0733. Von besonderem Interesse war dabei eine C-terminalen *coiled-coil*-Domäne von DIP0733, da diese nur in pathogenen Corynebakterien identifiziert wurde. Durch den Nachweis der Bindung an extrazelluläre Matrixproteine, der Adhäsion an und Invasion in

Epithelzellen, der schädlichen Auswirkungen auf Epithelzellen und der Abtötung von Nematoden konnten wir zeigen, dass die Mutanten ohne *coiled-coil*-Domäne weniger virulent waren, während die Fusion der *coiled-coil*-Domäne mit DIP0733 eines nicht pathogenen Stammes, desen Pathogenität erhöhte. Damit wurde in dieser Studie die entscheidende Rolle der *coiled-coil*-Domäne von DIP0733 bei der Virulenz von Corynebakterien aufgeklärt (Weerasekera et al., 2018).

Die Pathogenität von Corynebakterien ist ein multifaktorieller Prozess, wobei Corynebakterien auch neue Virulenzfaktoren durch horizontalen Gentransfer erwerben können. Die kürzlich erfolgte Identifizierung des putativen ribosomenbindenden Proteins (Rbp) von *C. ulcerans* 809, zeigte eine auffällige strukturelle Ähnlichkeit mit der A-Kette von Shiga-ähnlichen Toxinen aus *Escherichia coli* (Trost et al., 2011) und stellt damit ein höheres Virulenzpotential dieser Spezies dar. In einer Studie erfolgte die erste funktionelle Charakterisierung dieses putativen Toxins im *C. ulcerans*-Stamm 809 zusammen mit einem homologen Protein, das im zuvor nicht beschriebenen *C. diphtheriae*-Stamm HC04 identifiziert wurde. Es konnte gezeigt werden, dass die Überexpression der entsprechenden *rbp*-Gene in *C. ulcerans* bzw. *C. diphtheriae* in Infektionsexperimenten mit verschiedenen Modellsystemen zu starken Schädigungen führte, während die *rbp*-Mutante eine verringerte zytotoxische Wirkung aufwies (Weerasekera et al., 2019b). Ferner zeigten FACS-Analysen, dass sowohl *C. ulcerans* 809 als auch *C. diphtheriae* HC04 Nekrose in menschlichen THP-1-Zellen verursachten (Weerasekera et al., in Vorbereitung).

Da die Wechselwirkung von Corynebakterien mit Makrophagen nicht gut verstanden ist, untersuchten wir die Aktivierung von Mustererkennungsrezeptoren, die bei *C. diphtheriae*-Kontakt auf verschiedenen Immunzellen exprimiert wurden, unter Verwendung von murinen und humanen Phagozyten. Die Studie ergab, dass die Abwesenheit von Mincle zu einer verringerten G-CSF-Produktion führte, während die Aufnahme der Bakterien nicht beeinflusst wurde. Im Gegensatz dazu wurden sowohl die Aufnahme der Bakterien als auch die Produktion von Zytokinen blockiert, wenn Myd88 fehlte. Daraus schließen wir, dass die Phagozytose von Corynebakterien nur auftritt, wenn der TLR/Myd88-Signalweg funktionsfähig

ist. Zusätzlich wurden stammspezifische Unterschiede bei der Internalisierung der Bakterien beobachtet, was darauf hinweist, dass obwohl alle *Corynebacterium*-Stämme in unserer Studie durch TLR2 erkannt wurden, einige Stämme durch nicht charakterisierte Mechanismen in der Lage waren, die Aufnahme durch die Wirtszellen, unabhängig vom Vorhandensein des Diphtherietoxins, zu verhindern (Weerasekera et al., 2019a).

2. AIM OF THE WORK

Diphtheria toxin is the best investigated major virulence factor of toxigenic *Corynebacterium diphtheriae* and *Corynebacterium ulcerans*. However, non-toxigenic strains of these two species also cause severe infections in animals and humans, indicating the presence of additional virulence factors.

With respect to host-pathogen interactions, one of the aims of this study was to characterize the role of C-terminal coiled-coil domain of DIP0733 protein of *C. diphtheriae*. To elucidate the impact of the coiled-coil domain on virulence, several DIP0733 truncated and domain-swapped mutant strains from *C. diphtheriae* were assessed utilizing epithelial cells and nematode model systems. Next, interaction of *C. diphtheriae* strains with primary mouse macrophages (C57BL/6, Clec4e$^{-/-}$ and MyD88$^{-/-}$) together with the human THP-1 cell line were focused. To get deeper insights into the early detection of invading pathogens in initiating early innate immune response, the activation of pattern recognition receptors expressed on different immune cells upon *C. diphtheriae* contact was investigated. In addition, to investigate the functional aspects of the putative ribosome-binding protein of a *C. ulcerans* strain with its newly identified homologous protein of a *C. diphtheriae* strain in this study, the first characterization of the cytotoxic effect of the ribosome-binding protein was aimed utilizing eukaryotic cell lines and nematode model systems.

3. CORYNEBACTERIA

The genus *Corynebacterium* was first described by Lehmann and Neumann in 1896 as a taxonomic group of bacteria with morphological similarities to the diphtheroid bacillus (Lehmann and Neumann, 1896). Corynebacteria belong to the class of Actinobacteria (high G+C Gram positive bacteria) and comprise a collection of morphologically similar, irregular or clubbed-shaped nonsporulating microorganisms (Ventura et al., 2007; Zhi et al., 2009). Corynebacteria form typical V-shaped cell dimers (Figure 1) during cell division. This is also called as the snapping division (Barksdale, 1970).

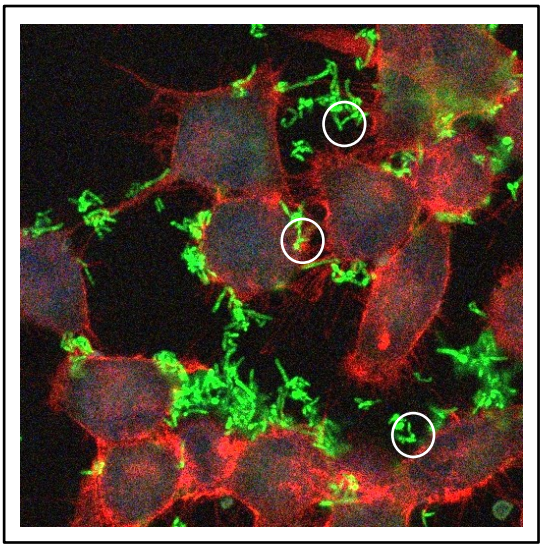

Figure 1. Fluorescence microscopy of corynebacteria and epithelial cells.
Adherence of *C. diphtheriae* CDC-E8392 to HeLa cells are shown. V-shaped cell dimers are indicated in white circles.

To date, 90 species have been assigned to the genus *Corynebacterium* with the most prominent member of the pathogenic species being *Corynebacterium diphtheriae*, which is also the type species of the whole genus. Some pathogenic species such as *Corynebacterium amycolactum* and *Corynebacterium jeikeium* are a part of the human skin flora, while others (*Corynebacterium ulcerans*, *Corynebacterium pseudotuberculosis* and *Corynebacterium xerosis*) are considered as commensals of humans or animals. Additionally, other species including *Corynebacterium glutamicum*, *Corynebacterium efficiens* and *Corynebacterium ammoniagenes* are well known for their biotechnological importance such as industrial production of nucleotides and amino acids (Bernard, 2012; Burkovski, 2013).

Corynebacteria are dedicated to the CMNR group (*Corynebacterium*, *Mycobacterium, Norcadia* and *Rhodococcus*), based on their molecular similarity of cell wall components. Almost all members of the genus are characterized by a complex cell wall architecture. The plasma membrane of these bacteria is covered by a peptidoglycan layer, which is covalently linked to arabinogalactan. Additionally, an outer layer of mycolic acids is found which is functionally equivalent to the outer membrane of Gram-negative bacteria. The outer surface material of the top-most layer is composed of free polysaccharides, glycolipids, and proteins which also includes S-layer proteins, pili and other surface proteins (reviewed in Daffé, 2005; Eggeling et al., 2008; Burkovski, 2013) (Figure 2).

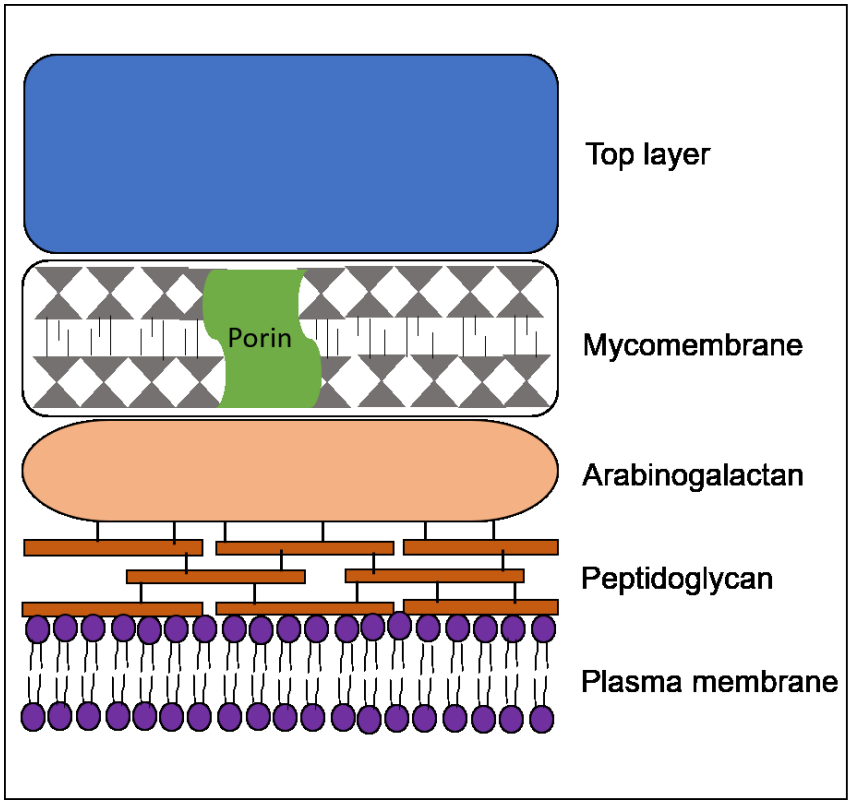

Figure 2. Schematic representation of the structure of corynebacterial cell envelope. The plasma membrane composed of a bilayer of proteins and phospholipids is covered by a peptidoglycan layer which is covalently linked to arabinogalactan. An outer layer of mycolic acids is found. The top layer is composed of polysaccharides, glycolipids and proteins which includes S-layer proteins, pili and other surface proteins. Porin proteins shown in mycomembrane might also be present in the top layer.

Pathogenic corynebacteria are mostly not highly virulent, and only immune-compromised patients get infected. However, virulence can be dramatically increased when

diphtheria toxin encoded β-corynebacteriophages are integrated into the chromosomes of *C. diphtheriae*, *C. ulcerans* and *C. pseudotuberculosis* (Sangal and Hoskisson, 2014). Toxigenic *C. diphtheriae* are the main causative agent of diphtheria. Although, historically humans are thought to be the sole reservoirs of *C. diphtheriae*, studies in 2010 reported isolation of *C. diphtheriae* from a domestic cat and a horse (Hall et al., 2010; Leggett et al., 2010). The prevention of diphtheria is achieved through mass immunization with toxoid molecules. (Vitek and Wharton, 1998; Hadfield et al., 2000).

C. ulcerans is a closely related emerging pathogen in domestic and wild animals (Schuhegger et al., 2009; Dixon, 2010; Sykes et al., 2010) that may serve as a reservoir for zoonotic infections and cause diphtheria-like illness in humans (Mattos-Guaraldi et al., 2014). Toxigenic *C. ulcerans* cause both respiratory and cutaneous diphtheria in humans and both toxigenic and non-toxigenic species have been increasingly isolated from a wide variety of animals including pet dogs (Lartigue et al., 2005; Meinel et al., 2015), cats (Berger et al., 2011), pigs (Schuhegger et al., 2009), cows (Murakami et al., 2014), goats (Morris et al., 2005), macaques (Venezia et al., 2012), ferrets (Marini et al., 2014), killer whales (Seto et al., 2008) and recently also in hedgehogs (Berger et al., 2019). Studies reported that some *C. ulcerans* are asymptomatic carriers in animals such as Ural owl and Japanese shrew-mole (Katsukawa et al., 2016), while others cause mastitis in cattle (Bostock et al., 1984; Hart, 1984), ulcerative skin lesions in water rats (Eisenberg et al., 2015), lung damage in otters (Foster et al., 2002), abscesses in wild boars (Eisenberg et al., 2014) and roe deers (Rau et al., 2012). Transmission occurs from animals to humans and usually adults get infected. The high risk in humans due to *C. ulcerans* infection is associated with consuming unpasteurized, contaminated milk and dairy products (Bostock et al., 1984; Hart, 1984) or close contact with domestic animals (Wagner et al., 2010). However, person-to-person transmission has not been reported until now.

C. pseudotuberculosis is the etiological agent of caseous lymphadenitis (CLA) in sheep and goats throughout the world (Dorella et al., 2006b; Baird and Fontaine, 2007) and occasionally cause disease in other species, including horses, cattle and humans (Batey,

1986). CLA is one of the most prevalent bacterial diseases in sheep resulting in reduced wool production, carcass condemnation and carcass trimming (Paton et al., 1988). Infections due to *C. pseudotuberculosis* are rare in humans, but there are some cases of suppurative cases of lymphadenitis in patients with close contact with sheep (Batey, 1986). Despite the putative presence of a diphtheria toxin, classical diphtheria of respiratory tract or skin is not observed. (Groman et al., 1984; Cianciotto and Groman, 1996).

Many other *Corynebacterium* species inhabit the human skin or mucosa as commensals (Tauch and Burkovski, 2015). Typical examples for skin inhabitants include *C. jeikeium*, *C. amycolatum*, *C. striatum* and *C. tuberculostearicum* whereas, *C. glucuronolyticum* and *C. urealyticum* are frequently found in urogenital tract. These species can cause invasive disease in immunocompromised as well as patients with compromised skin or mucosal barrier function (Chung et al., 2008; Martins et al., 2009; Schoen et al., 2009; Shao et al., 2015).

3.1. The disease diphtheria, epidemiology and occurrence

Diphtheria is potentially an acute disease mainly caused by exotoxin producing *Corynebacterium* species (Cerdeño-Tárraga et al., 2003). The classical forms of diphtheria are caused by toxigenic *C. diphtheriae* which is usually transmitted among people by direct contact, sneezing or coughing. It may also spread via contaminated objects (CDC, 2015). Diphtheria is an infection of the upper respiratory tract and characterized by the presence of a greyish pseudomembrane at the infection site due to the effect of diphtheria toxin production, multiplication of bacterial cells and the hosts immune response. Signs and symptoms of diphtheria may vary from mild to severe, they usually start two to five days after exposure. Symptoms often appear gradually with sore throat, low fever and malaise. In severe cases, the involvement of cervical lymph nodes may cause a profound swollen neck sometimes referred to as a “bull-neck” (Murphy, 1996). Later, barking cough develops due to the progressive formation of the pseudomembrane which renders breathing difficulties (Figure 3) (Gilbert, 1997; Lozhnikova et al., 1997; Hadfield et al., 2000; Holmes, 2000; Burkovski, 2014).

Coughing can remove parts of the pseudomembrane, easing the situation of the patient temporarily, and after several fits of coughing, the pseudomembrane might even be removed and healing might be achieved. However, in severe cases, obstruction of airways results in suffocation, agony and death of the patient (Burkovski, 2014). A form of diphtheria that involves the skin, eyes or genitals also exists (CDC, 2015). Complications may include myocarditis, inflammation of nerves, kidney problems and frequent bleeding due to low level of blood platelets. Cutaneous diphtheria prevails over the respiratory tract form in tropical and subtropical regions of the world (Höfler, 1991). Poverty, poor hygiene, overcrowding and slow healing of the wounds favor the infection. Cutaneous diphtheria is characterized by skin lesions located predominantly on feet, lower legs and hands (Figure 3) (Mattos-Guaraldi et al., 2008; Wagner et al., 2010; Lowe et al., 2011; Corti et al., 2012). The disease may spread by contact with infected skin, respiratory droplets or exposure to dust or clothing contaminated with *C. diphtheriae* (Höfler, 1991).

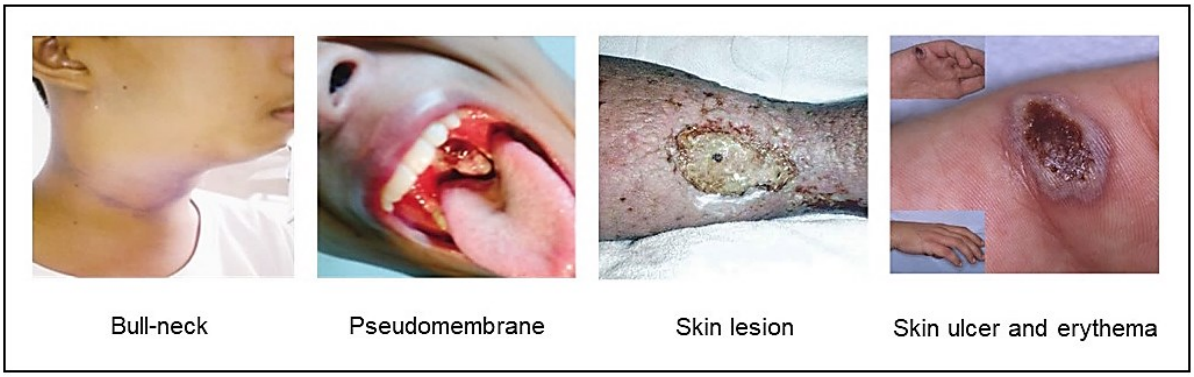

Figure 3. Disease manifestations in humans due to *C. ulcerans* infection. Bull-neck appearance and pseudomembrane formation also manifest upon *C. ulcerans* infection which otherwise is generally seen in diphtheria. It was identified on the tonsils of a 15-year old male from the Philippines (Putong et al., 2011), skin lesion with a yellowish membrane on leg of an 80-year old woman from Brazil (Mattos-Guaraldi et al., 2008) and skin ulcer with an undetermined edge covered with a grey-brown membrane and erythema on the back of the hand of a 29-year old male from Switzerland are shown (Corti et al., 2012).

Treatment of diphtheria is unproblematic today since *C. diphtheriae* can be eliminated easily using antibiotics, and the diphtheria toxin can be neutralized by antitoxin application. However, the best means to control diphtheria is the mass immunization of the population.

Although the availability of the highly effective toxoid vaccine makes diphtheria an extremely rare disease in industrialized countries, reporting of several thousand cases to the World Health Organization every year indicate that diphtheria is not completely eradicated and reservoirs still exist (Burkovski, 2014; WHO, 2015). Putative carriers are people in poor parts of developing countries who has insufficient access to medical care including vaccination programs. Consequently, for citizens of industrialized countries, a major risk factor for infection with *C. diphtheriae* might be traveling to an endemic country. Moreover, isolation of *C. diphtheriae* strains from domestic cats and horses indicate that animals too play an important role in transmission of the infection. For other toxigenic *Corynebacterium* species, animal reservoirs serve as a common source of infection which might be connected to diphtheria-like illness. For instance, *C. ulcerans* strains producing diphtheria toxin are reported with an increasing frequency from industrialized countries. *C. ulcerans* has been primarily recognized as a commensal bacterium in domestic and wild animals however, also frequent and severe human infections associated with *C. ulcerans* are observed (Burkovski, 2014).

The occurrence of diphtheria reflects inadequate coverage of childhood immunization programs. Therefore, obstacles to optimal vaccine delivery must be identified and forceful measure need to be taken to improve immunization coverage (Tiwari, 2012). Today, revaccination of adults against diphtheria (and tetanus) every 10 years may be necessary to sustain immunity in some epidemiological settings (CDC, 2015; WHO, 2015). Therefore, in all countries, easy access to laboratory facilities for reliable identification of toxigenic *C. diphtheriae* should be established to ensure early detection of diphtheria outbreaks.

4. VIRULENCE FACTORS OF CORYNEBACTERIA

Bacterial virulence factors in general are compounds (toxins, enzymes or other molecules) contributing to the infectious potential of a pathogenic microbe and can either confer the ability to attach to and colonize specific host tissues or cause damage to the host (Madigan et al., 2009). Virulence factors help bacteria to invade the host, cause disease and evade host defenses.

4.1. Diphtheria toxin

Diphtheria toxin (DT) is the best analyzed virulence factor in *C. diphtheriae* (Pappenheimer, 1993; Wang and London, 2009). This toxin is also the major virulence factor of the closely related species, *C. ulcerans* and is responsible for the classical symptoms of the respiratory disease diphtheria, characterized by a sore throat, a typical sweetish-putrid smell of the patients' breath and formation of pseudomembrane due to the accumulation of dead cells resulting in a thick, grey coating in the throat or nose. DT is a 535 amino acids polypeptide chain with a molecular weight of about 62 KDa (Holmes, 2000) and composed of two fragments, the amino-terminal fragment A and the carboxy-terminal fragment B, which are linked by disulfide bonds. Fragment A contains the catalytic domain (C-domain), fragment B corresponds to the translocation and receptor binding domains (T-domain and R-domain) (Figure 4), respectively (Varol et al., 2014).

The delivery of DT to the cytosol is a sequential process. First, the toxin binds to the receptor on the cell surface via R-domain and is internalized by clathrin-mediated endocytosis. The diphtheria toxin receptor has been identified as the precursor of heparin-binding epidermal growth factor (proHB-EGF) like-growth factor (Naglich et al., 1992). Second, the toxin enters the cell by receptor-driven endocytosis and the acidic pH inside the endosome triggers a translocation of the catalytic domain (Figure 4), leading to the insertion of the T-and C-domains in the membrane. The active C-domain crosses the endosomal membrane into the cytoplasm and the inhibition of protein synthesis occurs via ADP-ribosylation of its cellular target, the

elongation factor 2 (EF-2) (Collier, 1975; Pappenheimer, 1977; Lord et al., 1999; Falnes and Sandvig, 2000). A single molecule of DT, when introduced directly into the cytoplasm, is sufficient to kill a eukaryotic cell (Yamaizumi et al., 1978).

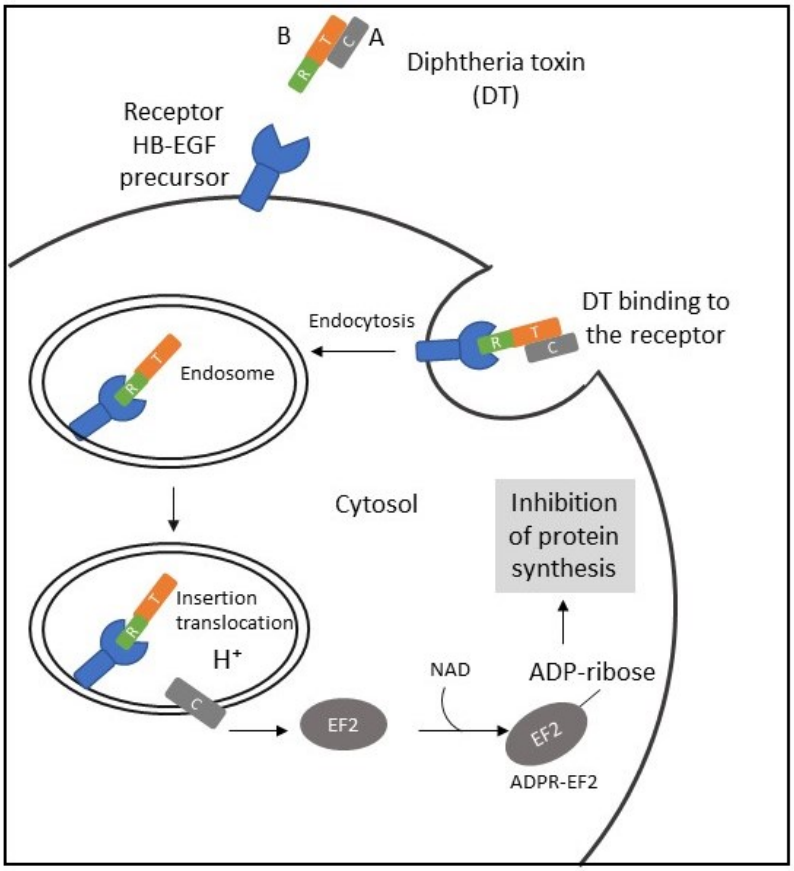

Figure 4. Schematic representation of the cellular entry of diphtheria toxin. The toxin binds to heparin-binding EGF-like receptor on the surface via R-domain and initiate endocytosis by clathrin-mediated endocytosis. The low pH induced conformational change of T-domain initiates the membrane translocation steps. The transfer of C- domain from the early endosome to cytosol occur under regulation of cytosolic translocation factor EF-2. Following disulfide bond reduction and chaperon-dependent refolding, the C-domain becomes active, ADP-ribosylates EF-2 in the presence of NAD and induces depolymerization of F-actin leading to the halting of protein synthesis.

The *tox* gene for diphtheria toxin expression is located in the genomes of corynebacteriophages, which are able to integrate into the chromosomes of *C. diphtheriae*, *C. ulcerans* and *C. pseudotuberculosis* (Sangal and Hoskisson, 2014). As a result, not all strains produce the toxin, but only those gets lysogenized by corynephages. DT is synthesized under iron starvation and is extracellularly secreted as a single polypeptide chain (Pappenheimer, 1977; Holmes, 2000). In this conformation, the toxin is inactive, can be absorbed into the

circulatory system and disseminated to remote parts of the body. The expression of the *tox* gene is regulated by the bacterial host via a chromosome-encoded regulatory element, the diphtheria toxin repressor (DtxR), which is an iron-dependent regulatory protein. Under high iron conditions, DtxR represses the transcription of the *tox* gene, the synthesis of the corynebacterial siderophore as well as other components of the high affinity iron-uptake system (Lee et al., 1997). Among both *C. diphtheriae* and *C. ulcerans*, differences in nucleotide sequences of the *tox* genes may occur (Mekada et al., 1988; Bitragunta et al., 2010). In fact, significant differences between the sequences of the *tox* genes of two *C. ulcerans* isolates have been identified but interestingly, it showed higher similarity to *C. diphtheriae tox* gene (Contzen et al., 2011). Therefore, individuals vaccinated with diphtheria toxoid or undergoing serum therapy may not present full protection against infections caused by toxigenic corynebacteria. Vaccination only prevents the action of DT and does not impede the colonization by toxigenic corynebacteria (Neal and Efstratiou, 2007; Bégué, 2010; Möller et al., 2019). In *C. ulcerans*, a novel putative DT-encoding pathogenicity island (PAI) was found which is not phage related. The location of the PAI in the genome of *C. ulcerans* is a target of other events of horizontal gene transfer (Hacker et al., 2016a). However, the specificity of PAI to *C. ulcerans* and the mechanisms involved in transferring to bacterial genome is yet to be elucidated (Meinel et al., 2014).

4.2. Phospholipase D

Phospholipase D (PLD) is the major virulence determinant in *C. pseudotuberculosis* and thought to be another major virulence factor in *C. ulcerans* (Lipsky et al., 1982; Hodgson et al., 1992; Dorella et al., 2006a). It is a secreted exotoxin that possesses sphingomyelinase activity (Hodgson et al., 1990). PLD has been shown to increase vascular permeability *in vivo*, have dermonecrotic properties and exhibit synergistic haemolysis of sheep blood cells (McKean et al., 2007).

Studies with *C. pseudotuberculosis* PLD-mutant strains showed that PLD is an essential virulence factor that is involved in the dissemination of the bacteria from initial infection sites to secondary sites within the host. Strains with inactivated PLD were unable to cause abscesses of the lymph nodes and establish caseous lymphadenitis (Hodgson et al., 1992; McNamara et al., 1994). PLD also seems to be involved in killing of macrophages, as a PLD-deficient mutant strain caused significantly less cell death in murine J774 macrophages than did the wild type strain (McKean et al., 2007). PLD genes from *C. pseudotuberculosis* and *C. ulcerans* share 80 % homology in the nucleotide sequence and 87 % homology in their amino acid sequence (Cuevas and Songer, 1993). Cytotoxic effects and death of caprine macrophages due to the action of PLD was observed during infection with *C. pseudotuberculosis* (Tashjian and Campbell, 1983). Expression of PLD is regulated by multiple environmental factors, including cell density and heat shock (McKean et al., 2007).

The occurrence of necrosis and mucosal ulceration as well as other clinical manifestations in the lower respiratory tract caused by *C. ulcerans* were attributed to the production of both DT and PLD (Dessau et al., 1995; Seto et al., 2008). However, experimental data on the involvement of PLD in virulence in *C. ulcerans* is scarce. While a reduction in cytotoxicity was observed in THP-1 macrophages when infected with the PLD-deficient mutant compared to *C. ulcerans* wild-type strain (Hacker et al., 2016b), no significant differences were observed in the adhesion and invasion rates in epithelial cells (Hacker et al., 2015). Furthermore, infection with *C. ulcerans* and *C. pseudotuberculosis* strains showed colonization in *Caenorhabditis elegans* and induced death in *Galleria mellonella* models. The strongest effects on *Galleria* larvae which included high degree of melanization, immobility and rapid death were attributed to PLD production (Ott et al., 2012).

4.3. Shiga-like toxin

During a large epidemic in the 19th century, the great Japanese bacteriologist Kiyoshi Shiga, isolated the bacterium *Bacillus dysenteriae* from stools of patients suffering from dysentery. For his discovery, the bacterium was renamed as *Shigella dysenteriae* and the toxin produced by this bacterium was named as Shiga toxin (Stx). As Stx when injected to rabbits caused limb paralysis, the toxin was first described as a neurotoxin. However, in 1970s, the relevance of Stx to gastrointestinal toxicity was revealed (Keusch et al., 1981). A few years later, *in vitro* studies showed that some strains of *Escherichia coli* produced toxins that killed Vero cells (Konowalchuk et al., 1978) and behaved similar to Stx, leading to often deadly and frequently debilitating hemolytic uremic syndrome. Therefore, these toxins were named as verotoxins. Moreover, the verotoxins shared a remarkable identity with Stx, as application of antibodies against Stx also worked for neutralizing verotoxins. Therefore, the verotoxins were re-designated as Shiga-like toxins (SLTs) (Chan and Ng, 2016). As two very different bacterial species produced a similar toxin, it was believed that there was a transfer of genes to the bacteria. It was proved that the lambdoid bacteriophages that encode Shiga toxins incorporate their genome into host bacterial cells and produce the toxin (Cornick et al., 2006). Stx-1 and Stx-2 are the two main types of Shiga toxins produced by Shiga-like toxin producing *E. coli* (STEC). They are antigenically different but have the same mode of action. While Stx-1 shows a remarkable homology to the amino acid sequence of Stx identified in *S. dysenteriae*, Stx-2 shows only about 55 % similarity. Stx-1 can therefore be neutralized by antibodies raised against Stx, as they only differ in one amino acid residue however, antibodies from Stx cannot inactivate Stx-2 (Calderwood et al., 1987).

Shiga-like toxin requires a couple of steps to exert its toxicity to the target cells. After binding to the target cell surface receptor Globotriaosylceramide-3 (Gb3), the toxin requires a complicated process to be transported into the cytosol of the host cell before it can approach the ribosomes. SLT-1 usually consists of a catalytic A chain that is non-covalently linked to a pentamer of B chains. These B subunits of SLT-1 are essential for binding to a specific

glycolipid receptor and the translocation of the toxin into the host cell. After endocytosis of the toxin, it is transported to the Golgi network and then to the endoplasmic reticulum (ER). The toxin is finally translocated across the ER membrane into the cytosol to exert its catalytic action on ribosomes (Figure 5). The A chain inhibits protein synthesis by cleaving the N-glycosidic bond by depurination of a single adenosine residue in 28S eukaryotic ribosome (O'Loughlin and Robins-Browne, 2001). However, the mechanism involved in recognizing the specific adenine, the catalytic action and why the depurination of single adenine arrests protein synthesis is not properly understood.

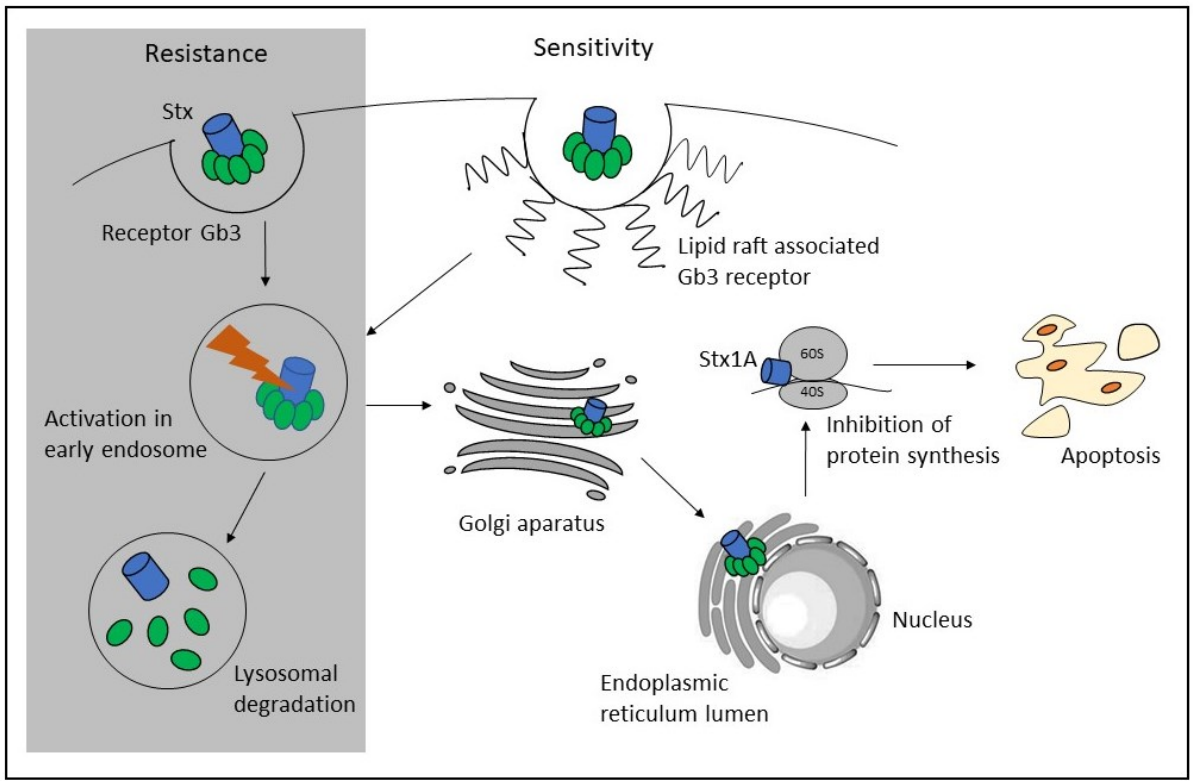

Figure 5. Mechanism of action of Shiga-like toxin. Binding of Stx to Gb3 in Stx-resistant cells leads to the transport of Stx via endosomal/lysosomal pathway which ultimately gets degraded in lysosomes. In a sensitive cell, after binding to the lipid raft associated Gb3, Stx is internalized into the early endosome, and travels further to the trans-Golgi network. During this early stage, furin cleaves the A subunit of Stx into an active A1 subunit and an A2 fragment that is associated with the B pentamer. At this stage, StxA1 is still linked to StxA2 and B subunits via a disulfide bond. From the Golgi apparatus, the toxin is transported to the ER and then to the nuclear membrane. The reduction of the disulfide bond in the ER results in retro-translocation of StxA1 into the cytoplasm where it binds to the large ribosomal subunit and inhibits protein synthesis by cleaving off a single adenine residue from the 28S rRNA. The inhibition of protein synthesis triggers a ribotoxic stress response in the host cell which ultimately leads to apoptosis. (Modified from Schüller, 2011).

C. ulcerans genome is equipped with a broad spectrum of virulence factors, including a novel ribosome-binding protein (Rbp) that is encoded only in the human isolate *C. ulcerans* 809. The search for unique genes by basic local alignment search tool (BLAST) matches revealed 90 strain-specific genes for *C. ulcerans* 809, of which to our interest, a *rbp* gene encoding a putative ribosome binding protein containing a ribosome-inactivating protein domain (RIP) was annotated with putative physiological function (Trost et al., 2011). The *rbp* gene (CULC809_00177) containing Pfam 00161 represent a candidate virulence factor of *C. ulcerans* 809 (Marchler-Bauer et al., 2010). A lateral transfer of *rbp* to *C. ulcerans* 809 was suggested since *rbp* is located between a gene coding for a putative phage integrase and a transposase gene with a low G+C content of 45.1 %, compared to the complete genome sequence comprising a G+C content of 53.3 % (Trost et al., 2011).

The amino acid sequence of Rbp showed weak similarity of about 24 % to the A chains of Shiga-like toxins SLT-1 and SLT-2 from *E. coli* but comprised all highly conserved amino acid residues needed for the catalytic *N*-glycosidase activity (O'Loughlin and Robins-Browne, 2001; LaPointe et al., 2005). SLT-1 belongs to Rbp type-II family with a low similarity to amino acid sequences but with a highly conserved tertiary structure of type-II family members. In silico comparison of tertiary structures of Rbps and A chain of SLT-1 revealed significant structural similarities of both proteins. It has been identified that the amino acid sequence of Rbp lacks the typical ER-targeting sequence at the C-terminal end. The ER-targeting sequence is known to be necessary for the retranslocation of the catalytic domain of SLT-1 from the ER into the cytosol of the host cell (O'Loughlin and Robins-Browne, 2001). However, as *C. ulcerans* still persist as an intracellular pathogen in mammalian host cells, it was suggested that the retranslocation of the Rbp into the cytosol for the activity is not necessary, instead, it was proposed that the secretion of the putative toxin into the cytosol is supported by a signal sequence at the N-terminus of the Rbp (Trost et al., 2011).

Until now, the only corynebacterial strain for which the corresponding Rbp has been described is *C. ulcerans* 809. However, based on multiple sequence comparisons, a recent study indicates an amino acid identity of 26 % and a query coverage of 76 % of the Rbp to a

homologous putative secreted protein (CDHC04_0155) identified in the non-toxigenic *C. diphtheriae* HC04 strain (Weerasekera et al., 2019b). Moreover, the alignment of the tertiary structure of Rbp from *C. diphtheriae* HC04 showed a confidence of 96.89 % and an identity of 26 % to the A chain of SLT-1. Interestingly, *in vivo* and *in vitro* studies revealed similar functions of the Rbps identified in *C. ulcerans* and *C. diphtheriae* with respect to the detrimental effects observed in invertebrate model organisms as well as animal and human epithelial and macrophage cell lines (Weerasekera et al., 2019b). Although these findings as well as previous studies suggest a horizontal transfer of the coding region to corynebacteria, it is unclear whether the *rbp* gene was a former part of a corynephage or associated with a transposable element. In this respect, future studies concerning secretion and delivery mechanisms of the toxin need to be characterized to elucidate molecular basis of the gene transfer mechanisms.

4.4. DIP0733: a multi-functional pathogenicity determinant

Besides diphtheria toxin, only a few other virulence factors have been characterized in detail in *C. diphtheriae*. One of the best characterized virulence factors that play an important role in pathogenicity of *C. diphtheriae* is the protein DIP0733 (Sabbadini et al., 2012; Antunes et al., 2015; Weerasekera et al., 2018). *C. diphtheriae* strains express non-fimbrial surface proteins and utilize them in binding to specific host cell receptors. DIP0733 was initially described as a non-fimbrial surface protein of 67-72p according to its appearance as two bands with distinct apparent masses in SDS-PAGE (Colombo et al., 2001). It was also demonstrated that both polypeptides 67-72p, bind to erythrocyte receptors, leading to hemagglutination (Colombo et al., 2001). 67-72p not only served as adhesins involved in the interaction of *C. diphtheriae* with human erythrocytes, but also successful in interacting with human epidermoid laryngeal carcinoma cell line HEp-2. Furthermore, by applying anti 67-72p IgG antibodies it was shown that the binding was effectively blocked (Hirata et al., 2004).

A comparative analysis of MALDI-TOF MS and *in silico* proteome deduced from the complete genome sequence of *C. diphtheriae* indicated 67-72p as the protein DIP0733, encoded by the single gene *dip0733*. Moreover, experiments on 67-72p protein-coated latex beads suggested an effect of the protein on the internalization and induction of apoptosis (Sabbadini et al., 2012). Despite the different properties ascribed to DIP0733, i.e. hemagglutination, binding to host cell receptors and induction of apoptosis, unfortunately, a detailed molecular analysis of the protein was difficult due to complete lack of an annotation of functional domains within the protein.

To characterize this functionally astonishing and diverse protein, *in vivo* and *in vitro* experiments were carried out to elucidate its interaction utilizing wild type CDC-E8392 and mutant strains. DIP0733 is widely distributed in Actinobacteria including pathogenic and non-pathogenic *Corynebacterium*, *Mycobacterium*, *Nocardia* and *Rhodococcus* species. It is also found in other bacteria having a high GC content like *Dietzia* and *Amycolatopsis* species. This distribution indicates many other physiological functions of DIP0733, besides its role as a virulence property in *C. diphtheriae*. A study by Antunes et al. demonstrated that the *dip0733* disrupted CAM-1 mutant significantly attenuated the colonization and killing of the nematode *C. elegans* and decreased the adherence and internalization rate in epithelial cells (Antunes et al., 2015). The invasion of epithelial cells represents an important step of infection as it allows *C. diphtheriae* to maintain an intracellular location. Moreover, the necessity of cytoskeletal rearrangement for bacterial entry is suggested as invasion was completely blocked by cytochalasin E, an inhibitor known for eukaryotic microfilament formation (Hirata Jr. et al., 2008). In addition to an altered adhesion and invasion process in epithelial cells, the mutant CAM-1 also exhibited drastically reduced internalization in human THP-1 cells, indicating that DIP0733 influences the survival of bacteria within macrophages. Moreover, the subsequent experiments revealed DIP0733 has an influence in the binding to extracellular matrix proteins such as collagen and fibronectin (Antunes et al., 2015).

DIP0733 is a membrane protein characterized by seven amino terminal transmembrane helices and a long carboxy terminal segment predicted to be located outside

the cell (Sabbadini et al., 2012). Weerasekera and co-workers carried out extensive mutagenesis studies to investigate the contribution of functional elements of DIP0733 in the process of host-pathogen interactions (Weerasekera et al., 2018). For this purpose, short linear motifs and structural elements of DIP0733 with a putative importance in virulence were identified using bioinformatic approaches. The examination of Short Linear Motifs (SLiMs) of DIP0733 homolog sequences by means of Eukaryotic Linear Motif (ELM) database revealed, DIP0733 sequences from closely related pathogenic corynebacteria shared higher similarity in SLiMs compared to non-pathogenic corynebacteria. In this respect, a particular importance was given to the C-terminal coiled-coil region of the protein as it was found only in DIP0733 homologs of pathogenic but not in non-pathogenic corynebacteria. In fact, the coiled-coil domain was found to be present in all *C. diphtheriae* and *C. pseudotuberculosis* strains whereas it was not identified in *C. glutamicum* and *C. ulcerans* strains (Weerasekera et al., 2018). Taking the above into consideration, it was assumed that the virulence property of DIP0733 could be influenced by the coiled-coil domain. Therefore, the function of the domain was studied by constructing several truncated mutant variants (Weerasekera et al., 2018).

Coiled-coil domains are protein structural motifs that consist of two or more α-helical peptides that are enfolded around each other in a superhelical fashion (Apostolovic et al., 2010). They are ubiquitous in nature, found in proteins of both eukaryotes and prokaryotes, play an important role in various intracellular regulation processes as well as membrane fusion (Apostolovic et al., 2010). While in eukaryotes coiled-coil domains are found in transcription factors and in a whole class of fibrous proteins such as keratin, myosin, epidermin and fibrinogen, in prokaryotes it can be found in murein lipoproteins of *E. coli*, colicin E3 in *Salmonella* Typhimurium and Pep M5 protein in group A streptococci (Manjula and Fischetti, 1986; Apostolovic et al., 2010). A recent study by Weerasekera et al. indicated that the coiled-coil domain of DIP0733 is important for the binding to certain microbial surface component recognizing adhesion matrix molecules (MSCRAMMs), play a key role in the pathogenicity of invertebrate model organisms and is crucial for adherence and internalization of *C. diphtheriae* to HeLa cells (Weerasekera et al., 2018). Interestingly, this effect was not observed with the

coiled-coil domain lacking DIP0733 homolog mutant of *C. ulcerans* (CULC22_00609) (Hacker et al., 2015). To address if the coiled-coil domains of DIP0733 are solely responsible for the interaction with host cells or with holding of protein oligomers, crystallization of the protein and its oligomerization status need to be investigated in future studies.

4.5. Other pathogenicity determinants and niche factors of corynebacteria

Pathogenic bacteria are equipped with a plethora of proteins and other components for successful colonization of the host, which are often designated as virulence factors. These virulence factors are often involved in colonization of a specific ecological niche, rather than exhibiting any specific function such as detrimental effect on the host. However, since these virulence factors have a specific function with respect to pathogenicity only in combination with other proteins and in a certain environment, it was argued that they might better be designated as 'niche factors' (Hill, 2012; Tauch and Burkovski, 2015). This concept should be true within a distinct taxonomical group of bacteria. In this respect, the genus *Corynebacterium* is in the light of interest due to its high diverse composition.

Derivatives of lipomannan (LM) and lipoarabinomannan (LAM) were found in different *Corynebacterium* species (Puech et al., 2001) and the distribution of it seems to be species specific. For example, in *C. diphtheriae* an equal distribution of LM and LAM were observed. While in *C. glutamicum*, LM-like substances were dominating, in *C. xerosis* and *C. amycolatum*, LAM-like substances were preferentially found (Puech et al., 2001). CdiLAM is the 10 kDa lipoarabinomannan polymer identified in *C. diphtheriae* which shows a structural similarity to mycobacterial LAM. CdiLAM is known to contribute in the adherence of *C. diphtheriae* to epithelial cells (Moreira et al., 2008). Additionally, the role of LAM in *C. glutamicum* with respect to the initiation of immune responses by interacting with Toll-like receptor-2 (TLR-2) was addressed (Mishra et al., 2012). Nevertheless, further studies are required to support the idea that CdiLAM is able to modulate the immune responses.

The suborder *Corynebacterineae* of the order Actinomycetales, which also includes *Mycobacterium* spp., *Nocardia* spp., *Rhodococcus* spp., and *Tsukamurella* spp., are characterized by a lipid rich cell wall with an outer layer of mycolic acids. They are termed also as corynomycolic acids in *Corynebacterium.* This mycolic acid layer is dominated by long-chain α-alkyl-β-hydroxy fatty acids, which are covalently linked to arabinogalactan, and trehalose monomycolate (TMM) and trehalose dimycolate (TDM) (Schick et al., 2017). Mycolic acids and trehalosyl mycolates are the second permeability barrier equivalent to the outer membrane of Gram-negative bacteria, where the functionality is strongly depending on the mycolic acid content of this barrier (Gebhardt et al., 2007). In *Mycobacterium tuberculosis*, TDM is known as the mycobacterial cord factor and is the most abundant cell wall lipid of pathogenic mycobacteria. TDM plays an important role in inducing inflammatory response, granuloma formation and adjuvant activity for T-cell responses in mycobacteria (Geisel et al., 2005; Hunter et al., 2006). It was also shown that trehalose monocorynomycolates (TMCM) and trehalose dicorynomycolates (TDCM) from corynebacteria activate human and mouse inducible C-type lectin Mincle as effectively as the cord factor (van der Peet et al., 2015).

Pili and fimbriae are proteinaceous protuberances that play an important role in the attachment of bacteria to abiotic and biotic surfaces. The genome of *C. diphtheriae* NCTC 13129 encodes three distinct adhesive pili, i.e., SpaA (SpaABC), SpaD (SpaDEF) and SpaH (SpaGHI). Interestingly, mutant strains lacking proper pilus structures have demonstrated lower adhesion rate to epithelial cells, although the adhesion property was not completely lost (Mandlik et al., 2007). It was also shown that only the SpaA-type pili contribute to corynebacterial adherence to human pharyngeal cells (Detroit 562), whereas SpaD and SpaH-type pili support adhesion to laryngeal (HEp-2) and lung cells (A549) (Mandlik et al., 2007). Moreover, atomic force microscopy revealed that the pili formation in *C. diphtheriae* is highly variable and strains that lack visible pili also showed adhesion to epithelial cells (Ott et al., 2010b). The identification of a fourth type of pili and the differential distribution indicate a high degree of genetic variability of the pili structures and locations on genomic islands which hint to a frequent horizontal gene transfer (Trost et al., 2012). However, adhesive pili are not only

identified in pathogenic corynebacteria, but also found in non-pathogenic species such as *C. glutamicum*, *C. efficiens*, *C. casei* and *C. vitaeruminis.* Hence, they are not considered as virulence factors *sensu stricto* (Wassenaar and Gaastra, 2001; Tauch and Burkovski, 2015).

The virulence factors responsible for the adhesion of pathogenic corynebacteria are partially characterized and the molecular basis of the invasion is still unclear. DIP1281 is a member of the NIpC/P60 family, which is a large superfamily of several diverse groups of proteins (Anantharaman and Aravind, 2003). They are highly conserved among pathogenic and non-pathogenic corynebacteria and can be found in bacteriophages, viruses, prokaryotes and eukaryotes. DIP1281 mutant completely lacked the ability to adhere and invade into host cells (Ott et al., 2010a). Proteome analysis and atomic force microscopy revealed that DIP1281 is a pleotropic effector of the outer surface of *C. diphtheriae* rather than a specific virulence factor. Nevertheless, the results obtained with the mutant suggested that the corynebacterial cell envelope components are important determinants of host-pathogen interaction (Ott et al., 2010a).

Sialidases are enzymes also known as neuraminidases. They are glycosyl hydrolases that catalyze the removal of terminal sialic acid residues from a variety of glycoconjugates of the host surface (Vimr, 1994). In *C. diphtheriae,* sialic acids are expressed on the outer surface and are associated with the bacterial adherence ability to biotic or abiotic surfaces (Mattos-Guaraldi et al., 1999) and assist in the invasion and spread of the organisms within various hosts (Müller, 1974; Miyagi and Yamaguchi, 2012). Sialidases are capable in modifying the ability of the host to respond to an infection by scavenging sialic acids from host cells and decorating its surface. By doing so, pathogenic bacteria elude the host immune mechanisms and play an important role in the interaction with the host cell contributing to virulence property (Vimr and Lichtensteiger, 2002). Sialidase activity was first identified in a crude preparation of a diphtheria toxin (Blumberg and Warren, 1961). In *C. diphtheriae*, the production of sialidases and the composition of cell surface carbohydrates seem to be directly depending on the iron concentration in the medium (Warren and Spearing, 1963; Moreira et al., 2003; Kim et al., 2010). Although a putative exosialidase (DIP0543) designated as NanH was identified in *C.*

diphtheriae NCTC 13129 strain (Kim et al., 2014), it is still to be clarified whether or not NanH is involved in the sialic acid decoration (Burkovski, 2014; Kim et al., 2014). Sialidases are present in a diverse group of organisms including vertebrates, viruses and microorganisms, while absent in plants (Roggentin et al., 1993). It also represents a potential virulence factor in *C. ulcerans*. More than 70 known microorganisms with sialidase activity have close contact to mammals, either as commensals or pathogens (Roggentin et al., 1993; Varki, 1993). *C. ulcerans* when introduced into the skin of guinea pigs or rabbits, induced the production of high levels of sialidases and rapidly developed purulent lesions (Arden et al., 1972). Furthermore, it has been shown that sialidases exerted a direct toxic effect on host tissues or interfered with host immunologic and other defense mechanisms (Corfield, 1992).

Another putative virulence factor of *C. ulcerans* is the corynebacterial protease 40 (Cpp), encoded by the *cpp* gene. The corresponding enzyme is known to have a proteolytic activity in *C. pseudotuberculosis* (Wilson et al., 1995). An amino acid sequence alignment of *cpp* from *C. pseudotuberculosis* and *C. ulcerans* with the α-domain of the secreted endoglycosidase EndoE from the human pathogen *Enterococcus faecalis* revealed that all three proteins shared a conserved motif FGH18 (Collin and Fischetti, 2004; Trost et al., 2011), which is a common catalytic motif with endo-β-*N*-acetylglucosaminidase activity (Terwisscha van Scheltinga et al., 1996). Interestingly, an involvement of the protein in the modification of host glycoproteins was suggested (Trost et al., 2011). Moreover, the human isolate *C. ulcerans* KL387 harboring a prophage which encodes the virulence factor RhuM, shares homology with *Salmonella enterica* at a molecular level (Meinel et al., 2014). Although the function of RhuM has not been characterized in detail (Trost et al., 2011; Meinel et al., 2014), noteworthy, a *rhuM* mutant from *S. enterica* exhibited a significant decrease in epithelial cell invasion (Tenor et al., 2004).

Taken together, not only the definition of microbial components acting on host cells as virulence factors need to be ascertained, but also the context of the bacterium-host interaction and host cell damage need to be perceived (Wassenaar and Gaastra, 2001; Hill, 2012; Casadevall and Pirofski, 2015). One attempt in this respect is the introduction of the concept

of ‘niche factors’ (Hill, 2012). So far, many components identified as important for the interaction of *Corynebacterium* with host cells were also seemed to be present in non-pathogenic corynebacteria (Tauch and Burkovski, 2015). Many *Corynebacterium* species developed into ‘pathogens-by-chance’ by acquiring the high capacity for gene uptake by horizontal gene transfer, while others became the real threat for humans due to the uptake of different toxin genes. Therefore, a reconsideration of many virulence factors as niche factors seems to be a valid concept which might help to understand the development of pathogens as well as characterizing the composition and associated functional aspects.

5. INVERTEBRATE MODEL ORGANISMS FOR HOST-PATHOGEN INTERACTION STUDIES OF CORYNE-BACTERIA

Model organisms serve as ideal systems to study the molecular basis of the pathogenicity of infectious agents and the corresponding mechanisms of the host defense (Kurz and Ewbank, 2000). Intuitively, the more closely related a model of an infectious disease is to the natural pathology, the greater its relevance, therefore the higher reliance on rodent and mammalian tissue culture studies. Although certain pathogens such as *Listeria* and *Salmonella* species restrict the range of possible model hosts, other pathogens exhibit virulence in a diverse array of hosts. *C. diphtheriae* has not only been isolated from humans but also from cats, cows and horses, while *C. ulcerans* colonizes a wide variety of mammals (Mattos-Guaraldi et al., 2014). Recent studies indicated that hosts might not be restricted to mammals, since *C. diphtheriae*, *C. ulcerans* and *C. glutamicum* can colonize the nematode, *C. elegans* and induce morphological changes (Antunes et al., 2016), which were typically observed in nematode pathogens like *Leucobacter* isolates (Clark and Hodgkin, 2015) and *Microbacterium nematophilum* (Hodgkin et al., 2000). The greater wax moth *Galleria mellonella* has also been successfully used to characterize bacterial virulence in a range of strains including *Pseudomonas aeruginosa*, Burkholderia (Jander et al., 2000), *Listeria monocytogenes* (Mukherjee et al., 2010)*, Staphylococcus aureus* (Desbois and Coote, 2011) as well as *C. diphtheriae* and *C. ulcerans* (Ott et al., 2012; Weerasekera et al., 2018). Amid ever-growing concerns for the welfare of animals in scientific research, there is a heightened need to find organisms that could be studied ethically and on a large-scale. Therefore, from a microbiological standpoint, the discovery of simple surrogate model organisms that are susceptible to human pathogens such as *C. elegans* and *G. mellonella* has been a remarkable advance in this field to gain insights into host-pathogen interface.

5.1. *Caenorhabditis elegans* as a model organism for pathogenic corynebacteria

C. elegans is a free-living, globally distributed nematode that feeds on bacteria. It was used as a model host for a wide variety of microorganisms that have implications on human health. *C. elegans* can be found predominantly in soil and human-associated habitats including compost heaps and rotting fruits (Andersen et al., 2012). It has developed into one of the attractive model systems in biology based on several advantageous properties such as ease of maintenance, short life span, transparency and genetic tractability. The standard *C. elegans* laboratory strain N2 was introduced in the early 1970s by Sydney Brenner as a model for neural development due to its genetic convenience, small size and simplicity (Brenner, 1974). Later, it was developed as a model system for host-pathogen interactions to study microbial virulence factors and innate immunity (Clark and Hodgkin, 2014).

C. elegans exclusively rely on their innate immune system to defend themselves against pathogens. The response of *C. elegans* to various fungal and bacterial infections revealed that their immune system employs an evolutionary conserved signaling pathway (Engelmann and Pujol, 2010). *C. elegans* possesses three major mechanisms of defenses against microbial attacks which comprise its avoidance behavior, anatomy composition and inducible defense mechanisms (Engelmann and Pujol, 2010). They can remember odors and even learn to avoid certain bacteria, particularly the pathogenic bacteria that are recognized as noxious (Zhang et al., 2005; Antunes et al., 2016). The anatomical composition of *C. elegans* which includes the olfactory neurons, G protein coupled receptors and TOL-1 (the only Toll-like receptor in *C. elegans*) seem to be involved in triggering the avoidance (Pujol et al., 2001; Pradel et al., 2007). Partly, this discrimination relies on asymmetric chemosensory neurons (Wes and Bargmann, 2001). Secondly, they harbor a strong physical barrier cuticle composed of collagen and chitin which constitute the exoskeleton of the worm. Additionally, they harbor a pharyngeal grinder which would destroy the pathogens and prevents them from reaching the intestine. Thirdly, the inducible defense system of *C. elegans* involves in multiple

signaling cascades that regulate the production of antimicrobial peptides and proteins (Engelmann and Pujol, 2010). Considering the given importance on the tractability of bacteria and the availability of range of mutant nematodes to investigate the host response (Ott et al., 2012), *C. elegans* might serve as the best model system for pathogenic corynebacteria.

Ott and co-workers provided a proof for application of the nematode as an infection model for pathogenic corynebacteria. In their study, they have developed *C. elegans* as a suitable model for pathogenic *C. diphtheriae*, *C. ulcerans* and *C. pseudotuberculosis*, while comparing the exerted virulence with the non-pathogenic *C. glutamicum* (Ott et al., 2012). When the nematodes were infected with *C. diphtheriae* strain ISS3319, a faster death of the worms were observed in comparison to the *C. diphtheriae* strain DSM43988. Strain ISS3319 colonized both the foregut (buccal cavity and pharynx) and the midgut of the nematodes while strain DSM43988 colonized only the midgut. Conversely, infecting worms with the non-pathogenic *C. glutamicum* ATCC 13032 or *E. coli* OP50 resulted in clearance of the bacteria, indicating that these bacteria were unable to colonize the worms (Ott et al., 2012). These results suggested that pathogenic corynebacteria were able to colonize the worms in a strain-specific manner (Ott et al., 2012). Interestingly, while diphtheria toxin-carrying *C. diphtheriae* DSM43989 and the diphtheria toxin-negative *C. ulcerans* 809 colonized only the hindgut of the worms, colonization of the bacteria all over the worm body was observed when infected with *C. ulcerans* BR-AD22 and *C. pseudotuberculosis* FRC41. The localization and killing kinetics exerted by pathogenic corynebacteria in this study reflected the different virulence properties and mechanisms used by those strains. The colonization in the foregut of the nematodes reflected the natural niche of these organisms in their mammalian hosts in contrast to the dispersed colonization in the gut observed in *Pseudomonas* or *Serratia* (Mahajan-Miklos et al., 2000; Kurz et al., 2003).

In another study, *C. elegans* were utilized to address the role of pili in corynebacterial pathogenesis. The toxigenic *C. diphtheriae* strain NCTC 13129 harbors three distinct pili structures SpaA, SpaD and SpaH, which makes up the shaft structure and are known to mediate bacterial adherence to epithelial cells. It has been observed that in contrast to NCTC

13129, its isogenic mutants lacking SpaA pili or devoid of toxin and SpaA type pili exhibited delayed killing of the nematodes. Furthermore, it was also observed that toxigenic or non-toxigenic strains that lack either one, two or all three pilus types were also attenuated in virulence. Therefore, this study emphasized the significance and the utilization of *C. elegans* as a simple host model to identify additional virulence factors in corynebacteria (Broadway et al., 2013).

A study by Antunes et al. demonstrated that the *dip0733* disrupted mutant CAM-1 attenuated in its ability to colonize and kill *C. elegans* in comparison to the wild-type strain *C. diphtheriae* CDC-E8392. (Antunes et al., 2015). Moreover, this defect could be complemented when the strain CAM-1 was transformed with the plasmid pXMJ19_*dip0733mCherry*, while both the mutant and the wild-type strains showed enhanced nematode toxicity when carrying the DIP0733 expression vector (Antunes et al., 2015). Further studies by Weerasekera et al. indicated that the coiled-coil domain of DIP0733 is responsible for the pathogenicity of *C. elegans* (Weerasekera et al., 2018). The fusion of the coiled-coil sequence to the DIP0733 homolog from the non-pathogenic *C. glutamicum* resulted in increased pathogenicity, while bacteria expressing the truncated form of DIP0733 were less virulent (Weerasekera et al., 2018).

In a recent study, overexpression of the Rbp (Rbp shares an amino acid sequence similarity to Shiga-like toxins in *E. coli*) in *C. ulcerans* 809 (*CULC809_00177*) and *C. diphtheriae* HC04 (*CDHC04_0155*) showed detrimental effects in *C. elegans*. In contrast, the mutant constructed by disruption of the *rbp* designated as DW-1, led to a significant prolongation of the survival of the nematodes (Weerasekera et al., 2019b). Interestingly, the non-toxigenic *C. diphtheriae* strain BR-INCA5015 tested in a *C. elegans* survival assay showed strong colonization and killing by this strain (Peixoto et al., 2016). Additionally, a mutant constructed for the tellurite-resistant gene (Te^R) in *C. diphtheriae* (*CDCE8392_0813*) showed an attenuation in killing of the nematodes when compared to the wild-type *C. diphtheriae* CDC-E8392 (dos Santos et al., 2010). Similarly, a study indicated that the mutation

of Te^R of *Bacillus anthracis* (*yceGH*) reduced the survival of *C. elegans* and increased the susceptibility to TeO_3^{2-} compounds (Franks et al., 2014).

Although *C. elegans* is a predator of bacteria, it is susceptible to infections by nematopathogenic coryneform bacteria which are known as natural pathogens of *C. elegans*. These bacteria include *Microbacterium* and *Leucobacter* species, which display intriguing and diverse modes of pathogenicity. In fact, *M. nematophilum* was isolated from a fortuitously contaminated culture of the nematode (Hodgkin et al., 2000). The unusual infection caused by *M. nematophilum* resulted in a distinctive Dar phenotype in the nematode, that was characterized by a deformed anal region indicated by a swollen tail. Although the infection was non-lethal, the localized swelling led to constipation and slowed growth in the infected worms (Hodgkin et al., 2000; Akimkina et al., 2006). Conversely, certain mutant worms isolated from screens of a bacterially unswollen (*bus*) phenotype were resistant to the infection and exhibited little or no rectal infection when challenged with bacteria. These worms have probably altered the surface properties so that the bacteria can no longer infect the worms (Gravato-Nobre et al., 2005). In the presence of *M. nematophilum*, most of the uninfectable mutants except for *sur*-2 mutant which was hypersensitive, were able to grow better than the wild type. This observation suggests that the Dar formation by *C. elegans* is indicated as associated with a survival strategy against the bacteria (Gravato-Nobre et al., 2005; Yook and Hodgkin, 2007).

A study demonstrated the formation of Dars due to infection with *Leucobacter* strains. One *C. elegans* isolate collected from Japan exhibited visibly adherent bacteria, swollen tail and poor growth and was identified to be infected by *Leucobacter.* Another Dar isolate with swollen tail and a dense covering of adherent bacteria over the surface of the body was obtained from rotting banana trunks in Cape Verde. These *Leucobacter* species were referred to as Verde1 and Verde2 were highly virulent and lethal to the nematodes (Hodgkin et al., 2013). When examined microscopically, infected worms had a dense covering of adherent bacteria, however, no Dar phenotype was observed. Interestingly, within 2 minutes after the exposure of worms to Verde1 in liquid culture, worms started to swim and began to stick to

each other in their tail regions forming star-like aggregates which were termed as ‘worm-stars’ (Hodgkin et al., 2013). In contrast, Verde2 infection resulted in Dar phenotype as well as distorted internal organs and vacuole formation within the worms (Hodgkin et al., 2013).

Furthermore, these phenotypes were studied in the genus *Corynebacterium*. Remarkably, not only *C. diphtheriae*, *C. ulcerans* and *C. glutamicum* were able to induce worm-stars in liquid culture but also, they were able to induce severe rectal swelling, the so-called Dar formation in *C. elegans* (Figure 6) (Antunes et al., 2016) previously described only for *M. nematophilum* and *Leucobacter* species (Hodgkin et al., 2000; Hodgkin et al., 2013).

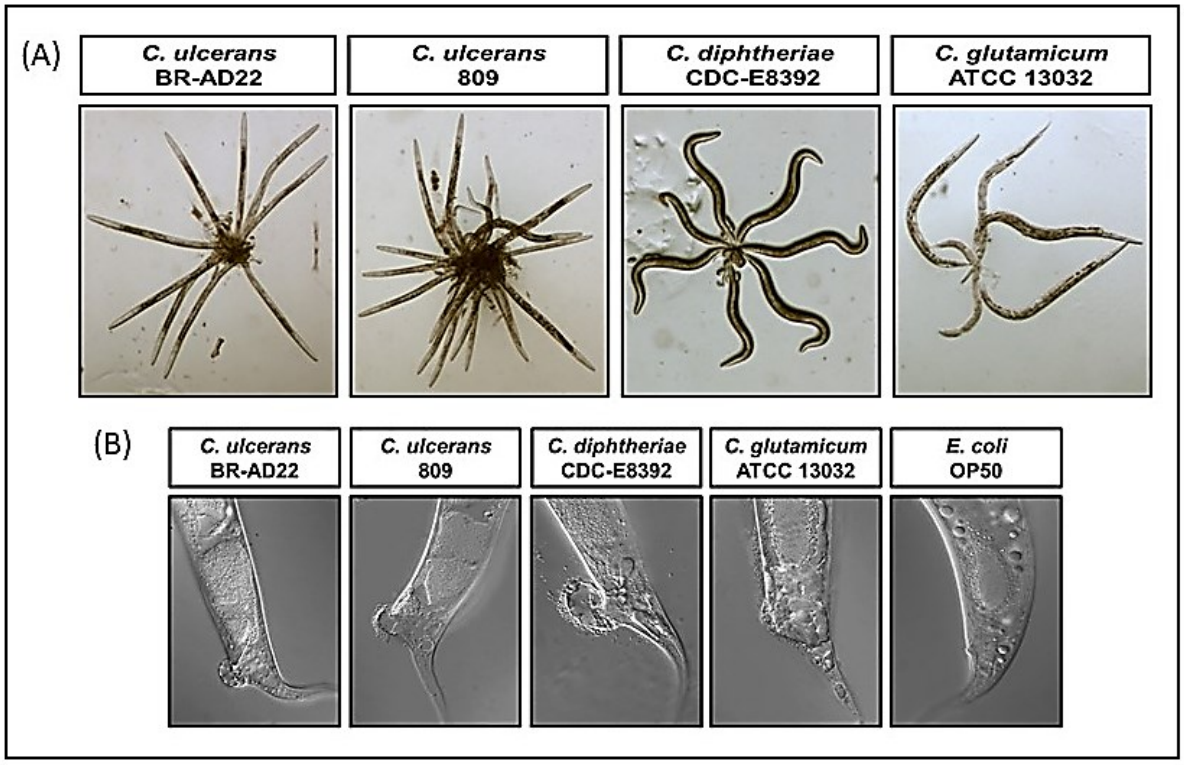

Figure 6. Induction of "worm star" (A) and “Dar” (B) formation by species of the genus *Corynebacterium*. Worm stars were observed after incubation for 2-4 days in liquid medium and Dar formation in the solid medium in the presence of *C. ulcerans* BR-AD22, *C. ulcerans* 809, *C. diphtheriae* CDC-E8392 and *C. glutamicum* ATCC 13032. *E. coli* OP50 was used as control. (Modified from Antunes et al., 2016).

Studies have shown that different strains of *C. ulcerans* irrespective of the presence or the absence of *pld* gene, were capable of inducing Dar phenotype, worm-star aggregates and internal egg hatching known as ‘bagging’ phenotype (Simpson-Lourêdo et al., 2019). As in the case of worm-star formation, all *Corynebacterium* strains tested induced Dars and

interestingly, significant species-specific differences were observed in respect to the Dar formation depending on the culture medium (Figure 6). The Dar formation in liquid medium was more pronounced in *C. ulcerans* when compared to *C. glutamicum* and *C. diphtheriae*. Moreover, Dar formation was observed to be more abundant on solid media, indicating that the pathogenicity of strains differs depending on the culture conditions (Antunes et al., 2016).

Additionally, it was demonstrated that *C. elegans* were able to avoid pathogenic corynebacteria and choose the non-pathogenic *C. glutamicum* as the preferred food source. Moreover, worms that were previously in contact with pathogenic corynebacteria known as 'trained worms' avoided those pathogens in contrast to the untrained worms indicating a learning behavior of *C. elegans* that is beneficial in avoiding tainted, detrimental food sources (Antunes et al., 2016).

In future studies, it is important to address the question of which host factors and host signaling pathways are involved in the infection process of corynebacteria by employing mutant worms which would help to unravel the ecologically relevant processes in the nematodes' natural habitat.

5.2. *Galleria mellonella* as a model organism

The larvae of *Galleria mellonella*, (also known as the greater wax moth or honeycomb moth larvae) is widely being used as an infection model to study virulence factors and pathogenesis of many bacterial and fungal human pathogens (Cook and McArthur, 2013). Many of the attractive features highlight the importance of *G. mellonella* as a model for investigating bacterial pathogens. They have a short life cycle of 6-8 weeks, easy to obtain in large numbers, inexpensive, simple to use, easy to maintain in laboratory conditions, do not require ethical approval to use and unlike many alternative models, *G. mellonella* can be maintained at 37 °C (Champion et al., 2016). Therefore, they are ideal for large-scale studies. Additionally, their size simplifies host-pathogen studies as it requires only one hind pro leg and a syringe to apply the precise dose of desired bacteria (Pereira et al., 2018), which would allow

the relative virulence of strains and mutants to be compared (Champion et al., 2016). Recently, *G. mellonella* genome has been sequenced (Lange et al., 2018) and have access to transcriptome and microRNA data (Vogel et al., 2011; Mukherjee and Vilcinskas, 2014).

5.2.1. Melanization and immune response of *G. mellonella*

Melanin formation is catalyzed by phenoloxidase which is produced as the inactive zymogen pro-phenoloxidase in hemocytes. Conversion of pro-phenoloxidase to active enzyme can be brought about by lipopolysaccharides, peptidoglycans and β-1,3 glucans from microorganisms (Söderhäll and Cerenius, 1998). Pro-phenoloxidase is an important innate immunity protein in insects due to its involvement in cellular and humoral defense. The pathway of pro-phenoloxidase incorporates several proteins including pattern recognition receptors (PRRs), serine proteases and serine protease inhibitors. Melanization is initiated after the engagement of soluble PRRs with target surfaces such as lipopolysaccharides (Altincicek et al., 2007), lipoteichoic acids (Halwani et al., 2000) or thermolysin (Altincicek et al., 2007). Activated phenoloxidase oxidizes phenolic molecules to produce melanin around invading pathogens and wounds (Lu et al., 2014). Phenoloxidation is highly controlled by protease inhibitors and it produces cell damaging reactive oxygen species (Söderhäll and Cerenius, 1998). It has been reported that antimicrobial peptides such as lysozyme, *Galleria* defensin, proline-rich peptide 1, and anionic peptide 2 decreased the hemolymph phenoloxidase activity suggesting a role of these antimicrobial peptides in immune modulation (Zdybicka-Barabas et al., 2014; Tsai et al., 2016).

The immune response of *G. mellonella* exhibits remarkable structural and functional similarities to the innate immune response of mammals (Browne et al., 2013; Tsai et al., 2016). Hemolymph in *G. mellonella* is equivalent to mammalian blood, and contains immune cells called hemocytes which act similar to mammalian neutrophils by phagocytosing pathogens and killing them by producing superoxides (Bergin et al., 2005). Among the six types of hemocytes, pre-dominant are the plasmatocytes and granular cells which are of great importance in cellular defense against invasive pathogens (Tojo et al., 2000). During

phagocytosis, enzymes are released, and the pathogen is destroyed by degranulation (Baggiolini and Wymann, 1990). Although phagocytosis in *G. mellonella* is mediated by plasmocytes, granular cells also contribute indirectly to this process. Hemocytes in *G. mellonella* recognize pathogens through calreticulin or apolipophorin receptors. In mammals, calreticulin is known to be important for adhesion into cells, phagocytosis, antigen presentation and in the process of inflammation. Apolipophorin III is associated with innate immunity which binds to Gram positive bacteria and lipoteichoic acid which promotes phagocytosis (Halwani et al., 2000; Browne et al., 2013).

In addition to phagocytosis, hemocytes exhibit cellular events such as nodulation and encapsulation. Nodulation allows large number of pathogens to be eliminated from hemolymph by activation of prophenoloxidase followed by melanization (Lavine and Strand, 2002). Certain large foreign bodies such as nematodes, protozoa and parasitic eggs are killed by encapsulation (Grizanova et al., 2018). However, encapsulation and nodulation can occur when phagocytosis fails to eliminate pathogens and the type of response is usually determined by pathogen characteristics and concentration (Grizanova et al., 2018; Pereira et al., 2018).

5.2.2. *Galleria mellonella* as a model host to study fungal pathogens, viruses and bacteria

G. mellonella was first described as a model for studying virulence in the human yeast *Candida albicans*, to distinguish between pathogenic and non-pathogenic strains (Cotter et al., 2000). Since then, *G. mellonella* have been used as a model for virulence of other fungi (Cotter et al., 2000; Fallon et al., 2011). Mutants of *Aspergillus fumigatus* tested in *G. mellonella* correlated closely with mice as well as data from infected human (Slater et al., 2011). This indicates that *G. mellonella* is a suitable host to assess virulence determinants by screening attenuation of mutants. Furthermore, the larvae have been used to study tissue invasion capabilities between biofilm producing and non-producing strains (Borghi et al.,

2014), role of filamentation in virulence (Fuchs et al., 2010) and as a model to screen the efficacy of antifungal compounds (Kelly and Kavanagh, 2011).

G. mellonella have been used to investigate viral disease as well. In some cases, the larvae have been challenged with viruses and in others, haemocytes of larvae have been infected (Champion et al., 2016). However, it was suggested that *Galleria* is not so far been proven to be suitable for research into viral pathogens of mammals. One reason for this could be that the insect cells incubated at 25-30 °C may not support the growth of mammalian viruses. In addition, tropism of viral receptors may not be shared by insect cell lines (Champion et al., 2016).

G. mellonella have been studied using a wide range of Gram-positive and Gram-negative bacterial genera including *Streptococcus* (Olsen et al., 2011; Evans and Rozen, 2012; Loh et al., 2013), *Enterococcus* (Lebreton et al., 2011; La Rosa et al., 2013), *Staphylococcus* (Desbois and Coote, 2011), *Listeria monocytogenes* (Joyce and Gahan, 2010), *Pseudomonas* (Andrejko and Mizerska-Dudka, 2012), *Francisella* (Aperis et al., 2007; Thelaus et al., 2018) and *E. coli* (Ciesielczuk et al., 2015). A study reported that *Streptococcus pyogenes* SF370 killed the larvae in a dose-dependent manner by more rapidly progressing the melanin accumulation and hemolymph coagulation in larvae. More importantly, the survival in *G. mellonella* strongly correlated with the survival in mice (Loh et al., 2013). The *Galleria* model system was further improved by introducing a health index that enabled the measurement of more subtle differences including cocoon formation and melanization (Loh et al., 2013). In another study, differences in virulence between the serotypes of *Streptococcus pneumoniae* were assessed using *G. mellonella* larvae by correlating the presence or absence of known virulence factors (Evans and Rozen, 2012). Larvae infected with *E. faecalis* resulted in intense melanization within 5 min followed by death in 30 min. Moreover, when injected into the hemolymph of *G. mellonella*, the putative virulence factor extracellular gelatinase (GelE) of *E. faecalis* destroyed the defense system of the larvae. As a result, the antimicrobial peptide, *G. mellonella* cecropin (Gm cecropin) was degraded which is known to perform a critical role in host defense during microbial infections (Park et al., 2007).

G. mellonella has been successfully used to illustrate inter-strain variation in bacterial virulence in respect to infection with *Pseudomonas aeruginosa* (Jander et al., 2000) and *Burkholderia pseudomallei* (Wand et al., 2011). The larvae showed high sensitivity resulting in melanization in response to infection, and when injected into the hemolymph, a 50 % lethal dose of < 10 bacteria were reported (Jander et al., 2000; Wand et al., 2011). In another study, it was shown that *G. mellonella* larvae infected with *S. aureus* were killed both in a dose- and temperature-dependent manner. Moreover, the killing was more efficient with increasing temperatures when tested at 25 °C, 30 °C and 37 °C (Desbois and Coote, 2011).

The Sec pathway in *S. aureus* plays a prominent role in the secretion of major bacterial virulence determinants. Interestingly, it was shown that the SecDF deletion mutant of *S. aureus* significantly reduced virulence in *G. mellonella* (Quiblier et al., 2013). Furthermore, a study by Mukherjee et al. demonstrated the suitability of *G. mellonella* to distinguish between pathogenic and non-pathogenic *Listeria* species. Deletion mutants with deficiencies in phospholipase B and listeriolysin showed increased survival rates of *G. mellonella* larvae. The virulence of the mutant strains correlated well with previous results obtained from mouse models (Mukherjee et al., 2010).

Thus, it is clear that the susceptibility of *G. mellonella* to bacterial and fungal infections, the correlation of its virulence to mouse model systems and the ability to initiate a defense response making them not only an excellent infection model but also provide more insights on mammalian infection processes.

5.2.3. Application of *G. mellonella* as a model system to study virulence in corynebacteria

C. elegans serve as a model system for pathogenic corynebacteria to investigate host response, given the tractability of bacteria and the availability of a range of mutant nematodes (Ott et al., 2012). However, insects offer a complex cell-based immune system compared to the simple innate immune system of nematodes. When different corynebacterial strains were

tested, distinct differences in response of the larvae were detected (Ott et al., 2012). The non-pathogenic *C. glutamicum* led to the development of small black spots, although the larvae remained active and beige in color. Injection of non-toxigenic *C. diphtheriae* DSM43988 led to brown larvae and the toxigenic *C. diphtheriae* DSM43989 caused strong melanization resulting in immobility of the larvae. The strongest effects in larvae including melanization, immobility and rapid death were observed in response to the infection with *C. ulcerans* and *C. pseudotuberculosis* (Ott et al., 2012). These results indicated that *G. mellonella* are more susceptible to the infection with *C. ulcerans* and *C. pseudotuberculosis* reflecting their broader host range compared to *C. diphtheriae*, which is an effect also observed in the wide host range pathogen *P. aeruginosa* (Jander et al., 2000).

To further test the proof of principle, *C. diphtheriae* wild type ISS3319 and its corresponding transposon mutant Tn5-*46* as well as phospholipase D-deficient *C. ulcerans* mutant ELHA1 with its parental wild type strain *C. ulcerans* BR-AD22 were tested in *G. mellonella*. Although, Tn5-*46* showed a decreased adhesion rate in Detroit 562 cells compared to its wild type ISS3319, no difference was observed upon injection in *G. mellonella.* In contrast, although the adhesion rates of the wild type and the mutant were identical, the phospholipase D-deficient ELHA1 showed less severe virulence in *G. mellonella* compared to its wild type BR-AD22 (Ott et al., 2012).

G. mellonella was used as a simple model host to study various virulence factors of corynebacteria including one of the best characterized DIP0733 transmembrane protein. Remarkably, a study by Weerasekera et al. demonstrated a key role of DIP0733 and its C-terminal coiled-coil domain in the melanization process induced by infection with *C. diphtheriae* (Weerasekera et al., 2018). While the melanization of the larvae became more pronounced in response to injection with the toxigenic *C. diphtheriae* CDC-E8392, injection of the corresponding *dip0733* disrupted mutant CAM-1 showed less severe effects. Moreover, while the larvae infected with the coiled coil lacking truncated forms of *C. diphtheriae* DIP0733 and *C. glutamicum* DIP0733 were less virulent to *G. mellonella*, the coiled-coil sequence carrying *C. glutamicum* DIP0733 homolog increased the pathogenicity as indicated by less

active brown larvae. The health index score measurements of the subtle differences of the larvae in response to infection verified these observations (Weerasekera et al., 2018).

Furthermore, the effects of corynebacterial *rbp* genes were studied in *G. mellonella* model system (Weerasekera et al., 2019b). Preparations of bacteria have been applied in numerous studies to test their toxicity to *G. mellonella*. In many cases, the studied toxins were insecticidal and therefore *G. mellonella* larvae served as an attractive model to further investigate the toxicity (Brown et al., 2004; Champion et al., 2016). *Pseudomonas fluorescens* insecticidal toxin (Fit) produced by some *P. fluorescence* strains was lethal to *G. mellonella*, while the deletion mutant of the *fit* gene significantly attenuated in its virulence to the larvae (Péchy-Tarr et al., 2008). Furthermore, the bacterium *Xenorhabdus nematophila* was shown to kill *G. mellonella* when injected at doses of around 30–40 ng/g larvae. Studies have shown the importance of *G. mellonella* as a model host in understanding *Shigella* pathogenesis. *Shigella* sp. injected through forelegs caused death of the larvae whereas plasmid-cured mutants were rapidly cleared (Barnoy et al., 2017). As corynebacterial Rbps share striking structural homology with SLT from *E. coli* Stx-1A, *G. mellonella* were applied to study the effect of Rbps from *C. ulcerans* 809 and *C. diphtheriae* HC04 (Weerasekera et al., 2019b). While injection of buffer or the non-pathogenic *C. glutamicum* did not impair the larvae, the overexpression of Rbps in *C. ulcerans* 809 and *C. diphtheriae* HC04 led to strong melanization and death of the larvae within 5 days of infection. The *rbp* disrupted mutant DW-1 evoked less detrimental effects compared to its corresponding wild type strain HC04. The quantitative analysis of these results indicated that the presence of the two corynebacterial *rbp* genes is involved in the virulence exerted in *G. mellonella* (Weerasekera et al., 2019b).

Therefore, based on previous studies and current observations, *G. mellonella* can be acknowledged as a useful model system in corynebacteria to detect differences in response to the presence or absence of toxins and other virulence factors.

6. RECOGNITION, ENGULFMENT AND CLEARANCE OF CORYNEBACTERIA BY MACROPHAGES

For bacterial pathogens, infection consists of a series of steps. After entering the body, the bacteria will undergo cycles of replication, phagocytosis, reinfection of new phagocytes and ultimately exit from the host, thereby allowing a new cycle to begin. For the bacteria to survive and scavenge nutrients required for their viability and replication, the extracellular and intracellular environment of the macrophages require adaptations. Macrophages can be heterogenous with regard to their ability to kill facultative intracellular bacteria. Although macrophages are able to kill most of the bacteria quickly, some may bind, bind and internalize, yet not be able to kill it. The receptors on the macrophage that recognize and internalize a bacterium may influence the intracellular fate of this organism (Hilbi et al., 1997). Eukaryotic cells may undergo programmed cell death as an ultimate response to an infection with a pathogen. Therefore, modulation of apoptosis is often a prerequisite to establish a host-pathogen relationship. Some pathogens kill macrophages by inducing apoptosis and thus overcome the microbicidal weapons of the phagocyte. Apoptotic macrophages, on the other hand, elicit an inflammation by secretion of proinflammatory cytokines (Hilbi et al., 1997).

It is suggested that the uptake of corynebacteria by non-phagocytic cells and their migration across epithelial cell barriers might be important in the early stages of respiratory and systemic infections (dos Santos et al., 2010). It is widely studied that macrophages are important in both innate and acquired immunity and play a key role in the defense against viruses, bacteria and fungi. However, several factors such as recent and chronic infection, environmental exposures, cytokines, drug therapy and gene transfer can modulate macrophage function (Gordon and Read, 2002). Therefore, mechanisms that involve corynebacteria to reach deeper tissues need further investigation.

6.1. Phagocytosis

Phagocytosis is a process by which cells ingest particles larger than 0.5 μm including microbes into membrane-bound vesicles called phagosomes, then these particles undergo enzymatic degradation by lysosomes (Underhill and Goodridge, 2012). More than a century ago, Elie Metchnikoff first described the occurrence of internalization of the particles via an action-based mechanism (Merien, 2016). Since then it has been extensively studied in both unicellular and multicellular organisms (Titus, 1999). Phagocytosis is a dynamic process that requires the reorganization of the actin cytoskeleton and the involvement of actin binding proteins and signaling molecules (Aderem and Underhill, 1999). Although many cells are capable of phagocytosis (non-professional phagocytes), macrophages, neutrophils and the immature dendritic cells in the immune system, known as 'professional phagocytes' truly excel in this process (Silva and Correia-Neves, 2012). The engulfed microorganisms get either contained, killed or processed by professional phagocytes for antigen presentation and plays an essential role in the innate immune response to pathogens as well as the subsequent initiation of adaptive immunity.

PRRs expressed on the phagocyte membrane detects molecules typical for pathogens and play a crucial role in the proper function of the innate immune system which plays a key role in first-line defense until more specific adaptive immunity is developed (Jang et al., 2015). PRRs differ in their activated host response and signaling cascade as well as their distribution in the tissue. These include Toll-like receptors (TLRs), C-type lectin receptors (CLRs), nucleotide-binding oligomerization domain-like receptors (NLRs), retinoic acid-inducible gene-I-like receptors (RLRs), and AIM2-like receptor (ALR). PRRs recognize mainly two types of molecules i.e., pathogen-associated molecular patterns (PAMPs), present on the surface of pathogens and damage-associated molecular patterns (DAMPs), components released by host cells during cell damage or death. Binding of PAMPs to PRRs causes actin polymerization at the site of ingestion and deformation of the plasma membrane, which triggers phagocytosis. During phagocytosis, first the cell membrane extends around the target,

eventually enveloping it and pinching-off to form a discrete phagosome (Flannagan et al., 2012). The ability to kill pathogens and degrade the ingested particles are acquired during the phagosomal maturation where a drastic sequential process of remodeling of the phagosomal membrane and contents occur (Vieira et al., 2002; Flannagan et al., 2012). After the phagosome becomes matured, the lysosome fuses with the phagosome, acidifies and forms the phagolysosome. At this point, the action of lysosomal hydrolases degrades the contents in the phagolysosome. This degradation can be either oxygen-dependent, which requires NADPH and the production of reactive oxygen species, or oxygen-independent, which depends on the release of granules containing lysozymes, defensins or lactoferrin. Numerous pathogen-associated and endogenous molecules such as lipopolysaccharides and cytokines also influence phagocytosis.

Although one of the primary functions of professional phagocytosis is to effectively engulf pathogens and eliminate them, some pathogens have developed mechanisms to evade degradation within the phagocytes and take advantage of the internalization step by attaching to the host cells to enter and spread infection (Sarantis and Grinstein, 2012). Pathogens accomplish this by either binding to certain host phagocyte receptors that can initiate signaling for internalization or by injecting microbial effectors into the host, that can overtake the host cellular machinery to force pathogen uptake and establish a safe survival niche (Sarantis and Grinstein, 2012).

6.2. Interaction of corynebacteria with macrophages: current knowledge

Bacterial exotoxins including DT are powerful in activating macrophages (Mookerjee et al., 1982). However, studies have shown that the phagocytosis of human macrophages was significantly impaired in response to prolonged incubation with DT (Saelinger et al., 1975; D'Onofrio and Paradisi, 1983) and that human macrophages are more susceptible to DT than mouse phagocytes (Saelinger et al., 1975; Weerasekera et al., 2019a). Beside the mode of

action of DT, studies on the molecular mechanisms of *C. diphtheriae* interaction with host cells and the activation of macrophages especially with non-toxigenic strains is scarce.

Invasive infections caused by some Gram-positive bacteria may be partially related to inappropriate opsonization due to the lack of type-specific antibodies (Schuchat, 1999). In this respect, receptors that recognize microbial surface adhesins mediated by non-opsonic phagocytosis have gained increasing interest as a potential host defense mechanism against extracellular pathogens and as a mode of survival in the host for intracellular pathogens (Ofek et al., 1995). Infectious agents employ heterogenous pathways to enter macrophages and modify vacuolar maturation in order to favor their survival (Aderem and Underhill, 1999). To elucidate molecular mechanisms underlying phagocytosis, differences in cytoskeletal elements that mediate internalization and identification of inflammatory responses are given a prime importance. In order to study *C. diphtheriae* interaction with macrophages, dos Santos and co-workers investigated the ability of phagocytosis by homologous toxigenic (ATCC 27012) and non-toxigenic (ATCC 27010) strains in human U-937 macrophages in the absence of opsonins (dos Santos et al., 2010). Their results indicated that the presence and the expression of the *tox* gene in *C. diphtheriae* may have favored a non-opsonic interaction with U-937 enhancing bacterial adherence and internalization. The investigated *C. diphtheriae* tox^- strain adhered weakly to U-937 cells with only a small proportion of viable bacteria being phagocytosed. This result indicated that *C. diphtheriae* is capable of avoiding non-opsonic phagocytosis by human macrophages. Despite the vigorous immune cell infiltration by macrophages, *C. diphtheriae* remains alive and cause the disease. Although the adherence of the studied tox^- strain was less efficient, the phagocytosed bacteria remained alive for 24 h indicating that tox^- *C. diphtheriae* can remain alive long periods intracellularly as also observed for other Gram-positive bacteria (Cornacchione et al., 1998). Conversely, the investigated tox^+ strain did not replicate or survive inside U-937 cells and was killed 24 h post-infection (dos Santos et al., 2010). Interestingly, *C. diphtheriae* strains exhibited strategies to survive within macrophages and exerted apoptosis and necrosis in human phagocytic cells independent of the *tox* gene (dos Santos et al., 2010).

The internalization process of *C. diphtheriae* is dependent on actin polymerization-coupled phosphotyrosine signaling. The PKC signal transduction pathway is a useful intracellular target to ensure survival of pathogens inside macrophages. Inhibition of the PKC pathway by a tyrosine kinase inhibitor genistein, prevented the survival of *C. diphtheriae tox*$^{+}$ strain within U-937 macrophages. Moreover colchicine, a microtubule disrupting drug completely inhibited intracellular viability of the *tox*$^{+}$ strain (dos Santos et al., 2010). Furthermore, in less than 3 h post-infection, a higher cytotoxicity rate in U-937 cells was observed with the *tox*$^{+}$ strain when compared to *tox*$^{-}$ strain. Therefore, intracellular replication of the bacteria is not a necessity to induce cytopathogenicity, as also observed with other human pathogens (Gao and Kwaik, 1999). Although, both *tox*$^{+}$ and *tox*$^{-}$ exhibited cytotoxicity independent of DT, the cytotoxicity was enhanced by the *tox*$^{+}$ strain (dos Santos et al., 2010). Moreover, the demonstration of survival of *C. diphtheriae* in U-937 cells by dos Santos et al. revealed that in the absence of opsonins, human macrophages are not effective in killing *C. diphtheriae*.

Further investigations by Peixoto and co-workers indicated that the non-toxigenic strains are involved in maintaining invasive infectious processes. Their study revealed that the intracellular survival of the non-toxigenic osteomyelitis-related *C. diphtheriae* strain BR-INCA5015 in human THP-1 and murine RAW 264.7 macrophages was significantly higher compared to non-toxigenic (ATCC 27010) and toxigenic (ATCC 27012) *C. diphtheriae* strains (Peixoto et al., 2016). Moreover, the work by Antunes and co-workers demonstrated that *C. diphtheriae* DIP0733 protein influences survival of *C. diphtheriae* within human THP-1 cells by avoiding and/or delaying host defense mechanisms (Antunes et al., 2015). These studies suggest that the intracellular localization of *C. diphtheriae* in macrophages protects *C. diphtheriae* from microbicidal activities and from antimicrobial agents. In addition, Weerasekera and co-workers demonstrated that the infection of human THP-1 cells with *rbp* overexpression strains from *C. ulcerans* 809 and *C. diphtheriae* HC04 led to a significant reduction in the internalized colony forming units and indicated detrimental effects on human macrophage cells (Weerasekera et al., 2019b).

The properties of adherence and intracellular survival of *C. diphtheriae* within human macrophages might involve in throat colonization, hence contributing to the failure of eradicating the bacteria and perhaps also support asymptomatic carriage. Moreover, adherence and intracellular survival in professional phagocytes may help understand the virulence of *C. diphtheriae* in endovascular infections, independent of toxin production, to establish metastatic foci of infection. Furthermore, it was hypothesized that *C. diphtheriae* may infect heart valves partially through phagocyte-facilitated invasion, also known as the 'Trojan horse' mechanism (Drevets, 1999; dos Santos et al., 2010). This may help to explain the aggressive nature of the disease leading to death of the patients despite antimicrobial therapy in many situations.

Recent studies indicated that human macrophages show a delay of phagolysosome maturation when infected with *C. diphtheriae* (Ott et al., 2017) and *C. ulcerans* (Hacker et al., 2016b), a process resembling the situation of *M. tuberculosis* macrophage infection. Almost all members of CMNR group are characterized by mycolic acid layer which is on one hand linked to arabinogalactan-peptidoglycan meshwork of the cell wall and on the other hand to glycolipids located on the outer leaflet of mycomembrane. TDM is a prominent member of these glycolipids and play a role in the pathogenicity of *M. tuberculosis*, which is a closely related species of corynebacteria. While mycolic acid synthesis and the role of TDM in virulence has been well studied in *M. tuberculosis*, information on corynebacterial mycolates are very limited (Takayama et al., 2005; Lee et al., 2012; Lang, 2013). Therefore, Ott and co-workers investigated the influence of mycolic acids on the interaction of corynebacteria with macrophage-like cell lines (Ott et al., 2017). Their results indicated that mycolic acids are not crucial for the interaction of pathogenic corynebacteria with host cells. Although, all genes previously known for the synthesis of mycolic acids were found intact in the Park-Williams strain *C. diphtheriae* DSM43989, comparative sequence analyses revealed DIP0789 (annotated as enoyl-CoA hydratase) as a pseudogene in DSM43989 with a capacity to partially restore corynomycolic acids (Ott et al., 2017). Furthermore, it was suggested that

after internalization in human and murine macrophages, *C. diphtheriae* is able to delay phagolysosome maturation, independent of the presence of mycolic acids (Ott et al., 2017).

To get deeper insights into the pathogenicity of the emerging pathogen *C. ulcerans*, Hacker and co-workers studied the interaction of two *C. ulcerans* strains with human macrophages (Hacker et al., 2016b). Their study revealed that at 8 h post-infection, *C. ulcerans* were able to multiply within macrophages and delayed the phagolysosome formation, which might serve as an effective mechanism for immune evasion and spreading of *C. ulcerans* within the body (Hacker et al., 2016b). In addition to *C. ulcerans* as well as *C. diphtheriae*, delay of phagolysosome formation was also reported in a Gram-positive species *Rhodococcus equi* before the late endocytic stage (Sydor et al., 2013). As it was shown that the membrane lipids of *C. pseudotuberculosis* have a lethal effect on murine (Hard, 1975) and caprine (Tashjian and Campbell, 1983) macrophages, in future studies, elucidating the role of mycolic acids in the interaction of *C. ulcerans* might be important. Furthermore, as uptake of *C. ulcerans* induced detrimental effects of macrophages and indicated a necrotic mode of cell death (Hacker et al., 2016b; Weerasekera et al., in preparation), *C. ulcerans* harboring more than one active mechanism to cope with macrophages is suggested which also supports the necessity of the constant surveillance of this emerging pathogen.

Studies have reported that the closely related animal pathogen *C. pseudotuberculosis* is able to survive and grow within J774A.1 mouse macrophage in order to disseminate within the host (McKean et al., 2007). Expression of the secreted exotoxin PLD in *C. pseudotuberculosis* was shown to make a significant contribution to the reduction in macrophage viability and plays a role in macrophage death. Several methods have been proposed to explain this observation (McKean et al., 2007). First, it was suggested that the sphingomyelinase activity of PLD might have caused a reduction in the integrity of the macrophage plasma membrane. Given that sphingomyelin is located on the outer leaflet of the plasma membrane, its effect may be mediated by an extracellular mechanism. Following the death of the macrophage, the cellular contents are released, and extracellular PLD was then able to attack sphingomyelin present on the outer leaflet of the plasma membrane of still

viable macrophages. Alternatively, sphingomyelin is a major phospholipid component of the phagosomal membranes of murine J774E macrophages (Desjardins et al., 1994). Therefore, the effect of PLD on macrophage viability may also be mediated by reducing the viability of intracellular compartments of macrophages, which would potentially allow the bacteria to escape from this restricted area. Thirdly, it was suggested that the action of PLD within the macrophages may primarily mediate through disruption of mammalian signaling pathways which is advantageous for the pathogen (McKean et al., 2007).

6.3. Host immune response

The mammalian immune system comprises innate and adaptive components, with the innate immunity providing the first line of defense against invading pathogens, which is essential for the control of common bacterial infections, while the adaptive immune system providing a more versatile means of defense with increased protection against subsequent reinfection with the same pathogen. The innate immune system initially recognizes microorganisms that invade a vertebrate host through germline encoded PRRs. PRRs that recognize PAMPs are expressed constitutively on host cells and detect pathogens regardless of their life-cycle stage. Different PRRs react with specific PAMPs and activate a specific signaling pathway leading to distinct antipathogen response. Microbial components are recognized by several classes of PRRs including Toll-like receptors and cytoplasmic receptors which directly activate immune cells (Akira et al., 2006). TLRs are evolutionarily conserved from the worm *C. elegans* to mammals (Janeway and Medzhitov, 2002; Hoffmann, 2003; Akira and Takeda, 2004; Beutler, 2004). TLR family members recognize lipopolysaccharide from Gram-negative bacteria and lipoteichoic acids, mycolic acids and arabinogalactan from Gram-positive bacteria including corynebacteria, mycobacteria and nocardia (Akira et al., 2006). The activation of TLRs first leads to the activation and recruitment of phagocytic cells such as macrophages and neutrophils to the site of infection. Next, TLR signaling leads to transcription

of distinct proinflammatory genes which produce cytokines, interferons, chemokines and cell surface molecules (Sioud, 2005).

The activation of intracellular signaling pathways lead to the transcription of genes involved in antimicrobial host defense mechanisms which was first investigated in *C. diphtheriae* with respect to septic arthritis in mice. Puliti et al. demonstrated that the intravenous injection of non-toxigenic *C. diphtheriae* leads to lethal infections in mice (Puliti et al., 2006). Similar findings were reported when Swiss Webster mice were infected with a non-toxigenic *C. diphtheriae* strain (Peixoto et al., 2014). The appearance of arthritic lesions is undoubtedly a multifactorial process involving bacterial virulence factors and host immune system (Puliti et al., 2000). For instance, in both animal and human models, the role of proinflammatory cytokines such as IL-6, IL-1β and TNF-α in the arthritis pathogenesis has been well documented (Feldmann et al., 1996). However, the mechanisms of host cell signaling and innate immune recognition by corynebacteria are not well studied. Macrophage activation by *C. diphtheriae* is mediated via TLR2-dependent yet TLR4-independent manner (Takeuchi et al., 1999). LM and LAM of *C. glutamicum* interact with TLR2 (Mishra et al., 2012). A stimulatory effect of purified TDCM from *C. glutamicum* on mouse macrophages was shown previously but the involvement of the receptors has not been characterized (Chami et al., 2002). A study by van der Peet et al. demonstrated the recognition of synthetic corynomycolates by mouse and human Mincle receptors (van der Peet et al., 2015). To address the role of Mincle and TLR2 in the recognition of corynebacteria and activation of macrophages, binding of glycolipid extracts from cell wall preparations of several pathogenic and non-pathogenic *Corynebacterium* strains to Mincle was studied (Schick et al., 2017). Macrophages deficient in Mincle or its adapter protein Fc receptor gamma chain (FcRγ) produced severely reduced amount of granulocyte colony stimulating factor (G-CSF) and nitric oxide (NO) upon challenge with corynebacterial glycolipids. Interestingly, cell wall extracts of the toxigenic *C. diphtheriae* DSM43989 strain lacking mycolic acids neither bound to Mincle nor activated macrophages (Schick et al., 2017). Furthermore, their results indicated that TLR2 was in fact critical for sensing cell wall extracts and whole corynebacteria. Thus,

macrophage activation by the corynebacterial cell wall relies on TLR2-driven robust Mincle expression and the co-operative action of both receptors (Schick et al., 2017).

The activation of TLR signaling pathway originates from the cytoplasmic Toll/IL-1 receptor (TIR) domain that associates with a TIR domain-containing adaptor, Myd88. IL-1 receptor or TLR family members are linked by Myd88 to IL-1R-associated kinases (IRAK) via homotypic protein-protein interactions. Activation of IRAK leads to a variety of functional outputs, including the activation of nuclear factor kappa B (NF-κB), which makes Myd88 a central node of inflammatory pathways (Deguine and Barton, 2014). To get deeper insights into the molecular mechanisms of *C. diphtheriae* driven macrophage activation, a combination of murine and human phagocytes was used recently to investigate the interaction of *C. diphtheriae* (Weerasekera et al., 2019a). Bone marrow-derived macrophages (BMM), Mincle$^{-/-}$ and Myd88$^{-/-}$ cells were used as murine and THP-1 cells as human phagocytes. The infection of BMM and THP-1 cells with toxigenic *C. diphtheriae* DSM43989 strain showed the lowest intracellular colony forming units (CFUs) indicating that the bacteria are not endocytosed. It was confirmed by TLR9, a receptor that is expressed in the ER and located in endolysosomal compartments showing a low signal for DSM43989 strain. Interestingly, although no intracellular CFUs were detected with respect to the infection with *C. glutamicum* ATCC 13032 independent of the host cell, they were recognized by TLR9 indicating that the bacteria were degraded immediately after endocytosis. No significant differences were observed in terms of G-CSF and Interleukin-6 (IL-6) production in between BMM and THP-1, while all *C. diphtheriae* strains investigated in this study showed higher G-CSF production in comparison to IL-6 (Weerasekera et al., 2019a).

C. diphtheriae not only were able to cause host immune response by inducing inflammatory cytokines but also were able to induce the production of NO. They were able to delay phagolysosome formation and had a cytotoxic effect on host cells (Weerasekera et al., 2019a). Furthermore, *C. diphtheriae* strains were able to activate NF-KB signal transduction pathway (Ott et al., 2013; Weerasekera et al., 2019a). Interestingly, in the absence of Mincle, G-CSF production was reduced, while the uptake of bacteria was not influenced. In contrast,

in the absence of Myd88, both the uptake of the bacteria and the production of cytokines were blocked (Weerasekera et al., 2019a). The TLR2/Myd88 pathway is in fact required for the phagocytosis of *C. diphtheriae* and the upregulation of CLR Mincle. Since the detected intracellular CFUs are strain-and cell line-specific, the bacterial antigen that is recognized by host cell receptor might be expressed in various amounts across different *C. diphtheriae* strains. Moreover, as both pathogenic and non-pathogenic corynebacteria bind to TLR2 and Mincle, *C. diphtheriae* might express various other proteins/molecules, which are advantageous in interacting with host cells, enabling the bacteria to trigger host-immune response (Weerasekera et al., 2019a).

6.4. Cell death

Macrophages can act differently in the way of killing toxigenic and non-toxigenic corynebacteria. Some microorganisms are able to avoid killing by macrophages by inhibiting the attachment to phagocytes or by inhibiting the phagocytosis itself (Wood et al., 2001). A study by dos Santos and co-workers demonstrated that the adherence of *C. diphtheriae tox*$^-$ strain to U-937 cells was weak and that only a very low number of bacteria were phagocytosed indicating that *C. diphtheriae* is capable of escaping non-opsonic phagocytosis by human macrophages. It was suggested that there might be differences in the molecules expressed on *tox*$^+$ and *tox*$^-$ strains which are involved in non-opsonic phagocytosis in U-937 cells (dos Santos et al., 2010). Furthermore, about 80 % macrophages remained viable upon infection with *tox*$^-$ strain which suggested that non-opsonic phagocytosis was not due to macrophage cytotoxicity. However, *tox*$^-$ strain also caused death of some phagocytes. Therefore, the possibility of bacteria that grew in and killed macrophages and grew extracellularly afterwards cannot be excluded. In contrast, the *tox*$^+$ strain did not survive or replicate inside U-937 macrophages. In fact, a rapid reduction of the number of intracellular bacteria was observed in macrophages infected with *tox*$^+$ strain, most probably due to the cytotoxic activity of DT (dos Santos et al., 2010). Taken together, non-opsonic phagocytosis of *tox*$^+$ and *tox*$^-$ strains

inhibited bacterial growth and induced cytopathogenicity at different levels in U-937 cells. *Tox*$^{+}$ strain killed more than 42 % cells indicating higher cytotoxicity compared to *tox*$^{-}$ strain which only killed about 18 %. Therefore, cytopathogenicity is not dependent on bacterial intracellular replication in U-937 cells. However, both strains exhibited cytotoxicity irrespective of the presence or absence of DT.

Purified DT mediates cell lysis and DNA fragmentation (Thorburn et al., 2004). Studies revealed that mice treated with DT, depleted alveolar macrophages by apoptosis (Mookerjee et al., 1982; Miyake et al., 2007). Although cytotoxicity of DT to host cells has been well documented, *C. diphtheriae*-induced cell death has not been well understood.

During the last decades, many forms of cell death have been identified. However, the most prominent and well-known forms of cell death are apoptosis and necrosis (Galluzzi et al., 2018). Apoptosis is an active process which requires protein synthesis for its execution and is characterized by morphological and biochemical alterations. In contrast, necrosis is a degenerative phenomenon that follows irreversible injury where the cells may lose their membrane integrity at almost all stages of dying (Walker et al., 1988; Munoz et al., 2013). Studies reported that the death of macrophages due to bacterial infection may be partially activated by apoptotic machinery (Leek et al., 1990; Ruckdeschel et al., 1997; Gao and Kwaik, 1999; Thorburn et al., 2004; Miyake et al., 2007). The microtubule cytoskeleton plays an important role in preserving plasma membrane integrity during apoptosis. In many cell types, under different apoptotic stimuli, the cytoskeleton is reformed (Sánchez-Alcázar et al., 2007).

Thus far, at least two main mechanisms are discussed by which corynebacteria induce cell death, i.e., necrosis and/or apoptosis (dos Santos et al., 2010; Hacker et al., 2016b; Weerasekera et al., in preparation). During *C. diphtheriae* infection, cytoskeleton rearrangement stimulated the death of U-937 macrophages. Interestingly, a *tox*$^{-}$ strain also caused necrosis and apoptosis. Therefore, the mechanisms of cell death induced by *C. diphtheriae* are not exclusively associated with DT production or presence of the *tox* gene (dos Santos et al., 2010). Cell surface components such as 67-72p protein, also known as DIP0733 is not only able to interact with macrophages but also with non-phagocytic HEp-2 epithelial cells and

involve in the induction of apoptosis and necrosis favoring the persistence and dissemination in human tissues (Sabbadini et al., 2012). Bacteria released from the apoptotic cells may initiate another round of host cell infection (Tsai et al., 1999). Since apoptosis is usually not simply a result of exoproduct toxicity, bacterial expression of specific adhesins and invasins may contribute in evoking apoptosis even in susceptible cells (Jendrossek et al., 2003; Choi et al., 2005). In the initial stages of apoptosis, due to the extrusion of water, cells undergo shrinkage followed by fragmentation leading to the formation of apoptotic bodies. At this stage, microfilament assembly may be important in the formation of apoptotic bodies (Cotter et al., 1992). Treatment of HEp-2 cells with DIP0733 caused cell shrinkage and reduction in cell volume. In addition, other signs of apoptosis such as prominent blebs on cell surface, rounding up cells and budding were observed within 3 to 6 hours of infection. Furthermore, during later stages of infection (24 h), formation of higher amount of apoptotic bodies, changes in membrane permeability and a significant reduction in cell viability was observed suggesting late apoptosis or secondary necrosis (Sabbadini et al., 2012).

In a recent study, infection of human THP-1 macrophages with *C. ulcerans* indicated a lytic cell death mechanism resembling necrosis (Hacker et al., 2016b). Although infections of *C. ulcerans* in humans are rare, some *C. ulcerans* strains seem to be more aggressive towards human cells at least *in vitro* indicating that *C. ulcerans* may also use similar strategies to interact with human host as *C. diphtheriae* (Weerasekera et al., in preparation). In a recent study, infection with *C. diphtheriae* HC04 and *C. ulcerans* 809 strains resulted in condensation of DNA in macrophage nuclei and induced cell lysis. Depending on the time of incubation, an increase in the detachment of macrophages from cell culture surface was observed. Live cell imaging experiments revealed that these detrimental effects on macrophages depend on bacterial endocytosis and replication within macrophages. Interestingly, at 14 h of infection, almost all the cells were found dead (Weerasekera et al., in preparation). Primary necrosis has often been described as a consequence of extreme stress and is thus considered as accidental. It is characterized by rapid plasma membrane rupture (Walker et al., 1988). Weerasekera et al. demonstrated that flow cytometry analyses using Annexin V as a FITC

conjugate in combination with propidium iodide was able to identify phosphatidyl serine (PS) exposure of the cells and plasma membrane damage. In addition, mitochondrial membrane potential and nuclear DNA content was determined by staining with DiIC and Hoechst 33342, respectively. Additionally, upon infection with *C. diphtheriae* HC04 and *C. ulcerans* 809, several stages of cell-death and associated changes such as viable, stressed, early/late apoptosis, primary/secondary necrosis have been distinguished (Weerasekera et al., in preparation).

In summary, the interaction of *C. diphtheriae* and *C. ulcerans* with hosts is much more complex than initially expected. Although until now several different mechanisms have been elucidated, there is still the existing need for research especially regarding interactions at the molecular level. Therefore, the results already described, and the on-going research may most certainly contribute to the understanding of the mechanisms involved in virulence and pathogenicity of corynebacteria.

7. THE ROLE OF RIBOSOME-INACTIVATING PROTEINS

The biological activity of RIPs is not completely clarified, and sometimes they are independent of the inhibition of protein synthesis. There are differences in the cytotoxicity of RIPs and, consequently, in their toxicity to animals. Some RIPs are potent toxins, the best-known being ricin, a potential biological weapon. RIPs cause apoptotic and necrotic lesions and induce production of cytokines causing inflammation (Hajto et al., 1990; Ferri and Kroemer, 2001). However, the distribution, mechanism of action and role in nature of RIPs are not completely understood. Cellular events and apoptosis induced by various RIPs suggests an important role played by mitochondria acting as an integrator of cellular stress and cell death (Stirpe and Battelli, 2006). As the preliminary data suggested a necrotic cell death induced by *C. ulcerans* 809 and *C. diphtheriae* HC04, the early events leading to necrosis need to be investigated in detail by monitoring the morphological changes in human THP-1 cell line. Furthermore, numerous bacterial toxins recognize the actin cytoskeleton as a target. The bacterial toxins that modify the actin cytoskeleton induce various cell disfunctions including changes in cell barrier permeability and disruption of intracellular junctions (Richard et al., 1999). Therefore, in response to the putative toxin, morphological changes in the nuclei, changes in actin cytoskeleton, host cell responses need to be further investigated using TLR reporter cells, secretion of cytokines as well as NF-κB induction. Furthermore, the analysis of the amino acid sequence of Rbp revealed lack of the ER-targeting sequence at the C-terminal end of the protein from *C. ulcerans* 809 (Trost et al., 2011). Therefore, it is suggested that the secretion of the putative toxin into the cytosol of the host cell is instead supported by a typical signal sequence at the N-terminus of the protein. To characterize the delivery mechanisms and secretion of the toxin, overexpression and purification of the protein and raising antibodies against these purified recombinant proteins need to be performed in future experiments to identify *stx* gene variants.

Based on the structure, RIPs have been divided into two groups: type I and type II. Type II RIPs, including ricin and Shiga toxin, possess a dimeric structure with an active A-

subunit (homologous to type I RIPs) and a larger B subunit that attaches to galactose containing surface receptors of target cells (Hogg et al., 2015). The entry process of type I and type II RIPs appears to be dependent largely on the protein structure. Thus, the differences are ascribed to the presence or absence of B chains which allow binding to the cell membrane and facilitate their endocytosis process. However, the presence of the B chain is not sufficient to confer a high level of cytotoxicity on type II RIPs. Type I RIPs can also enter cells in various ways, by enclosure into carriers that can fuse with cells such as liposomes, erythrocytes or by subjecting the cells to shock waves (Delius and Adams, 1999). Therefore, with respect to the structural analyses, protein domains and linear motifs need to be analyzed in detail to elucidate the mechanisms of cell entry and intracellular trafficking of RIPs in future studies. For this purpose, firstly, the RIPs investigated in our study need to be assigned to either type I or type II. Although the amino acid sequences of Rbps from *C. ulcerans* 809 are about 24 % similar to A chains of SLT-1A and SLT-2A from *E. coli*, it contained all highly conserved amino acid residues needed for the catalytic activity and exhibited strong structural similarity between both proteins (Trost et al., 2011). These SLT-1 belong to Rbp type-II family with a highly conserved tertiary structure of type-II family members. The preliminary data of this study revealed that the alignment of the tertiary structures of *C. diphtheriae* HC04 protein and SLT-1A demonstrated overlapping regions between the two proteins with a confidence of 97 % and an identity of 26 %. Moreover, the Rbps of *C. diphtheriae* HC04 belong to the family of plant cytotoxins, hence can serve as type-II family RIPs. To understand the assembly of subunits of these putative toxins, the interfaces between the A-chain and B-chain in type-II proteins need to be analyzed by superimposing with 1R4Q (Shiga-Toxin) or 1M2T (Lectin) in corynebacteria. To investigate detrimental effects and host cell responses, RIPs associated candidate domains and motifs need to be identified and extensive mutagenesis studies need to be carried out. This work will help shedding new light on complex pathophysiological or bacteria induced cell death processes in corynebacteria.

8. OUTLOOK

The interaction of pathogenic corynebacteria with host cells seems to be very often a multifactorial process. The observed internalization into epithelial cells, multiplication within macrophages and delaying the phagolysosome formation might be effective mechanisms for immune evasion and spreading of corynebacteria within the body which supports the establishment and progress of infections. Moreover, next-generation sequencing revealed that horizontal gene transfer plays an important role in the acquiring of new virulence factors due to intraspecies genome plasticity. Unfortunately, due to the lack of specialized diagnostics and under reporting of infections especially in developing countries, *C. diphtheriae* still present on the list of the most important global death-provoking pathogens. Therefore, more detailed studies on the interaction of corynebacteria with macrophages are crucial to enhance the global surveillance of pathogenic corynebacteria to get further insights into the molecular basis, gene transfer and toxin delivery mechanisms.

9. REFERENCES

Aderem, A. & Underhill, D. M. 1999. Mechanisms of phagocytosis in macrophages. *Annual Review of Immunology,* 17**,** 593-623.

Akimkina, T., Yook, K., Curnock, S. & Hodgkin, J. 2006. Genome characterization, analysis of virulence and transformation of *Microbacterium nematophilum*, a coryneform pathogen of the nematode *Caenorhabditis elegans*. *FEMS Microbiology Letters,* 264**,** 145-51.

Akira, S. & Takeda, K. 2004. Toll-like receptor signalling. *Nature Reviews Immunology,* 4**,** 499-511.

Akira, S., Uematsu, S. & Takeuchi, O. 2006. Pathogen recognition and innate immunity. *Cell,* 124**,** 783-801.

Altincicek, B., Linder, M., Linder, D., Preissner, K. T. & Vilcinskas, A. 2007. Microbial metalloproteinases mediate sensing of invading pathogens and activate innate immune responses in the lepidopteran model host *Galleria mellonella*. *Infection and Immunity,* 75**,** 175.

Anantharaman, V. & Aravind, L. 2003. Evolutionary history, structural features and biochemical diversity of the NlpC/p60 superfamily of enzymes. *Genome Biology,* 4**,** R11.

Andersen, E. C., Gerke, J. P., Shapiro, J. A., Crissman, J. R., Ghosh, R., Bloom, J. S., Félix, M.-A. & Kruglyak, L. 2012. Chromosome-scale selective sweeps shape *Caenorhabditis elegans* genomic diversity. *Nature Genetics,* 44**,** 285.

Andrejko, M. & Mizerska-Dudka, M. 2012. Effect of *Pseudomonas aeruginosa* elastase B on level and activity of immune proteins/peptides of *Galleria mellonella* hemolymph. *Journal of Insect Science,* 12.

Antunes, C. A., Clark, L., Wanuske, M.-T., Hacker, E., Ott, L., Simpson-Louredo, L., De Luna, M. D. G., Hirata, R., Mattos-Guaraldi, A. L., Hodgkin, J. & Burkovski, A. 2016. *Caenorhabditis elegans* star formation and negative chemotaxis induced by infection with corynebacteria. *Microbiology,* 162**,** 84-93.

Antunes, C. A., Sanches Dos Santos, L., Hacker, E., Köhler, S., Bösl, K., Ott, L., De Luna, M. D. G., Hirata, R., Azevedo, V. a. D. C., Mattos-Guaraldi, A.-L. & Burkovski, A. 2015. Characterization of DIP0733, a multi-functional virulence factor of *Corynebacterium diphtheriae*. *Microbiology,* 161**,** 639-47.

Aperis, G., Burgwyn Fuchs, B., Anderson, C. A., Warner, J. E., Calderwood, S. B. & Mylonakis, E. 2007. *Galleria mellonella* as a model host to study infection by the *Francisella tularensis* live vaccine strain. *Microbes and Infection,* 9**,** 729-34.

Apostolovic, B., Danial, M. & Klok, H. A. 2010. Coiled coils: attractive protein folding motifs for the fabrication of self-assembled, responsive and bioactive materials. *Chemical Society Reviews,* 39**,** 3541-75.

Arden, S. B., Chang, W.-H. & Barksdale, L. 1972. Distribution of neuraminidase and n-acetylneuraminate lyase activities among corynebacteria, mycobacteria, and nocardias. *Journal of Bacteriology,* 112**,** 1206.

Baggiolini, M. & Wymann, M. P. 1990. Turning on the respiratory burst. *Trends in Biochemical Sciences,* 15**,** 69-72.

Baird, G. J. & Fontaine, M. C. 2007. *Corynebacterium pseudotuberculosis* and its role in ovine caseous lymphadenitis. *Journal of Comparative Pathology,* 137**,** 179-210.

Barksdale, L. 1970. *Corynebacterium diphtheriae* and its relatives. *Bacteriological reviews,* 34**,** 378-422.

Barnoy, S., Gancz, H., Zhu, Y., Honnold, C. L., Zurawski, D. V. & Venkatesan, M. M. 2017. The *Galleria mellonella* larvae as an in vivo model for evaluation of Shigella virulence. *Gut Microbes,* 8**,** 335-50.

Batey, R. G. 1986. Pathogenesis of caseous lymphadenitis in sheep and goats. *Australian Veterinary Journal,* 63**,** 269-72.

Bégué, P. 2010. Consequences of opposition to vaccination in france and europe. How to maintain effective vaccine coverage in 2010?. *Bulletin de l'Academie nationale de medecine,* 194**,** 719-32.
Berger, A., Dangel, A., Peters, M., Mühldorfer, K., Braune, S., Eisenberg, T., Szentiks, C. A., Rau, J., Konrad, R., Hörmansdorfer, S., Ackermann, N. & Sing, A. 2019. Tox-positive *Corynebacterium ulcerans* in hedgehogs, Germany. *Emerging Microbes and Infections,* 8**,** 211-7.
Berger, A., Huber, I., Merbecks, S.-S., Ehrhard, I., Konrad, R., Hörmansdorfer, S., Hogardt, M. & Sing, A. 2011. Toxigenic *Corynebacterium ulcerans* in woman and cat. *Emerging infectious diseases,* 17**,** 1767-9.
Bergin, D., Reeves, E. P., Renwick, J., Wientjes, F. B. & Kavanagh, K. 2005. Superoxide production in *Galleria mellonella* hemocytes: identification of proteins homologous to the nadph oxidase complex of human neutrophils. *Infection and Immunity,* 73**,** 4161.
Bernard, K. 2012. The genus *Corynebacterium* and other medically relevant coryneform-like bacteria. *Journal of Clinical Microbiology,* 50**,** 3152-8.
Beutler, B. 2004. Inferences, questions and possibilities in Toll-like receptor signalling. *Nature,* 430**,** 257-63.
Bitragunta, S., Murhekar, M. V., Chakravarti, A., Verma, V., Namjoshi, G. S., Parekh, S. S., Sharma, H. J., Kumar, B. K. & Gupte, M. D. 2010. Safety and immunogenicity of single dose of tetanus–diphtheria (TD) vaccine among non/partially immune children against diphtheria and/or tetanus, Hyderabad, India, 2007. *Vaccine,* 28**,** 5934-38.
Blumberg, B. S. & Warren, I. 1961. The effect of sialidase on transferrins and other serum proteins. *Biochimica et Biophysica Acta,* 50**,** 90-101.
Borghi, E., Romagnoli, S., Fuchs, B. B., Cirasola, D., Perdoni, F., Tosi, D., Braidotti, P., Bulfamante, G., Morace, G. & Mylonakis, E. 2014. Correlation between *Candida albicans* biofilm formation and invasion of the invertebrate host *Galleria mellonella*. *Future Microbiology,* 9**,** 163-73.
Bostock, A. D., Gilbert, F. R., Lewis, D. & Smith, D. C. M. 1984. *Corynebacterium ulcerans* infection associated with untreated milk. *Journal of Infection,* 9**,** 286-8.
Brenner, S. 1974. The genetics of *Caenorhabditis elegans*. *Genetics,* 77**,** 71.
Broadway, M. M., Rogers, E. A., Chang, C., Huang, I. H., Dwivedi, P., Yildirim, S., Schmitt, M. P., Das, A. & Ton-That, H. 2013. Pilus gene pool variation and the virulence of *Corynebacterium diphtheriae* clinical isolates during infection of a nematode. *Journal of Bacteriology,* 195**,** 3774.
Brown, S. E., Cao, A. T., Hines, E. R., Akhurst, R. J. & East, P. D. 2004. A novel secreted protein toxin from the insect pathogenic bacterium *Xenorhabdus nematophila*. *Journal of Biological Chemistry,* 279**,** 14595-601.
Browne, N., Heelan, M. & Kavanagh, K. 2013. An analysis of the structural and functional similarities of insect hemocytes and mammalian phagocytes. *Virulence,* 4**,** 597-603.
Burkovski, A. 2013. Cell envelope of corynebacteria: structure and influence on pathogenicity. *ISRN Microbiology,* 2013**,** 935736.
Burkovski, A. 2014. Diphtheria and its etiological agents. *In:* Burkovski, A. (ed.) *Corynebacterium diphtheriae* and related toxigenic species. Dordrecht: Springer Netherlands. pp. 1-10.
Calderwood, S. B., Auclair, F., Donohue-Rolfe, A., Keusch, G. T. & Mekalanos, J. J. 1987. Nucleotide sequence of the Shiga-like toxin genes of *Escherichia coli*. *Proceedings of the National Academy of Sciences,* 84**,** 4364.
Casadevall, A. & Pirofski, L.-A. 2015. What is a host? incorporating the microbiota into the damage-response framework. *Infection and Immunity,* 83**,** 2.
CDC, Center For Disease Control and Prevention. 2015. Diphtheria vaccination [Online]. Available: http://www.cdc.gov/vaccines/vpd-vac/diphtheria/ [Accessed 02 June 2019].
Cerdeño-Tárraga, A. M., Efstratiou, A., Dover, L. G., Holden, M. T. G., Pallen, M., Bentley, S. D., Besra, G. S., Churcher, C., James, K. D., De Zoysa, A., Chillingworth, T., Cronin, A., Dowd, L., Feltwell, T., Hamlin, N., Holroyd, S., Jagels, K., Moule, S., Quail, M. A., Rabbinowitsch, E., Rutherford, K. M., Thomson, N. R., Unwin, L., Whitehead, S.,

Barrell, B. G. & Parkhill, J. 2003. The complete genome sequence and analysis of *Corynebacterium diphtheriae* NCTC13129. *Nucleic Acids Research,* 31**,** 6516-23.
Chami, M., Andréau, K., Lemassu, A., Petit, J.-F., Houssin, C., Puech, V., Bayan, N., Chaby, R. & Daffé, M. 2002. Priming and activation of mouse macrophages by trehalose 6,6′-dicorynomycolate vesicles from *Corynebacterium glutamicum*. *Pathogens and Disease,* 32**,** 141-7.
Champion, O. L., Wagley, S. & Titball, R. W. 2016. *Galleria mellonella* as a model host for microbiological and toxin research. *Virulence,* 7**,** 840-5.
Chan, Y. S. & Ng, T. B. 2016. Shiga toxins: from structure and mechanism to applications. *Applied Microbiology and Biotechnology,* 100**,** 1597-610.
Choi, C. H., Lee, E. Y., Lee, Y. C., Park, T. I., Kim, H. J., Hyun, S. H., Kim, S. A., Lee, S.-K. & Lee, J. C. 2005. Outer membrane protein 38 of *Acinetobacter baumannii* localizes to the mitochondria and induces apoptosis of epithelial cells. *Cellular Microbiology,* 7**,** 1127-38.
Chung, C. S., Liao, C. H., Cheng, S. L., Lin, T. H. & Hsueh, P. R. 2008. Percutaneous nephrostomy tube-associated bacteremia caused by *Corynebacterium urealyticum*. *Journal of Microbiology Immunology and Infection,* 41**,** 525-7.
Cianciotto, N. P. & Groman, N. B. 1996. Extended host range of a β-related corynebacteriophage. *FEMS Microbiology Letters,* 140**,** 221-5.
Ciesielczuk, H., Betts, J., Phee, L., Doumith, M., Hope, R., Woodford, N. & Wareham, D. W. 2015. Comparative virulence of urinary and bloodstream isolates of extra-intestinal pathogenic *Escherichia coli* in a *Galleria mellonella* model. *Virulence,* 6**,** 145-51.
Clark, L. C. & Hodgkin, J. 2014. Commensals, probiotics and pathogens in the *Caenorhabditis elegans* model. *Cellular Microbiology,* 16**,** 27-38.
Clark, L. C. & Hodgkin, J. 2015. *Leucobacter musarum* subsp. *Musarum* sp. Nov., subsp. Nov., *Leucobacter musarum* subsp. *Japonicus* subsp. Nov., and *Leucobacter celer* subsp. *Astrifaciens* subsp. Nov., three nematopathogenic bacteria isolated from *Caenorhabditis*, with an emended description of *Leucobacter celer*. *International journal of systematic and evolutionary microbiology,* 65**,** 3977-84.
Collier, R. J. 1975. Diphtheria toxin: mode of action and structure. *Bacteriological reviews,* 39**,** 54-85.
Collin, M. & Fischetti, V. A. 2004. A novel secreted endoglycosidase from *Enterococcus faecalis* with activity on human immunoglobulin G and ribonuclease B. *Journal of Biological Chemistry,* 279**,** 22558-70.
Colombo, A. V., Hirata, R., Jr., De Souza, C. M. R., Monteiro-Leal, L. H., Previato, J. O., Formiga, L. C. D., Andrade, A. F. B. & Mattos-Guaraldi, A. L. 2001. *Corynebacterium diphtheriae* surface proteins as adhesins to human erythrocytes. *FEMS Microbiology Letters,* 197**,** 235-9.
Contzen, M., Sting, R., Blazey, B. & Rau, J. 2011. *Corynebacterium ulcerans* from diseased wild boars. *Zoonoses and Public Health,* 58**,** 479-88.
Cook, S. M. & Mcarthur, J. D. 2013. Developing *Galleria mellonella* as a model host for human pathogens. *Virulence,* 4**,** 350-3.
Corfield, T. 1992. Bacterial sialidases—roles in pathogenicity and nutrition. *Glycobiology,* 2**,** 509-21.
Cornacchione, P., Scaringi, L., Fettucciari, K., Rosati, E., Sabatini, R., Orefici, G., Hunolstein, V. C., Modesti, A., Modica, A., Minelli, F. & Marconi, P. 1998. Group B streptococci persist inside macrophages. *Immunology,* 93**,** 86-95.
Cornick, N. A., Helgerson, A. F., Mai, V., Ritchie, J. M. & Acheson, D. W. K. 2006. *In vivo* transduction of an stx-encoding phage in ruminants. *Applied and Environmental Microbiology,* 72**,** 5086.
Corti, M. A. M., Bloemberg, G. V., Borelli, S., Kutzner, H., Eich, G., Hoelzle, L. & Lautenschlager, S. 2012. Rare human skin infection with *Corynebacterium ulcerans*: transmission by a domestic cat. *Infection,* 40**,** 575-8.
Cotter, G., Doyle, S. & Kavanagh, K. 2000. Development of an insect model for the *in vivo* pathogenicity testing of yeasts. *Pathogens and Disease,* 27**,** 163-9.

Cotter, T. G., Lennon, S. V., Glynn, J. M. & Green, D. R. 1992. Microfilament-disrupting agents prevent the formation of apoptotic bodies in tumor cells undergoing apoptosis. *Cancer Research,* 52**,** 997.

Cuevas, W. A. & Songer, J. G. 1993. *Arcanobacterium haemolyticum* phospholipase D is genetically and functionally similar to *Corynebacterium pseudotuberculosis* phospholipase D. *Infection and Immunity,* 61**,** 4310.

D'onofrio, C. & Paradisi, F. 1983. The influence of bacterial exotoxins and endotoxins on the phagocytic activity of human macrophages in culture. *Infection,* 11**,** 137-43.

Daffé, M. 2005. The cell envelope of corynebacteria. *In:* Eggeling, L. & Bott, M. (eds.) Handbook of *Corynebacterium glutamicum.* Boca Raton, Fla, USA: Taylor & Francis. pp. 121-48.

Deguine, J. & Barton, G. M. 2014. Myd88: a central player in innate immune signaling. *F1000Prime Reports,* 6**,** 97.

Delius, M. & Adams, G. 1999. Shock wave permeabilization with ribosome inactivating proteins: a new approach to tumor therapy. *Cancer Research,* 59**,** 5227.

Desbois, A. P. & Coote, P. J. 2011. Wax moth larva (*Galleria mellonella*): An in vivo model for assessing the efficacy of antistaphylococcal agents. *Journal of Antimicrobial Chemotherapy,* 66**,** 1785-90.

Desjardins, M., Celis, J. E., Van Meer, G., Dieplinger, H., Jahraus, A., Griffiths, G. & Huber, L. A. 1994. Molecular characterization of phagosomes. *Journal of Biological Chemistry,* 269**,** 32194-200.

Dessau, R. B., Brandt-Christensen, M., Jensen, O. J. & Tonnesen, P. 1995. Pulmonary nodules due to *Corynebacterium ulcerans*. *European Respiratory Journal,* 8**,** 651.

Dixon, B. 2010. Sick as a dog. *The Lancet Infectious Diseases,* 10**,** 73.

Dorella, F. A., Pacheco, L. G., Oliveira, S. C., Miyoshi, A. & Azevedo, V. 2006. *Corynebacterium pseudotuberculosis*: microbiology, biochemical properties, pathogenesis and molecular studies of virulence. *Veterinary Research,* 37**,** 201-18.

dos Santos, C. S., dos Santos, L. S., de Souza, M. C., dos Santos Dourado, F., de Souza de Oliveira Dias, A. A., Sabbadini, P. S., Pereira, G. A., Cabral, M. C., Junior, R. H. & de Mattos-Guaraldi, A. L. 2010. Non-opsonic phagocytosis of homologous non-toxigenic and toxigenic *Corynebacterium diphtheriae* strains by human U-937 macrophages. *Microbiology and Immunology,* 54**,** 1-10.

Drevets, D. A. 1999. Dissemination of *Listeria monocytogenes* by infected phagocytes. *Infection and Immunity,* 67**,** 3512.

Eggeling, L., Gurdyal, S. B. & Alderwick, L. 2008. Structure and synthesis of the cell wall *In:* Burkovski, A. (ed.) Corynebacteria: genomics and molecular biology. Norfolk, UK: Caister Academic Press. pp. 267-94.

Eisenberg, T., Kutzer, P., Peters, M., Sing, A., Contzen, M. & Rau, J. 2014. Nontoxigenic tox-bearing *Corynebacterium ulcerans* infection among game animals, Germany. *Emerging infectious diseases,* 20**,** 448-52.

Eisenberg, T., Mauder, N., Contzen, M., Rau, J., Ewers, C., Schlez, K., Althoff, G., Schauerte, N., Geiger, C., Margos, G., Konrad, R. & Sing, A. 2015. Outbreak with clonally related isolates of *Corynebacterium ulcerans* in a group of water rats. *BMC Microbiology,* 15**,** 42.

Engelmann, I. & Pujol, N. 2010. Innate immunity in *C. elegans*. *In:* Söderhäll, K. (ed.) Invertebrate immunity. Boston, MA: Springer US. pp. 105-21.

Evans, B. A. & Rozen, D. E. 2012. A *Streptococcus pneumoniae* infection model in larvae of the wax moth *Galleria mellonella*. *European Journal of Clinical Microbiology and Infectious Diseases,* 31**,** 2653-60.

Fallon, J. P., Troy, N. & Kavanagh, K. 2011. Pre-exposure of *Galleria mellonella* larvae to different doses of *Aspergillus fumigatus* conidia causes differential activation of cellular and humoral immune responses. *Virulence,* 2**,** 413-21.

Falnes, P. Ø. & Sandvig, K. 2000. Penetration of protein toxins into cells. *Current Opinion in Cell Biology,* 12**,** 407-13.

Feldmann, M., Brennan, F. M. & Maini, R. N. 1996. Role of cytokines in rheumatoid arthritis. *Annual Review of Immunology,* 14**,** 397-440.
Ferri, K. F. & Kroemer, G. 2001. Organelle-specific initiation of cell death pathways. *Nature Cell Biology,* 3**,** E255-63.
Flannagan, R. S., Jaumouillé, V. & Grinstein, S. 2012. The cell biology of phagocytosis. *Annual Review of Pathology: Mechanisms of Disease,* 7**,** 61-98.
Foster, G., Patterson, T., Howie, F., Simpson, V., Davison, N., Efstratiou, A. & Lai, S. 2002. *Corynebacterium ulcerans* in free-ranging otters. *The Veterinary record,* 150**,** 524.
Franks, S. E., Ebrahimi, C., Hollands, A., Okumura, C. Y., Aroian, R. V., Nizet, V. & Mcgillivray, S. M. 2014. Novel role for the YCEGH tellurite resistance genes in the pathogenesis of *Bacillus anthracis*. *Infection and Immunity,* 82**,** 1132.
Fuchs, B. B., Eby, J., Nobile, C. J., El Khoury, J. B., Mitchell, A. P. & Mylonakis, E. 2010. Role of filamentation in *Galleria mellonella* killing by *Candida albicans*. *Microbes and Infection,* 12**,** 488-96.
Galluzzi, L., Vitale, I., Aaronson, S. A., Abrams, J. M., Adam, D., Agostinis, P., Alnemri, E. S., Altucci, L., Amelio, I., Andrews, D. W., Annicchiarico-Petruzzelli, M., Antonov, A. V., Arama, E., Baehrecke, E. H., Barlev, N. A., Bazan, N. G., Bernassola, F., Bertrand, M. J. M., Bianchi, K., Blagosklonny, M. V., et al. 2018. Molecular mechanisms of cell death: recommendations of the nomenclature committee on cell death 2018. *Cell Death and Differentiation,* 25**,** 486-541.
Gao, L.-Y. & Kwaik, Y. A. 1999. Apoptosis in macrophages and alveolar epithelial cells during early stages of infection by *Legionella pneumophila* and its role in cytopathogenicity. *Infection and Immunity,* 67**,** 862.
Gebhardt, H., Meniche, X., Tropis, M., Krämer, R., Daffé, M. & Morbach, S. 2007. The key role of the mycolic acid content in the functionality of the cell wall permeability barrier in *Corynebacterineae*. *Microbiology,* 153**,** 1424-34.
Geisel, R. E., Sakamoto, K., Russell, D. G. & Rhoades, E. R. 2005. *In vivo* activity of released cell wall lipids of *Mycobacterium bovis* bacillus calmette-guérin is due principally to trehalose mycolates. *The Journal of Immunology,* 174**,** 5007.
Gilbert, L. 1997. Infections with *Corynebacterium diphtheriae*--changing epidemiology and clinical manifestations. Report of the third international meeting of the European Laboratory Working Group on Diphtheria (ELWGD), Institute Pasteur, Paris 7-8 June 1996.
Gordon, S. B. & Read, R. C. 2002. Macrophage defences against respiratory tract infections: the immunology of childhood respiratory infections. *British Medical Bulletin,* 61**,** 45-61.
Gravato-Nobre, M. J., Nicholas, H. R., Nijland, R., Rourke, D., Whittington, D. E., Yook, K. J. & Hodgkin, J. 2005. Multiple genes affect sensitivity of *Caenorhabditis elegans* to the bacterial pathogen *Microbacterium nematophilum*. *Genetics,* 171**,** 1033.
Grizanova, E. V., Semenova, A. D., Komarov, D. A., Chertkova, E. A., Slepneva, I. A. & Dubovskiy, I. M. 2018. Maintenance of redox balance by antioxidants in hemolymph of the greater wax moth *Galleria mellonella* larvae during encapsulation response. *Archives of Insect Biochemistry and Physiology,* 98**,** e21460.
Groman, N., Schiller, J. & Russell, J. 1984. *Corynebacterium ulcerans* and *Corynebacterium pseudotuberculosis* responses to DNA probes derived from corynephage beta and *Corynebacterium diphtheriae*. *Infection and Immunity,* 45**,** 511.
Hacker, E., Antunes, C. A., Mattos-Guaraldi, A. L., Burkovski, A. & Tauch, A. 2016a. *Corynebacterium ulcerans*, an emerging human pathogen. *Future Microbiology,* 11**,** 1191-208.
Hacker, E., Ott, L., Hasselt, K., Mattos-Guaraldi, A. L., Tauch, A. & Burkovski, A. 2015. Colonization of human epithelial cell lines by *Corynebacterium ulcerans* from human and animal sources. *Microbiology,* 161**,** 1582-91.
Hacker, E., Ott, L., Schulze-Luehrmann, J., Lührmann, A., Wiesmann, V., Wittenberg, T. & Burkovski, A. 2016b. The killing of macrophages by *Corynebacterium ulcerans*. *Virulence,* 7**,** 45-55.

Hadfield, T. L., Mcevoy, P., Polotsky, Y., Tzinserling, V. A. & Yakovlev, A. A. 2000. The pathology of diphtheria. *The Journal of Infectious Diseases,* 181**,** S116-20.
Hajto, T., Hostanska, K., Frei, K., Rordorf, C. & Gabius, H. J. 1990. Increased secretion of tumor necrosis factors alpha, interleukin 1, and interleukin 6 by human mononuclear cells exposed to beta-galactoside-specific lectin from clinically applied mistletoe extract. *Cancer Research,* 50**,** 3322-6.
Hall, A. J., Cassiday, P. K., Bernard, K. A., Bolt, F., Steigerwalt, A. G., Bixler, D., Pawloski, L. C., Whitney, A. M., Iwaki, M., Baldwin, A., Dowson, C. G., Komiya, T., Takahashi, M., Hinrikson, H. P. & Tondella, M. L. 2010. Novel *Corynebacterium diphtheriae* in domestic cats. *Emerging Infectious Diseases,* 16**,** 688-91.
Halwani, A. E., Niven, D. F. & Dunphy, G. B. 2000. Apolipophorin-III and the interactions of lipoteichoic acids with the immediate immune responses of *Galleria mellonella*. *Journal of Invertebrate Pathology,* 76**,** 233-41.
Hard, G. C. 1975. Comparative toxic effect of the surface lipid of *Corynebacterium ovis* on peritoneal macrophages. *Infection and Immunity,* 12**,** 1439.
Hart, R. J. C. 1984. *Corynebacterium ulcerans* in humans and cattle in North Devon. *Journal of Hygiene,* 92**,** 161-4.
Hilbi, H., Zychlinsky, A. & Sansonetti, P. J. 1997. Macrophage apoptosis in microbial infections. *Parasitology,* 115**,** 79-87.
Hill, C. 2012. Virulence or niche factors: What's in a name? *Journal of Bacteriology,* 194**,** 5725.
Hirata Jr., R., Pereira, G. A., Filardy, A. A., Gomes, D. L. R., Damasco, P. V., Rosa, A. C. P., Nagao, P. E., Pimenta, F. P. & Mattos-Guaraldi, A. L. 2008. Potential pathogenic role of aggregative- adhering *Corynebacterium diphtheriae* of different clonal groups in endocarditis. *Brazilian Journal of Medical and Biological Research,* 41**,** 986-91.
Hirata, R., Souza, S. M. S., Rocha-De-Souza, C. M., Andrade, A. F. B., Monteiro-Leal, L. H., Formiga, L. C. D. & Mattos-Guaraldi, A. L. 2004. Patterns of adherence to hep-2 cells and actin polymerisation by toxigenic *Corynebacterium diphtheriae* strains. *Microbial Pathogenesis,* 36**,** 125-30.
Hodgkin, J., Félix, M.-A., Clark, L. C., Stroud, D. & Gravato-Nobre, M. J. 2013. Two *Leucobacter* strains exert complementary virulence on *Caenorhabditis* including death by worm-star formation. *Current Biology,* 23**,** 2157-61.
Hodgkin, J., Kuwabara, P. E. & Corneliussen, B. 2000. A novel bacterial pathogen, *Microbacterium nematophilum*, induces morphological change in the nematode *C. elegans*. *Current Biology,* 10**,** 1615-18.
Hodgson, A. L., Bird, P. & Nisbet, I. T. 1990. Cloning, nucleotide sequence, and expression in *Escherichia coli* of the phospholipase D gene from *Corynebacterium pseudotuberculosis*. *Journal of Bacteriology,* 172**,** 1256.
Hodgson, A. L., Krywult, J., Corner, L. A., Rothel, J. S. & Radford, A. J. 1992. Rational attenuation of *Corynebacterium pseudotuberculosis*: potential cheesy gland vaccine and live delivery vehicle. *Infection and Immunity,* 60**,** 2900.
Hoffmann, J. A. 2003. The immune response of *Drosophila*. *Nature,* 426**,** 33-8.
Höfler, W. 1991. Cutaneous diphtheria. *International Journal of Dermatology,* 30**,** 845-7.
Hogg, T., Mendel, J. T. & Lavezo, J. L. 2015. Structural analysis of a type 1 ribosome inactivating protein reveals multiple l-asparagine-n-acetyl-d-glucosamine monosaccharide modifications: implications for cytotoxicity. *Molecular Medicine Reports,* 12**,** 5737-45.
Holmes, R. K. 2000. Biology and molecular epidemiology of diphtheria toxin and the tox gene. *The Journal of Infectious Diseases,* 181**,** S156-67.
Hunter, R. L., Olsen, M. R., Jagannath, C. & Actor, J. K. 2006. Multiple roles of cord factor in the pathogenesis of primary, secondary, and cavitary tuberculosis, including a revised description of the pathology of secondary disease. *Annals of Clinical and Laboratory Science,* 36**,** 371-86.
Jander, G., Rahme, L. G. & Ausubel, F. M. 2000. Positive correlation between virulence of *Pseudomonas aeruginosa* mutants in mice and insects. *Journal of Bacteriology,* 182**,** 3843.

Janeway, C. J. & Medzhitov, R. 2002. Innate immune recognition. *Annual Review of Immunology,* 20**,** 197-216.
Jang, J.-H., Shin, H. W., Lee, J. M., Lee, H.-W., Kim, E.-C. & Park, S. H. 2015. An overview of pathogen recognition receptors for innate immunity in dental pulp. *Mediators of Inflammation,* 2015**,** 12.
Jendrossek, V., Fillon, S., Belka, C., Müller, I., Puttkammer, B. & Lang, F. 2003. Apoptotic response of chang cells to infection with *Pseudomonas aeruginosa* strains PAK and PAO-I: molecular ordering of the apoptosis signaling cascade and role of type iv pili. *Infection and Immunity,* 71**,** 2665.
Joyce, S. A. & Gahan, C. G. M. 2010. Molecular pathogenesis of *Listeria monocytogenes* in the alternative model host *Galleria mellonella*. *Microbiology,* 156**,** 3456-68.
Katsukawa, C., Umeda, K., Inamori, I., Kosono, Y., Tanigawa, T., Komiya, T., Iwaki, M., Yamamoto, A. & Nakatsu, S. 2016. Toxigenic *Corynebacterium ulcerans* isolated from a wild bird (ural owl) and its feed (shrew-moles): comparison of molecular types with human isolates. *BMC Research Notes,* 9**,** 181.
Kelly, J. & Kavanagh, K. 2011. Caspofungin primes the immune response of the larvae of *Galleria mellonella* and induces a non-specific antimicrobial response. *Journal of Medical Microbiology,* 60**,** 189-96.
Keusch, G. T., Donohue-Rolfe, A. & Jacewicz, M. 1981. Shigella toxin(s) : description and role in diarrhea and dysentery. *Pharmacology & Therapeutics,* 15**,** 403-38.
Kim, S., Oh, D.-B. & Kwon, O. 2014. Sialidases of corynebacteria and their biotechnological applications. *In:* Burkovski, A. (ed.) *Corynebacterium diphtheriae* and related toxigenic species. Dordrecht: Springer Netherlands. pp. 247-60.
Kim, S., Oh, D.-B., Kwon, O. & Kang, H. A. 2010. Identification and functional characterization of the NanH extracellular sialidase from *Corynebacterium diphtheriae*. *The Journal of Biochemistry,* 147**,** 523-33.
Konowalchuk, J., Dickie, N., Stavric, S. & Speirs, J. I. 1978. Properties of an *Escherichia coli* cytotoxin. *Infection and Immunity,* 20**,** 575.
Kurz, C. L., Chauvet, S., Andrès, E., Aurouze, M., Vallet, I., Michel, G. P. F., Uh, M., Celli, J., Filloux, A., De Bentzmann, S., Steinmetz, I., Hoffmann, J. A., Finlay, B. B., Gorvel, J. P., Ferrandon, D. & Ewbank, J. J. 2003. Virulence factors of the human opportunistic pathogen *Serratia marcescens* identified by *in vivo* screening. *The EMBO Journal,* 22**,** 1451.
Kurz, C. L. & Ewbank, J. J. 2000. *Caenorhabditis elegans* for the study of host–pathogen interactions. *Trends in Microbiology,* 8**,** 142-4.
La Rosa, S. L., Casey, P. G., Hill, C., Diep, D. B., Nes, I. F. & Brede, D. A. 2013. *In vivo* assessment of growth and virulence gene expression during commensal and pathogenic lifestyles of luxABCDE-tagged *Enterococcus faecalis* strains in murine gastrointestinal and intravenous infection models. *Applied and Environmental Microbiology,* 79**,** 3986.
Lang, R. 2013. Recognition of the mycobacterial cord factor by mincle: relevance for granuloma formation and resistance to tuberculosis. *Frontiers in Immunology,* 4, 5.
Lange, A., Beier, S., Huson, D. H., Parusel, R., Iglauer, F. & Frick, J.-S. 2018. Genome sequence of *Galleria mellonella* (greater wax moth). *Genome announcements,* 6**,** e01220-17.
Lapointe, P., Wei, X. & Gariepy, J. 2005. A role for the protease-sensitive loop region of Shiga-like toxin 1 in the retrotranslocation of its A1 domain from the endoplasmic reticulum lumen. *Journal of Biological Chemistry,* 280**,** 23310-8.
Lartigue, M. F., Monnet, X., Le Fleche, A., Grimont, P. A., Benet, J. J., Durrbach, A., Fabre, M. & Nordmann, P. 2005. *Corynebacterium ulcerans* in an immunocompromised patient with diphtheria and her dog. *Journal of Clinical Microbiology,* 43**,** 999-1001.
Lavine, M. D. & Strand, M. R. 2002. Insect hemocytes and their role in immunity. *Insect Biochemistry and Molecular Biology,* 32**,** 1295-309.

Lebreton, F., Le Bras, F., Reffuveille, F., Ladjouzi, R., Giard, J. C., Leclercq, R. & Cattoir, V. 2011. *Galleria mellonella* as amodel for studying *Enterococcus faecium* host persistence. *Journal of Molecular Microbiology and Biotechnology,* 21**,** 191-6.

Lee, J. H., Wang, T., Ault, K., Liu, J., Schmitt, M. P. & Holmes, R. K. 1997. Identification and characterization of three new promoter/operators from *Corynebacterium diphtheriae* that are regulated by the diphtheria toxin repressor (DtxR) and iron. *Infection and Immunity,* 65**,** 4273.

Lee, W.-B., Kang, J.-S., Yan, J.-J., Lee, M. S., Jeon, B.-Y., Cho, S.-N. & Kim, Y.-J. 2012. Neutrophils promote mycobacterial trehalose dimycolate-induced lung inflammation via the mincle pathway. *PLOS Pathogens,* 8**,** e1002614.

Leek, M. D., Sivaloganathan, S., Devarj, S. K., Zamiri, I., Griffiths, G. D. & Green, M. A. 1990. Diphtheria with a difference—a rare *Corynebacterium* fatality with associated apoptotic cell death. *Histopathology,* 16**,** 187-9.

Leggett, B. A., De Zoysa, A., Abbott, Y. E., Leonard, N., Markey, B. & Efstratiou, A. 2010. Toxigenic *Corynebacterium diphtheriae* isolated from a wound in a horse. *Veterinary Record,* 166**,** 656-7.

Lehmann, K. B. & Neumann, R. O. 1896. *Atlas und grundriss der bakteriologie und lehrbuch der speziellen bakteriologischen diagnostik,* München.

Lipsky, B. A., Goldberger, A. C., Tompkins, L. S. & Plorde, J. J. 1982. Infections caused by nondiphtheria corynebacteria. *Clinical Infectious Diseases,* 4**,** 1220-35.

Loh, J. M. S., Adenwalla, N., Wiles, S. & Proft, T. 2013. *Galleria mellonella* larvae as an infection model for group A streptococcus. *Virulence,* 4**,** 419-28.

Lord, J. M., Smith, D. C. & Roberts, L. M. 1999. Toxin entry: how bacterial proteins get into mammalian cells. *Cellular Microbiology,* 1**,** 85-91.

Lowe, C. F., Bernard, K. A. & Romney, M. G. 2011. Cutaneous diphtheria in the urban poor population of Vancouver, British Columbia, Canada: a 10-year review. *Journal of Clinical Microbiology,* 49**,** 2664.

Lozhnikova, S. M., Pirogov, V. N., Piradov, M. A., Sakharova, A. V. & Liudkovskaia, I. G. 1997. [Diphtheritic polyneuropathy: clinico-morphologic study]. *Arkhiv patologii,* 59**,** 11-17.

Lu, A., Zhang, Q., Zhang, J., Yang, B., Wu, K., Xie, W., Luan, Y.-X. & Ling, E. 2014. Insect prophenoloxidase: the view beyond immunity. *Frontiers in Physiology,* 5**,** 252.

Madigan, M. T., Martinko, J. M., Dunlap, P. V. & Clark, D. P. 2009. Brock biology of microorganisms*,* 12 ed. Upper Saddle River, NJ, Pearson Education Inc. pp. 1061.

Mahajan-Miklos, S., Rahme, L. G. & Ausubel, F. M. 2000. Elucidating the molecular mechanisms of bacterial virulence using non-mammalian hosts. *Molecular Microbiology,* 37**,** 981-8.

Mandlik, A., Swierczynski, A., Das, A. & Ton-That, H. 2007. *Corynebacterium diphtheriae* employs specific minor pilins to target human pharyngeal epithelial cells. *Molecular Microbiology,* 64**,** 111-24.

Manjula, B. N. & Fischetti, V. A. 1986. Sequence homology of group A streptococcal Pep M5 protein with other coiled-coil proteins. *Biochemical and Biophysical Research Communications,* 140**,** 684-90.

Marchler-Bauer, A., Lu, S., Anderson, J. B., Chitsaz, F., Derbyshire, M. K., Deweese-Scott, C., Fong, J. H., Geer, L. Y., Geer, R. C., Gonzales, N. R., Gwadz, M., Hurwitz, D. I., Jackson, J. D., Ke, Z., Lanczycki, C. J., Lu, F., Marchler, G. H., Mullokandov, M., Omelchenko, M. V., Robertson, C. L., Song, J. S., Thanki, N., Yamashita, R. A., Zhang, D., Zhang, N., Zheng, C. & Bryant, S. H. 2010. CDD: a conserved domain database for the functional annotation of proteins. *Nucleic Acids Research,* 39**,** D225-9.

Marini, R. P., Cassiday, P. K., Venezia, J., Shen, Z., Buckley, E. M., Peters, Y., Taylor, N., Dewhirst, F. E., Tondella, M. L. & Fox, J. G. 2014. *Corynebacterium ulcerans* in ferrets. *Emerging infectious diseases,* 20**,** 159-61.

Martins, C., Faria, L., Souza, M., Camello, T., Velasco, E., Hirata Jr, R., Thuler, L. & Mattos-Guaraldi, A. 2009. Microbiological and host features associated with corynebacteriosis in cancer patients: a five-year study. *Memórias do Instituto Oswaldo Cruz,* 104**,** 905-13.

Mattos-Guaraldi, A., Sampaio, J., Santos, C., Pimenta, F., Pereira, G., Pacheco, L., Miyoshi, A., Azevedo, V., Moreira, L., Gutierrez, F., Costa, J., Costa-Filho, R., Damasco, P., Camello, T. & Hirata Jr, R. 2008. First detection of *Corynebacterium ulcerans* producing a diphtheria-like toxin in a case of human with pulmonary infection in the Rio de Janeiro metropolitan area, Brazil. *Memórias do Instituto Oswaldo Cruz,* 103**,** 396-400.

Mattos-Guaraldi, A. L., Cappelli, E. A., Previato, J. O., Formiga, L. C. D. & Andrade, A. F. B. 1999. Characterization of surface saccharides in two *Corynebacterium diphtheriae* strains. *FEMS Microbiology Letters,* 170**,** 159-166.

Mattos-Guaraldi, A. L., Hirata, R. & Azevedo, V. C. 2014. *Corynebacterium diphtheriae*, *Corynebacterium ulcerans* and *Corynebacterium pseudotuberculosis*—general aspects. *In:* Burkovski, A. (ed.) *Corynebacterium diphtheriae* and related toxigenic species. Dordrecht: Springer Netherlands. pp. 15-27.

Mckean, S. C., Davies, J. K. & Moore, R. J. 2007. Expression of phospholipase D, the major virulence factor of *Corynebacterium pseudotuberculosis*, is regulated by multiple environmental factors and plays a role in macrophage death. *Microbiology,* 153**,** 2203-11.

Mcnamara, P. J., Bradley, G. A. & Songer, J. G. 1994. Targeted mutagenesis of the phospholipase D gene results in decreased virulence of *Corynebacterium pseudotuberculosis*. *Molecular Microbiology,* 12**,** 921-30.

Meinel, D. M., Konrad, R., Berger, A., Konig, C., Schmidt-Wieland, T., Hogardt, M., Bischoff, H., Ackermann, N., Hormansdorfer, S., Krebs, S., Blum, H., Margos, G. & Sing, A. 2015. Zoonotic transmission of toxigenic *Corynebacterium ulcerans* strain, Germany, 2012. *Emerging Infectious Diseases,* 21**,** 356-8.

Meinel, D. M., Margos, G., Konrad, R., Krebs, S., Blum, H. & Sing, A. 2014. Next generation sequencing analysis of nine *Corynebacterium ulcerans* isolates reveals zoonotic transmission and a novel putative diphtheria toxin-encoding pathogenicity island. *Genome Medicine,* 6**,** 113.

Mekada, E., Okada, Y. & Uchida, T. 1988. Identification of diphtheria toxin receptor and a nonproteinous diphtheria toxin-binding molecule in vero cell membrane. *The Journal of Cell Biology,* 107**,** 511.

Merien, F. 2016. A journey with Elie Metchnikoff: from innate cell mechanisms in infectious diseases to quantum biology. *Frontiers in Public Health,* 4**,** 125.

Mishra, A. K., Alves, J. E., Krumbach, K., Nigou, J., Castro, A. G., Geurtsen, J., Eggeling, L., Saraiva, M. & Besra, G. S. 2012. Differential arabinan capping of lipoarabinomannan modulates innate immune responses and impacts T helper cell differentiation. *Journal of Biological Chemistry,* 287**,** 44173-83.

Miyagi, T. & Yamaguchi, K. 2012. Mammalian sialidases: physiological and pathological roles in cellular functions. *Glycobiology,* 22**,** 880-96.

Miyake, Y., Kaise, H., Isono, K.-I., Koseki, H., Kohno, K. & Tanaka, M. 2007. Protective role of macrophages in noninflammatory lung injury caused by selective ablation of alveolar epithelial type II cells. *The Journal of Immunology,* 178**,** 5001.

Möller, J., Kraner, M., Sonnewald, U., Sangal, V., Tittlbach, H., Winkler, J., Winkler, T. H., Melnikov, V., Lang, R., Sing, A., Mattos-Guaraldi, A. L. & Burkovski, A. 2019. Proteomics of diphtheria toxoid vaccines reveals multiple proteins that are immunogenic and may contribute to protection of humans against *Corynebacterium diphtheriae*. *Vaccine,* 37**,** 3061-70.

Mookerjee, B. K., Kanegasaki, S. & Kato, I. 1982. Effects of diphtheria toxin and other exotoxins on oxidant generation by human and murine phagocytes. *Developmental and Comparative Immunology,* 6**,** 161-70.

Moreira, L. D. O., Andrade, A. F. B., Vale, M. D., Souza, S. M. S., Hirata, R., Asad, L. M. O. B., Asad, N. R., Monteiro-Leal, L. H., Previato, J. O. & Mattos-Guaraldi, A. L. 2003. Effects of iron limitation on adherence and cell surface carbohydrates of *Corynebacterium diphtheriae* Strains. *Applied and Environmental Microbiology,* 69**,** 5907.

Moreira, L. O., Mattos-Guaraldi, A. L. & Andrade, A. F. B. 2008. Novel lipoarabinomannan-like lipoglycan (CdiLAM) contributes to the adherence of *Corynebacterium diphtheriae* to epithelial cells. *Archives of Microbiology,* 190**,** 521-30.

Morris, W. E., Uzal, F. A. & Cipolla, A. L. 2005. Pyogranulomatous meningoencephalitis in a goat due to *Corynebacterium ulcerans*. *Veterinary Record,* 156**,** 317.

Mukherjee, K., Altincicek, B., Hain, T., Domann, E., Vilcinskas, A. & Chakraborty, T. 2010. *Galleria mellonella* as a model system for studying *Listeria* pathogenesis. *Applied and Environmental Microbiology,* 76**,** 310.

Mukherjee, K. & Vilcinskas, A. 2014. Development and immunity-related micrornas of the lepidopteran model host *Galleria mellonella*. *BMC Genomics,* 15**,** 705.

Müller, H. E. 1974. Neuraminidase activity in *Streptococcus sanguis* and in the viridans group, and occurrence of acylneuraminate lyase in viridans organisms isolated from patients with septicemia. *Infection and Immunity,* 9**,** 323.

Munoz, L. E., Maueroder, C., Chaurio, R., Berens, C., Herrmann, M. & Janko, C. 2013. Colourful death: six-parameter classification of cell death by flow cytometry-dead cells tell tales. *Autoimmunity,* 46**,** 336-41.

Murakami, K., Hata, E., Hatama, S., Wada, Y., Ito, M., Ishikawa, Y. & Kadota, K. 2014. Eosinophilic granuloma with splendore-hoeppli material caused by toxigenic *Corynebacterium ulcerans* in a heifer. *Journal of Veterinary Medical Science,* 76**,** 931-5.

Murphy, J. R. 1996. *Corynebacterium diphtheriae*. *In:* Baron, S. (ed.) Medical microbiology. 4 ed. Galveston: Galveston (TX): University of Texas Medical Branch. pp. 32.

Naglich, J. G., Metherall, J. E., Russell, D. W. & Eidels, L. 1992. Expression cloning of a diphtheria toxin receptor: identity with a heparin-binding EGF-like growth factor precursor. *Cell,* 69**,** 1051-61.

Neal, S. & Efstratiou, A. 2007. Dipnet - establishment of a dedicated surveillance network for diphtheria in europe. Euro surveillance : bulletin Europeen sur les maladies transmissibles = European communicable disease bulletin [Online], 12**,** E-9-10. Available: http://europepmc.org/abstract/MED/18076863 [Accessed 02 June 2019].

O'loughlin, E. V. & Robins-Browne, R. M. 2001. Effect of Shiga toxin and Shiga-like toxins on eukaryotic cells. *Microbes and Infection,* 3**,** 493-507.

Ofek, I., Goldhar, J., Keisari, Y. & Sharon, N. 1995. Nonopsonic phagocytosis of microorganisms. *Annual Review of Microbiology,* 49**,** 239-76.

Olsen, R. J., Watkins, M. E., Cantu, C. C., Beres, S. B. & Musser, J. M. 2011. Virulence of serotype M3 group A streptococcus strains in wax worms (*Galleria mellonella* larvae). *Virulence,* 2**,** 111-9.

Ott, L. 2018. Adhesion properties of toxigenic corynebacteria. *AIMS Microbiology,* 4**,** 85-103.

Ott, L., Hacker, E., Kunert, T., Karrington, I., Etschel, P., Lang, R., Wiesmann, V., Wittenberg, T., Singh, A., Varela, C., Bhatt, A., Sangal, V. & Burkovski, A. 2017. Analysis of *Corynebacterium diphtheriae* macrophage interaction: dispensability of corynomycolic acids for inhibition of phagolysosome maturation and identification of a new gene involved in synthesis of the corynomycolic acid layer. *PLOS One,* 12**,** e0180105.

Ott, L., Höller, M., Gerlach, R. G., Hensel, M., Rheinlaender, J., Schäffer, T. E. & Burkovski, A. 2010a. *Corynebacterium diphtheriae* invasion-associated protein (DIP1281) is involved in cell surface organization, adhesion and internalization in epithelial cells. *BMC Microbiology,* 10**,** 2.

Ott, L., Höller, M., Rheinlaender, J., Schäffer, T. E., Hensel, M. & Burkovski, A. 2010b. Strain-specific differences in pili formation and the interaction of *Corynebacterium diphtheriae* with host cells. *BMC Microbiology,* 10**,** 257.

Ott, L., Mckenzie, A., Baltazar, M. T., Britting, S., Bischof, A., Burkovski, A. & Hoskisson, P. A. 2012. Evaluation of invertebrate infection models for pathogenic corynebacteria. *FEMS Immunology and Medical Microbiology,* 65**,** 413-21.

Ott, L., Scholz, B., Holler, M., Hasselt, K., Ensser, A. & Burkovski, A. 2013. Induction of the NF*κ*-B signal transduction pathway in response to *Corynebacterium diphtheriae* infection. *Microbiology,* 159**,** 126-35.

Pappenheimer, A. M. 1993. The story of a toxic protein, 1888–1992. *Protein Science,* 2**,** 292-8.

Pappenheimer, A. M., Jr. 1977. Diphtheria toxin. *Annual Review of Biochemistry,* 46**,** 69-94.

Park, S. Y., Kim, K. M., Lee, J. H., Seo, S. J. & Lee, I. H. 2007. Extracellular gelatinase of *Enterococcus faecalis* destroys a defense system in insect hemolymph and human serum. *Infection and Immunity,* 75**,** 1861.

Paton, M. W., Mercy, A. R., Wilkinson, F. C., Gardner, J. J., Sutherland, S. S. & Ellis, T. M. 1988. The effects of caseous lymphadenitis on wool production and body weight in young sheep. *Australian Veterinary Journal,* 65**,** 117-9.

Péchy-Tarr, M., Bruck, D. J., Maurhofer, M., Fischer, E., Vogne, C., Henkels, M. D., Donahue, K. M., Grunder, J., Loper, J. E. & Keel, C. 2008. Molecular analysis of a novel gene cluster encoding an insect toxin in plant-associated strains of *Pseudomonas fluorescens*. *Environmental Microbiology,* 10**,** 2368-86.

Peixoto, R. S., Hacker, E., Antunes, C. A., Weerasekera, D., Dias, A., Martins, C. A., Hirata Jr, R., Santos, K. R. N. D., Burkovski, A. & Mattos-Guaraldi, A. L. 2016. Pathogenic properties of a *Corynebacterium diphtheriae* strain isolated from a case of osteomyelitis. *Journal of Medical Microbiology,* 65**,** 1311-21.

Peixoto, R. S., Pereira, G. A., Sanches Dos Santos, L., Rocha-De-Souza, C. M., Gomes, D. L. R., Silva Dos Santos, C., Werneck, L. M. C., Dias, A. D. S. D. O., Hirata, R., Nagao, P. E. & Mattos-Guaraldi, A. L. 2014. Invasion of endothelial cells and arthritogenic potential of endocarditis-associated *Corynebacterium diphtheriae*. *Microbiology,* 160**,** 537-46.

Pereira, C. T., De Barros, P. P., Fugisaki, R. L., Rossoni, D. R., Ribeiro, D. F., De Menezes, T. R., Junqueira, C. J. & Scorzoni, L. 2018. Recent advances in the use of *Galleria mellonella* model to study immune responses against human pathogens. *Journal of Fungi,* 4**,** pii E128.

Pradel, E., Zhang, Y., Pujol, N., Matsuyama, T., Bargmann, C. I. & Ewbank, J. J. 2007. Detection and avoidance of a natural product from the pathogenic bacterium *Serratia marcescens* by *Caenorhabditis elegans*. *Proceedings of the National Academy of Sciences,* 104**,** 2295.

Puech, V., Chami, M., Lemassu, A., Lanéelle, M.-A., Schiffler, B., Gounon, P., Bayan, N., Benz, R. & Daffé, M. 2001. Structure of the cell envelope of corynebacteria: importance of the non-covalently bound lipids in the formation of the cell wall permeability barrier and fracture plane. *Microbiology,* 147**,** 1365-82.

Pujol, N., Link, E. M., Liu, L. X., Kurz, C. L., Alloing, G., Tan, M.-W., Ray, K. P., Solari, R., Johnson, C. D. & Ewbank, J. J. 2001. A reverse genetic analysis of components of the Toll signaling pathway in *Caenorhabditis elegans*. *Current Biology,* 11**,** 809-21.

Puliti, M., Nizet, V., Von Hunolstein, C., Bistoni, F., Mosci, P., Oreflci, G. & Tissi, L. 2000. Severity of group B streptococcal arthritis is correlated with β-hemolysin expression. *The Journal of Infectious Diseases,* 182**,** 824-32.

Puliti, M., Von Hunolstein, C., Marangi, M., Bistoni, F. & Tissi, L. 2006. Experimental model of infection with non-toxigenic strains of *Corynebacterium diphtheriae* and development of septic arthritis. *Journal of Medical Microbiology,* 55**,** 229-35.

Putong, N., Agustin, G., Pasubillo, M., Miyagi, K. & Dimaano, E. M. 2011. Diphtheria-like illness due to *Corynebacterium ulcerans* infection. *Tropical Medicine and Health,* 39**,** 1-2.

Quiblier, C., Seidl, K., Roschitzki, B., Zinkernagel, A. S., Berger-Bächi, B. & Senn, M. M. 2013. Secretome analysis defines the major role of secDF in *Staphylococcus aureus* virulence. *PLoS One,* 8**,** e63513.

Rau, J., Blazey, B., Contzen, M. & Sting, R. 2012. *Corynebacterium ulcerans* infection in roe deer (capreolus capreolus). *Berliner und Munchener tierarztliche Wochenschrift,* 125**,** 159-62.

Richard, J. F., Petit, L., Gibert, M., Marvaud, J. C., Bouchaud, C. & Popoff, M. R. 1999. Bacterial toxins modifying the actin cytoskeleton. *International Microbiology,* 2**,** 185-94.

Roggentin, P., Schauer, R., Hoyer, L. L. & Vimr, E. R. 1993. The sialidase superfamily and its spread by horizontal gene transfer. *Molecular Microbiology,* 9**,** 915-21.

Ruckdeschel, K., Roggenkamp, A., Lafont, V., Mangeat, P., Heesemann, J. & Rouot, B. 1997. Interaction of *Yersinia enterocolitica* with macrophages leads to macrophage cell death through apoptosis. *Infection and Immunity,* 65**,** 4813.

Sabbadini, P. S., Assis, M. C., Trost, E., Gomes, D. L. R., Moreira, L. O., Dos Santos, C. S., Pereira, G. A., Nagao, P. E., Azevedo, V. a. D. C., Hirata Júnior, R., Dos Santos, A. L. S., Tauch, A. & Mattos-Guaraldi, A. L. 2012. *Corynebacterium diphtheriae* 67-72p hemagglutinin, characterized as the protein DIP0733, contributes to invasion and induction of apoptosis in hep-2 cells. *Microbial Pathogenesis,* 52**,** 165-76.

Saelinger, C., Bonventre, P. F. & Imhoff, J. 1975. Interaction of toxin of *Corynebacterium diphtheriae* with phagocytes from susceptible and resistant species. *The Journal of Infectious Diseases,* 131**,** 431-8.

Sánchez-Alcázar, J. A., Rodríguez-Hernández, Á., Cordero, M. D., Fernández-Ayala, D. J. M., Brea-Calvo, G., Garcia, K. & Navas, P. 2007. The apoptotic microtubule network preserves plasma membrane integrity during the execution phase of apoptosis. *Apoptosis,* 12**,** 1195-208.

Sangal, V. & Hoskisson, P. A. 2014. Corynephages: infections of the infectors. *In:* Burkovski, A. (ed.) *Corynebacterium diphtheriae* and related toxigenic species*.* Dordrecht: Springer Netherlands. pp. 67-81.

Sarantis, H. & Grinstein, S. 2012. Subversion of phagocytosis for pathogen survival. *Cell Host and Microbe,* 12**,** 419-31.

Schick, J., Etschel, P., Bailo, R., Ott, L., Bhatt, A., Lepenies, B., Kirschning, C., Burkovski, A. & Lang, R. 2017. Toll-like receptor 2 and mincle cooperatively sense corynebacterial cell wall glycolipids. *Infection and Immunity,* 85**,** e00075-17.

Schoen, C., Unzicker, C., Stuhler, G., Elias, J., Einsele, H., Grigoleit, G. U., Abele-Horn, M. & Mielke, S. 2009. Life-threatening infection caused by daptomycin-resistant *Corynebacterium jeikeium* in a neutropenic patient. *Journal of Clinical Microbiology,* 47**,** 2328.

Schuchat, A. 1999. Group B streptococcus. *The Lancet,* 353**,** 51-6.

Schuhegger, R., Schoerner, C., Dlugaiczyk, J., Lichtenfeld, I., Trouillier, A., Zeller-Peronnet, V., Busch, U., Berger, A., Kugler, R., Hormansdorfer, S. & Sing, A. 2009. Pigs as source for toxigenic *Corynebacterium ulcerans*. *Emerging Infectious Diseases,* 15**,** 1314-5.

Schüller, S. 2011. Shiga toxin interaction with human intestinal epithelium. *Toxins,* 3**,** 626-39.

Seto, Y., Komiya, T., Iwaki, M., Kohda, T., Mukamoto, M., Takahashi, M. & Kozaki, S. 2008. Properties of corynephage attachment site and molecular epidemiology of *Corynebacterium ulcerans* isolated from humans and animals in japan. *Japanese Journal of Infectious Diseases,* 61**,** 116-22.

Shao, H., Luo, R., Wang, X., Pan, X. & Chen, G. 2015. Management of a patient with small-area burns, severe sepsis and superficial vein thrombosis. *Journal of Wound Care,* 24**,** 73-8.

Silva, M. & Correia-Neves, M. 2012. Neutrophils and macrophages: the main partners of phagocyte cell systems. *Frontiers in Immunology,* 3**,** 174.

Simpson-Lourêdo, L., Silva, C. M. F., Hacker, E., Souza, N. F., Santana, M. M., Antunes, C. A., Nagao, P. E., Hirata, R., Burkovski, A., Villas Bôas, M. H. S. & Mattos-Guaraldi, A. L. 2019. Detection and virulence potential of a phospholipase D-negative *Corynebacterium ulcerans* from a concurrent diphtheria and infectious mononucleosis case. *Antonie van Leeuwenhoek*, 112**,** 1055-65.

Sioud, M. 2005. Induction of inflammatory cytokines and interferon responses by double-stranded and single-stranded sirnas is sequence-dependent and requires endosomal localization. *Journal of Molecular Biology,* 348**,** 1079-90.

Slater, J. L., Gregson, L., Denning, D. W. & Warn, P. A. 2011. Pathogenicity of *Aspergillus fumigatus* mutants assessed in *Galleria mellonella* matches that in mice. *Medical Mycology,* 49**,** S107-13.

Söderhäll, K. & Cerenius, L. 1998. Role of the prophenoloxidase-activating system in invertebrate immunity. *Current Opinion in Immunology,* 10**,** 23-8.
Stirpe, F. & Battelli, M. G. 2006. Ribosome-inactivating proteins: Progress and problems. *Cellular and Molecular Life Sciences CMLS,* 63**,** 1850-66.
Sydor, T., Von Bargen, K., Hsu, F. F., Huth, G., Holst, O., Wohlmann, J., Becken, U., Dykstra, T., Sohl, K., Lindner, B., Prescott, J. F., Schaible, U. E., Utermohlen, O. & Haas, A. 2013. Diversion of phagosome trafficking by pathogenic *Rhodococcus equi* depends on mycolic acid chain length. *Cellular Microbiology,* 15**,** 458-73.
Sykes, J. E., Mapes, S., Lindsay, L. L., Samitz, E. & Byrne, B. A. 2010. *Corynebacterium ulcerans* bronchopneumonia in a dog. *Journal of Veterinary Internal Medicine,* 24**,** 973-6.
Takayama, K., Wang, C. & Besra, G. S. 2005. Pathway to synthesis and processing of mycolic acids in *Mycobacterium tuberculosis*. *Clinical Microbiology Reviews,* 18**,** 81.
Takeuchi, O., Hoshino, K., Kawai, T., Sanjo, H., Takada, H., Ogawa, T., Takeda, K. & Akira, S. 1999. Differential roles of TLR2 and TLR4 in recognition of Gram-negative and Gram-positive bacterial cell wall components. *Immunity,* 11**,** 443-51.
Tashjian, J. J. & Campbell, S. G. 1983. Interaction between caprine macrophages and *Corynebacterium pseudotuberculosis*: an electron microscopic study. *American journal of veterinary research,* 44**,** 690-3.
Tauch, A. & Burkovski, A. 2015. Molecular armory or niche factors: virulence determinants of *Corynebacterium* species. *FEMS Microbiology Letters,* 362.
Tenor, J. L., Mccormick, B. A., Ausubel, F. M. & Aballay, A. 2004. *Caenorhabditis elegans*-based screen identifies salmonella virulence factors required for conserved host-pathogen interactions. *Current Biology,* 14**,** 1018-24.
Terwisscha van Scheltinga, A. C., Hennig, M. & Dijkstra, B. W. 1996. The 1.8 å resolution structure of hevamine, a plant chitinase/lysozyme, and analysis of the conserved sequence and structure motifs of glycosyl hydrolase family 18. *Journal of Molecular Biology,* 262**,** 243-57.
Thelaus, J., Lundmark, E., Lindgren, P., Sjödin, A. & Forsman, M. 2018. *Galleria mellonella* reveals niche differences between highly pathogenic and closely related strains of *Francisella* spp. *Frontiers in cellular and infection microbiology,* 8**,** 188.
Thorburn, A., Thorburn, J. & Frankel, A. E. 2004. Induction of apoptosis by tumor cell-targeted toxins. *Apoptosis,* 9**,** 19-25.
Titus, M. A. 1999. A class vii unconventional myosin is required for phagocytosis. *Current Biology,* 9**,** 1297-303.
Tiwari, T. S. P. 2012. Diphtheria. *In:* Brunette GW (ed) CDC health information for international travel 2012. The yellow book. Oxford Iniversity Press, Inc. New York, pp. 162–5.
Tojo, S., Naganuma, F., Arakawa, K. & Yokoo, S. 2000. Involvement of both granular cells and plasmatocytes in phagocytic reactions in the greater wax moth, *Galleria mellonella*. *Journal of Insect Physiology,* 46**,** 1129-35.
Trost, E., Al-Dilaimi, A., Papavasiliou, P., Schneider, J., Viehoever, P., Burkovski, A., Soares, S. C., Almeida, S. S., Dorella, F. A., Miyoshi, A., Azevedo, V., Schneider, M. P., Silva, A., Santos, C. S., Santos, L. S., Sabbadini, P., Dias, A. A., Hirata, R., Mattos-Guaraldi, A. L. & Tauch, A. 2011. Comparative analysis of two complete *Corynebacterium ulcerans* genomes and detection of candidate virulence factors. *BMC Genomics,* 12**,** 383.
Trost, E., Blom, J., De Castro Soares, S., Huang, I. H., Al-Dilaimi, A., Schröder, J., Jaenicke, S., Dorella, F. A., Rocha, F. S., Miyoshi, A., Azevedo, V., Schneider, M. P., Silva, A., Camello, T. C., Sabbadini, P. S., Santos, C. S., Santos, L. S., Hirata, R., Mattos-Guaraldi, A. L., Efstratiou, A., Schmitt, M. P., Ton-That, H. & Tauch, A. 2012. Pangenomic study of *Corynebacterium diphtheriae* that provides insights into the genomic diversity of pathogenic isolates from cases of classical diphtheria, endocarditis, and pneumonia. *Journal of Bacteriology,* 194**,** 3199.
Tsai, C. J.-Y., Loh, J. M. S. & Proft, T. 2016. *Galleria mellonella* infection models for the study of bacterial diseases and for antimicrobial drug testing. *Virulence,* 7**,** 214-29.

Tsai, P.-J., Lin, Y.-S., Kuo, C.-F., Lei, H.-Y. & Wu, J.-J. 1999. Group A streptococcus induces apoptosis in human epithelial cells. *Infection and Immunity,* 67**,** 4334.
Underhill, D. M. & Goodridge, H. S. 2012. Information processing during phagocytosis. *Nature Reviews Immunology,* 12**,** 492.
Van Der Peet, P. L., Gunawan, C., Torigoe, S., Yamasaki, S. & Williams, S. J. 2015. Corynomycolic acid-containing glycolipids signal through the pattern recognition receptor mincle. *Chemical Communications,* 51**,** 5100-3.
Varki, A. 1993. Biological roles of oligosaccharides: All of the theories are correct. *Glycobiology,* 3**,** 97-130.
Varol, B., Özerman Edis, B. & Bektaş, M. 2014. Toxin structure, delivery and action. *In:* Burkovski, A. (ed.) *Corynebacterium diphtheriae* and related toxigenic species. Dordrecht: Springer Netherlands. pp. 83-91.
Venezia, J., Cassiday, P. K., Marini, R. P., Shen, Z., Buckley, E. M., Peters, Y., Taylor, N., Dewhirst, F. E., Tondella, M. L. & Fox, J. G. 2012. Characterization of *Corynebacterium* species in macaques. *Journal of medical microbiology,* 61**,** 1401-8.
Ventura, M., Canchaya, C., Tauch, A., Chandra, G., Fitzgerald, G. F., Chater, K. F. & Van Sinderen, D. 2007. Genomics of actinobacteria: tracing the evolutionary history of an ancient phylum. *Microbiology and Molecular Biology Reviews,* 71**,** 495-548.
Vieira, O. V., Botelho, R. J. & Grinstein, S. 2002. Phagosome maturation: aging gracefully. *Biochemical Journal,* 366**,** 689.
Vimr, E. & Lichtensteiger, C. 2002. To sialylate, or not to sialylate: that is the question. *Trends in Microbiology,* 10**,** 254-7.
Vimr, E. R. 1994. Microbial sialidases: does bigger always mean better? *Trends in Microbiology,* 2**,** 271-7.
Vitek, C. R. & Wharton, M. 1998. Diphtheria in the former soviet union: reemergence of a pandemic disease. *Emerging infectious diseases,* 4**,** 539-50.
Vogel, H., Altincicek, B., Glockner, G. & Vilcinskas, A. 2011. A comprehensive transcriptome and immune-gene repertoire of the lepidopteran model host *Galleria mellonella*. *BMC Genomics,* 12**,** 308.
Wagner, K. S., White, J. M., Crowcroft, N. S., De Martin, S., Mann, G. & Efstratiou, A. 2010. Diphtheria in the united kingdom, 1986–2008: the increasing role of *Corynebacterium ulcerans*. *Epidemiology and Infection,* 138**,** 1519-30.
Walker, N. I., Harmon, B. V., Gobe, G. C. & Kerr, J. F. 1988. Patterns of cell death. *Methods and Achievments in Experimental Pathology,* 13**,** 18-54.
Wand, M. E., Müller, C. M., Titball, R. W. & Michell, S. L. 2011. Macrophage and *Galleria mellonella* infection models reflect the virulence of naturally occurring isolates of B. *pseudomallei*, B. *thailandensis* and B. *oklahomensis*. *BMC Microbiology,* 11**,** 11.
Wang, J. & London, E. 2009. The membrane topography of the diphtheria toxin T domain linked to the a chain reveals a transient transmembrane hairpin and potential translocation mechanisms. *Biochemistry,* 48**,** 10446-56.
Warren, L. & Spearing, C. W. 1963. Sialidase (neuraminidase) of *Corynebacterium diphtheriae*. *Journal of Bacteriology,* 86**,** 950.
Wassenaar, T. M. & Gaastra, W. 2001. Bacterial virulence: can we draw the line? *FEMS Microbiology Letters,* 201**,** 1-7.
Weerasekera, D., Fastner, T., Lang, R., Burkovski, A. & Ott, L. 2019a. Of mice and men: Interaction of *Corynebacterium diphtheriae* strains with murine and human phagocytes. *Virulence,* 10**,** 414-28.
Weerasekera, D., Möller, J., Kraner, M. E., Antunes, C. A., Mattos-Guaraldi, A.-L. & Burkovski, A. 2019b. Beyond diphtheria toxin: cytotoxic proteins of *Corynebacterium ulcerans* and *Corynebacterium diphtheriae*. *Microbiology,* DOI 10.1099/mic.0.000820.
Weerasekera, D., Stengel, F., Sticht, H., De Mattos Guaraldi, A. L., Burkovski, A. & Azevedo Antunes, C. 2018. The C-terminal coiled-coil domain of *Corynebacterium diphtheriae* DIP0733 is crucial for interaction with epithelial cells and pathogenicity in invertebrate animal model systems. *BMC Microbiology,* 18**,** 106.

Wes, P. D. & Bargmann, C. I. 2001. *C. elegans* odour discrimination requires asymmetric diversity in olfactory neurons. *Nature,* 410**,** 698-701.
WHO, World Health Organization. 2015. Diphtheria reported cases [Online]. Available: https://apps.who.int/immunization_monitoring/globalsummary/timeseries/tsincidenced iphtheria.html [Accessed 02 June 2019].
Wilson, M. J., Brandon, M. R. & Walker, J. 1995. Molecular and biochemical characterization of a protective 40-kilodalton antigen from *Corynebacterium pseudotuberculosis*. *Infection and Immunity,* 63**,** 206.
Wood, G. E., Dutro, S. M. & Totten, P. A. 2001. *Haemophilus ducreyi* inhibits phagocytosis by U-937 cells, a human macrophage-like cell line. *Infection and Immunity,* 69**,** 4726.
Yamaizumi, M., Mekada, E., Uchida, T. & Okada, Y. 1978. One molecule of diphtheria toxin fragment A introduced into a cell can kill the cell. *Cell,* 15**,** 245-50.
Yook, K. & Hodgkin, J. 2007. Mos1 mutagenesis reveals a diversity of mechanisms affecting response of *Caenorhabditis elegans* to the bacterial pathogen *Microbacterium nematophilum*. *Genetics,* 175**,** 681.
Zdybicka-Barabas, A., Mak, P., Jakubowicz, T. & Cytryńska, M. 2014. Lysozyme and defense peptides as suppressors of phenoloxidase activity in *Galleria mellonella*. *Archives of Insect Biochemistry and Physiology,* 87**,** 1-12.
Zhang, Y., Lu, H. & Bargmann, C. I. 2005. Pathogenic bacteria induce aversive olfactory learning in *Caenorhabditis elegans*. *Nature,* 438**,** 179-84.
Zhi, X. Y., Li, W. J. & Stackebrandt, E. 2009. An update of the structure and 16S rRNA gene sequence-based definition of higher ranks of the class actinobacteria, with the proposal of two new suborders and four new families and emended descriptions of the existing higher taxa. *International Journal of Systemic and Evolutionary Microbiology,* 59**,** 589-608.

10. ABBREVIATIONS

Adenosine diphosphate	ADP
AIM2-like receptor	ALR
Basic local alignment search tool	BLAST
Bone marrow-derived macrophage	BMM
Caseous lymphadenitis	CLA
Catalytic domain	C-domain
Corynebacterium, *Mycobacterium, Norcadia* and *Rhodococcus*	CMNR
Colony forming unit	CFU
C-type lectin receptor	CLR
Damage-associated molecular patterns	DAMPs
Deoxyribonucleic acid	DNA
Diphtheria toxin	DT
Diphtheria toxin repressor	DtxR
Elongation factor-2	EF-2
Endoplasmic reticulum	ER
Eukaryotic linear motif	ELM
Extracellular gelatinase	GelE
Fc receptor gamma chain	FcRγ
Fluorescence insecticidal toxin	Fit
Galleria mellonella cecropin	Gm cecropin
Globotriaosylceramide-3	Gb3
Granulocyte colony stimulating factor	G-CSF
Heparin binding-epidermal growth factor	HB-EGF
Interleukin-6	IL-6
Interleukin-1 receptor associated kinase	IRAK
Lipoarabinomannan	LAM
Lipomannan	LM
Matrix-assisted laser desorption ionization with time-of-flight	MALDI-TOF
Microbial surface component recognizing adhesion matrix molecules	MSCRAMMs
Nicotinamide adenine dinucleotide	NAD
Nitric oxide	NO
Nuclear factor kappa B	NF-κB
Nucleotide-binding oligomerization domain-like receptors	NLRs

Pattern recognition receptors	PRRs
Pathogen-associated molecular patterns	PAMPs
Pathogenicity island	PAI
Phosphatidyl serine	PS
Phospholipase D	PLD
Receptor binding domain	R-domain
Retinoic acid-inducible gene-1-like receptors	RLRs
Ribosome-binding protein	Rbp
Ribosome-inactivating protein	RIP
Shiga-like toxins	SLTs
Shiga toxin	Stx
Shiga-like toxin producing *E. coli*	STEC
Short linear motifs	SLiMs
Sodium dodecyl sulfate polyacrylamide gel electrophoresis	SDS-PAGE
Tellurite resistance	Te^R
Toll-like receptor	TLR
Toll/IL-1 receptor	TIR
Translocation domain	T-domain
Trehalose dicorynomycolates	TDCM
Trehalose dimycolate	TDM
Trehalose monocorynomycolates	TMCM
Trehalose monomycolate	TMM
Tumor necrosis factor-alpha	TNFα

11. CONTRIBUTIONS

11.1. Beyond diphtheria toxin: cytotoxic proteins of *Corynebacterium ulcerans* and *Corynebacterium diphtheriae* (Weerasekera et al., 2019b)

Dulanthi Weerasekera, Jens Möller, Max Edmund Kraner, Camila Azevedo Antunes, Ana Luíza Mattos-Guaraldi and Andreas Burkovski. *Microbiology*, 2019, DOI 10.1099/mic.0. 000820

- *In vivo* and *in vitro* experiments
    - *C. elegans* colonization and survival assays
    - Infection of *G. mellonella* and health index score measurements
    - Transepithelial resistance assays
    - Vero cell cytotoxicity assay
    - LDH release assay
    - Phagocytosis and survival assay
    - Sample preparation for mass spectrometry analyses
- Bioinformatic analyses
- Cloning: construction of the mutant strain and overexpression plasmids
- RNA isolation and hybridization experiments
- Microscopy
- Analysis and presentation of the data
- Involved in writing of the manuscript

11.2. Of mice and men: Interaction of *Corynebacterium diphtheriae* strains with murine and human phagocytes (Weerasekera et al., 2019a)

Dulanthi Weerasekera, Tamara Fastner, Roland Lang, Andreas Burkovski and Lisa Ott. *Virulence*, 2019, 10: 414-428

- *In vitro* experiments
  - Phagocytosis and survival assays: primary macrophages from C57BL/6, Clec4e$^{-/-}$ and Myd88$^{-/-}$ mice
  - Phagocytosis and survival assays: human THP-1 cells
  - NF-κB reporter assay
  - Determination of cytokine excretion
  - LDH release assay
  - Griess assay
  - TLR2 reporter assay
- Preparation of the diagram and schematic illustration of the data
- Analysis and presentation of the data
- Involved in writing and proofreading of the manuscript

11.3. The C-terminal coiled-coil domain of *Corynebacterium diphtheriae* DIP0733 is crucial for interaction with epithelial cells and pathogenicity in invertebrate animal model systems (Weerasekera et al., 2018)

Dulanthi Weerasekera, Franziska Stengel, Heinrich Sticht, Ana Luíza de Mattos-Guaraldi, Andreas Burkovski and Camila Azevedo Antunes. *BMC Microbiology*, 2018, 18: 106

- *In vivo* and *in vitro* experiments
    - Infection of *G. mellonella* and health index score measurements
    - Extracellular matrix and plasma protein binding assays
    - Adhesion and invasion assays
    - Transepithelial resistance assays
- RNA isolation and hybridization experiments
- Analysis and presentation of the data
- Involved in writing of the manuscript

11.4. Pathogenic properties of *a Corynebacterium diphtheriae* strain isolated from a case of osteomyelitis (Peixoto et al., 2016)

Renata Stavracakis Peixoto, Elena Hacker, Camila Azevedo Antunes, **Dulanthi Weerasekera**, Alexandre Alves de Souza de Oliveira Dias, Carlos Alberto Martins, Raphael Hirata Júnior, Kátia Regina Netto dos Santos, Andreas Burkovski and Ana Luíza Mattos-Guaraldi. *Journal of Medical Microbiology*, 2016, 65: 1311–1321

- Extracellular matrix and plasma protein binding assays
- Involved in revising the manuscript

12. PUBLICATIONS

MICROBIOLOGY

RESEARCH ARTICLE

Weerasekera *et al.*, *Microbiology*

DOI 10.1099/mic.0.000820

MICROBIOLOGY SOCIETY

Beyond diphtheria toxin: cytotoxic proteins of *Corynebacterium ulcerans* and *Corynebacterium diphtheriae*

Dulanthi Weerasekera[1], Jens Möller[1], Max Edmund Kraner[2], Camila Azevedo Antunes[1,3], Ana Luiza Mattos-Guaraldi[3] and Andreas Burkovski[1,*]

Abstract

Diphtheria toxin is one of the best investigated bacterial toxins and the major virulence factor of toxigenic *Corynebacterium diphtheriae* and *Corynebacterium ulcerans* strains. However, also diphtheria toxin-free strains of these two species can cause severe infections in animals and humans, indicating the presence of additional virulence factors. In this study, we present a first characterization of two proteins with cytotoxic effect in corynebacteria. A putative ribosome-binding protein (AEG80717, CULC809_00177), first annotated in a genome sequencing project of *C. ulcerans* strain 809, was investigated in detail together with a homologous protein identified in *C. diphtheriae* strain HC04 (AEX80148, CDHC04_0155) in this study. The corresponding proteins show striking structural similarity to Shiga-like toxins. Interaction of wild-type, mutant and complementation as well as overexpression strains with invertebrate model systems and cell lines were investigated. Depending on the presence of the corresponding genes, detrimental effects were observed *in vivo* in two invertebrate model systems, *Caenorhabditis elegans* and *Galleria mellonella*, and on various animal and human epithelial and macrophage cell lines *in vitro*. Taken together, our results support the idea that pathogenicity of corynebacteria is a multifactorial process and that new virulence factors may influence the outcome of potentially fatal corynebacterial infections.

INTRODUCTION

Diphtheria is a paradigm of an infectious disease caused by toxigenic bacteria. Classical diphtheria of the upper respiratory tract, which are transmitted by respiratory droplets, is characterized by a thick, dirty-grayish or brownish pseudomembrane, which renders breathing difficult. By coughing the pseudomembrane might be removed and healing might be achieved; however, more often obstruction of airways results in suffocation and death (for review, see [1]).

In 1884, Loeffler demonstrated that *Corynebacterium diphtheriae* is the etiological agent of diphtheria, not only providing key evidence for Koch's postulates on the germ theory, but also postulating that the secretion of a toxin by *C. diphtheriae* is causing the often fatal damage on distant organs [2]. This idea was supported by Roux and Yersin, who showed that sterile filtrates of *C. diphtheriae* cultures can evoke damages upon injection in animals that are similar to those caused by diphtheria in humans, indicating that diphtheria toxin is the main virulence factor of *C. diphtheriae* and responsible for the life-threatening symptoms of respiratory diphtheria [3]. At the beginning of the twentieth century, the work of scientists in North America and Europe including Ehrlich, Fraenkel, Park, Ramon, von Behring and others, laid the basis for diphtheria vaccination and a consequent sharp decline of diphtheria cases (for a review, see [4]). However, the disease was never fully eliminated, still a few thousand cases are reported to the World Health Organization every year [5, 6] and even today, *C. diphtheriae* is present on the list of the most important global death-provoking pathogens [7].

Diphtheria toxin is encoded on a temperate bacteriophage, which during lysogeny is capable of toxin production (for

Received 28 November 2018; Accepted 24 May 2019; Published 04 June 2019

Author affiliations: [1]Microbiology Division, Friedrich-Alexander-University of Erlangen-Nuremberg, Erlangen, Germany; [2]Biochemistry Division, Friedrich-Alexander-University of Erlangen-Nuremberg, Erlangen, Germany; [3]Laboratory of Diphtheria and Corynebacteria of Clinical Relevance-LDCIC, Faculty of Medical Sciences, Rio de Janeiro State University, Rio de Janeiro, Brazil.

***Correspondence:** Andreas Burkovski, andreas.burkovski@fau.de

Keywords: diphtheria; exotoxin; ribosome-binding protein; toxigenic corynebacteria; Vero cells.

Abbreviations: c.f.u., colony-forming units; DEMEM, Dulbecco's modified Eagle's medium; FBS, fetal bovine serum; FDR, false discovery rate; FDR, false discovery rate; m.o.i., multiplicity of infection; NGM, nematode growth medium; SD, standard deviation; SEM, standard error of the mean; TFA, trifluoroacetic acid.

Two supplementary figures and one supplementary table are available with the online version of this article.

a recent review, see [8]). Besides *C. diphtheriae*, two closely related species, *Corynebacterium pseudotuberculosis* and *Corynebacterium ulcerans*, can be lysogenized by *tox*-positive corynephages and subsequently allow diphtheria toxin production under certain conditions, i.e. during iron limitation [8–10]. Recently, a novel putative diphtheria toxin-encoding pathogenicity island and a corynephage-independent transmission pathway for the *tox* gene was identified in *C. ulcerans* [11].

The pathogenicity of *C. ulcerans* does not necessarily depend on the production of diphtheria toxin [12, 13]. When the genome of *C. ulcerans* strain 809, isolated from an 80-year-old woman with fatal pulmonary infection [14, 15] was sequenced and annotated, no β-corynephage encoding the diphtheria toxin was detected [16], despite the fact that preliminary experiments hint to the presence of a diphtheria toxin B subunit [14]. Therefore, the sequenced *C. ulcerans* 809 isolate was regarded as non-toxigenic with respect to the synthesis of the diphtheria toxin [16]. The absence of the *tox* gene in *C. ulcerans* 809 may also explain why the medical treatment of the elderly patient with the diphtheria antitoxin was unsuccessful [14, 16].

In contrast, a gene encoding a putative ribosome-binding protein (Rbp), comprising a ribosome-inactivating protein domain was found [16]. Despite a low amino acid identity of only 24 % between the deduced amino acid sequence of *C. ulcerans* Rbp and the A chain of the *Escherichia coli* Shiga-like toxins SLT-1 and SLT-2, all conserved amino acid residues needed for the catalytic N-glycosidase activity were identified. Furthermore, an *in silico* structure model of Rbp showed significant similarities to the A chain of SLT-1 from *E. coli* [16].

Shiga-like toxins comprise two domains, A and B. The A subunit has N-glycosidase activity, which is responsible for cleavage of an adenine from the 28S rRNA of the 60S ribosome. This renders the 28S rRNA unable to interact with the elongation factors EF-1 and EF-2, stops protein synthesis resulting in cell death. The B subunit forms a pentamer that binds to the receptor globotriaosylceramide (Gb3) in eukaryotic cells and facilitates receptor-mediated endocytosis [17–19].

The *rbp* gene of strain 809 (CULC809_00177) has a significantly lower G+C content of 45.1 % compared to the complete genome sequence, which comprises a G+C content of 53.3 %. Together with the fact that the gene is located between genes encoding a putative phage integrase (CULC809_00176) and a transposase (CULC809_00178), this suggests acquisition by horizontal gene transfer [16]. Until now, *C. ulcerans* 809 is the only corynebacterial strain for which a corresponding Rbp has been described, while experimental data for this putative toxin were completely lacking until now.

In this study, we present a functional characterization of *C. ulcerans* Rbp in respect to its effect on different invertebrate model systems and cell lines. In addition, we identified and characterized a homologous protein in the non-toxigenic *C. diphtheriae* strain HC04 (CDHC04_0155), isolated from a fatal case of endocarditis [20].

METHODS

Bacterial strains and culture conditions

Bacteria were incubated at 37 °C. For *E. coli* and *Salmonella* strains Luria–Bertani (LB) medium and for *C. diphtheriae*, *C. ulcerans* and *C. glutamicum* strains heart infusion (HI) was used. When appropriate, 50 µg ml^{-1} kanamycin or 25 µg ml^{-1} chloramphenicol and 1 mM IPTG was added. Bacterial strains, cell lines and plasmids used in this study are listed in Table 1.

Bioinformatic analyses of putative Rbps

Multiple amino acid sequence alignments were generated with the Clustal Omega program at web services from EMBL-EBL [31, 32]. The signal peptides and the cleavage sites were predicted using the SignalP 4.1 server [33]. The three-dimensional model of the hypothetical Rbp-like from *C. diphtheriae* HC04 (CDHC04_0155) was predicted using the Phyre2 protein fold recognition server [34] and the resulting structure model was aligned with the template SLT-1A. The overlapping and the similarity matches between the two models were carried out using the program UCSF Chimera [35].

Molecular biology techniques

Standard molecular biology techniques were used for plasmid isolation, transformation of *E. coli* and cloning [36].

Construction of the *C. diphtheriae* HC04 mutant strain DW-1 with insertion plasmid pK18mob_0155′

For cloning of the insertion vector, a 369 bp fragment of the gene CDHC04_0155 was amplified by PCR using chromosomal DNA of strain *C. diphtheriae* HC04 as a template and the following primers: 5′-GCGCCCCGGGCGCGGT ACCGCAATAGTGCG-3′ and 5′-GCGCCCCGGGCT TAGGGTGAAGTTATATGG-3′. Using the XmaI site introduced via the PCR primers, the DNA fragment was ligated to XmaI-restricted and dephosphorylated pK18mob DNA. The resulting vector pK18mob_0155′ was amplified in *E. coli* DH5αMCR. One microgram of unmethylated plasmid isolated from this *E. coli* strain was used to transform *C. diphtheriae* HC04 using a GenePulser II (Bio-Rad, Munich Germany). Electroporated cells were added to 1 ml of HI broth and incubated for 2 h at 37 °C. An appropriate volume of culture was plated on medium containing kanamycin. The insertion of the plasmid into the chromosome of *C. diphtheriae* HC04 strain was confirmed by Southern blotting (Fig. S1, available in the online version of this article) and the corresponding strain was designated as DW-1.

Table 1. Bacterial strains, plasmids and cell lines used in this study

Bacterial strains	**Genotype/description**	**Reference/source**
C. diphtheriae HC04	Isolated from a 7-year-old female with a fatal endocarditic infection, wild-type, non-toxigenic (tox$^-$)	[20, 21]
C. diphtheriae DW-1	HC04 *0155*::pK18*mob0155*'	This work
C. ulcerans 809	Isolated from an 80-year-old woman with a fatal pulmonary infection, non-toxigenic (tox$^-$)	[15]
C. glutamicum ATCC 13032	Type strain	[22]
E. coli DH5αMCR	*endA1 supE44 thi-1λ$^-$ recA1 gyrA96 relA1 deoR Δ(lacZYA-argF) U196ϕ80 ΔlacZΔM15 mcrA Δ(mmrhsdRMS mcrBC)*	[23]
E. coli OP50	Uracil-auxotrophic *E. coli* B strain	[24]
Salmonella enterica serovar Typhimurium NCTC 12023	Wild-type identical to ATCC 14028	NCTC, Colindale, UK
Plasmids	**Description**	**Reference/source**
pK18*mob*	Insertion vector, Km^R, *ori* pUC, *mob*	[25]
pK18*mob-0155*	pK18*mob* with a 369 bp internal fragment of gene *CDHC04_0155*	This work
pXMJ19	*ori colE1, ori$_{cg}$, ptac,* Cm^R	[26]
pXMJ19_00177	*ori colE1, ori$_{cg}$, ptac*, Cm^R, carrying 921 bp *CULC809_00177* gene	This work
pXMJ19_0155	*ori colE1, ori$_{cg}$, ptac,* Cm^R, carrying 690 bp *CDHC04_0155* gene	This work
pXMJ19*mCherry*	*ori colE1, ori$_{cg}$, ptac, mCherry*, Cm^R	[27]
pXMJ19*_00177_mCherry*	*ori colE1, ori$_{cg}$, ptac, CULC809_0017, mCherry*, Cm^R	This work
pXMJ19*_0155_mCherry*	*ori colE1, ori$_{cg}$, ptac, CDHC04_0155, mCherry*, Cm^R	This work
Cell lines	**Description**	**Reference/source**
Detroit 562	Human hypopharyngeal carcinoma cells	[28]
THP-1	Human leukemic monocytic cells	[29]
THP1-Blue NFκB	THP-1 cells with stable integrated NFκB inducible SEAP reporter construct	Invivogen
Vero	African green monkey kidney epithelial cells	[30]

Construction of overexpression plasmids pXMJ19_00177 and pXMJ19_0155

For cloning of the overexpression vector pXMJ19_00177, the gene *CULC809_00177* was amplified by PCR using chromosomal DNA of strain *C. ulcerans* 809 as a template and the following primers: 5′-CGCGCTGCAGCGACGTATTG ATATCGCAGG-3′ and 5′-CGCGCCCGGGGTGGCCACAC TTAGCAGTATG-3′. Using the PstI and XmaI sites introduced via the PCR primers, the DNA fragment was ligated to PstI/XmaI-restricted and dephosphorylated pXMJ19 DNA downstream of the IPTG-inducible *tac*-promoter. The resulting overexpression plasmid pXMJ19_00177 was amplified in *E. coli* DH5αMCR. One microgram of unmethylated plasmid isolated from this *E. coli* strain was used to transform *C. ulcerans* 809 using a GenePulser II (Bio-Rad, Munich, Germany). Similarly, for cloning of the overexpression vector pXMJ19_0155, the gene *CDHC04_0155* was amplified by PCR using chromosomal DNA of strain *C. diphtheriae* HC04 as a template and the following primers: 5′-CGCGGTCGACGGATATATGAGAATG AAGG-3′ and 5′-CGCGCCCGGGGGTGGCTCCTTCTTTTATCG-3′. Using the SalI and XmaI sites introduced via the PCR primers, the DNA fragment was ligated to SalI/XmaI-restricted and dephosphorylated pXMJ19 DNA. The resulting overexpression plasmid pXMJ19_0155 was amplified and used to transform *C. diphtheriae* HC04 as described above. An appropriate volume of culture was plated on HI agar containing 10 μg ml^{-1} chloramphenicol.

For fluorescence microscopy experiments, plasmid pXMJ19_00177mCherry was constructed. For this purpose, a 711 bp KpnI/EcoRI DNA fragment carrying the *mCherry* gene was isolated from pXMJ19mCherry and ligated downstream of the *CULC809_00177* gene in plasmid pXMJ19_00177. Plasmid pXMJ19_0155mCherry was constructed carrying the *CDHC04_0155* gene between *tac* promoter and mCherry. For this purpose, a 708 bp XmaI/EcoRI DNA fragment carrying the *mCherry* gene was isolated from pXMJ19mCherry and ligated downstream of the *CDHC04_0155* gene in plasmid pXMJ19_0155.

RNA isolation and hybridization

RNA isolation and hybridization were carried out as described [37]. For hybridization of the digoxigenin-labelled RNA probes (prepared by PCR using the oligonucleotide primer pairs 5′-GCAGCCGCGGTAATACGTAG-3′; 5′-GGGCCCTAATACGACTCACTATAGGGACATCTCACGACACGAGCTG-3′ for the 16S rRNA gene, 5′-CAGCACCTAGCGGGCTCGG-3′; 5′-CCCGGGTAATACGACTCACTATAGGGAGAGAATCGTTCCGCGGTTGGG-3′ for CDHC04_0155 and 5′-CTCATGCGTCTGCTGACGACC-3′; 5′-GGGCCCTAATACGACTCACTATAGGGAGCTCGGGCAGCAGAT-3′ for the CULC809_00177 probe) and detection, alkaline phosphatase-conjugated anti-digoxigenin Fab fragments and CSPD [Disodium 3-(4-methoxyspiro {1,2-dioxetane-3,2′-(5′-chloro)tricyclo [3.3.1.13,7]decan}−4-yl)phenyl phosphate] as the light-emitting substrate were used as recommended by the supplier (Roche). Chemiluminescence detection was carried out using a ChemiDoc XRS+ system (BioRad).

Sample preparation and mass spectrometry analyses

For the preparation of crude cell extracts, bacteria were grown as described above and protein concentrations were determined after cell disruption (Bertin precellys 24) using a standard Bradford assay [38].

For mass spectrometry analyses, 20 µg protein samples were loaded onto 10 kDa vivacon 500 membrane filters, the flow-through was discarded by centrifugation for 30 min at 12 000 ***g*** and a modified Filter Aided Sample Preparation (FASP) protocol was carried out [39]. In short, proteins samples were incubated for 1 h at 37 °C after addition of 200 µl of reduction buffer [25 mM 1,4-dithiotreitol (DTT), 8 M urea, 50 mM tris(hydroxymethyl)aminomethane (Tris), pH 8.0]. Samples were centrifuged and the flow through was discarded. Alkylation of sulfhydryl groups was carried out for 1 h at room temperature on a shaker at 600 r.p.m. in the dark after addition of 200 µl alkylation buffer [20 mM chloroacetamide (CAA), 8 M urea, 50 mM Tris, pH 8.0]. Filters were washed with 300 µl of 1 M urea in 50 mM Tris, pH 8. For protein digestion, 1 µg trypsin in 100 µl 1 M urea, 50 mM Tris, pH 8.0 was added and over-night incubation was carried out on a shaker at 37 °C and 600 r.p.m. Peptides were collected by centrifugation at 12 000 ***g*** for 20 min. Then, 10 % trifluoroacetic acid (TFA) was added to a final concentration of 0.5 % TFA and a clean-up with C18 stage tips were performed to desalt the peptides. Prior to LC-MS/MS analysis, peptides were vacuum dried and resuspended in 10 % formic acid.

Mass spectrometric analyses were carried out on an electrospray Orbitrap Fusion Tribrid and peptides were separated on a nano flow Dionex 3000 uHPLC with general settings as described [40]. Each MS run took 160 min and peptides were separated by an increasing acetonitrile gradient on a 50 cm C18 EASY-Spray column (ThermoFisher Scientific).

Resulting raw data files were analysed using the PEAKS Studio 8.5 (Bioinformatics Solutions) software package [41]. Searches were performed against the *C. diphtheriae* (strain HC04) database (Proteome Id: UP000007154) or *C. ulcerans* 809 database (Proteome Id: UP000008886) (www.uniprot.org/proteomes). Global parameters for identification were trypsin digestion with a maximum of two missed cleavages, carbamidomethyl modification on cysteine as fixed and oxidation of methionine as dynamic modification. For label-free quantification a maximum retention time shift of 10.0 min, mass tolerance of 10.0 ppm for survey scans and a 1 % false discovery rate (FDR) was applied.

C. elegans and *G. mellonella* invertebrate model systems

The assays were performed as described recently [42].

Infection of *C. elegans*

C. elegans N2 were maintained on nematode growth medium (NGM) agar plates inoculated with *E. coli* OP50 for 3 to 7 days until the worms become starved, indicated by clumping behaviour [43]. The nematodes were synchronized and used in infection assays with *C. ulcerans* and *C. diphtheriae* strains. *E. coli* OP50 was used as a control. For the survival assay, 20 L4 stage larval worms were infected with 20 µl of each bacterial strain ($O.D_{600}$ 1.0) on NGM plates at 20 °C for 24 h. Worms were assessed each day following infection, and the dead nematodes were counted and removed every 24 h. For each strain, approximately 60 nematodes were used.

For the colonization of *C. elegans*, the nematodes were infected with *C. ulcerans*, *C. diphtheriae* and *E. coli* OP50 transformed with pXMJ19mCherry. Infection of 20 L4 stage larval worms was carried out with 20 µl of each bacteria strain on NGM plates at 20 °C for 24 h. Worms were then transferred to plates with 20 µl of unlabelled *E. coli* OP50 for further 24–48 h, to allow the gut to clear of fluorescent bacteria and cell debris. Worms were assessed each day following infection. Nematodes were paralysed with 20 mM sodium azide (Sigma, Munich, Germany), mounted onto agar pads and photographed using a Leica DMI4000B fluorescence microscope.

Infection and monitoring of *G. mellonella*

Briefly, bacteria from an overnight culture were inoculated in fresh medium and grown until an OD_{600} of 0.6 was reached. Bacteria were harvested by centrifugation (10 min, 4500 ***g***) and resuspended in 10 mM $MgSO_4$ to an OD_{600} of 10 (approximately 3×10^9 c.f.u. ml^{-1}). For the infection, a 50 µl Hamilton syringe was used to inject 5 µl aliquots into *G. mellonella* larvae via the hindmost left proleg. Larvae were monitored daily during 5 days for their activity, melanization and survival on incubation at 25 °C, and the pictures were taken on the fifth day of infection. A score was provided for each monitored attribute that supported a global health index of each individual larvae. Healthy, uninfected wax moth larvae typically score between 10 and 11, while infected dead larvae score between 0 and 1 [42, 44].

Cell culture

Detroit562 and Vero cells were cultivated and maintained in Dulbecco's modified Eagle's medium (DMEM), high glucose with L-glutamine and sodium pyruvate (PAA Laboratories, Austria), supplemented with 120 µg ml^{-1} penicillin, 120 µg ml^{-1} streptomycin and 10 % (v/v) FBS (Life Technologies, Germany). Human monocytic THP-1 cells were cultured in 10 % FBS supplemented RPMI medium 1640 containing 100 U ml^{-1} penicillin and 100 mg ml^{-1} streptomycin. The cell lines were incubated at 37 °C with 5 % CO_2 in a humidified incubator and passaged at a ratio of 1 : 10 twice per week. The antibiotics were removed from the medium prior to infection with bacteria.

Transepithelial resistance measurements

Detroit562 cells were seeded in transwells (12 mm, 0.4 µm, polyester membrane, 12-well plate, Corning Costar) at a density of 1×10^5 cells per well and cultivated in DMEM (high glucose, 10 % FBS, 2 mM glutamine) for 14 days until they build a transepithelial resistance of at least 800 Ω cm^{-2}. Bacteria were grown in HI broth (*C. ulcerans* and *C. diphtheriae*) or LB medium (*S.* Typhimurium) until an OD_{600} of 0.4 to 0.6 was reached, harvested by centrifugation and the pellet was resuspended in 500 µl PBS. An OD_{600} of 5 was adjusted in 500 µl PBS and 100 µl of this suspension were used to infect one well. Measurements of transepithelial resistance of Detroit562 cells after infection were carried out with a volt-ohm-meter (EVOM2, World Precision Instruments, Berlin, Germany) every 60 min. After 180 min, the supernatant of infected Detroit562 cells was removed and the cells were incubated in fresh DMEM overnight to avoid detrimental effects of excessive bacterial growth.

Cytotoxicity assay

Bacteria were grown in HI broth until an OD_{600} of 0.4 to 0.6 was reached with constant shaking at 125 r.p.m. Mitomycin C (Carl Roth GmbH) was added to a final concentration of 2 µg ml^{-1} during mid-logarithmic-phase and grown for 2–3 h for optimal synthesis of toxin. The bacterial cultures were centrifuged (8000 ***g***, 5 min) and cell-free supernatants were stored in sterile tubes. Additionally, bacterial pellets were lysed with glass beads at 5.5 m s^{-1}, 30 s, three cycles (FastPrep-24 5G high-speed homogenizer), centrifuged at 8000 ***g*** for 5 min at 4 °C, the supernatants were collected and combined with the original cell-free supernatants and filtered through 0.45 µm filters. Vero cells were cultivated in tissue culture flasks with DMEM (high glucose, 10 % FBS, 2 mM glutamine). Confluent monolayers were removed with trypsin EDTA, resuspended to approximately 1×10^5 cells ml^{-1} in DMEM without antibiotics and 100 µl of samples were pipetted into each well of 24-well plates. After incubation at 37 °C in 5 % CO_2 for 24 h, the medium in each well was replaced with 400 µl DMEM and 100 µl of the bacterial filtrate. For the control wells, only DMEM was used. Vero monolayer morphology was observed and photographed using a Leica DMI4000B and checked for cytotoxic effect for 72 h. For the cytotoxicity of Vero cells with bacterial infection, bacteria were inoculated to an OD_{600} of 0.1 from overnight cultures and grown in HI broth to an OD_{600} of 0.4 to 0.6. Subsequently, the bacteria were harvested by centrifugation and cell density was adjusted to an OD_{600} of 1. A master mix of the inoculum with an m.o.i. of 25 was prepared in DMEM and 500 µl per well was used to infect the cells. The plates were centrifuged for 5 min at 350 ***g*** to synchronize the infection and subsequently incubated for 90 min. The cells were washed with PBS and incubated for 20 h in DMEM (500 µl per well), containing 50 µg ml^{-1} gentamicin to kill the remaining extracellular bacteria. After 20 h, Vero monolayer morphology was observed and photographed using Leica DMI4000B. The supernatants were collected and checked for cytotoxicity with cytotoxicity detection kit (Roche).

Phagocytosis and survival assays in THP-1 macrophages

For phagocytosis and survival assays, THP-1 cells were seeded in 24-well plates (Nunc) at a density of 2×10^5 and differentiated by addition of 10 ng ml^{-1} phorbol 12-myristate 13-acetate (PMA) 24 h prior to infection. *C. ulcerans* and *C. diphtheriae* were grown in HI to an OD_{600} of 0.4 to 0.6. An inoculum with an m.o.i. of 25 was prepared in RPMI 1640 without antibiotics and 500 µl per well was used to infect the cells. The plates were centrifuged for 5 min at 350 ***g*** to synchronize the infection and incubated for 30 min (37 °C, 5 % CO_2, 90 % humidity) to allow phagocytosis of bacteria. Subsequently, the supernatant containing non-engulfed bacteria was aspirated, cells were washed once with PBS and remaining extracellular bacteria were killed by addition of 100 µg ml^{-1} gentamicin in cell culture medium. After 2 h, cells were either lysed and intracellular bacteria were recovered or further incubated with medium containing 10 µg ml^{-1} gentamicin for analysis at later time points. To recover intracellular bacteria, the medium was aspirated and cells were lysed by adding 500 µl of 0.1 % Triton-X100 in PBS. Serial dilutions of lysate and inoculum were plated on blood agar plates using an Eddy Jet Version 1.22 (IUL Instruments). After incubation at 37 °C for2 days, the number of c.f.u. was determined. The ratio of bacteria used for the infection (number of colonies on inoculum plates) and bacteria in the lysate (number of colonies on the lysate plates) multiplied with 100 gave the percentage of viable intracellular bacteria at different time points. When the survival of intracellular bacteria in THP-1 cells was analysed over the time, the number of c.f.u. at 2 h was set to 100 % and later time points were calculated based on this value.

LDH measurement

The release of cytosolic lactate dehydrogenase as a sign of host cell damage during infection was measured using the cytotoxicity detection kit (LDH) according to the supplier (Roche). Briefly, 100 µl supernatant of infected cells were mixed with 2.5 µl of the provided catalyst solution and 112.5 µl of the provided dye solution in 96-well plates, incubated in the dark for 30 min and the absorbance was measured at 490 nm and wavelength correction at 620 nm in a multiplate reader (TECAN Infinite 200 PRO). Cells treated

with 2 % Triton X-100 served as the positive control for maximal LDH release and were set to 100 %, untreated cells served as the negative control.

Statistical analysis

Statistical analyses were performed using GraphPad Prism 7.0 (GraphPad, CA, USA) software. For the Kaplan–Meier survival analysis, the Mantel–Cox log-rank test (95 % CI) was performed to compare the survival distributions. Unless indicated, data were normally distributed, and graphs show means and SD or SEM for each group. Results were compared with two-tailed *t*-tests with a minimal level of significance set at $P<0.05$. Results of all the groups were compared with ANOVA column statistics and Bonferroni corrections were applied for multiple comparisons. Each experiment was performed at least three times (independent biological replicates).

RESULTS

Bioinformatic analyses of putative Rbps

When the whole genome of *C. ulcerans* strain 809 was sequenced and analysed [16], bioinformatic analysis revealed the presence of a gene annotated as *rbp*, encoding a putative Rbp based on the presence of a ribosome-inactivating protein (RIP) domain (Pfam domain 00161). Multiple sequence alignments of this putative Rbp, initially also designated as Shiga-like toxin based on a striking structural similarity to these toxins, revealed a considerable amino acid identity of 26 % and a query coverage of 76 % with a putative secreted protein from *C. diphtheriae* HC04 (RIP; Pfam domain 00161) (Fig. 1a). The predicted molecular weight of the putative Rbps were 33 and 25 KDa for *C. ulcerans* 809 and *C. diphtheriae* HC04, respectively.

The analysis of signal sequences revealed the presence of signal peptides with cleavage sites between 22–23 for *E. coli* SLT-1A and SLT-2A, cleavage sites between amino acid residues 41 and 42 for *C. ulcerans* 809 and residues 34 and 35 for *C. diphtheriae* HC04 respectively. The alignment of the tertiary structure of Rbp from *C. diphtheriae* HC04 (CDHC04_0155) and the A chain of SLT-1 demonstrated overlapping regions between the two proteins (Fig. 1b). The sequence alignment of the Rbp from *C. diphtheriae*, CDHC04_0155, showed a confidence of 96.89 % and an identity of 26 % to the A chain of SLT-1 (Fig. 1b).

Since we are interested in virulence determinants of *C. ulcerans* [45] and *C. diphtheriae* [46], we started a first characterization of the putative Rbps from strains 809 and HC04

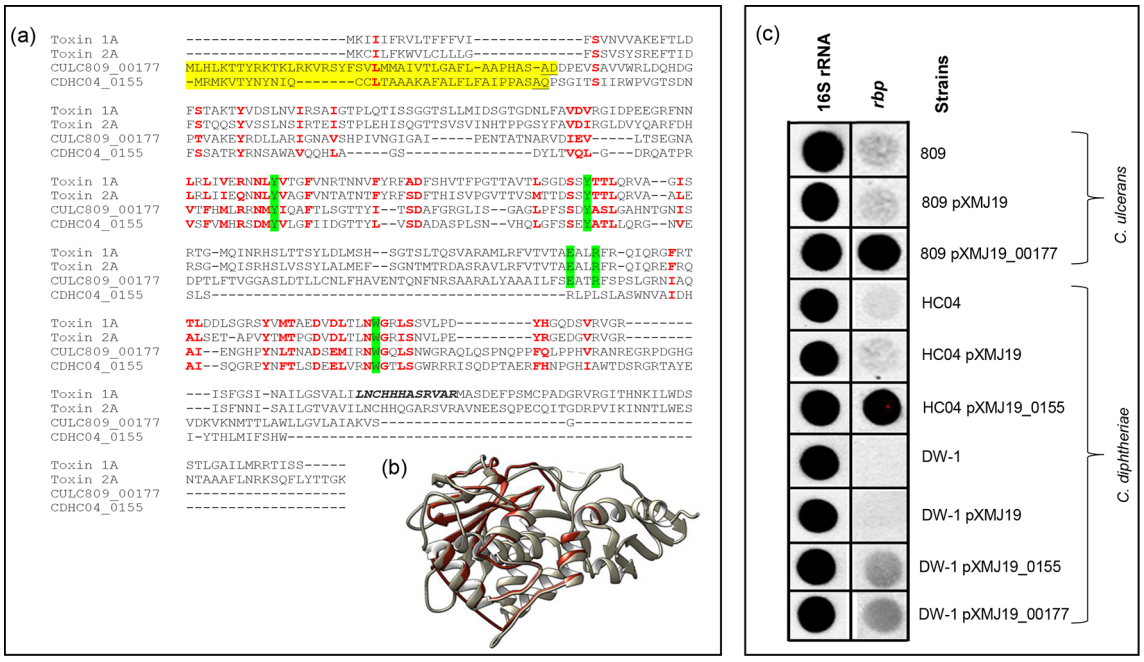

Fig. 1. Analysis of putative corynebacterial Rbps. (a) Amino acid sequence alignment of the Rbp from *C. ulcerans* 809 and the putative secreted protein from *C. diphtheriae* HC04 with A chains of the Shiga-like toxins SLT-1 and SLT-2 from *E. coli*. The predicted signal peptides of corynebacterial Rbps are highlighted in yellow, while underlined amino acids represent the cleavage sites. The common conserved catalytic residues shared among SLT-1A, SLT-2A, *C. ulcerans* CULC809_00177 (as previously shown [16]) and *C. diphtheriae* CDHC04_0155 are marked in green. The conserved amino acids are indicated in red and the re-translocation domain of SLT-1A is shown in bold italics. (b) Three-dimensional model representing the overlapping regions between the Rbp-like from *C. diphtheriae* (CDHC04_0155) and the A chain of SLT-1. The predicted structure model of Rbp from *C. diphtheriae* HC04 is indicated in red while the template SLT-1A is shown in grey. (c) Transcription levels of the putative *rbp* genes of *C. ulcerans* 809 and *C. diphtheriae* HC04. RNA was isolated and hybridized with probes monitoring 16S rRNA for control as well as transcripts of the *CULC809_00177* and *CDHC04_0155* genes.

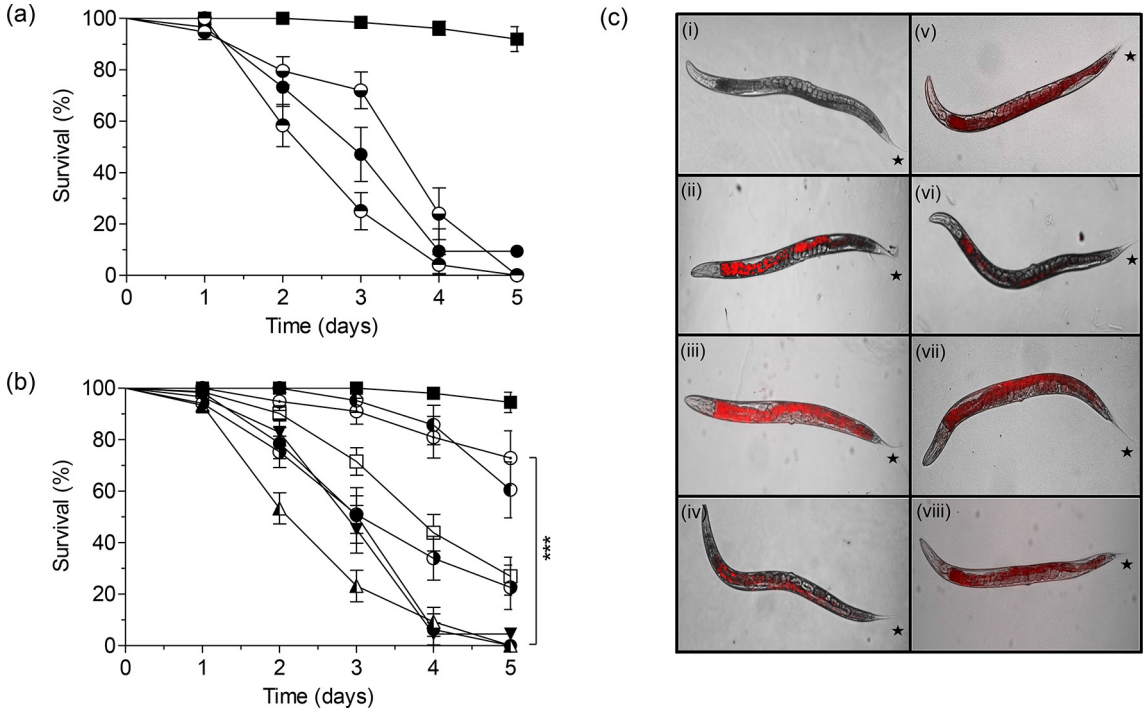

Fig. 2. *C. elegans* survival and colonization upon infection with *C. ulcerans* and *C. diphtheriae* strains. (a) Infection with *E. coli* OP50 (■), *C. ulcerans* 809 (●), 809 pXMJ19 (◒) and 809 pXMJ19_00177 (◓). (b) Infection with *E. coli* OP50 (■), *C. diphtheriae* HC04 (●), HC04 pXMJ19 (▼), HC04 pXMJ19_0155 (▲), DW-1 (Θ), DW-1 pXMJ19 (◐), DW-1 pXMJ19_0155 (◑) and DW-1 pXMJ19_00177 (□). Experiments were carried out in triplicate and data shown are mean values and SD of at least three independent biological replicates. Statistical significance between *C. diphtheriae* wild-type HC04 and mutant DW-1 is shown with ***$P<0.0001$. (c) Fluorescence microscopy of *C. elegans* colonization. *C. elegans* were infected with fluorescent labelled bacteria for 24 h and transferred to unlabelled *E. coli* OP50 for 48 h to allow the gut to clear of fluorescent bacteria and cell debris. After 48 h, nematodes were mounted onto agar pads, paralyzed with 20 mM sodium azide and photographed using a Leica DMI4000B. In each of the three independent experiments, approximately 20 worms were infected. Representative results are shown. *C. elegans* fed with *E. coli* OP50 pXMJ19mCherry (i), *C. ulcerans* 809 pXMJ19mCherry (ii), *C. ulcerans* 809 pXMJ19_00177mCherry (iii), *C. diphtheriae* HC04 pXMJ19mCherry (iv), *C. diphtheriae* HC04 pXMJ19_0155mCherry (v), *C. diphtheriae* DW-1 pXMJ19mCherry (vi) *C. diphtheriae* DW-1 pXMJ19_0155mCherry (vii) and *C. diphtheriae* DW-1 pXMJ19_00177mCherry (viii). Asterisks indicate the tail end of the worms.

in respect to their influence on host–pathogen interaction. In the case of *C. ulcerans* 809, which is not fully accessible by molecular biology tools [47], an overexpression strain was constructed and analysed in comparison to control strains, while for *C. diphtheriae* HC04, besides corresponding strains, also mutant and complementation strains were generated and studied.

Expression of putative Rbps

As a first approach, transcription levels of the putative cytotoxin-encoding genes were tested in the different strains. RNA hybridization experiments hint to a low transcription level of the corresponding genes in *C. ulcerans* 809 and *C. diphtheriae* HC04. No mRNA signal was detected for *C. diphtheriae* strains DW-1 and DW-1 pXMJ19, while complementation strains DW-1 pXMJ19_0155 and DW-1 pXMJ19_00177 showed moderate mRNA levels. The highest transcript levels were observed for overexpression strains 809 pXMJ19_00177 and HC04 pXMJ19_0155 (Fig. 1c).

In addition, mass spectrometry analyses were carried out. In the case of the *C. ulcerans* Rbp, one unique peptide with a coverage of 3 % was detected in the overexpression strain, while it was not detectable in the wild-type. This result is in accordance with recent secretome analyses of strain 809 [48]. Also in this study, the putative Rbp of *C. ulcerans* was not detected, indicating a very low abundance. In the case of the *C. diphtheriae* protein, three unique peptides with a coverage of 18 % were observed, when the cytoplasm of the overexpression strain was analysed, while in the wild-type HC04 only one unique peptide with a coverage of 6 % was found (Fig. S2 and Table S1).

Influence of Rbps on growth of *C. ulcerans* and *C. diphtheriae*

For a proper strain-dependent analysis of pathogen interactions, knowledge about the growth behaviour of strains is crucial. Therefore, bacterial growth was tested. In the case of *C. ulcerans*, growth of the wild-type 809, control strain

809 pXMJ19 and overexpression strain 809 pXMJ19_00177 were identical with doubling times of 58.3±2.0 min, 59.4±2.1 min and 62.2±2.5 min, respectively, when at least three independent biological replicates were analysed. Also *C. diphtheriae* wild-type HC04 and corresponding *rbp* mutant DW-1 showed identical doubling times with 77.3±3.5 min and 77.0±3.2 min. Compared to HC04 wild-type, plasmid-carrying strains HC04 pXMJ19 and HC04 pXMJ19_0155 showed a slightly increased doubling time of 91.1±1.3 min and 96.0±3.4 min, respectively. A similar effect was observed for strains DW-1 pXMJ19 and DW-1 pXMJ19_0155 with 91.4±3.2 min and 111.5±3.2 min, respectively. Taken together, the experiments revealed that *rbps* mutations induce no detrimental effects on growth or fitness of the analysed corynebacteria, while overexpression of *C. diphtheriae* Rbp was slightly detrimental to growth of the corresponding strain, an effect, which may mask a putative influence of the expressed proteins on host cells.

As a first approach to analyse host effects, the influence of the corynebacterial *rbp* genes was tested in two invertebrate model systems established for the investigation of *Corynebacterium*–host interaction, the nematode *Caenorhabditis elegans* and larvae of the greater wax moth *Galleria mellonella* [27, 42].

Rbp-dependent interaction with *C. elegans*

Typically, *C. elegans* are feeding on *E. coli*, which supported their survival during the time of the experiment and therefore, were used as a control group. In contrast, approximately 50 % of the nematodes died within less than 3 days, when *C. elegans* were infected with *C. ulcerans* 809 (Fig. 2a). Since a deletion of the *rbp* gene could not be obtained in this strain (see also [47]), the correspondent gene was overexpressed. In contrast to empty vector control, overexpression strain 809 pXMJ19_00177 showed a decreased survival rate. The effect was more pronounced for the *C. diphtheriae* Rbp. Strain HC04 led to a 50 % killing rate within 3 days. Deletion of the corresponding gene significantly prolonged the survival of 70 % of the worms to 5 days. Infection of *C. elegans* with the control strain HC04 pXMJ19 had no additional detrimental effect compared to the untransformed strain (Fig. 2b), while the strain HC04 pXMJ19_0155 led to killing of 50 % of the worms within 2 days. Additionally, the mutant DW-1 was complemented with the *rbp* gene (*CULC809_00177*) from *C. ulcerans* 809. In comparison to the mutant DW-1, infection with the strain DW-1 pXMJ19_00177 enhanced the killing rate to about 40 %. Interestingly, a similar effect observed with DW-1 pXMJ19_0155 (Fig. 2b) illustrate that the expression of *CDHC04_0155* has a deleterious effect on *C. elegans*.

The data obtained by the nematode-killing assay were consistent with fluorescence microscopy investigations of nematode colonization by mCherry-expressing strains (Fig. 2c). While *E. coli* OP50 were not able to colonize the worms and were readily digested, strains 809 and HC04 colonized the intestinal tract of the worms completely. Colonization by DW-1 was weak, but could be restored by complementation with the plasmids pXMJ19_0155mCherry and pXMJ19_00177mCherry.

Influence of Rbps on *G. mellonella*

The effect of the corynebacterial *rbp* genes was also studied in the *G. mellonella* model system and the representative images were taken on the fifth day post-infection (Fig. 3a). Injection of buffer or the non-pathogenic *C. glutamicum* strain ATCC 13032 used as the control did not impair the larvae, while infection with *Salmonella enterica* sv. Typhimurium (*S.* Typhimurium) led to strong melanization, inactivity and finally to death of the larvae. Compared to *S.* Typhimurium, the effect of *C. ulcerans* 809 infection was less severe but also accompanied by melanization and decreased activity. Similar effects were observed on larvae infected with *C. ulcerans* 809 pXMJ19, while the overexpression strain 809 pXMJ19_00177 led to stronger melanization and finally to death of the larvae. *C. diphtheriae* strain HC04 and HC04 pXMJ19 evoked similar symptoms, while overexpression strain HC04 pXMJ19_0155 had more severe effects on the larvae. *C. diphtheriae rbp* mutant DW-1 and empty vector control DW-1 pXMJ19 were less detrimental compared to HC04 and HC04 pXMJ19, while the virulence was restored by the complementation of the *rbp* gene. For a quantitative analysis of this effect, the wax larvae were monitored daily and their activity, melanization and survival were scored according to the health index scoring system described recently [42, 44].

The quantitative analysis of the health index score of *G. mellonella* revealed that while the control wax moth larvae (injected with buffer) remained the typical beige colour and were highly active over all days, *S.* Typhimurium ATCC 12023 used as a positive control showed a high degree of melanization and immobility leading to death within 2–3 days of infection (Fig. 3b). Injection of the non-pathogenic *C. glutamicum* ATCC 13032 led to the development of small black spots after 3 days post-infection, while the larvae remained active. The melanization process of the larvae became more pronounced in response to injection of *C. ulcerans* 809 and 809 pXMJ19. Upon injection with the *rbp* overexpression strain 809 pXMJ19_00177, a severe detrimental effect of the larvae with a health index score of 4 was observed on the fourth day (Fig. 3b). Similarly, while *C. diphtheriae* strains HC04 and HC04 pXMJ19 led to less active brown larvae during 5 days of infection, a strong effect was already observed on day 1 as indicated by a health index score of 8, which later reduced dramatically during the 5 days of infection and ranged between 2 and 2.5. *C. diphtheriae* HC04 pXMJ19_0155 overexpression strain resulted in severe detrimental effect on the fourth day (health index score of 2.5) leading to death of the larvae (Fig. 3c). Infection of the larvae with *C. diphtheriae rbp* mutant DW-1 and empty vector control DW-1 pXMJ19 showed a slow melanization process with a slight reduction of the health index from a score of 10 to a score of 7 until day 4, while the complementation strain led to a stronger melanization (health index score of 0) over 5 days of infection leading to death of the larvae (Fig. 3d).

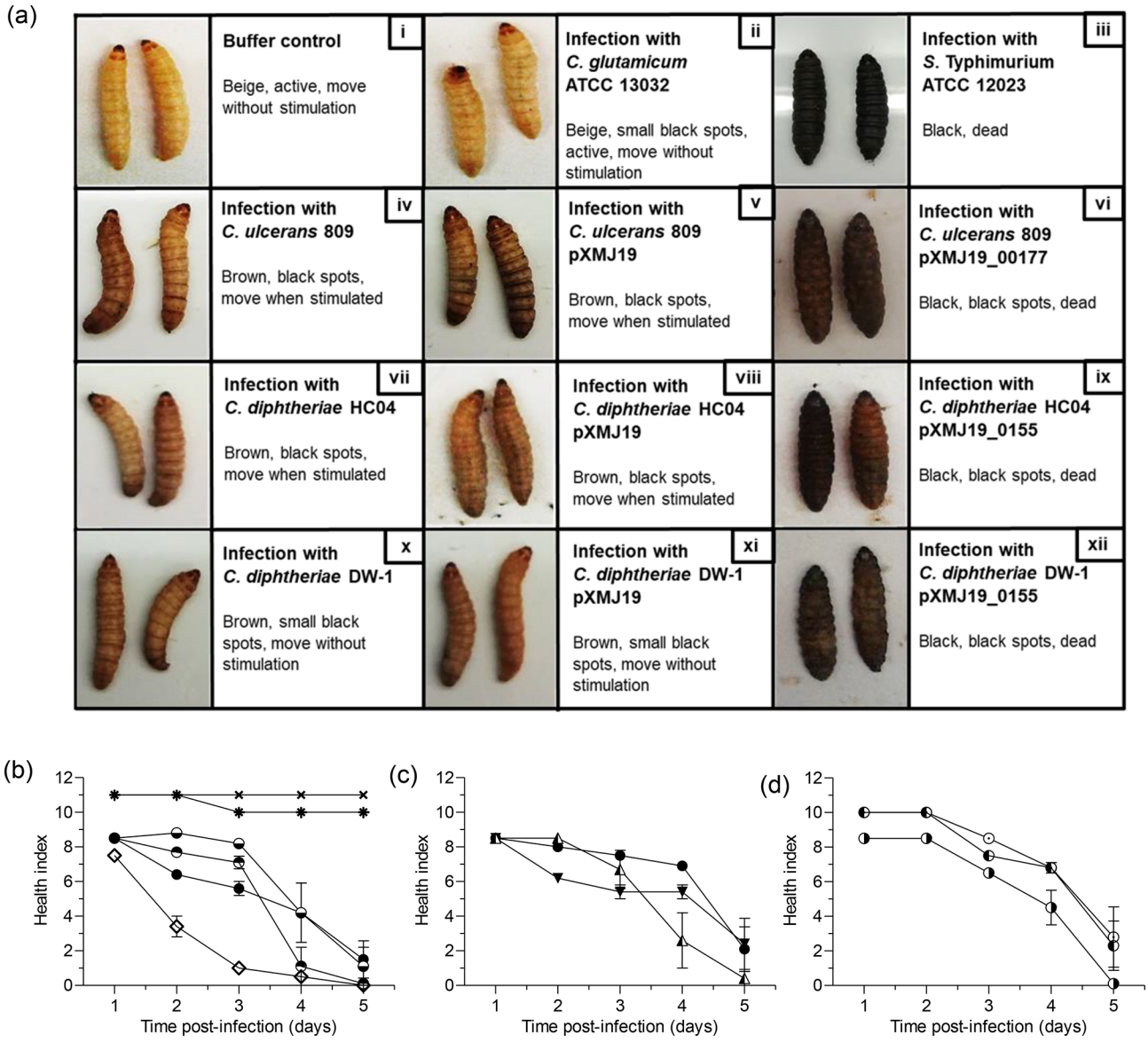

Fig. 3. Response and health index score monitoring of *G. mellonella* upon bacterial infections. (a) *G. mellonella* larvae were injected with 10 mM $MgSO_4$ buffer as the control (i), non-pathogenic corynebacteria *C. glutamicum* ATCC 13032 (ii), positive control for melanization *S.* Typhimurium ATCC 12023 (iii), *C. ulcerans* strains 809 (iv), 809 pXMJ19 (v), 809 pXMJ19_00177 (vi) and *C. diphtheriae* strains HC04 (vii), HC04 pXMJ19 (viii), HC04 pXMJ19_0155 (ix), DW-1 (x), DW-1 pXMJ19 (xi), DW-1 pXMJ19_0155 (xii). Images were taken on the fifth day post-infection. *G. mellonella* were monitored post-infection and the activity, melanization and survival features were scored according to their health index. (b) The wax worms were injected with 10 mM $MgSO_4$ buffer (x), *S.* Typhimurium ATCC 12023 (◊), non-pathogenic *C. glutamicum* ATCC 13032 (*), pathogenic *C. ulcerans* strain 809 (●), 809 pXMJ19 (◒), 809 pXMJ19_00177 (◓) (c) *C. diphtheriae* strain HC04 (●), HC04 pXMJ19 (▼), HC04 pXMJ19_0155 (▲) and (d) *C. diphtheriae* mutant DW-1 (Θ), DW-1 pXMJ19 (◐) and DW-1 pXMJ19_0155 (◑). For each strain at least five larvae were infected and experiments were carried out in triplicate (independent biological replicates). Error bars represent mean±SEM.

Taken together, the presence of the two corynebacterial *rbp* genes was obviously connected to virulence in the invertebrate model systems investigated here. To further characterize the function of *C. ulcerans* and *C. diphtheriae rbp* genes, interaction of the bacterial strains with different animal and human epithelial cell lines and human macrophages was studied.

Rbps are involved in the break-down of transepithelial resistance of epithelial cell monolayers

As shown previously, infection with *C. diphtheriae* and *C. ulcerans* can damage cells and due to the resulting loss of cell integrity, the transepithelial resistance of cell monolayers is reduced [47, 49]. Infection of polarized

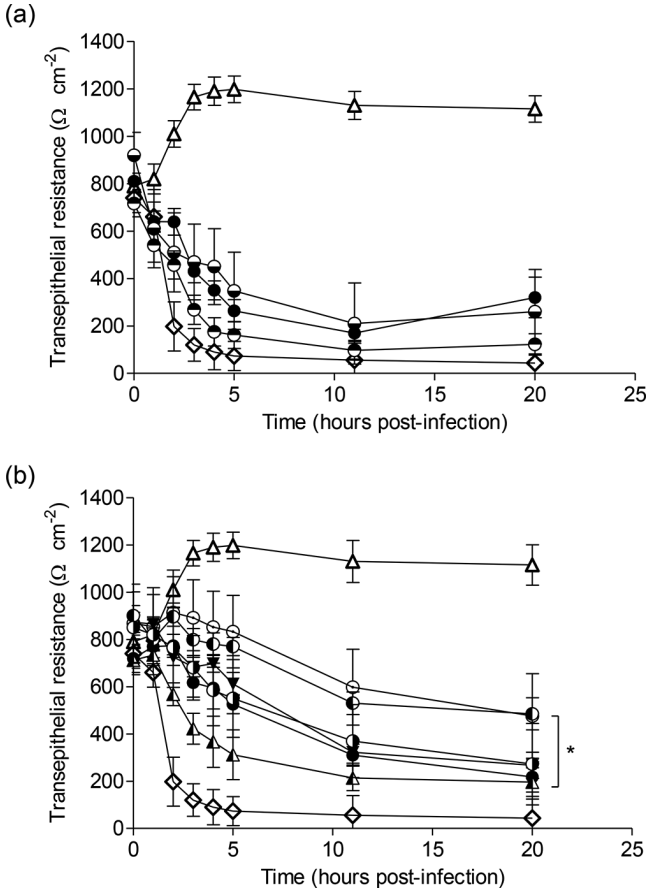

Fig. 4. Influence of Rbps on transepithelial resistance. Polarized Detroit562 monolayers were grown on transwells and challenged with different bacteria. (a) Response to infection with *C. ulcerans* strains 809 (●), 809 pXMJ19 (◒) and 809 pXMJ19_00177 (◓). For the negative control, cells were incubated without bacteria (Δ) and for the positive control with *S.* Typhimurium (◊). (b) Response to infection with *C. diphtheriae* strains HC04 (●), HC04 pXMJ19 (▼), HC04 pXMJ19_0155 (▲), DW-1 (Θ), DW-1 pXMJ19 (◐) and DW-1 pXMJ19_0155 (◑). For the negative control, cells were incubated without bacteria (Δ) and for the positive control with *S.* Typhimurium (◊). Experiments were carried out in triplicate (biological replicates) and error bars represent SD as a percentile of the mean. Statistically relevant differences between *C. diphtheriae* HC04 pXMJ19_0155 and DW-1 (based on one-way ANOVA) are indicated by **P*<0.05.

Detroit562 monolayers with *S.* Typhimurium used as the positive control in this study caused a dramatic break-down of transepithelial resistance within approximately 2 h. *C. ulcerans* 809 and *C. diphtheriae* HC04 were less detrimental, showing a slow break-down of transepithelial resistance over time. A basal level was reached at about 10 h after infection. Similar data were observed for *C. ulcerans* 809 and *C. diphtheriae* HC04 transformed with empty vector pXMJ19, while overexpression of the corresponding *rbp* genes accelerated the break-down of transepithelial resistance significantly (Fig. 4). Vice versa, infection with *C. diphtheriae rbp* mutant DW-1 and DW-1 pXMJ19 only slightly decreased the transepithelial resistance from 800 to 500 Ω cm^{-2} (Fig. 4b).

C. ulcerans and *C. diphtheriae* Rbps are cytotoxic

In transepithelial resistance measurements, it is not possible to distinguish between detrimental effects of invasion of bacteria or of proteins or metabolites secreted by the bacteria. A classical test in this respect is the treatment of Vero cells, African green monkey kidney cells, with bacterial culture filtrates. In this case, only modest differences were observed (data not shown), most likely due to the low expression of the Rbps and their dilution in the medium. Therefore, Vero cells were challenged by infection with bacteria in a subsequent set of experiments. In this case, detachment of cells from the well surface was observed depending on the presence of corynebacterial *rbp* genes (Fig. 5a ii-x), which was more pronounced in the case of *C. ulcerans* (Fig. 5a ii-iv) compared to *C. diphtheriae* (Fig. 5a v-x), while control Vero cell monolayers (i) appeared unchanged over 72 h. To quantify the suggested cytotoxic effect of Rbps, the number of viable Vero cells depending on the infection with different strains was determined using a lactate dehydrogenase (LDH) release assay. Viability of control cells without bacterial contact showed no damage to the cells, whereas Triton X-100 used as the positive control reached almost 100 % cytotoxicity. Infection with *C. ulcerans* 809 and 809 pXMJ19 resulted in a cytotoxicity of about 10 to 15 %, while Rbp-overexpressing strain 809 pXMJ19_00177 reached about 40 % (Fig. 5b). In the case of infection with *C. diphtheriae* HC04 and HC04 pXMJ19 cytotoxicity reached 8 to 12 %, while in the case of HC04 pXMJ19_0155, a cytotoxicity of about 25 % was observed. Disruption of the *rbp* gene resulted in almost no LDH release, while the cytotoxicity of the complementation strain DW-1 pXMJ19_0155 reached approx. 20 % (Fig. 5c).

Influence of corynebacterial Rbps on macrophages

The detrimental effects observed for invertebrate model systems and epithelial cell lines prompted us to characterize macrophage cell lines as well. For this purpose, the interaction of human THP-1 macrophages with *C. ulcerans* and *C. diphtheriae* was analysed together with *C. glutamicum* ATCC 13032, which was expected to be eliminated quickly by the macrophages as it is non-pathogenic. The fate of the bacteria was monitored for 2, 8 and 20 h. The number of bacteria within the macrophages appeared to be constant or declining within the 20 h for *C. glutamicum* ATCC 13032 (Fig. 6a). When the low number of viable *C. glutamicum* at 2 h post-infection was set to 100 %, a constant decline of c.f.u. could be observed at later time points (Fig. 6c). In contrast, a significant increase of the number of bacteria was determined for *C. ulcerans* 809 until 8 h, which then reduced dramatically over 20 h of incubation time (Fig. 6a, c). The internalized c.f.u. by the overexpression strain 809 pXMJ19_00177 showed a significant reduction possibly due to the killing of the macrophages, which was also supported by the microscopic observations of macrophage detachment (data not shown). This result indicates that in contrast to

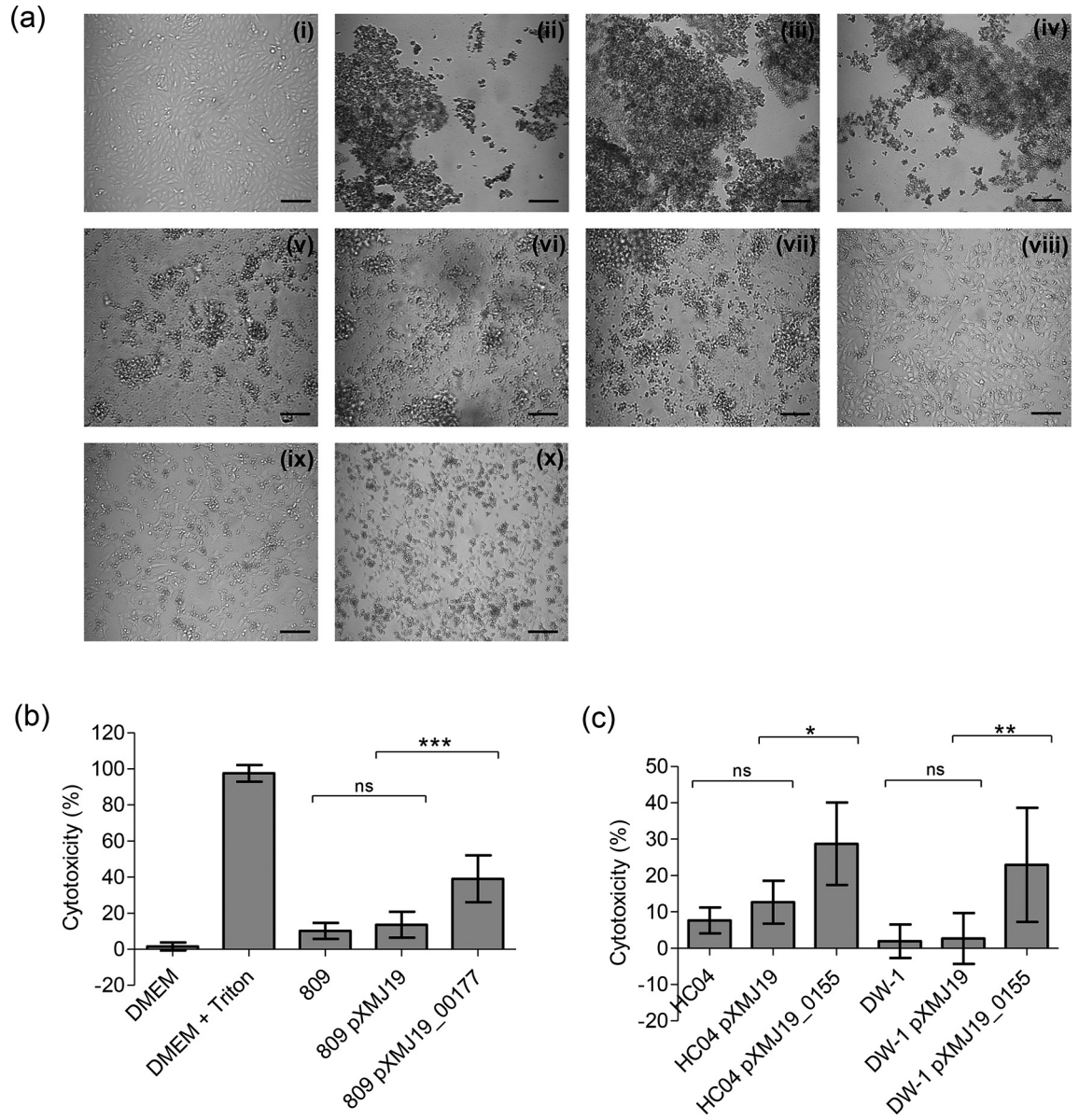

Fig. 5. Cytotoxic effect on Vero cell monolayers and quantification of the release of LDH upon infection with bacteria. (a) Vero cells were treated with bacteria at an MOI of 25 (ii–x). The control cells received only DMEM (i). Vero monolayer morphology was monitored for cytotoxic effects for 72 h and photographed using a Leica DMI4000B. Vero cells were infected with *C. ulcerans* 809 (ii), *C. ulcerans* 809 pXMJ19 (iii), *C. ulcerans* 809 pXMJ19_00177 (iv), *C. diphtheriae* HC04 (v), *C. diphtheriae* HC04 pXMJ19 (vi), *C. diphtheriae* HC04 pXMJ19_0155 (vii), *C. diphtheriae* DW-1 (viii), *C. diphtheriae* DW-1 pXMJ19 (ix) and *C. diphtheriae* DW-1 pXMJ19_0155 (x). Scale bars (right lower corner of the images) represent 100 µm. Experiments were carried out in triplicate (biological replicates). LDH release of Vero cells infected with *C. ulcerans* (b) and *C. diphtheriae* (c). Vero cells were infected with bacteria at an m.o.i. of 25 for 90 min. To kill extracellular bacteria, cells were incubated with medium containing gentamicin and after 20 h, the release of LDH was determined. Data shown are mean values of eight independent biological replicates each performed in triplicates±SD. Statistically relevant differences between the strains (based on Student's *t*-test) are indicated by **P*<0.05.

C. glutamicum, *C. ulcerans* is able to proliferate in macrophages within the first hours of internalization. However, internalization of *C. diphtheriae* by macrophages was less compared to *C. ulcerans* and appeared to be significantly decreasing in a time-dependent manner (Fig. 6b, d). The *C. diphtheriae* mutant DW-1 showed the lowest c.f.u. indicating a successful elimination by the macrophages. After 20 h, the number of c.f.u. declined for both *C. ulcerans* and *C. diphtheriae* indicating successful inactivation of bacteria at this late time point by macrophages (Fig. 6a, b).

To quantify the detrimental effect on macrophages, the release of lactate dehydrogenase by lysed cells was measured (Fig. 6e, f). When the cytotoxicity was analysed with this assay,

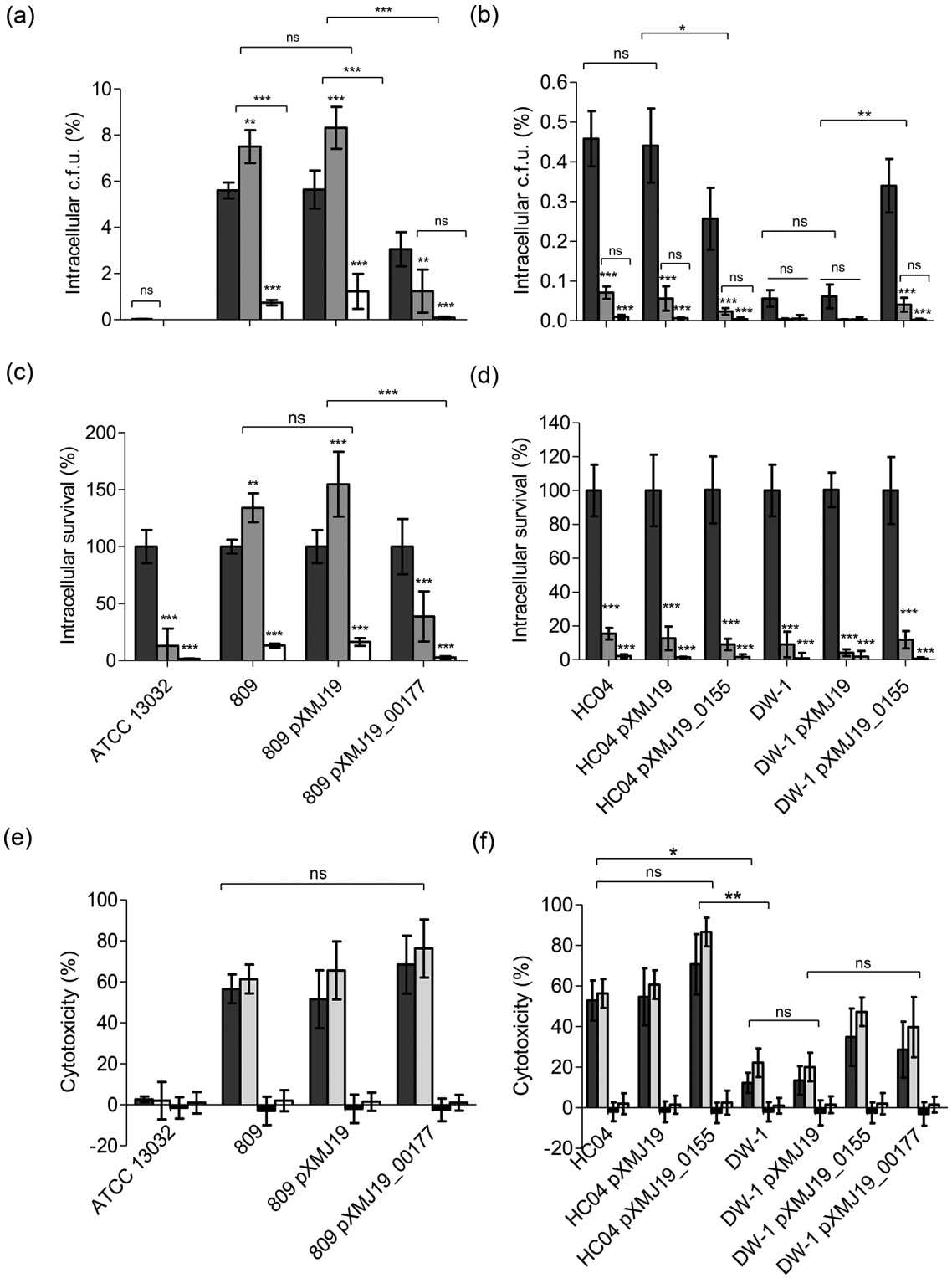

Fig. 6. Quantitative analysis of viable intracellular bacteria in THP-1 cells and the release of LDH in THP1-Blue cells infected with bacteria. THP-1 cells were infected with *C. glutamicum* ATCC 13032, *C. ulcerans* (a and c) and *C. diphtheriae* (b and d) strains at an m.o.i. of 25 for 30 min. To kill extracellular bacteria, cells were incubated with medium containing gentamicin and after 2 h (dark grey bars), 8 h (light grey bars) and 20 h (white bars), cells were harvested, lysed and the lysates were plated on blood agar plates to recover intracellular c.f.u.. Intracellular c.f.u. (a and b) in percent referred to the inoculum and intracellular survival (c and d) in percent referred to the bacteria that were taken up after 2 h. LDH release of THP-1 Blue cells infected with *C. glutamicum* ATCC 13032, *C. ulcerans* (e) and *C. diphtheriae* (f) strains. Grey bars indicate infection with living bacteria, black and white bars show results using UV-killed bacteria. Dark grey and black bars indicate an m.o.i. of 1, light grey and white bars an m.o.i. of 10. Data shown are mean values of at least three independent biological replicates each performed in triplicates±SD. ANOVA column statistics show **P*<0.05, ***P*<0.01 and ****P*<0.001.

supernatants of cells in contact with the non-pathogenic *C. glutamicum* ATCC 13032 showed no LDH activity, independent of used m.o.i. or whether living or dead cells were used. In contrast, strain 809 and HC04 led to cell lysis, when bacteria were added to an m.o.i. 1 or 10. This was not the case when bacteria were inactivated by UV light before infection. Similar results were obtained for strain 809 transformed with pXMJ19 and pXMJ19_00177. A slight but not a significant effect of overexpression of the *rbp* was found. In the case of the *C. diphtheriae rbp* mutant DW-1, a significant effect was observed in comparison to the wild-type strain HC04. Cytotoxicity of the living bacteria reached approximately one-third to half of the level of the corresponding wild-type strain. This was also the case when DW-1 was transformed with pXMJ19 (empty vector control), while DW-1 pXMJ19_0155 and DW-1 pXMJ19_00177 showed enhanced pathogenicity.

DISCUSSION

C. ulcerans strain 809 was isolated from an 80-year-old woman with a fatal pulmonary infection [14]. Based on the symptoms of the patient, production of diphtheria toxin by the strain was assumed and anti-toxin was admitted; however, without success. When the genome sequence of *C. ulcerans* strain 809 was analysed, in fact no gene encoding diphtheria toxin, but a gene encoding a putative Rbp with significant structural similarity to the A chain of SLT-1 from *E. coli* was found [16]. In this study, we were able to provide first experimental evidence for the proposed cytotoxic function of this protein. We were able to demonstrate *in vivo* toxicity of *C. ulcerans* depending on the presence of the *rbp* gene in two invertebrate model systems and provided data for cytotoxic effects exerted *in vitro* on different animal and human epithelial cells and human macrophage cell lines. The severe effects of 809 and *rbp* overexpression may indicate that this protein might have had a significant influence on the fatal outcome of infection with this strain. The fact that Vero cells, kidney epithelial cells from an African green monkey, were damaged may also explain the observed kidney problems of the patient [14].

In principle, also phospholipase D (PLD), a major virulence factor of *C. ulcerans* [50], may have an influence on infection. In fact, strain 809 was described as PLD-positive when isolated and sequenced [14, 16]; however, in a recent proteome study, PLD was not detected [48]. Therefore, the impact of this virulence factor on the macrophages studied here is unclear for *C. ulcerans*, while it can be excluded for *C. diphtheriae*, since strain HC04 is as all other known *C. diphtheriae* strains PLD-negative.

Interestingly, we were able to identify a protein in *C. diphtheriae* HC04, which comprised similar functions and was not reported for *C. diphtheriae* before. These observations may indicate that more toxins than expected may be found in corynebacteria, most likely acquired via horizontal gene transfer. The donor of the corresponding gene and the transfer mechanism for the investigated Rbps is unclear; however, a recent study suggested that conjugation from proteobacteria to actinobacteria might happen frequently in soil [51] and recently also carry-back of antibiotic resistance genes was proposed [52]. Taken together, the results show that more research is necessary and also surveillance of pathogenic corynebacteria is indicated as suggested before [53, 54].

In respect to the studied putative cytotoxic proteins, a more detailed biochemical analysis including overexpression and purification is crucial in future experiments to understand the molecular basis of cytotoxic activity. Furthermore, it is important to characterize the delivery mechanisms in respect to secretion of the toxins by *C. ulcerans* 809 and *C. diphtheriae* HC04 and uptake by the host cells in future studies.

Funding information
The authors received no specific grant from any funding agency.

Acknowledgements
D.W. was supported by a fellowship of the Deutscher Akademischer Austauschdienst (DAAD) and by the Deutsche Forschungsgemeinschaft in frame of SFB796 (MGK). C. A. A. gratefully acknowledge the support by the Coordination for the Improvement of Higher Education Personnel (CAPES) program and the Förderung von Frauen in Forschung und Lehre (FFL) of the Friedrich-Alexander-Universität Erlangen-Nürnberg. The authors are grateful to Dr A. Lührmann for kindly providing the Vero cells and S. Gastiger for the excellent technical assistance.

Author contributions
Conceptualization, project and post project administration, A.B.; investigation, D.W., J.M., M.E.K. and C.A.A.; supervision, C.A.A. and A.B.; methodology and visualization, D.W.; writing and original draft, D.W., A.L.M.G. and A.B.; writing, review and editing: A.B.

Conflicts of interest
The authors declare that there are no conflicts of interest.

References

1. Burkovski A. Diphtheria. In: Rosenberg E, DeLong EF, Thompson F, Lory S *et al* (editors). *The Prokaryotes*, 5, 4th ed. New York: Springer; 2013. pp. 237–246.
2. Loeffler F. Untersuchungen über die bedeutung der mikroorganismen für die entstehung der diphtherie beim menschen, bei der taube und beim kalbe. *Mitteilung Klinische Gesundheit Berlin* 1884;2:451–499.
3. Roux E, Yersin A. Contribution l'étude de la diphtérie. *Ann Inst Pasteur* 1888;2:629–661.
4. Rappuoli R, Malito E. History of diphtheria vaccine development. In: Burkovski A (editor). *Corynebacterium diphtheriae and Related Toxigenic Species*. Dordrecht: Springer; 2014. pp. 225–238.
5. Burkovski A. Pathogenesis of *Corynebacterium diphtheriae* and *Corynebacterium ulcerans*. In: Singh SK (editor). *Human Emerging and Re-emerging Infections: Viral and Parasitic Infections*. Wiley Blackwell Press: John Wiley & Sons; 2015. pp. 699–709.
6. World Health Organization. Immunization, vavvines and biologicals. diphtheria. http://www.who.int/immunization/monitoring_surveillance/burden/diphtheria/en/ [accessed 30th September 2018].
7. Hessling M, Feiertag J, Hoenes K. Pathogens provoking most deaths worldwide: a review. *Biosci Biotech Res Comm* 2017;10:1–7.
8. Sangal V, Hoskisson PA. Corynephages: infections of the infectors. In: Burkovski A (editor). *Corynebacterium diphtheriae and Related Toxigenic Species*. Dordrecht: Springer; 2014. pp. 67–81.
9. Riegel P, Ruimy R, de Briel D, Prévost G, Jehl F *et al*. Taxonomy of *Corynebacterium diphtheriae* and related taxa, with recognition

of *Corynebacterium ulcerans* sp. nov. nom. rev. *FEMS Microbiol Lett* 1995;126:271–276.

10. Burkovski A. Diphtheria and its etiological agents. In: Burkovski A (editor). *Corynebacterium Diphtheriae And Related Toxigenic Species*. Dordrecht: Springer; 2014. pp. 1–14.
11. Meinel DM, Margos G, Konrad R, Krebs S, Blum H *et al*. Next generation sequencing analysis of nine *Corynebacterium ulcerans* isolates reveals zoonotic transmission and a novel putative diphtheria toxin-encoding pathogenicity island. *Genome Med* 2014;6:113.
12. Sing A, Hogardt M, Bierschenk S, Heesemann J. Detection of differences in the nucleotide and amino acid sequences of diphtheria toxin from *Corynebacterium diphtheriae* and *Corynebacterium ulcerans* causing extrapharyngeal infections. *J Clin Microbiol* 2003;41:4848–4851.
13. Sing A, Bierschenk S, Heesemann J. Classical diphtheria caused by *Corynebacterium ulcerans* in Germany: amino acid sequence differences between diphtheria toxins from *Corynebacterium diphtheriae* and *C. ulcerans*. *Clin Infect Dis* 2005;40:325–326.
14. Mattos-Guaraldi AL, Sampaio JLM, Santos CS, Pimenta FP, Pereira GA *et al*. First detection of *Corynebacterium ulcerans* producing a diphtheria-like toxin in a case of human with pulmonary infection in the Rio de Janeiro metropolitan area, Brazil. *Mem Inst Oswaldo Cruz* 2008;103:396–400.
15. Dias AA, Silva FC Jr, Pereira GA, Souza MC, Camello TCF *et al*. *Corynebacterium ulcerans* isolated from an asymptomatic dog kept in an animal shelter in the metropolitan area of Rio de Janeiro, Brazil. *Vector Borne Zoonotic Dis* 2010;10:743–748.
16. Trost E, Al-Dilaimi A, Papavasiliou P, Schneider J, Viehoever P *et al*. Comparative analysis of two complete *Corynebacterium ulcerans* genomes and detection of candidate virulence factors. *BMC Genomics* 2011;12:383.
17. Endo Y, Tsurugi K, Yutsudo T, Takeda Y, Ogasawara T *et al*. Site of action of a Vero toxin (VT2) from *Escherichia coli* O157:H7 and of Shiga toxin on eukaryotic ribosomes. RNA N-glycosidase activity of the toxins. *Eur J Biochem* 1988;171:45–50.
18. Lingwood CA. Verotoxins and their glycolipid receptors. *Adv Lipid Res* 1993;25:189–211.
19. Sandvig K, van Deurs B. Endocytosis and intracellular sorting of ricin and Shiga toxin. *FEBS Lett* 1994;346:99–102.
20. HirataR Jr, Pereira GA, Filardy AA, Gomes DLR, Damasco PV *et al*. Potential pathogenic role of aggregative-adhering *Corynebacterium diphtheriae* of different clonal groups in endocarditis. *Braz J Med Biol Res* 2008;41:986–991.
21. Trost E, Blom J, Soares Sde C, Huang IH, Al-Dilaimi A *et al*. Pangenomic study of *Corynebacterium diphtheriae* that provides insights into the genomic diversity of pathogenic isolates from cases of classical diphtheria, endocarditis, and pneumonia. *J Bacteriol* 2012;194:3199–3215.
22. Abe S, Takayama K, Kinoshita S. Taxonomical studies on glutamic acid-producing bacteria. *J Gen Appl Microbiol* 1967;13:279–301.
23. Grant SG, Jessee J, Bloom FR, Hanahan D. Differential plasmid rescue from transgenic mouse DNAs into *Escherichia coli* methylation-restriction mutants. *Proc Natl Acad Sci USA* 1990;87:4645–4649.
24. Brenner S. The genetics of *Caenorhabditis elegans*. *Genetics* 1974;77:71–94.
25. Schäfer A, Tauch A, Jäger W, Kalinowski J, Thierbach G *et al*. Small mobilizable multi-purpose cloning vectors derived from the *Escherichia coli* plasmids pK18 and pK19: selection of defined deletions in the chromosome of *Corynebacterium glutamicum*. *Gene* 1994;145:69–73.
26. Jakoby M, Ngouoto-Nkili CE, Burkovski A. Construction and application of new *Corynebacterium glutamicum* vectors. *Biotechnol Tech* 1999;13:437–441.
27. Ott L, McKenzie A, Baltazar MT, Britting S, Bischof A *et al*. Evaluation of invertebrate infection models for pathogenic corynebacteria. *FEMS Immunol Med Microbiol* 2012;65:413–421.
28. Peterson WD Jr, Stulberg CS, Swanborg NK, Robinson AR. Glucose-6-phosphate dehydrogenase isoenzymes in human cell cultures determined by sucrose-agar gel and cellulose acetate zymograms. *Exp Biol Med* 1968;128:772–776.
29. Tsuchiya S, Yamabe M, Yamaguchi Y, Kobayashi Y, Konno T *et al*. Establishment and characterization of a human acute monocytic leukemia cell line (THP-1). *Int J Cancer* 1980;26:171–176.
30. Yasumura Y, Kawakita Y. Studies on SV40 in tissue culture: preliminary step for cancer research *in vitro*. *Nihon Rinsho* 1963;21:1201–1215.
31. McWilliam H, Li W, Uludag M, Squizzato S, Park YM *et al*. Analysis tool web services from the EMBL-EBI. *Nucleic Acids Res* 2013;41:W597–W600.
32. Sievers F, Wilm A, Dineen D, Gibson TJ, Karplus K *et al*. Fast, scalable generation of high-quality protein multiple sequence alignments using Clustal omega. *Mol Syst Biol* 2011;7:539.
33. Petersen TN, Brunak S, von Heijne G, Nielsen H. SignalP 4.0: Discriminating signal peptides from transmembrane regions. *Nat Methods* 2011;8:785–786.
34. Kelley LA, Mezulis S, Yates CM, Wass MN, Sternberg MJE. The Phyre2 web portal for protein modeling, prediction and analysis. *Nat Protoc* 2015;10:845–858.
35. Pettersen EF, Goddard TD, Huang CC, Couch GS, Greenblatt DM *et al*. UCSF Chimera--a visualization system for exploratory research and analysis. *J Comput Chem* 2004;25:1605–1612.
36. Sambrook J, Fritsch EF, Maniatis T. *Molecular Cloning: a Laboratory Manual*, 2nd ed. Cold Spring Harbor, NY: Cold Spring Harbor Laboratory Press; 1989.
37. Ott L, Höller M, Rheinlaender J, Schäffer TE, Hensel M *et al*. Strain-specific differences in pili formation and the interaction of *Corynebacterium diphtheriae* with host cells. *BMC Microbiol* 2010;10:257.
38. Bradford MM. A rapid and sensitive method for the quantitation of microgram quantities of protein utilizing the principle of protein-dye binding. *Anal Biochem* 1976;72:248–254.
39. Wiśniewski JR, Zougman A, Nagaraj N, Mann M. Universal sample preparation method for proteome analysis. *Nat Methods* 2009;6:359–362.
40. Kraner ME, Müller C, Sonnewald U. Comparative proteomic profiling of the choline transporter-like1 (CHER1) mutant provides insights into plasmodesmata composition of fully developed *Arabidopsis thaliana* leaves. *Plant J* 2017;92:696–709.
41. Zhang J, Xin L, Shan B, Chen W, Xie M *et al*. Peaks DB: *de Novo* sequencing assisted database search for sensitive and accurate peptide identification. *Mol Cell Proteomics* 2012;11:M111.010587.
42. Weerasekera D, Stengel F, Sticht H, de Mattos Guaraldi AL, Burkovski A *et al*. The C-terminal coiled-coil domain of *Corynebacterium diphtheriae* DIP0733 is crucial for interaction with epithelial cells and pathogenicity in invertebrate animal model systems. *BMC Microbiol* 2018;18:106.
43. de Bono M, Bargmann CI. Natural variation in a neuropeptide Y receptor homolog modifies social behavior and food response in *C. elegans*. *Cell* 1998;94:679–689.
44. Loh JMS, Adenwalla N, Wiles S, Proft T. *Galleria mellonella* larvae as an infection model for group A streptococcus. *Virulence* 2013;4:419–428.
45. Hacker E, Ott L, Schulze-Luehrmann J, Lührmann A, Wiesmann V *et al*. The killing of macrophages by *Corynebacterium ulcerans*. *Virulence* 2016;7:45–55.
46. Ott L, Burkovski A. Toxigenic corynebacteria: adhesion, invasion and host response. In: Burkovski A (editor). *Corynebacterium diphtheriae and Related Toxigenic Species*. Dordrecht: Springer; 2014. pp. 143–170.
47. Hacker E, Ott L, Hasselt K, Mattos-Guaraldi AL, Tauch A *et al*. Colonization of human epithelial cell lines by *Corynebacterium ulcerans* from human and animal sources. *Microbiology* 2015;161:1582–1591.

48. Bittel M, Gastiger S, Amin B, Hofmann J, Burkovski A. Surface and extracellular proteome of the emerging pathogen *Corynebacterium ulcerans*. *Proteomes* 2018;6:18.
49. Ott L, Höller M, Rheinlaender J, Schäffer TE, Hensel M *et al*. Strain-specific differences in pili formation and the interaction of *Corynebacterium diphtheriae* with host cells. *BMC Microbiol* 2010;10:257.
50. Hacker E, Antunes CA, Mattos-Guaraldi AL, Burkovski A, Tauch A. *Corynebacterium ulcerans*, an emerging human pathogen. *Future Microbiol* 2016;11:1191–1208.
51. Klümper U, Riber L, Dechesne A, Sannazzarro A, Hansen LH *et al*. Broad host range plasmids can invade an unexpectedly diverse fraction of a soil bacterial community. *ISME J* 2015;9:934–945.
52. Jiang X, Ellabaan MMH, Charusanti P, Munck C, Blin K *et al*. Dissemination of antibiotic resistance genes from antibiotic producers to pathogens. *Nat Commun* 2017;8:15784.
53. Efstratiou A, Engler KH, Mazurova IK, Glushkevich T, Vuopio-Varkila J *et al*. Current approaches to the laboratory diagnosis of diphtheria. *J Infect Dis* 2000;181:S138–S145.
54. Wagner KS, White JM, Neal S, Crowcroft NS, Kuprevičiene N *et al*. Screening for *Corynebacterium diphtheriae* and *Corynebacterium ulcerans* in patients with upper respiratory tract infections 2007-2008: a multicentre European study. *Clin Microbiol Infect* 2011;17:519–525.

Edited by: J. Stülke and E. L Denham

VIRULENCE
2019, VOL. 10, NO. 1, 414–428
https://doi.org/10.1080/21505594.2019.1614384

Taylor & Francis
Taylor & Francis Group

RESEARCH PAPER

Of mice and men: Interaction of *Corynebacterium diphtheriae* strains with murine and human phagocytes

Dulanthi Weerasekera[a], Tamara Fastner[a], Roland Lang [b], Andreas Burkovski [a], and Lisa Ott[a]

[a]Department Biologie, Friedrich-Alexander-Universität Erlangen-Nürnberg, Erlangen, Germany; [b]Institut für Klinische Mikrobiologie, Immunologie und Hygiene, Universitätsklinikum Erlangen, Friedrich-Alexander-Universität Erlangen-Nürnberg, Erlangen, Germany

ABSTRACT

Seven non-toxigenic *C. diphtheriae* strains and one toxigenic strain were analyzed with regard to their interaction with murine macrophages (BMM) and human THP-1 macrophage-like cells. Proliferation assays with BMM and THP-1 revealed similar intracellular CFUs for *C. diphtheriae* strains independent of the host cell. Strain ISS4060 showed highest intracellular CFUs, while the toxigenic DSM43989 was almost not detectable. This result was confirmed by TLR 9 reporter assays, showing a low signal for DSM43989, indicating that the bacteria are not endocytosed. In contrast, the non-pathogenic *C. glutamicum* showed almost no intracellular CFUs independent of the host cell, but was recognized by TLR9, indicating that the bacteria were degraded immediately after endocytosis. In terms of G-CSF and IL-6 production, no significant differences between BMM and THP-1 were observed. G-CSF production was considerably higher than IL-6 for all *C. diphtheriae* strains and the *C. glutamicum* did not induce high cytokine secretion in general. Furthermore, all corynebacteria investigated in this study were able to induce NFκB signaling but only viable *C. diphtheriae* strains were able to cause host cell damage, whereas *C. glutamicum* did not. The absence of Mincle resulted in reduced G-CSF production, while no influence on the uptake of the bacteria was observed. In contrast, when MyD88 was absent, both the uptake of the bacteria and cytokine production were blocked. Consequently, phagocytosis only occurs when the TLR/MyD88 pathway is functional, which was also supported by showing that all corynebacteria used in this study interact with human TLR2.

ARTICLE HISTORY
Received 21 December 2018
Revised 21 March 2019
Accepted 28 April 2019

KEYWORDS
Cytotoxicity; inflammation; interleukins; macrophages; NFκB; TLRs

Introduction

Corynebacterium diphtheriae is the classical etiological agent of diphtheria and the type species of the genus *Corynebacterium* [1,2]. The transmission of *C. diphtheriae* from person to person occurs by close physical contact or respiratory droplets [3]. Infections of the upper respiratory tract are characterized by sore throat, low fever, and malaise. Symptoms range from mild pharyngitis to severe hypoxia with pseudomembrane formation due to the toxin. Vaccination against classical respiratory diphtheria is available with toxoid vaccine that is directed against the toxin. Nevertheless, *C. diphtheriae* does not mandatorily produce the diphtheria toxin; it has to be infected by a toxin carrying β-corynephage, integrating into the genome of the bacteria [4]. Interestingly, toxigenic but also non-toxigenic *C. diphtheriae* strains are increasingly associated with invasive infections, such as endocarditis, osteomyelitis, splenic abscesses, meningitis, and septic arthritis [5–7]. Recent characterization of a non-toxigenic *C. diphtheriae* strain isolated from a cancer patient with osteomyelitis indicates that *C. diphtheriae* can colonize not only epithelia but can also infect deeper parts of the body [8].

Besides the mode of action of the diphtheria toxin, the molecular mechanisms of the interaction of *C. diphtheriae* with host cells, especially the activation of human macrophages by non-toxigenic strains, is poorly understood. In case of mycobacteria, which are closely related to corynebacteria, the molecular mechanisms of the infection process are investigated in more detail. For the human pathogen *Mycobacterium tuberculosis* it is known that direct recognition of trehalose dimycolate (TDM), the major lipid in the outer membrane of mycobacteria, by the C-type lectin receptor (CLR) Mincle triggers macrophage activation through the adaptor protein Fc receptor gamma chain (FcRγ), the kinase Syk and the Card9-Bcl10-Malt1 complex [9–11]. Mycobacteria possess a number of Toll-like receptor (TLR) ligands, e.g. the 19 kDa lipopeptide and lipoarabinomannans. The activation of the TLR signaling pathway originates from the cytoplasmic Toll/IL-1 receptor (TIR) domain that associates with a TIR domain-containing adaptor, MyD88. MyD88 links IL-1 receptor

CONTACT Lisa Ott lisa.baeumer@fau.de
Supplementary material data can be accessed here.

(IL-1R) or TLR family members to IL-1R-associated kinase (IRAK) family kinases via homotypic protein–protein interaction. Activation of IRAK family kinases leads to a variety of functional outputs, including the activation of nuclear factor-kappa B (NFκB) making MyD88 a central node of inflammatory pathways [12].

In case of *C. diphtheriae*, it is known that macrophages show a delay of phagolysosome formation when being infected with different *C. diphtheriae* strains [13]. Additionally, cell wall extracts of *C. diphtheriae* play a role in activating murine macrophages [14]. Furthermore, TLR2 was found to be required for the upregulation of Mincle expression upon corynebacterial infection [14]. To get deeper insights into the molecular mechanisms of macrophage activation by *C. diphtheriae*, we investigated the interaction of *C. diphtheriae* wild type strains with bone marrow-derived macrophages (BMM) in comparison to the human THP-1 cell line. By using a combination of BMM, Mincle$^{-/-}$ and MyD88$^{-/-}$ cells, we tested if viable *C. diphtheriae* strains bind and activate the C-type lectin receptor Mincle and the Toll-like receptor TLR2. Furthermore, the role of the adaptor protein Myd88 during uptake of the bacteria was investigated. By quantification of intracellular bacteria, detection of pro-inflammatory cytokines, analysis of NFκB activation as well as host cell damage, host immune response was studied during *C. diphtheriae* infection. The question of recognition of bacteria in endolysosomal compartments was addressed by using TLR9 reporter cells.

Materials and methods

Bacterial strains and growth conditions

C. diphtheriae strains as well as *C. glutamicum* (Table 1) were grown in Heart Infusion (HI) broth (Becton Dickinson, Sparks, MD, USA) or on HI and Brain Heart Infusion (BHI) (Oxoid, Wesel, Germany) agar plates as well as Columbia Blood Agar (CBA) containing 5% sheep blood (Oxoid, Wesel, Germany) at 37°C.

Isolation and culture of primary mouse macrophages and macrophage cell lines

Killing of mice by cervical dislocation for extraction of bone marrow from femural and tibial bones was registered according to German Animal Protection Law §4 with the Regierung von Mittelfranken (protocol number 12/08). C57BL/6, Clec4e$^{-/-}$ and MyD88$^{-/-}$ mice were bred at the Präklinisches Experimentelles Tierzentrum of the Medical Faculty of the Friedrich-Alexander University Erlangen-Nürnberg. Bone marrow cells from femurs and tibiae were differentiated to macrophages by culture in complete Dulbecco's modified Eagle's medium (DMEM) (Life Technologies, Carlsbad, USA) containing 100 U penicillin ml^{-1} and 0.1 mg streptomycin ml^{-1}, 10% fetal calf serum (FCS) (Gibco BRL, Germany) and 50 µM β-mercaptoethanol (complete DMEM [cDMEM]) plus 10% L929 cell-conditioned medium as a source of macrophage colony-stimulating factor (M-CSF), as previously described [15]. On day 7, adherent macrophages were harvested by Accutase (Sigma, Munich, Germany) treatment, washed with 1 x PBS and counted.

THP-1 human monocytes were cultured in 10% FCS supplemented RPMI medium 1640 (Gibco BRL, Eggenstein, Germany) (containing 100 U penicillin ml^{-1} and 0.1 mg streptomycin ml^{-1}) at 37°C in 5% CO_2 in a humidified cell culture incubator. The cells were harvested by centrifugation, washed with 1 x PBS and counted.

Replication assay

For gentamicin protection assays, cells were seeded in 24-well plates (Nunc, Wiesbaden, Germany) at a density of 2×10^5 cells per well 24 h prior to infection. In case of THP-1 cells, 10 ng ml^{-1} phorbol 12-myristate 13-acetate (PMA) were added for differentiation of the cells. Overnight cultures of *C. diphtheriae* grown in HI were re-inoculated to an OD_{600} of 0.1 in fresh medium and grown to an OD_{600} of 0.4 to 0.6. An inoculum with MOI of 1 or 10 was prepared in RPMI without antibiotics and 500 µl per well were used to infect the cells. Serial dilutions of the inoculum were plated on blood agar plates (Oxoid, Wesel, Germany) using an Eddy Jet Version 1.22 (IUL Instruments, Barcelona, Spain) and incubated at 37°C for 2 days. The infection plates were centrifuged for 5 min at 350 x g to synchronize the infection and incubated for 30 min (37°C, 5% CO_2, 95% humidity) to allow phagocytosis of bacteria. Subsequently, the supernatant containing non-engulfed bacteria was aspirated, cells were washed once with PBS and remaining extracellular bacteria were killed by addition of 100 mg ml^{-1} gentamicin in cell culture medium. After 2 h, cells were either lysed by adding 500 µl of 0.1% Triton X-100 in PBS and intracellular bacteria were recovered by plating serial dilutions of the lysates on blood agar plates or further incubated with medium containing 10 mg ml^{-1} gentamicin for analysis at later time points (4 and 20 h). After incubation at 37°C for 2 days, the number of colony forming units (CFU) was determined. The ratio of bacteria used for infection (number of colonies on inoculum plates) and bacteria in the lysate (number of colonies on the lysate plates) multiplied with 100 gave the percentage of viable intracellular bacteria at different time points. When the survival of intracellular bacteria in THP-1 cells was analyzed over the time, the number of CFU at 2 h was set to 100% and

Table 1. Bacterial strains and cell lines used in this study.

	Genotype/Description	Reference/Source
***C. diphtheriae* strains**		
ISS3319	*C. diphtheriae* var. mitis, non-toxigenic, isolated from patients affected by pharyngitis/tonsilitis	[29]
ISS4060	*C. diphtheriae* var. gravis, non-toxigenic, isolated from patients affected by pharyngitis/tonsilitis	[29]
ISS4746	*C. diphtheriae* var. gravis, non-toxigenic, isolated from patients affected by pharyngitis/tonsilitis	[6]
ISS4749	*C. diphtheriae* var. gravis, non-toxigenic, isolated from patients affected by pharyngitis/tonsilitis	[6]
DSM43988	strain 48,255, ATCC 11,913, avirulent throat culture	obtained from DSMZ, Braunschweig, Germany
DSM43989	PW strain, strain 5159, ATCC 13,812, producer of diphtheria toxin for toxoid production	[30], obtained from DSMZ, Braunschweig, Germany
DSM44123	type strain, C7s, ATCC 27,010, CIP 100,721, NCTC 11,397	obtained from DSMZ, Braunschweig, Germany
Inca-402	isolated from a bronchial wash specimen from a cancer patient with pneumonia in Rio de Janeiro, 2000	[31]
NCTC13129	biovar gravis; tox^+	[32]
***C. glutamicum* strains**		
ATCC 13032	type strain	[33], laboratory stock
Cell lines		
THP-1	human leukemic monocytic cells	[34]
THP-1-Blue NFκB	THP-1 cells with stable integrated NFκB inducible SEAP reporter construct	InvivoGen, San Diego, USA
HEK-Blue 293 hTLR2	human TLR2/NF-κB/SEAP reporter HEK293 cells	InvivoGen, San Diego, USA
HEK-Blue 293 hTLR9	human TLR9/NF-κB/SEAP reporter HEK293 cells	InvivoGen, San Diego, USA
Bone marrow-derived macrophages		
C57/BL6	bone marrow cells from femur and tibiae differentiated to macrophages	Präklinisches Experimentelles Tierzentrum of the Medical Faculty of the Friedrich-Alexander Universtity Erlangen-Nuremberg
$Clec4e^{-/-}$	bone marrow cells from femur and tibiae of Mincle-deficient mice differentiated to macrophages	Präklinisches Experimentelles Tierzentrum of the Medical Faculty of the Friedrich-Alexander Universtity Erlangen- Nuremberg
$MyD88^{-/-}$	bone marrow cells from femur and tibiae of Myd88-deficient mice differentiated to macrophages	Präklinisches Experimentelles Tierzentrum of the Medical Faculty of the Friedrich-Alexander Universtity Erlangen- Nuremberg

later time points were calculated based on this value. The assay was performed at least in three biological replicates each performed in triplicates and means and standard deviations were calculated.

NFκB reporter assay

THP1-Blue NFκB cells (InvivoGen, San Diego, USA) carrying a stable integrated NFκB-inducible secreted embryonic alkaline phosphatase (SEAP) reporter construct were used to analyze NFκB induction by *C. diphtheriae*. *C. diphtheriae* strains were inoculated from an overnight culture to an OD_{600} of 0.1 in fresh medium and grown to an OD_{600} of 0.4 to 0.6. An inoculum with an OD_{600} of 1.25 in 1,000 µl PBS was prepared and 20 µl of this inoculum or of the 10^{-1} and 10^{-2} dilutions were mixed with 180 µl of a suspension with 5×10^5 THP1-Blue NFκB cells in cell culture medium resulting in an MOI of 100, 10 or 1. UV-killed bacteria in the same concentrations were also studied. After incubation for 20 h at cell culture conditions, the 96-well plates were centrifuged (350 x g, 5 min) and 20 µl of the cell free supernatant was mixed with 180 µl pre-warmed SEAP detection reagent QUANTI-Blue (InvivoGen, San Diego, USA). After further incubation at cell culture conditions for 3 h, the levels of NFκB-induced SEAP resulting in a color change from pink to blue were measured in a microplate reader (TECAN Infinite 200 PRO, Männedorf, Switzerland) at 620 nm.

Determination of cytokine excretion

For determination of cytokine activation through *C. diphtheriae*, supernatants of infected cells were collected after different time points and stored at −20°C. IL-6 and G-CSF concentrations were measured using the DuoSet ELISA Kits according to the manufacturer's recommendations (R&D systems). Briefly, the ELISA plates were coated over night with a capture antibody at room temperature, washed 3 times with 0.05% Tween20 in PBS, blocked for 1 h at room temperature with 1% BSA in PBS and washed again 3 times. Subsequently, 100 µl supernatant of infected cells or standard dilutions were added, and the plates were incubated for 2 h, washed again three times and further incubated for 2 h at room temperature. After another washing step, a streptavidin-HRP solution was added and the plates were stored for 20 min under light exclusion, washed again, and incubated for another 20 min in the dark with substrate solution. To stop

the color reaction, 2 N H_2SO_4 was added to the wells and the optical density was determined using a microplate reader (TECAN Infinite 200 PRO, Männedorf, Switzerland) set to 450 nm with wavelength correction at 550 nm.

LDH release

The release of cytosolic lactate dehydrogenase (LDH) as a sign of host cell damage during infection was measured using the cytotoxicity detection kit according to the supplier (Roche).

Briefly, 100 µl supernatant of infected cells were mixed with 2.5 ml of the provided catalyst solution and 112.5 µl of the provided dye solution in 96-well plates, incubated in the dark for 30 min and the absorbance was measured at 490 nm and wavelength correction at 620 nm in a microplate reader (TECAN Infinite 200 PRO, Männedorf, Switzerland). Cells treated with 2% Triton X-100 served as positive control for maximal LDH release and were set to 100%, untreated cells served as negative control.

Griess assay

NO production was assessed via a Griess assay (Griess Reagent System, Promega). 50µl of the culture medium supernatant were gently mixed with an equal volume of sulfanilamide solution and incubated in the dark at room temperature for 10 min. Subsequently, 50 µl of NED solution was added and the reaction solution was incubated in the dark at room temperature for 10 min. The absorbance of this solution at 540 nm was measured in a microplate reader (TECAN Infinite 200 PRO, Männedorf, Switzerland) and the nitrite concentration was calculated from a nitrite standard reference curve.

TLR2 and TLR9 reporter assays

HEK-Blue-hTLR2 and hTLR9 cells (InvivoGen, San Diego, USA), carrying a stable integrated inducible secreted embryonic alkaline phosphatase (SEAP) reporter construct, were used to analyze TLR2 and TLR9 binding of *C. diphtheriae*. Stimulation with a TLR2 or TLR9 ligand activates NF-κB and AP-1, which induce the production of SEAP. TRL2 is a surface exposed receptor, while TLR9 is expressed in the endoplasmic reticulum and located in endolysosomal compartments, where it recognizes specific unmethylated CpG sequences, which are characteristic for bacterial DNA. Furthermore, TLR9 binding involves Myd88 signaling. *C. diphtheriae* strains were inoculated from an overnight culture to an OD_{600} of 0.1 in fresh medium and grown to an OD_{600} of 0.4 to 0.6. An inoculum with an OD_{600} of 1 in 1000 µl PBS was prepared and 20 µl of the 10^{-1} and 10^{-2} dilutions of this inoculum for hTLR2 and 1:1 and 1:10 dilutions for hTLR9 were mixed with 180 µl of a suspension with 5×10^5 HEK-Blue hTRL2 in cell culture medium or hTLR9 cells in HEK Blue detection medium. This resulted in an MOI of 10 or 1 for hTLR2 and an MOI 50 and 10 for hTLR9. UV-killed bacteria in the same amount were also investigated. After incubation of HEK-Blue hTLR2 cells for 20 h at cell culture conditions, 96-well plates were centrifuged (350 x g, 5 min) and 20 µl of the cell-free supernatant was mixed with 180 µl pre-warmed SEAP detection reagent Quanti-Blue (InvioGen, San Diego, USA). After further incubation at cell culture conditions for 3 h, SEAP activity was measured in a microplate reader (TECAN Infinite 200 PRO, Männedorf, Switzerland) at 620 nm. In contrast, HEK-Blue hTLR9 cells were incubated for 24 h under cell culture conditions and SEAP activity was measured as mentioned above.

Statistical analysis

All experiments were carried out in at least three independent biological replicates, each performed in technical triplicates and standard deviations were calculated. Data were analyzed using the software GraphPad Prism 7.0 (GraphPad, CA, USA).

Results

Survival of *C. diphtheriae* after internalization by primary macrophages from C57BL/6 mice, Clec4e- and Myd88-deficient mice

As a basis for subsequent experiments, *C. diphtheriae* interaction with bone marrow-derived murine macrophages (BMM), Clec4e- and Myd88-deficient cells was analyzed (Figure 1). Different *C. diphtheriae* wild type isolates and the non-pathogenic *C. glutamicum* strain ATCC 13032 were studied in respect to internalization (Figure 1(a)) and intracellular survival (Figure 1(b)). When the intracellular CFUs were analyzed, strain-specific and cell-specific differences were detectable. Almost no viable bacteria of the non-pathogenic *C. glutamicum* strain (ATCC 13032) and the toxigenic *C. diphtheriae* strain (DSM43989) were observed already after 2 h post-infection independent of the cell type (Figure 1(a)). For the other investigated strains, the CFUs after 2 h ranged between 0.5% and 1.5% of the inoculum in BMM, which is representatively shown for strain ISS3319. The 2 h values were set to 100% and the

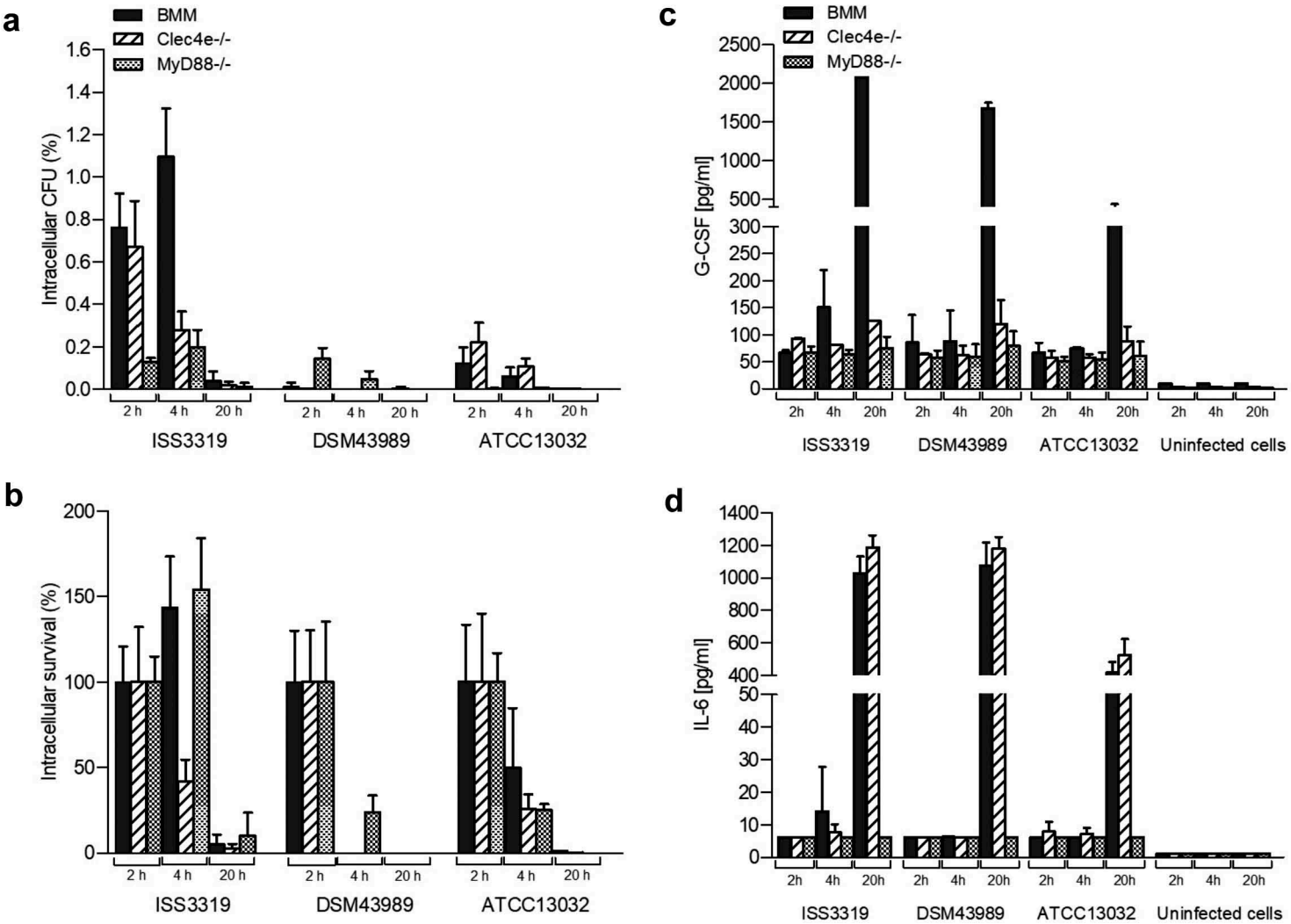

Figure 1. Quantitative analysis of viable intracellular corynebacteria and cytokine ELISA of bone marrow-derived murine macrophages from C57/BL6 (BMM), Clec4e- and MyD88-deficient mice after infection with bacteria. Cells were infected with *C. diphtheriae* wild type strains ISS3319, DSM43989 and *C. glutamicum* ATCC 13032 at an MOI of 10 for 2, 4 and 20 h, lysed and the lysates were plated on blood agar plates. (a) Intracellular CFU in percent of the inoculum. (b) intracellular survival in percent of the bacteria that were taken up after 2 h. Supernatants of primary bone marrow (BMM), Clec4e$^{-/-}$ and MyD88$^{-/-}$ macrophages infected with bacteria were collected at different time points post-infection (2, 4 and 20 h) and used for the determination of (c) G-CSF and (d) IL-6 concentrations. Data shown are mean values of at least three independent biological replicates each performed in triplicates ± standard deviation.

survival rates were calculated (Figure 1(b)). The calculated rates at 2 and 4 h showed, that strain ISS3319 is able to proliferate within the first 4 h post-infection in BMM and MyD88$^{-/-}$, while the survival rates of other *C. diphtheriae* strains, except the toxigenic strain DSM43989, remained at least constant. All strains were almost completely degraded overnight (Figure 1(b)). All other *C. diphtheriae* strains behaved similar to ISS3319 and the results for all eight strains are shown in the supplementary material (Fig. S1, S2, S3).

In summary, the different non-toxigenic *C. diphtheriae* isolates were able to persist longer periods within the BMM compared to *C. glutamicum* and toxigenic DSM43989, and were partially able to proliferate within the first 4 h post-infection. This result indicated that *C. diphtheriae* is able to cause a delay of phagolysosome maturation in macrophages, which was shown in a previous study for different *C. diphtheriae* strains [13].

Role of the C-type lectin receptor mincle on *C. diphtheriae* infection

In order to address if macrophage activation via Mincle is influenced when viable bacteria are used for infection, BMM from Mincle-deficient mice (Clec4e$^{-/-}$) were incubated with *C. diphtheriae* (Figure 1). These experiments revealed internalization rates between 0.6 and 1.0% for all *C. diphtheriae* strains, except the toxigenic strain DSM43989. Compared to the infection of BMM of wild type C57BL/6 mice, there was no significant reduction of the detectable CFUs in Clec4e$^{-/-}$ mice. As observed in infection of BMM wild type cells, in case of the toxigenic strain DSM43989 almost no viable intracellular CFUs were detectable already after 2 h of infection and the number of intracellular CFUs of *C. glutamicum* ATCC 13032 was significantly lower compared to the non-toxigenic *C. diphtheriae* strains, such as ISS3319 (Figure 1(a)). The survival rates reached about 30 to 60% of those of the non-toxigenic *C. diphtheriae* strains. Also *C. glutamicum* were still viable within the first 4 h post-infection. For strain DSM43989, no colony was detectable 4 h post-infection. After overnight incubation, the strains ISS4060, DSM44123 and Inca-402 showed the highest resistance to macrophage action with about 10 to 15% of the internalized bacteria being still viable (Fig. S2). The non-pathogenic control strain ATCC 13032 was almost entirely degraded overnight. Noteworthy, by comparing the intracellular CFUs in Clec4e$^{-/-}$ BMM to C57BL/6 BMM no significant difference was observed.

Influence of the adaptor protein Myd88 on *C. diphtheriae* infection

The Toll-like receptor/MyD88 pathway, a major pattern recognition system, plays an important role in immunity. The MyD88 adaptor molecule is recruited after activation of most TLRs. This pathway includes the recruitment and activation of several other proteins and leads finally to the activation of NFκB pathways and the production of pro-inflammatory cytokines [16,17]. In this study, the role of the MyD88 adapter protein in the activation of macrophages by viable *C. diphtheriae* strains in comparison to BMM and Clec4e$^{-/-}$ was analyzed (Figure 1). Replication assays carried out with cells derived from MyD88-deficient mice revealed that after 2 h of infection intracellular CFUs of maximum 0.3% of the inoculum were detectable for all *C. diphtheriae* strains and the number of intracellular CFUs remained almost constant within 4 h post-infection. Less than 0.01% of the inoculum was observed for strain *C. glutamicum* ATCC 13032 (Figure 1(a)). All *C. diphtheriae* strains, except the toxigenic one (DSM43989), were able to proliferate, or the number of viable bacteria remained constant at least the first 4 h post-infection. After overnight incubation, almost no CFUs were detectable for each strain (Figure 1(b)). Comparison the internalization rates of the different strains in MyD88-deficient cells with those in wild type cells after 2 h showed a reduction by 80 to 90% of the intracellular CFUs. The data indicated that the recruitment of the adaptor protein MyD88 is essential for TLR signaling in macrophage activation by viable *C. diphtheriae* strains.

Response of primary macrophages to *C. diphtheriae* infection

In order to address the immune response to the infection with *C. diphtheriae* in BMM, Clec4e- and Myd88-deficient cells, the supernatants were collected at 2, 4 and 20 h post-infection for determination of cytokine secretion, such as G-CSF (Figure 1(c)) and IL-6 (Figure 1(d)), respectively. Analysis of cytokines in the supernatants from BMM infected with non-toxigenic *C. diphtheriae* strains revealed about 2000 pg ml^{-1} of G-CSF after overnight incubation, which is shown representatively for strain ISS3319 (Figure 1(c)). The toxigenic strain DSM43989 reached slightly lower values of about 1700 pg ml^{-1} of G-CSF, while the non-pathogenic control strain ATCC 13032 reached only about 300 pg ml^{-1} of

G-CSF (Figure 1(c)). Interestingly, the weak cytokine production in response to *C. glutamicum* infection may not be due to the low intracellular CFUs that were detected in the proliferation assay for this strain. Rather it seems to indicate the non-pathogenic role of strain ATCC 13032, since the intracellular CFUs of strain DSM43989 were even lower than those of *C. glutamicum*, but were leading to high G-CSF production (Figure 1(a)). In Mincle-deficient cells, almost no G-CSF production was observed at 2 and 4 h post-infection, which was comparable to the wild type cells. Interestingly, after overnight incubation, the G-CSF concentrations were also almost at background levels between 100 and 270 pg ml^{-1}. Compared to macrophages derived from C57BL/6 mice, this is a reduction of about 90% (Figure 1(c)). The measurement of the G-CSF concentrations in the supernatant of Myd88-deficient cells revealed a reduction to background level at all time points (Figure 1(c)).

When IL-6 concentrations were measured in the supernatant of the different cell types, no significant differences were observed between BMM and Clec4e$^{-/-}$ cells (Figure 1(d)). Interestingly, after overnight incubation all *C. diphtheriae* strains lead to strong IL-6 production in both BMM and Clec4e$^{-/-}$ cells. The non-pathogenic strain ATCC 13032 reached the lowest IL-6 levels of about 400 pg ml^{-1} (Figure 1(d), S1). IL-6 concentrations in Mincle-deficient cells in response to *C. diphtheriae* infection reached values between 1000 and 1200 pg ml^{-1} for all *C. diphtheriae* strains, which was almost similar to wild type cells. Again, the lowest value of about 600 pg ml^{-1} was observed for strain ATCC 13032 (Figure 1(d)). When IL-6 secretion was analyzed in Myd88-deficient cells, all strains reached values only to background level of 6.15 pg ml^{-1} at all time-points (Figure 1(d)).

In summary, infection of BMM with *C. diphtheriae* induced production of the inflammatory cytokines G-CSF and IL-6 (Figure 1(c,d)). The non-pathogenic strain ATCC 13032 caused significantly lower inflammatory response compared to pathogenic corynebacteria. Furthermore, Mincle-binding of pathogenic corynebacteria seems not mandatory for the internalization of the bacteria. However, the inflammatory response in terms of G-CSF, but not of IL-6, is impaired when Mincle is absent. When the adaptor protein MyD88 is absent in macrophages neither phagocytosis of the bacteria nor G-CSF or IL-6 release occurred.

Survival of *C. diphtheriae* after internalization by THP-1 cells

While murine cells are an excellent model to test the influence of several signaling pathways due to the availability of the respective knockout cells, humans are the natural host of *C. diphtheriae*. Therefore, the human macrophage-like cell line THP-1 was applied to analyze internalization and survival of *C. diphtheriae* (Figure 2). In this case, strong strain-specific differences in the uptake of the bacteria were observed. After 2 h of incubation, the detected intracellular CFUs of the strains ISS4746, ISS4749 and the toxigenic strain DSM43989 were less than 0.2% of the inoculum. Highest internalization rates were reached for strains ISS3319 (~2.5%), ISS4060 (~5.0%) and strain DSM43988 (~3.0%) while the lowest internalization rates were observed for strains DSM44123 and Inca-402 with about 1.3% and 0.5%, respectively. The non-pathogenic strain ATCC 13032 was almost not detectable already 2 h post-infection (Figure 2(a)). By calculation of the survival rates, it became apparent that all *C. diphtheriae* strains were able to persist within the cells at least up to 4 h post-infection, but were completely degraded overnight (Figure 2(b)).

Response of THP-1 cells to *C. diphtheriae* infection

To investigate the reaction of unstimulated THP-1 cells in response to *C. diphtheriae* infection, culture supernatants were collected at 2, 4 and 20 h post-infection to measure G-CSF (Figure 2(c)), IL-6 (Figure 2(d)) and NO production (Figure 2(e)). Interestingly, in contrast to the strain-specific internalization of the bacteria into the cells, no significant differences in cytokine-production where observed (Figure 2(c,d)). After 4 h of infection *C. diphtheriae* strains led to G-CSF secretion of about 750 pg ml^{-1} (Figure 2(c)), while no IL-6 production was measurable (Figure 2(d)). After overnight, values of more than 3000 pg ml^{-1} were reached for G-CSF production (Figure 2(c)) and values between 800 and 1400 pg ml^{-1} were detectable for IL-6 (Figure 2(d)).

In THP-1 cells, reactive nitrogen species contributed to innate host defense against several *C. diphtheriae* wild type strains (Figure 2(e)). 17 µM nitrite for strains ISS4746 and IS4749, 27 µM nitrite for strain DSM43989 and 10 µM nitrite for strain Inca-402 at 20 h post-infection were detected. Remarkably, the NO production was contrary to the viable CFUs that were detectable at 2 h post-infection (Figure 2(a)), meaning

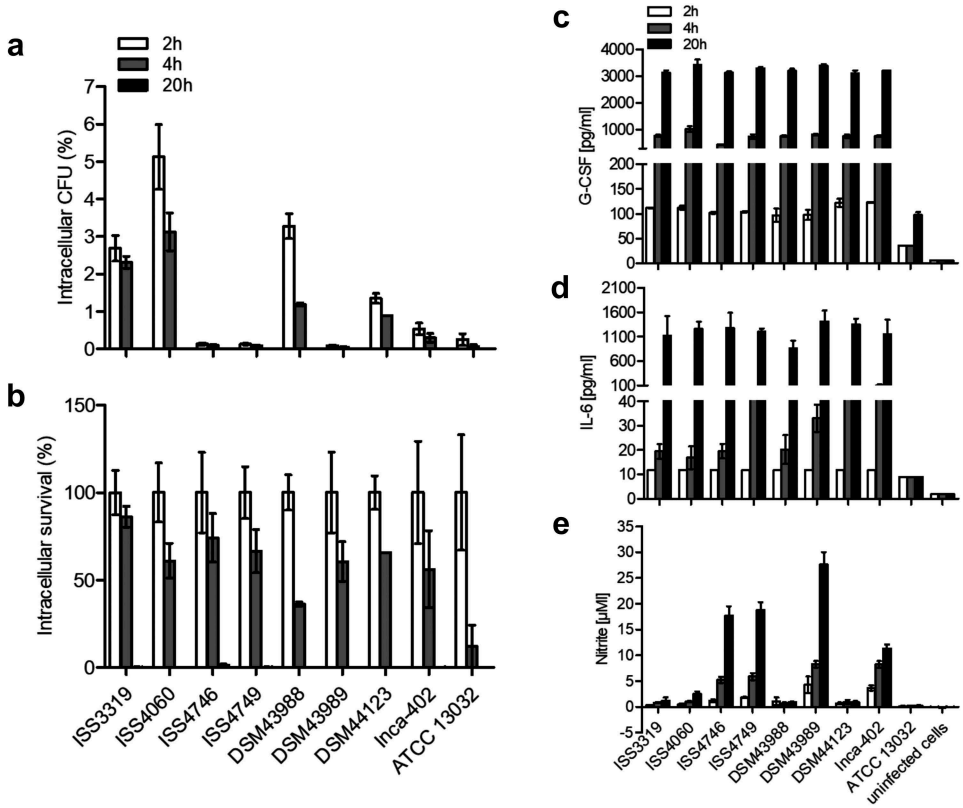

Figure 2. Quantitative analysis of viable intracellular corynebacteria in THP-1 cells and evaluation of cytokine and nitric oxide production. THP-1 cells were infected with different *C. diphtheriae* wild type strains and *C. glutamicum* ATCC 13032 at an MOI of 10 for 2, 4 and 20 h, lysed and the lysates were plated on blood agar plates. (a) Intracellular CFU in percent of the inoculum. (b) Intracellular survival in percent of the bacteria taken up after 2 h. Supernatants of THP-1 cells infected with bacteria were collected at different time points post-infection (2, 4 and 20 h) and used as samples for determination of (c) G-CSF and (d) IL-6 and (e) NO concentrations. Data shown are mean values of at least three independent biological replicates each performed in triplicates ± standard deviation.

that the strains that showed low numbers of intracellular CFUs induced high NO production in THP-1 cells. The high NO levels in response to some strains may result in fast degradation or inactivation of the bacteria and therefore no CFUs were detectable at 2 h post-infection. Considering this result, the 2 h values may not mandatory represent the uptake of the bacteria or the phagocytosis rate; most of the bacteria could already be killed by reactive nitrogen species within the first 2 h of infection in a strain-specific manner. Furthermore, it is conceivable that the high NO production leads to cell death of the macrophage [18].

When NFκB induction was analyzed in response to *C. diphtheriae* infection, cells of the reporter cell line THP-1-Blue NFκB were incubated for 20 h with MOI 1 and 10 of UV-killed and viable bacteria, respectively (Figure 3). Using MOI 1 and 10 of dead *C. diphtheriae* stains resulted in dose-dependent NFκB activation. The non-pathogenic strain ATCC 13032 led to similar NFκB signals independent of the MOI. In contrast, when viable *C. diphtheriae* strains were tested, using MOI 1 led to significant higher NFκB activation compared to MOI 10. A reduced NFκB signal up to 70% at MOI 10 (dead bacteria) was observed. This may indicate a specific reaction or detrimental effects of *C. diphtheriae* to the cells. Furthermore, strain DSM43989, which was shows very low numbers of intracellular CFUs at 2 h of infection (Figure 2(a)) and led to high NO production after 20 h (Figure 2(e)) showed a strong reduction of NFκB activation when MOI 10 of viable bacteria was used compared to MOI 1 (Figure 3). This observation may be explained by the fact that this strain is the only diphtheria toxin-producing strain used in this assay and THP-1 cells are expressing the corresponding receptor HB-EGF (heparin-binding EGF-like growth factor), which allows entrance of the toxin, leading to blocking of protein synthesis in the cell.

As mentioned above, the results of NFκB induction in THP-1 cells indicated that some *C. diphtheriae* strains may have detrimental effects on the cells. To test this idea, THP-1 reporter cells were infected for 20 h with the non-pathogenic *C. glutamicum* ATCC

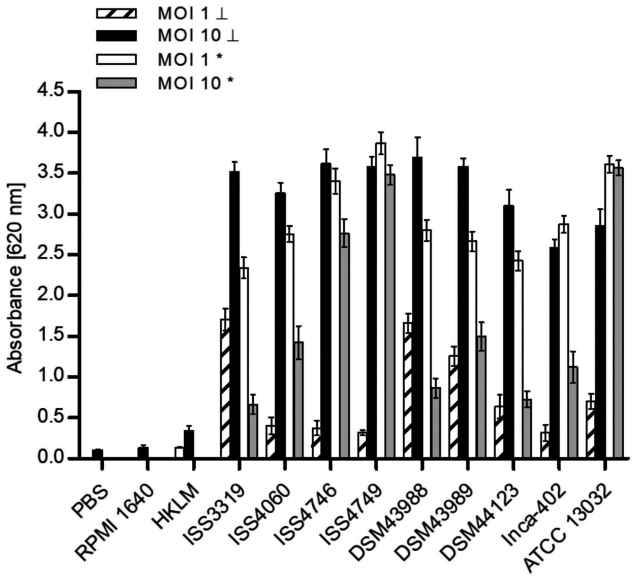

Figure 3. NF-KB activation in response to *C. diphtheriae* infection. THP1-Blue NF-KB cells were incubated for 20 h with viable and UV-killed bacteria of the non-pathogenic *C. glutamicum* ATCC 13032 and pathogenic *C. diphtheriae* strains at an MOI 1 and 10, respectively. Subsequently, supernatants were taken and mixed with QuantiBlue SEAP detection solution leading to a change in color upon NF-KB activation, which was detected by measuring absorbance at 620 nm. Dead bacteria are indicated with (□) and live bacteria with (*). Data shown are mean values of three independent biological replicates each performed in triplicates ± standard deviation.

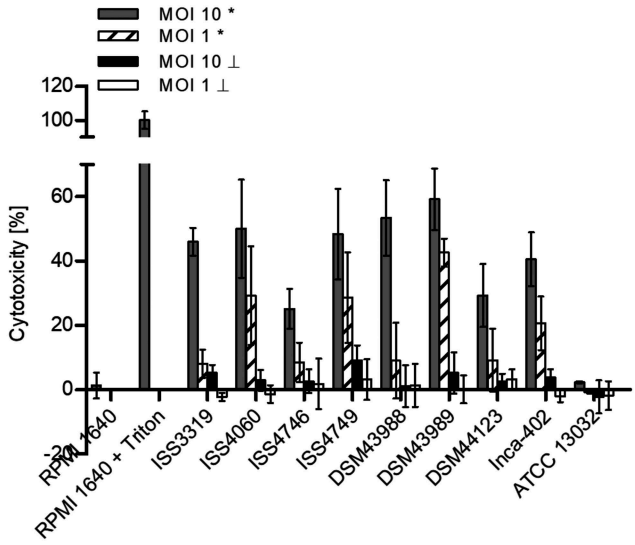

Figure 4. LDH release of cells. The release of lactate dehydrogenase (LDH) as a sign of host cell damage during infection of THP1-Blue NF-KB cells with *C. diphtheriae* was measured using the cytotoxicity detection kit (Roche). Cells were infected for 20 h with viable and UV-killed bacteria of the non-pathogenic strain *C. glutamicum* ATCC 13032 and different pathogenic *C. diphtheriae* wild type strains at an MOI 1 and 10, respectively. Cytotoxicity was calculated based on the absorbance values at 492 and 620 nm. Viable bacteria are indicated with (*) and dead bacteria with (□). Data shown are mean values of three independent biological replicates each performed in triplicates ± standard deviation.

13032 and pathogenic *C. diphtheriae* wild type strains to analyze the release of cytosolic lactate dehydrogenase (LDH) in the supernatant as a sign of host cell damage (Figure 4). In this case, all *C. diphtheriae* strains were able to damage host cells in a dose-dependent manner. The highest cytotoxicity was reached by the toxigenic strain DSM43989 with about 60 and 40% cell death when MOI 10 and MOI 1 of viable bacteria was tested, respectively. This may be most likely caused by diphtheria toxin produced by this strain. The lowest cytotoxic effects of about 25% cell death were detected for the strains ISS4746 and DSM44123 when MOI 10 was used. All other *C. diphtheriae* strains were able to cause at least 40% cell death at MOI 10 and the cytotoxic effect decreased significantly when MOI 1 was applied. As expected, no detrimental effect was observable when UV-killed bacteria, independent of the MOI, were used for infection, indicating that killing of macrophages is an active process conducted by the bacteria. In addition, the non-pathogenic control strain ATCC 13032 did not show any cytotoxic effect on the host cells, independent of the MOI and the physiological condition of the bacteria (Figure 4). In conclusion, decrease of NFκB activation when higher MOIs were used may be a consequence of lower transcription rates due to cell death caused by *C. diphtheriae*. Noteworthy, inducing cell death by *C. diphtheriae* is not only a characteristic of toxigenic strains, but the toxin may probably enhance the cytotoxic effect on the host cell and the diphtheria toxin is not the only mechanism to harm the host cell.

Recognition of *C. diphtheriae* by toll-like receptors in human epithelial cells

Recognition of corynebacterial cell wall glycolipids as well as whole heat-killed bacteria involves TRL2 binding in bone marrow-derived murine macrophages [14]. In order to investigate if TLR2 binding of *C diphtheriae* occurs also in human cells, HEK-Blue 293 hTRL2 were infected for 20 h with seven non-toxigenic strains, one toxigenic *C. diphtheriae* strain and the non-pathogenic *C. glutamicum* ATCC 13032 (Figure 5(a)). MOI 10 and 1 of viable and UV-killed bacteria were tested. As expected, the negative controls water and pure medium showed low absorbance values with less than 0.15. The positive control FSL-1, which is a TLR2 ligand, reached an absorbance value of about 1.75 at 620 nm, while

all *C. diphtheriae* strains as well as *C. glutamicum* reached high absorbance values between 1.0 and 2.4 for vital bacteria regardless to the MOI. The toxigenic strain seems to have again a detrimental effect to the cells when an MOI 10 was used, which may be due to the toxin. When UV-killed bacteria are used for infection, the activation of TRL2 seems to be dose-dependent.

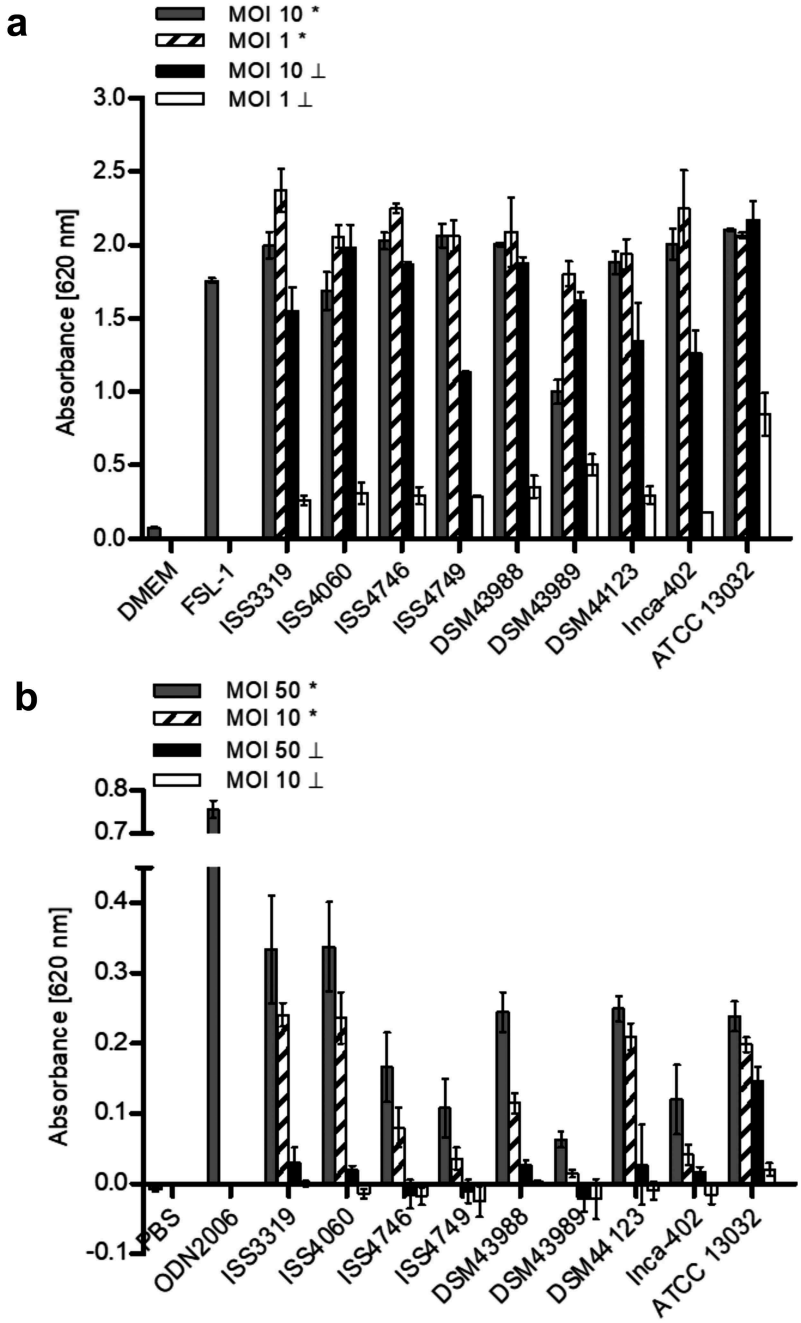

Figure 5. TLR reporter assays. (a) TLR binding of *C. diphtheriae* in HEK-Blue 293 hTLR2 cells. HEK-Blue 293 hTLR2 cells were incubated for 24 h with viable and UV-killed bacteria of pathogenic *C. diphtheriae* and the non-pathogenic *C. glutamicum* ATCC 13032 at an MOI 1 and 10, respectively. Subsequently, supernatants were taken and mixed with QuantiBlue SEAP detection solution leading to color change upon TLR activation. (b) TLR binding of *C. diphtheriae* in HEK-Blue 293 hTLR9 cells. HEK-Blue 293 hTLR9 cells were incubated for 24 h with viable and UV-killed bacteria of pathogenic *C. diphtheriae* and the non-pathogenic *C. glutamicum* ATCC 13032 in HEK-Blue Detection medium at an MOI 10 and 50, respectively. In both cases, TLR binding was detected by measuring absorbance at 620 nm. Viable bacteria are indicated with (*) and dead bacteria with (□). Data shown are mean values of three independent biological replicates each performed in triplicates ± standard deviation.

Recognition of intracellular bacteria by TLR9

In order to address the question, if bacteria that show low intracellular CFUs already 2 h post-infection are degraded or not internalized, TLR9 studies with HEK-Blue hTLR9 cells were performed. TLR9 is an intracellular receptor that is located in endolysosomal compartments, where it detects CpG DNA from bacteria and viruses [19]. Therefore, the cells were infected for 24 h with viable and UV-killed bacteria at MOI 10 and 50, respectively (Figure 5(b)). Interestingly, *C. diphtheriae* strains ISS4746, ISS4749 and DSM43989 showed the lowest TLR9 activation. TLR9 activation by *C. diphtheriae* was dose-dependent and dead bacteria showed no significant effect. Moreover, by using this assay, the pathogenicity of the bacteria could be evaluated. The non-pathogenic control strain ATCC 13032 showed very low internalization rates in THP-1 cells (Figure 2(a)), had no detrimental effect to the cells (Figure 4), but revealed high absorbance values in the TLR9 assay (Figure 5(b)). This means that *C. glutamicum* was internalized in high amounts, but much faster degraded than *C. diphtheriae* and was therefore not detectable already after 2 h post-infection. Taken together, these results indicate that strains ISS4746, ISS4749 and the toxigenic strain DSM43989 have unknown mechanisms to avoid to be taken up by the host cell, although they show TLR2 binding and induce inflammatory response in the host.

Influence of the diphtheria toxin

In all infection studies that have been made thus far with different *C. diphtheriae* wild type strains and epithelial cells [20] or human and murine macrophages in this study, the toxigenic strain DSM43989 was not able to adhere to or to invade into the host cells and it was obviously not taken up in macrophages. Additionally, former studies demonstrated that this strain does not contain mycolic acids in its cell wall [13]. In this study, it was shown that DSM43989 induces inflammatory response in the host as well as host cell damage. The question raised whether the diphtheria toxin or the lack of mycolic acids are responsible for the remarkable behavior of DSM43989. Therefore, we compared the intracellular CFUs of DSM43989 with another diphtheria toxin expressing strain, NCTC13129, in THP-1 cells at 2 and 4 h post-infection (Table 2). Compared to the non-toxigenic strain ISS3319 and the non-pathogenic *C. glutamicum* strain ATCC 13032, both DSM43989 and NCTC13129 are hardly detectable in THP-1 cells at 2 and 4 h post-infection. Since NCTC13129 contains mycolic acids [21] and shows low internalization rates, this result indicates that it may rather be the diphtheria toxin than the structure of the cell wall that influences the infection process.

Discussion

The innate immune system, an organism's first line of defense against invading pathogens, works together with the adaptive immune system to maintain physiological homeostasis of the host and to protect it against potentially pathogenic organisms [22,23]. Pattern recognition receptors (PRRs) expressed on the surface of immune cells are crucial for this early detection of invading pathogens as well as to recognize certain endogenous ligands belonging to the family of danger-associated molecular pattern molecules [24,25]. Toll-like receptors (TLRs) are a family of transmembrane receptors, which play a key role in both innate and adaptive immune responses. TLRs and C-type lectin receptors differ in their structures, localization pattern, and the types of ligands they recognize. As effector cells of the innate immune system, macrophages secrete pro-inflammatory and antimicrobial mediators upon phagocytosis of bacteria. The production of IL-6 and G-CSF leads to receptor-mediated activation of the JAK2/STAT3 (Janus Kinase/signal transducer and activator transcription) pathway [26,27], which subsequently leads to the induction of cell survival signals by producing increased levels of the anti-apoptotic proteins Bcl-2 and Bcl-X_L. In case of *C. diphtheriae*, the knowledge about molecular signaling upon infection of macrophages is scarce. A number of studies showed that *C. diphtheriae*, once considered as strict extracellular pathogen, is able to cause severe invasive diseases, such as osteomyelitis, septic arthritis and endocarditis [6–8], which enhances the compelling need to focus on the infection mechanism of *C. diphtheriae*. In the study presented here, seven non-toxigenic *C. diphtheriae* isolates as well as two toxin-producing strains were characterized with regard to their interaction with BMM and human THP-1 cells. A study conducted by Schick and co-workers on the interaction of heat killed corynebacteria and pure cell wall extracts with the C-type lectin receptor Mincle [14] provided the basis of this study. It was found that

Table 2. Intracellular CFUs [%] of different corynebacteria in THP-1 cells.

Strain	CFUs [%] at 2 h p.i.	CFUs [%] at 4 h p.i.
C. diphtheriae ISS3319	2.68 ± 0.34	2.31 ± 0.16
C. diphtheriae DSM43989 (*tox*$^+$)	0.08 ± 0.02	0.05 ± 0.01
C. diphtheriae NCTC13129 (*tox*$^+$)	0.10 ± 0.05	0.08 ± 0.01
C. glutamicum ATCC 13032	0.25 ± 0.06	0.06 ± 0.05

Mincle-Fc binds to cell wall extracts of corynebacteria and is required for the release of G-CSF in BMM, and Toll-like receptor 2 (TLR2) is essential for macrophage activation [14]. In order to address the role of Mincle as well as the TLR adaptor protein Myd88 in the infection process of *C. diphtheriae*, in this study, a combination of BMM, Mincle- and MyD88-deficient cells were tested. When phagocytosis of the different *C. diphtheriae* strains was analyzed, no significant difference between BMM and the respective knockout cell line Mincle$^{-/-}$ was observed. In contrast, when Myd88 was absent in BMM almost no intracellular bacteria were detectable. When Mincle was absent in BMM, the G-CSF production was dramatically reduced compared to wild type BMM. This was also the case, when Myd88 was absent. In conclusion, Mincle-binding is crucial for G-CSF production, but not essential for the phagocytosis of the bacteria. Phagocytosis of the bacteria only occurs when the TLR/MyD88 pathway is functional. Furthermore, in this study we could show that viable *C. diphtheriae* interacts with TLR2 of human HEK-Blue 293 hTLR2 cells, which was also the case for heat-killed bacteria and murine macrophages, shown in a previous study [14].

When the interaction of *C. diphtheriae* with THP-1 cells was investigated, the phagocytosis of the bacteria occurred in a strain-specific manner. Remarkably, former studies of Ott and co-workers [20], investigating the infection process of the human epithelial cell lines HeLa and Detroit 562, revealed a very similar infection pattern compared to THP-1 cells in this study. This means that strains that show highest adhesion and invasion rates were also the most phagocytosed in THP-1 cells and *vice versa*. Thereby, it is important to mention, that adhesion to and invasion into epithelial cells is regarded as an active process of the bacteria, while phagocytosis in macrophages is an active process of the host cell. These observations lead to the assumption that some of the *C. diphtheriae* wild type strains are preferentially internalized, while others seem to be avoided by the macrophage. Furthermore, this indicates that the recognition of the bacteria by human cells occurs via the same molecules independent of the cell type.

When NFκB induction in THP-1 cells was analyzed during infection with *C. diphtheriae* a detrimental effect of the bacteria to the cells was assumed, which was confirmed by the LDH release in the supernatant of infected cells, as a sign of host cell damage. Interestingly, the production of reactive nitrogen species in THP-1 cells was contrary to the intracellular CFUs at 2 h post-infection of the different *C. diphtheriae* strains. Due to this observation, the question raised whether the bacteria with low intracellular CFUs are already degraded by NO or are not internalized. The intracellular CFUs at 2 h post-infection were considered as phagocytosis rate thus far, but the bacteria may already be processed at this time point, indicated by high nitric oxide concentrations in infected THP-1 cells that contained almost no viable bacteria. By using TLR9 reporter cell lines, this question was addressed. Since TRL9 is an endolysosomal receptor, that binds CpG unmethylated bacterial and viral DNA, it became evident that bacteria that show low intracellular CFUs were not or weakly detected by TLR9, indicating that these strains were not endocytosed by the cell.

In conclusion, comparison of murine (BMM) and human phagocytes (THP-1) revealed similar intracellular CFUs for the different *C. diphtheriae* strains. TLR 9 reporter assays confirmed that *C. diphtheriae* that showed low intracellular CFUs were not detected by TLR9 in the endosome indicating that these strains were not taken up by the cell. In contrast, the non-pathogenic control *C. glutamicum* ATCC 13032 showing also almost no intracellular CFUs independent of the cell line, was recognized by TLR9, indicating that the bacteria are taken up by the cell and degraded immediately after endocytosis. In terms of G-CSF and IL-6 production, no significant differences between BMM and THP-1 for *C. diphtheriae* were observed, while the non-pathogenic *C. glutamicum* induced only half of the cytokine secretion in response to infection independent of the host cell. By using murine Mincle- and Myd88-deficient cells, it could be shown that the absence of Mincle resulted in reduced G-CSF production, while this had no influence on the uptake of the bacteria in comparison to BMM. In contrast, when MyD88 was absent, both the uptake of the bacteria as well as IL-6 and G-CSF production were blocked. Consequently, phagocytosis of the bacteria only occurs when the TLR/MyD88 pathway is functional, which was also confirmed by showing that all corynebacteria used in this study were able to interact with human TLR2.

However, it was not clear thus far, why the toxigenic strain DSM43989 showed very low adhesion to and invasion rates into Detroit 562 and HeLa cells and almost no intracellular CFUs in human macrophages [20]. A putative reason may be the lack of mycolic acids, which may consequently` lead to an impaired interaction of the bacteria by the host cell. The comparison with another toxigenic *C. diphtheriae* strain NCTC13129, that contains mycolic acids in its cell wall, revealed similar intracellular CFUs in THP-1 cells. These results indicate that the low number of intracellular CFUs of toxigenic strains is most likely not connected to the presence or absence of mycolic acids. Although the influence of the diphtheria toxin on the infection process of these strains may explain the cytotoxic

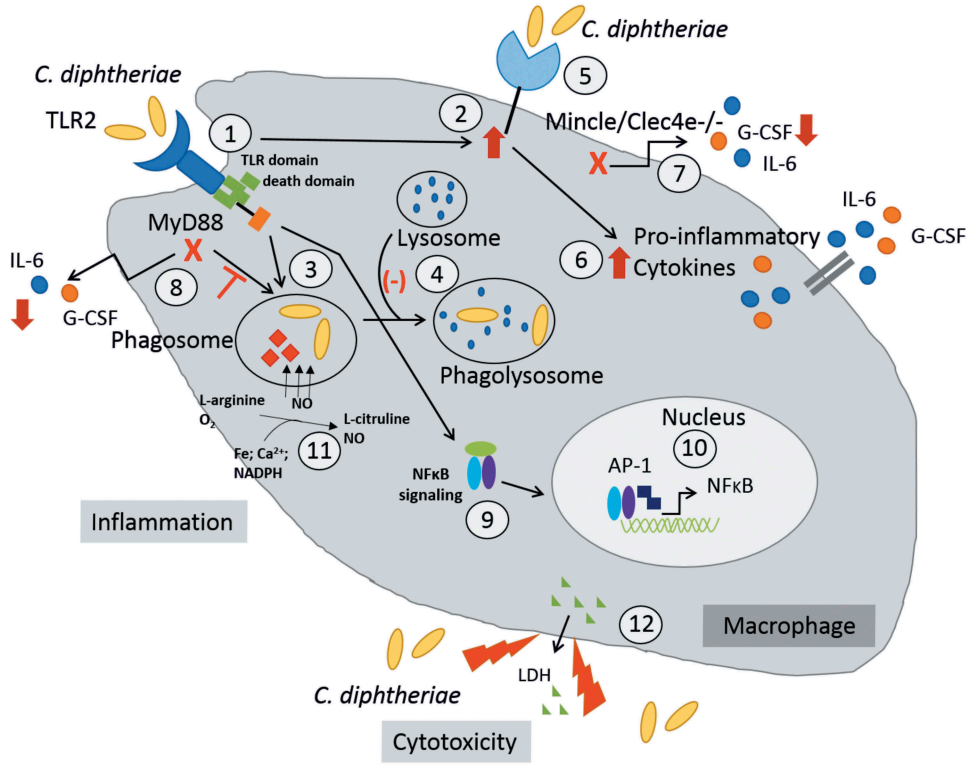

Figure 6. *C. diphtheriae* recognition by macrophages. Binding of *C. diphtheriae* by TLR2 (1) leads on the one hand to upregulation of the C-type lectin receptor Mincle (2) and on the other hand, to phagocytosis of the bacteria (3), resulting in phagosome-lysosome fusion, which is somehow delayed by *C. diphtheriae* (4). Furthermore, binding of *C. diphtheriae* to Mincle (5) triggers the production of pro-inflammatory cytokines (6), which was confirmed by reduced cytokine production in Clec4e$^{-/-}$ cells (7). Additionally, in Myd88-deficient cells the cytokine production as well as the uptake of the bacteria was completely blocked (8). Further signs of inflammation caused by pathogenic corynebacteria are the activation of NFκB-signaling (9), resulting in upregulation of pro-inflammatory genes (10), and the production of nitric oxide (NO) (11). In case of the infection of THP-1 cells, a cytotoxic effect of *C. diphtheriae* was detectable by LDH release (12).

effect of DSM43989 to THP-1 cells, this does not explain the low uptake by murine phagocytes, since murine cells are not susceptible to the diphtheria toxin [28]. To solve this question, future experiments have to be carried out concerning the susceptibility of murine cells toward the diphtheria toxin.

Summary

In contrast to the non-pathogenic strain *C. glutamicum* ATCC 13032, *C. diphtheriae* is able to cause host immune response by inducing inflammatory cytokine and NO production, is able to delay phagolysosome formation and has a cytotoxic effect on the cells (Figure 6). The TLR2/Myd88 pathway is required for phagocytosis of *C. diphtheriae* and leads to NFκB-signaling as well as upregulation of the C-type lectin receptor Mincle. Since the detected intracellular CFUs are strain-specific and/or cell line-specific, the bacterial antigen, which binds to the host cell receptor, may be expressed in various amounts across the different *C. diphtheriae* strains. On the one hand, these results emphasized the high virulence potential of *C. diphtheriae* by activating the innate immune system and causing inflammatory response in phagocytic cells. On the other hand, since both *C. diphtheriae* and *C. glutamicum* bind obviously to TLR2 and Mincle, *C. diphtheriae* may express further proteins/molecules interacting with host cells, enabling the bacteria to trigger host immune response. Based on the results carried out in this study, our future work will be focused on detailed elucidation of inflammatory pathways triggered by *C. diphtheriae* as well as the identification of the bacterial proteins that are recognized by the host cell.

Acknowledgments

DW was supported by a PhD fellowship of the Deutscher Akademischer Austauschdienst (DAAD) and the Förderung von Frauen in Forschung und Lehre (FFL) of the Friedrich-Alexander-Universität Erlangen-Nürnberg. LO gratefully acknowledges the Förderung von Frauen in Forschung und Lehre (FFL) of the Friedrich-Alexander-Universität Erlangen-

Nürnberg. The funding bodies had no role in the design of the study and collection, analysis and interpretation of data and in writing the manuscript.

Disclosure statement

No potential conflict of interest was reported by the authors.

ORCID

Roland Lang http://orcid.org/0000-0003-0502-3677
Andreas Burkovski http://orcid.org/0000-0003-1896-4521

References

[1] Lehmann KB, Neumann R. Atlas und Grundriss der Bakteriologie und Lehrbuch der speziellen bakteriologischen Diagnostik. Munich: Lehmann; 1896.
[2] Barksdale L. *Corynebacterium diphtheriae* and its relatives. Bacteriol Rev. 1970;34:378–422.
[3] Burkovski A. Diphtheria and its etiological agents. In: Burkovski A, editor. *Corynebacterium diphtheriae* and related toxigenic species. Dordrecht: Springer; 2014. p. 1–14.
[4] Sangal V, Hoskisson PA. Corynephages: infections of the infectors. In: Burkovski A, editor. *Corynebacterium diphtheriae* and related toxigenic species. Dordrecht: Springer; 2014. p. 67–81.
[5] Hirata R Jr., Pereira GA, Filardy AA, et al. Potential pathogenic role of aggregative -adhering *Corynebacterium diphtheriae* of different clonal groups in endocarditis. Braz J Med Biol Res. 2008;41:986–991.
[6] Puliti M, von Hunolstein C, Marangi M, et al. Experimental model of infection with non-toxigenic strains of *Corynebacterium diphtheriae* and development of septic arthritis. J Med Microbiol. 2006;55:229–235.
[7] Peixoto RS, Pereira GA, Sanches Dos Santos L, et al. Invasion of endothelial cells and arthritogenic potential of endocarditis-associated *Corynebacterium diphtheriae*. Microbiology. 2014;160:537–546.
[8] Peixoto RS, Hacker E, Antunes CA, et al. Pathogenic properties of a *Corynebacterium diphtheriae* strain isolated from a case of osteomyelitis. J Med Microbiol. 2016;65:1311–1321.
[9] Ishikawa E, Ishikawa T, Morita YS, et al. Direct recognition of the mycobacterial glycolipid, trehalose dimycolate, by C-type lectin Mincle. J Exp Med. 2009;206:2879–2888.
[10] Werninghaus K, Babiak A, Gross O, et al. Adjuvanticity of a synthetic cord factor analogue for subunit *Mycobacterium tuberculosis* vaccination requires FcRgamma-Syk-Card9 dependent innate immune activation. J Exp Med. 2009;206:89–97.
[11] Schoenen H, Bodendorfer B, Hitchens K, et al. Cutting edge: mincle is essential for recognition and adjuvanticity of the mycobacterial cord factor and its synthetic analog trehalose-dibehenate. J Immunol. 2010;184:2756–2760.
[12] Deguine J, Barton GM. MyD88: a central player in innate immune signaling. F1000Prime Rep. 2014;6:97.
[13] Ott L, Hacker E, Kunert T, et al. Analysis of *Corynebacterium diphtheriae* macrophage interaction: dispensability of corynomycolic acids for inhibition of phagolysosome maturation and identification of a new gene involved in synthesis of the corynomycolic acid layer. PLoS ONE. 2017;12:e0180105.
[14] Schick J, Etschel P, Bailo R, et al. Toll-like receptor 2 and Mincle cooperatively sense corynebacterial cell wall glycolipids. Infect Immun. 2017;85:e00075–17.
[15] Lang R, Rutschman RL, Greaves DR, et al. Autocrine deactivation of macrophages in transgenic mice constitutively overexpressing IL-10 under control of the human CD68 promoter. J Immunol. 2002;168:3402–3411.
[16] Kawai T, Adachi O, Ogawa T, et al. Unresponsiveness of MyD88-deficient mice to endotoxin. Immunity. 1999;11:115–122.
[17] O'Neill LA, Bowie AG. The family of five: TIR-domain containing adaptors in Toll-like receptor signaling. Nat Rev Immunol. 2007;7:353–364.
[18] Tripathi P, Tripathi P, Kashyap L, et al. The role of nitric oxide in inflammatory reactions. FEMS Immunol Med Microbiol. 2007;51:443–452.
[19] Hemmi H, Takeuchi O, Kawai T, et al. A Toll-like receptor recognizes bacterial DNA. Nature. 2000;408:740–745.
[20] Ott L, Scholz B, Hoeller M, et al. Induction of the NFκ-B signal transduction pathway in response to *Corynebacterium diphtheriae* infection. Microbiology. 2013;159:126–135.
[21] Cerdeño-Tárraga AM, Efstratiou A, Dover LG, et al. The complete genome sequence and analysis of *Corynebacterium diphtheriae* NCTC13129. Nucleic Acids Res. 2003;31:6516–6523.
[22] Kulkarni OP, Lichtnekert J, Anders HJ, et al. The immune system in tissue environments regaining homeostasis after injury: is "inflammation" always inflammation? Mediators Inflamm. 2016;2016:2856213.
[23] Medzhitov R, Janeway CA Jr. Decoding the patterns of self and nonself by the innate immune system. Science. 2002;296:298–300.
[24] Shcheblyakov DV, Logunov DY, Tukhvatulin AI, et al. Toll-like receptors (TLRs): the role in tumor progression. Acta Naturae. 2010;2:21–29.
[25] Takeuchi O, Akira S. Pattern recognition receptors and inflammation. Cell. 2010;140:805–820.
[26] Hirano T, Ishihara K, Hibi M. Roles of STAT3 in mediating the cell growth, differentiation and survival signals relayed through the IL-6 family of cytokine receptors. Oncogene. 2000;19:2548–2556.
[27] Solaroglu I, Cahill J, Jadhav V, et al. A novel neuroprotectant granulocyte-colony stimulating factor. Stroke. 2006;37:1123–1128.
[28] Mitamura T, Higashiyama S, Taniguchi N, et al. Diphtheria toxin binds to the epidermal growth factor (EGF)-like domain of human heparin-binding EGF-like growth factor/diphtheria toxin receptor and inhibits specifically its mitogenic activity. J Biol Chem. 1995;270:1015–1019.
[29] Bertuccini L, Baldassarri L, von Hunolstein C. Internalization of non-toxigenic *Coryne-bacterium*

diphtheriae by cultured human respiratory epithelial cells. Microb Pathog. 2004;37:111–118.

[30] Nakao H, Pruckler JM, Mazurova IZ, et al. Heterogeneity of diphtheria toxin gene, *tox*, and its regulatory element, *dtxR*, in *Corynebacterium diphtheriae* strains causing epidemic diphtheria in Russia and Ukraine. J Clin Microbiol. 1996;34:1711–1716.

[31] Trost E, Ott L, Schneider J, et al. The complete genome sequence of *Corynebacterium pseudotuberculosis* FRC41 isolated from a 12-year-old girl with necrotizing lymphadenitis reveals insights into gene-regulatory networks contributing to virulence. BMC Genomics. 2010;11:728.

[32] Public Health Laboratory Service. Diphtheria acquired during a cruise in the Baltic Sea. Commun Dis Rep CDR Wkly. 1997;7:207.

[33] Abe S, Takayama K, Kinoshita S. Taxonomical studies on glutamic acid producing bacteria. J Gen Microbiol. 1967;13:279–301.

[34] Tsuchiya S, Yamabe M, Yamaguchi Y, et al. Establishment and characterization of a human acute monocytic leukemia cell line (THP-1). Int J Cancer. 1980;26:171–176.

Weerasekera et al. BMC Microbiology (2018) 18:106
https://doi.org/10.1186/s12866-018-1247-z

BMC Microbiology

RESEARCH ARTICLE Open Access

The C-terminal coiled-coil domain of *Corynebacterium diphtheriae* DIP0733 is crucial for interaction with epithelial cells and pathogenicity in invertebrate animal model systems

Dulanthi Weerasekera[1], Franziska Stengel[1], Heinrich Sticht[2], Ana Luíza de Mattos Guaraldi[3], Andreas Burkovski[1] and Camila Azevedo Antunes[1,3*]

Abstract

Background: *Corynebacterium diphtheriae* is the etiologic agent of diphtheria and different systemic infections. The bacterium has been classically described as an extracellular pathogen. However, a number of studies revealed its ability to invade epithelial cells, indicating a more complex pathogen-host interaction. The molecular mechanisms controlling and facilitating internalization of *C. diphtheriae* still remains unclear. Recently, the DIP0733 transmembrane protein was found to play an important role in the interaction with matrix proteins and cell surfaces, nematode colonization, cellular internalization and induction of cell death.

Results: In this study, we identified a number of short linear motifs and structural elements of DIP0733 with putative importance in virulence, using bioinformatic approaches. A C-terminal coiled-coil region of the protein was considered particularly important, since it was found only in DIP0733 homologs in pathogenic *Corynebacterium* species but not in non-pathogenic corynebacteria. Infections of epithelial cells and transepithelial resistance assays revealed that bacteria expressing the truncated form of *C. diphtheriae* DIP0733 and *C. glutamicum* DIP0733 homolog are less virulent, while the fusion of the coiled-coil sequence to the DIP0733 homolog from *C. glutamicum* resulted in increased pathogenicity. These results were supported by nematode killing assays and experiments using wax moth larvae as invertebrate model systems.

Conclusions: Our data indicate that the coil-coiled domain of DIP0733 is crucial for interaction with epithelial cells and pathogenicity in invertebrate animal model systems.

Keywords: *Caenorhabditis elegans*, Corynebacteria, *Galleria mellonella*, Host pathogen interaction

* Correspondence: camila.a.azevedo@fau.de
[1]Microbiology Division, Friedrich-Alexander-University Erlangen-Nuremberg, Erlangen, Germany
[3]Laboratory of Diphtheria and Corynebacteria of Clinical Relevance-LDCIC, Faculty of Medical Sciences, Rio de Janeiro State University, Rio de Janeiro, Brazil
Full list of author information is available at the end of the article

Background

Corynebacterium diphtheriae is the causative agent of diphtheria, a toxemic infection of the upper respiratory tract [1]. Notably, *C. diphtheriae* is present on the list of the most important global pathogens. These pathogens cause global fatalities, and are often part of mixed infections or cause multiple different diseases, making them difficult to identify [2]. Besides classical diphtheria, an increasing number of systemic infections caused by non-toxigenic *C. diphtheriae* strains have been reported [3–7]. Moreover, it has been demonstrated that *C. diphtheriae* possesses various virulence factors that may act independently of diphtheria toxin [8–12]. Among these, only a few have been investigated in detail.

The DIP0733 protein - initially described as a non-fimbrial surface protein and designated as 67-72p [13] - was recently characterized as a multi-functional virulence factor of *C. diphtheriae* [14]. This protein plays an important role in the interaction process with extracellular matrix proteins and cell surfaces, nematode colonization, cellular internalization and induction of cell death [13, 14]. Despite its multiple roles in pathogenicity, DIP0733 was found to lack annotated functional domains within the protein besides seven transmembrane helices [14]. Therefore, the aim of this work was to identify functional elements in DIP0733 and its homologs and investigate how they contribute to the process of host pathogen interaction. In this study, short linear motifs and structural elements of DIP0733 with putative importance in virulence were identified using bioinformatic approaches. A C-terminal coiled-coil region of the protein was considered particularly important, since it was found only in DIP0733 homologs of pathogenic but not in non-pathogenic corynebacteria. Mutagenesis studies including the construction of truncated and variant forms of DIP0733 and their expression by its *C. diphtheriae* mutant strain were carried out and their involvement in interactions with biotic and abiotic surfaces were investigated. Furthermore, their interaction with epithelial cells and their influence in transepithelial resistance as well as with *Caenorhabditis elegans* and *Galleria mellonella,* invertebrate animal model systems [15], were also studied.

Methods

Bacterial strains and culture conditions

Escherichia coli OP50, *E. coli* DH5αMCR and *Salmonella enterica* serovar Typhimurium NCTC 12023 were grown in Luria Bertani (LB) medium at 37 °C [16]. *C. diphtheriae* strains were grown in heart infusion (HI) at 37 °C with constant shaking at 125 r.p.m. When appropriate, 50 μg kanamycin ml^{-1} or 25 μg chloramphenicol ml^{-1} were added to the medium. Bacterial strains, cell lines and plasmids used in this study are listed in Table 1.

Bioinformatic analysis of short linear motifs

In order to find functional structural units of the DIP0733, deposited information about the nucleotide and amino acid sequences were collected from databases. The DIP0733 protein sequences of 5 corynebacteria (*C. diphtheriae* CDC-E8392 and INCA-402, *Corynebacterium ulcerans* BR-AD22 and *Corynebacterium pseudotuberculosis* 258 as pathogenic strains and *Corynebacterium glutamicum* ATCC 13032 as a non-pathogenic species) were aligned using the compositional substitution matrix adjustment method executed on BLASTp (Additional file 1: Figure S1). Subsequently, the DIP0733 homolog sequences were examined by means of the Eukaryotic Linear Motif (ELM) database for short linear motifs (SLiMs). These motifs are categorised by different functions, such as CLV (cleavage sites), DEG (degradation sites), DOC (docking sites), LIG (ligand binding sites), MOD (post-translational modification sites) and TRG (targeting sites). The large number of possible linear motifs could be reduced by considering only highly conserved motifs. In addition, all motifs were compared, and those which were present only in pathogenic strains and not in non-pathogenic corynebacteria were considered in more detail. Subsequently, the presence and position of a coiled-coil area in different strains predicted with ELM database was considered for the construction of the recombinant DIP0733 mutant variants.

Molecular biology techniques and construction of recombinant DIP0733 variants

Standard molecular biology techniques were used for plasmid isolation, transformation of *E. coli* and cloning [16]. *C. diphtheriae* CDC-E8392 wild-type, the CAM-1 DIP0733 mutant strain [14] and their respective complementation and overexpression strains were used in this study. Additionally, different complementation plasmids encoding three recombinant forms of DIP0733 homologs were constructed (Table 1). The first comprised the complete nucleotide sequence of DIP0733 homolog from *C. glutamicum* ATCC 13032 and was designated as pXMJ19_Cg0896, according to its gene identifier. The second plasmid encoded a DIP0733 hybrid variant with the sequence of the *C. diphtheriae* C-terminal coiled-coil region fused downstream to *Cg0896* and it was consequently designated as pXMJ19_Cg0896 + cc. The third plasmid was constructed to encode a C-terminal truncated *C. diphtheriae* DIP0733 homolog lacking its coiled-coil region and was designated as pXMJ19_DIP0733-cc (Fig. 1a-e and Table 1). For easier comprehension, the constructs harbouring the sequences of DIP0733 homologs from *C. diphtheriae* remained named as DIP0733. Hence, the DIP0733 homolog sequences from the *C. diphtheriae* strains used in this study share high similarity with DIP0733 from NCTC 13129 (Additional file 1: Figure S1).

Table 1 Strains, cell lines, plasmids and primers used in this study

Strain	Description	Source
Escherichia coli		
DH5αMCR	*endA1 supE44 thi-1 λ- recA1 gyrA96 relA1 deoR Δ(lacZYA-argF) U196 Ø80 ΔlacZΔM15mcrA Δ (mmrhsdRMS mcrBC)*	[39]
OP50	Uracil-auxotrophic *E. coli* B strain	[40]
Salmonella enterica serovar Typhimurium		
NCTC 12023	Wild-type identical to ATCC 14028	National Collection of Type Cultures (Colindale, UK)
Corynebacterium diphtheriae		
CDC-E8392	Wild-type, Biovar. *mitis*, tox^+	[41]
CAM-1	CDC-E8392 *DIP0733*::pCR2.1 TOPO*DIP0733*'	[14]
INCA 402	Isolate from a patient with pneumonia, biovar. *Belfanti*, tox^-	[41]
Corynebacterium glutamicum		
ATCC 13032	Type strain, non-pathogenic	[42]
Cell lines		
Detroit562	Human hypopharyngeal carcinoma cells (ATCC CCL-2)	[43]
HeLa	Human cervical carcinoma cells (ATCC CCL-2)	[44, 45]
Plasmids		
pXMJ19	*ori colE1*, *oriCg*, *ptac*, Cm^R	[46]
pXMJ19_DIP0733	*ori colE1*, *oriCg*, *ptac*, *CDCE8392_0678*, Cm^R	[14]
pXMJ19_DIP0733-cc	pXMJ19 with 2700 bp insert of 3'-shortened *CDCE8392_0678* (DIP0733 homolog without sequence for *C*-terminal *disorder*- and *coiled-coil*-region) from *C. diphtheriae* CDC-E8392	This study
pXMJ19_Cg0896	*ori colE1*, *oriCg*, *ptac*, *Cg0896*, Cm^R	
pXMJ19_Cg0896 + cc	pXMJ19 with 2693 bp insert of 3'-shortened *Cg0896* (DIP0733 homolog without sequence for *C*-terminal *disorder*- and *coiled-coil*-region) from *C. glutamicum* ATCC 130323 and 268 bp insert of 5`-shortened *CDB402_0643* (DIP0733 homolog sequence for *C*-terminal *disorder*- and *coiled-coil*-region) from *C. diphtheriae* INCA-402	
Primers (5`- 3`)		
Probe 16SrRNA	GCAGCCGCGGTAATACGTAG	This study
	GGGCCCTAATACGACTCACTATAGGGACATCTCACGACACGAGCTG	
Probe DIP0733	CGACCCAGTGCTTAAGGCAT	
	GGGCCCTAATACGACTCACTATACCTGTGCCTGCTTTGGACCC	
Probe Cg0896	GTACGACGGAACTGTTGAAC	
	GGGCCCTAATACGACTCACTATAGCCTGCTTTGGACCCTGGGTC	
pXMJ19_DIP0733-cc	CGCG*CCTGCA*GGTTGGCGACCGGTTTTACGCG	
	CGCG*CCCGGG*TTACTTAGGGTCAATACCTACCT	
pXMJ19_Cg0896	CGCG*CCTGCA*GGTTGTCGACTGGTCTCACACC	
	CGCG*CCCGGG*CTACTGTGCGGACTGGTAGC	
pXMJ19_Cg0896 + cc	CGCGCCTGCAGGTTGTCGACTGGTCTCACACC	
	CGCG*CCTTA*GGCTGCGATAGGGCTTCAG	

The DIP0733 homolog nucleotide sequences from *C. diphtheriae* and *C. gutamicum* were amplified via PCR with primers containing specific restriction sites as described in Table 1, and the products were digested for 1 h at 37 °C. The vector pXMJ19 was digested with the same restriction enzymes as the respective inserts and dephosphorylated for 30 min at 37 °C. Ligations of inserts and pXMJ19 DNA were carried out with T4 DNA

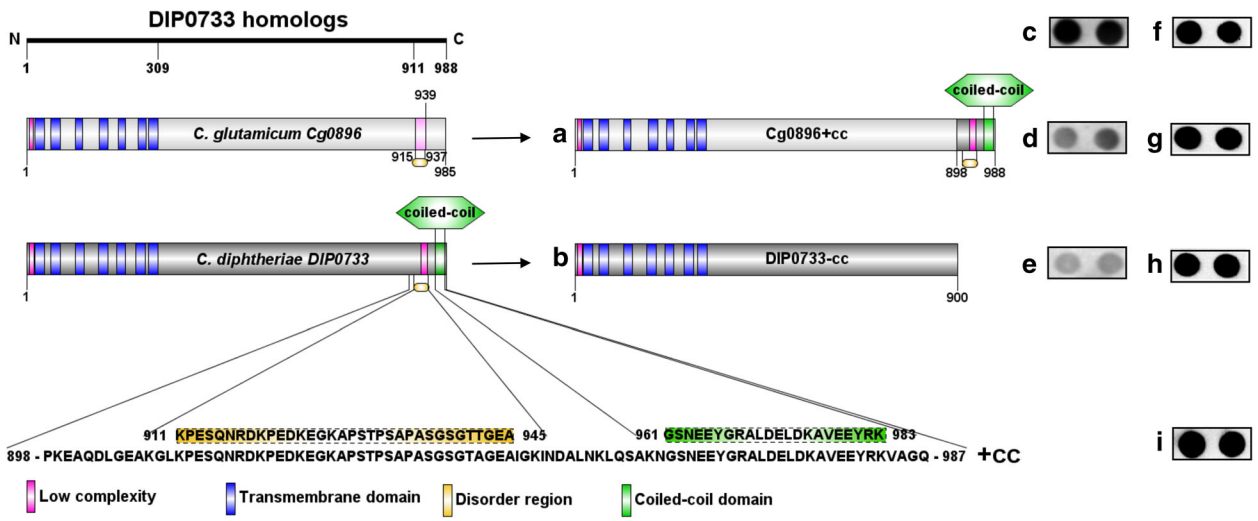

Fig. 1 Schematic representation of DIP0733 homologs and their truncated forms. Left: DIP0733 homologs in non-pathogenic (*C. glutamicum*) and pathogenic (*C. diphtheriae*) corynebacteria and their common features: low complexity regions (pink boxes), transmembrane helix domains (blue boxes), disorder regions (yellow boxes) and coiled-coil domain (green boxes). Right: strategy for the cloning of the truncated DIP0733 variants into pXMJ19. The *C. glutamicum* DIP0733 homolog sequence with the fused coding sequence for the coiled-coil domain from *C. diphtheriae* is represented by Cg0896 + cc (**a**). DIP0733 homolog sequence from *C. diphtheriae* without the coiled-coil domain and disorder region are represented by DIP0733-cc (**b**). Similar transcription levels of the DIP0733 homologs (Cg0896, Cg0896 + cc, DIP0733-cc) are demonstrated by RNA hybridization with the respective probes for DIP0733 homologs (**c**-**e**) and 16SrRNA respectively (**f**-**h**). The transcription levels of the control strains transformed with the empty plasmid was detected for 16SrRNA probe (**i**) and no signal for DIP0733 homolog probes was observed (data not shown)

ligase overnight at 22 °C. After transformation of *E. coli* DH5αMCR, positive clones were selected on LB medium containing 25 μg chloramphenicol ml^{-1}.

The resulting plasmids (Table 1) were isolated, sequenced and 1 μg of plasmid DNA was used to transform electrocompetent *C. diphtheriae* CAM-1 strain [14]. Transformants were selected on HI agar containing 12.5 μg chloramphenicol ml^{-1} and 25 μg kanamycin ml^{-1}. For verification of the transcription levels of the above mentioned DIP0733 constructions, RNA isolation and hybridization were carried out as previously described [17]. For hybridization of the digoxigenin-labelled RNA probes (oligonucleotide primers for the different probes are listed in Table 1) and its detection, alkaline phosphatase-conjugated anti-digoxigenin Fab fragments and CSPD (Disodium 3-(4-methoxyspiro {1,2-dioxetane-3,2′-(5′-chloro)tricyclo [3.3.1.1^{3,7}]decan}-4-yl)phenyl phosphate) as the light-emitting substrate were used as suggested by the supplier (Roche, Mannheim, Germany). Chemiluminescence was detected with a ChemiDoc XRS+ system (BioRad, Munich, Germany).

Extracellular matrix (ECM) and plasma protein binding assays

ECM protein binding assays were performed based on the combination of two protocols [7, 18] as previously described [12]. In summary, 96-well polystyrene microtiter plates were coated with collagen type I, collagen type IV and fibrinogen (Sigma, Munich, Germany) dissolved in PBS (Phosphate Buffered Saline) and incubated at 4 °C for 24 h. The coated wells were washed twice with PBS and subsequently filled with 200 μl of resuspended bacterial cells in HI medium (OD_{600} of 0.2). All experiments were carried out in triplicate. The biofilm formation occurred after incubation for 24 h at 37 °C under static conditions. Unattached bacterial cells were discarded and the wells were washed three times with PBS. Biofilms were heat-fixed for 1 h, stained with crystal violet for 15 min at room temperature and rinsed with distilled water. Plates were air dried for 1 h at 37 °C followed by re-solubilization of the stained biofilms in glacial acetic acid. The biofilm was quantified by spectrophotometry with the plate reader TECAN infinity F200 PRO (TECAN, Crailsheim, Germany), using an optical density of 620 nm.

Cell culture experiments

Detroit562 cells were cultivated in Dulbecco's modified Eagle's medium (DMEM), high glucose with L-glutamine and sodium pyruvate (PAA Laboratories, Austria), supplemented with 120 μg penicillin ml^{-1}, 120 μg streptomycin ml^{-1} and 10% (*v*/v) heat-inactivated fetal bovine serum (FBS) (Life Technologies, Germany) in a CO_2 incubator. HeLa cells were cultured in DMEM, high glucose with L-glutamine (PAA Laboratories, Austria) supplemented with 100 μg gentamicin ml^{-1} and 12 μg ciprofloxacin ml^{-1} and 10% heat-inactivated FBS in a CO_2 incubator. Cells were passaged at a ratio of 1:10 twice per week.

Adhesion and invasion assays

Cellular interaction assays were performed using epithelial cells derived from human cervical carcinoma as previously described protocols [12, 14]. In short, HeLa cells were infected with *C. diphtheriae* strains, washed with PBS, detached with trypsin solution, lysed with Tween 20 and the number of colony forming units (CFU) for adhesion was determined. Invasion of epithelial cells was determined as for the above mentioned adhesion assay, followed by further treatment with gentamicin for 90 min. The relative efficiency of invasion (%) was calculated based on the ratio of CFU prior to infection and CFU on the lysate plates after infection, multiplied by 100.

Measurement of transepithelial resistance

Transepithelial resistance assays were carried out in a modified version of a formerly described protocol [17]. Briefly, 1×10^5 Detroit562 cells were seeded per transwell and cultivated in DMEM for 2 weeks. Bacteria were grown until the beginning of the exponential phase was reached. 100 μl of resuspended bacterial cells in PBS (OD_{600} 5) were used to inoculate the transwells. All experiments were carried out in triplicate. After infection, the transepithelial resistance of Detroit562 cells was measured using a volt-ohm-meter (EVOM2, World Precision Instruments, Berlin, Germany). The putative detrimental effect of excessive bacterial growth towards Detroit562 cells was avoided by the replacement of the supernatant of infected cells with fresh DMEM for overnight incubation.

C. elegans survival assay

The assays were performed as previously described [12, 19–23]. Briefly, *C. elegans* N2 were maintained and synchronized on plates containing nematode growth medium (NGM) agar for approximately four to seven days at 20 °C and used in infection assays with *C. diphtheriae* strains. Twenty L4 stage larval worms were infected with 20 μl of each bacterial strain (OD_{600} 1.0) on NGM plates at 20 °C for 24 h. Worms were assessed each day following infection and the dead nematodes were counted and removed every 24 h. For each strain, approximately 60 nematodes were used in the experiments. *E. coli* OP50 was used as a control. *C. elegans* N2 was maintained on *E. coli* OP50 for six to seven days until the worms became starved, as indicated by clumping behaviour [20]. For the Kaplan-Meier survival plots, the Mantel-Cox log-rank test (95% CI) was used for comparing the survival distributions between the DIP0733 mutant strain CAM-1 or the wild-type strain CDC-E8392 versus each mutant variant construct, obtaining the average survival times and *p*-values of less than 0.05 considered significant. The data and all statistical analysis was performed with Prism 7.0 (GraphPad, CA, USA).

Infection and monitoring of *G. mellonella*

Infections of wax moth (*G. mellonella*) larvae were carried out as described previously [15]. In short, bacteria from an overnight culture were inoculated in fresh medium and grown until an OD_{600} of 0.6 was reached. Bacteria were harvested by centrifugation (10 min, 4500 x g) and resuspended in 10 mM $MgSO_4$ to an OD_{600} of 10 (approximately 3×10^9 CFU ml^{-1}). For the infection, a 50 μl Hamilton syringe was used to inject 5 μl aliquots into *G. mellonella* larvae via the hindmost left proleg. Larvae were incubated at 25 °C and pictures were taken on the third day of infection. Post-infection, *G. mellonella* larvae were monitored daily during 5 days for their activity, melanization and survival. A score was provided for each monitored attribute that supported a global health index of each individual wax worm (Additional file 2: Table S1; adapted from the Health Index Scoring System Table from [24]). Healthy, uninfected wax moth larvae typically score between 10 and 11, while infected dead larvae score between 0 and 1.5. For the health index scores of the wax moth larvae infected with *C. diphtheriae* strains, the 2-way ANOVA column statistics were calculated comparing values between the DIP0733 mutant strain CAM-1 or the wild-type strain CDC-E8392 versus each mutant variant construct. *P*-values of less than 0.05 considered significant.

Results

Analysis of short linear motifs of DIP0733 homologs

DIP0733 proteins are composed of seven transmembrane helices and a hydrophilic region. In order to unravel more structural and functional information, the protein sequence of DIP0733 homologs were examined by means of the ELM database for short linear motifs (SLiMs), which can be involved in different functions categorized from a repository of experimentally validated linear motif classes and instances that were manually curated from the literature [25]. SLiMs are functional segments of the protein sequence that are of fundamental importance for numerous biological processes by mediating protein–protein interactions, regulating the dynamic processes involved in cell signaling [26]. Almost seventy SLiMs were found along DIP0733 and its homologs. Among them, important linear motifs comprising docking sites, ligand binding sites and post-translational modification sites, such as DOC_MAPK_JIP1_4 (MAPK docking motifs or kinase interaction motif (KIM)), LIG_eIF4E_1 (motif binding to eIF4E, a key regulator of eukaryotic cap-dependent translation), LIG_SH3_4 (recognized by those SH3 domains with a non-canonical class II recognition specificity), LIG_SUMO_SIM_anti_2 (SUMO-interacting motif (SIM)), LIG_TYR_ITSM (ITSM (immunoreceptor tyrosine-based switch motif), MOD_PK_1/MOD_PKA_1 (phosphorylase kinase phosphorylation

site) and MOD_SUMO_for_1 (sumoylation site), were exclusively found in DIP0733 homologs from pathogenic corynebacteria. Furthermore, the C-terminal domain of DIP0733 is characterized by a pronounced coiled-coil region that is likely to be located extracellularly (Fig. 1). This coiled-coil domain was found to be present in all *C. diphtheriae* and *C. pseudotuberculosis* strains between amino acid positions 961 and 983 and 951 and 978, respectively, whereas it was not found in *C. glutamicum* and *C. ulcerans* DIP0733 homologs. This led to the idea that the virulence properties of DIP0733 in *C. diphtheriae* could be influenced by its C-terminal coiled-coil region and consequently, we constructed truncated variants (Fig. 1) to study the function of this domain.

Binding properties to collagen and fibrinogen

In previous studies, the interaction of *C. diphtheriae* with proteins of the extracellular matrix surrounding eukaryotic cells, e. g. collagen I and IV, was reported [12, 14, 19, 27]. Additionally, the interaction with fibrinogen, a major component of the human plasma, which is crucial for blood clot formation due to its conversion into insoluble fibrin, has also been investigated in corynebacteria [27–29].

To test the bacterial binding to extracellular matrix components and plasma proteins, the strains were incubated in microtitre plate wells previously coated with the corresponding proteins. Compared to the wild-type strain CDC-E8392, the binding of the DIP0733 mutant strain CAM-1 to collagen was significantly impaired (Fig. 2a, b). The binding level of CDC-E8392 to collagen type I was significantly higher (A_{620} 1.098 ± 0.128) than CAM-1 (A_{620} 0.34 ± 0.123). In the case of the overexpression strain, CDC-E8392 pXMJ19_DIP0733 and complementation strain CAM-1 pXMJ19_DIP0733, binding of collagen type I resulted in enhanced rates (A_{620} 1.554 ± 0.205 versus A_{620} 0.946 ± 0.107, respectively). These results supported the findings of the previous study [14]. The strains CAM-1 pXMJ19_Cg0896 and CAM-1 pXMJ19 DIP0733-cc showed a reduction in binding to collagen type I (A_{620} 0.158 ± 0.018 and A_{620} 0.233 ± 0.091, respectively). In contrast, CAM-1 pXMJ19_Cg0896 + cc showed an increased binding to collagen type I (A_{620} 0.475 ± 0.136) (Fig. 2a).

The pattern of binding to collagen type I was similar to the collagen type IV, when considering the complementation and overexpression behavior. CDC-E8392 pXMJ19_DIP0733 showed a higher binding rate of A_{620} 1.095 ± 0.122 compared to the wild-type CDC-E8392 (A_{620} 0.647 ± 0.023) and the binding of the full complementation strain to type IV collagen (A_{620} 0.7709 ± 0.046) presented similar value compared to CDC-E8392 and a significant higher binding than the mutant strain CAM-1 (A_{620} 0.293 ± 0.028 for CAM-1). The mutant variants showed a reduction in binding to collagen type IV; however, a significant difference in binding among the three strains were not observed (Fig. 2b).

The binding to fibrinogen was also reduced by the mutant compared to the wild-type (A_{620} 1.223 ± 0.113 for CDC-E8392 versus A_{620} 0.483 ± 0.134 for CAM-1; Fig. 2c). Similar to collagen type I, the binding to fibrinogen by the overexpression and complementation strains were higher compared to CDC-E8392 and CAM-1 (A_{620} 1.855 ± 0.102 for CDC-E8392 pXMJ19_DIP0733 versus A_{620} 1.466 ± 0.024 for CAM-1 pXMJ19_DIP0733). In contrast, the binding to fibrinogen was reduced by the strain expressing DIP0733 with a truncated coiled-coil domain (A_{620} 0.167 ± 0.04 for CAM-1 pXMJ19_DIP0733-cc). The strain CAM-1 pXMJ19_Cg0896 + cc showed about 4-fold higher binding to fibrinogen compared to CAM-1 pXMJ19_Cg0896 (A_{620} 0.340 ± 0.111 versus A_{620} 0.079 ± 0.016).

The binding to polystyrene surfaces by CDC-E8392 (A_{620} 0.680 ± 0.032) and its DIP0733 overexpression strain (A_{620} 1.563 ± 0.024) indicated that the whole DIP0733 protein could be involved in binding to abiotic surfaces. Moreover, the mutant strain CAM-1 presented a reduced ability to bind to polystyrene compared to the wild-type CDC-E8392 and its complementation strain (A_{620} 0.502 ± 0.020 for CAM-1 and A_{620} 0.680 ± 0.032 for CAM-1 pXMJ19_DIP0733). However, no significant difference in the binding to polystyrene surfaces was observed among the mutant variant strains, suggesting that the coiled-coil region is not interfering significantly with this process (Fig. 2d).

Influence on adhesion of *C. diphtheriae* to epithelial cells

The function of DIP0733 in host cell contact was quantitatively analyzed using wild-type and the mutant strain CAM-1 expressing recombinant versions of the protein in HeLa epithelial cell adhesion assays (Fig. 3a). While CDC-E8392 reached an adhesion rate of 21.4 ± 5%, the CAM-1 attachment was reduced to only 7.5 ± 1.8%. The rates were unchanged when the corresponding strains were transformed with plasmid pXMJ19 for control (20.9 ± 4.1% for the wild-type and 9.1 ± 1.4% for CAM-1). The overexpression of DIP0733 led to an adhesion rate of 51.5 ± 11.8% for the wild-type and 34.1 ± 9% for the mutant CAM-1. Interestingly, the strain CAM-1 pXMJ19_Cg0896 + cc, expressing the DIP0733 homolog of *C. glutamicum* fused with the C-terminal coiled-coil region from *C. diphtheriae*, showed an enhanced adherence rate of 19.2 ± 2.4% compared to the strain CAM-1 pXMJ19_Cg0896 (5.1 ± 1.5%).

Influence on invasion towards epithelial cells

When the internalization of the wild-type and the DIP0733 mutant strains were determined using gentamicin protection assays, the mutant showed a significant decreased

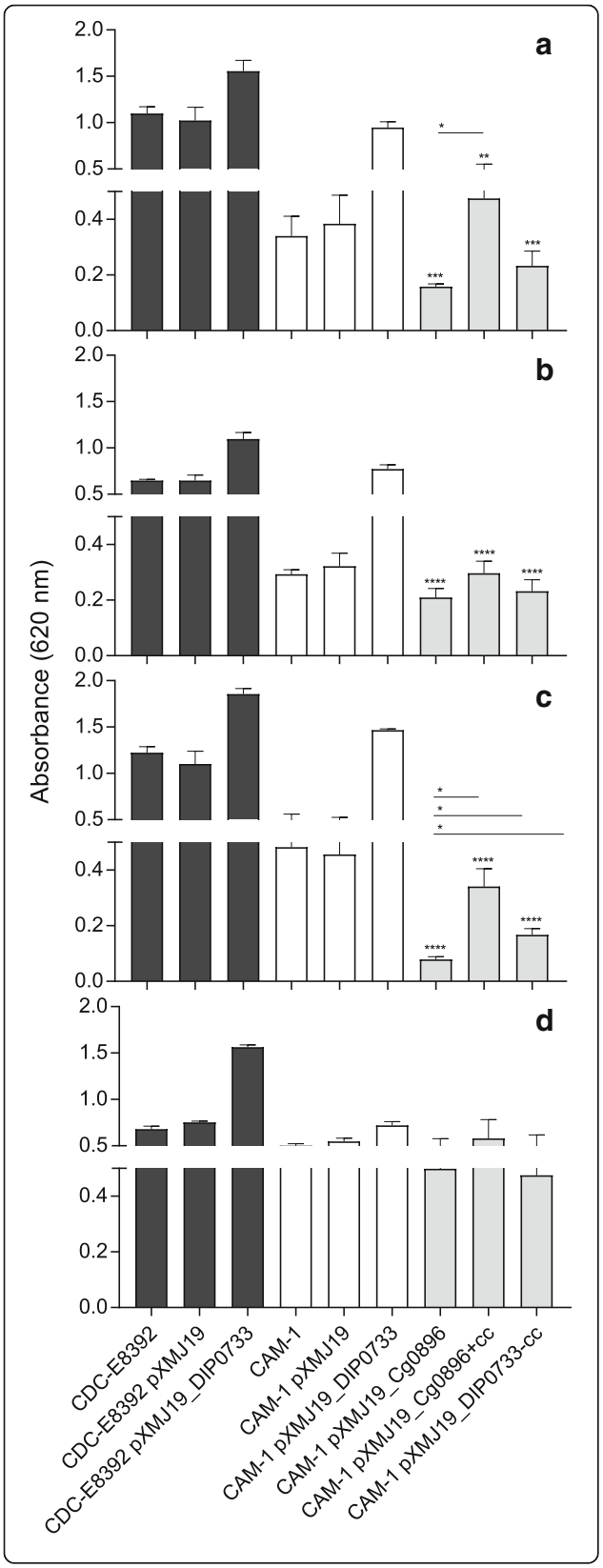

Fig. 2 Binding to extracellular matrix proteins and fibrinogen. Binding to human type I collagen (**a**) and type IV collagen (**b**), fibrinogen (**c**) and polystyrene (**d**) by *C. diphtheriae* strains. Dark grey and white columns represent reproduced assays with strains CDC-E8392 and CAM-1 respectively as previously shown [14]. Grey columns represent assays performed with new constructs for different truncated DIP0733 homologs (see Fig. 2). Data shown represent mean values ± SD of at least three independent biological replicates. Statistically relevant differences from CAM-1 pXMJ19_DIP0733 and its respective truncated forms (light grey columns) were based on Unpaired Student's t-test values below 0.05, 0.01, 0.001 and 0.0001 are indicated by one, two, three and four asterisks, respectively. Unpaired Student's t-test was performed using GraphPad Prism 7.0 (GraphPad, CA, USA)

internalization by HeLa cells. An invasion rate of 0.4 ± 0.12% was reached by the wild-type CDC-E8392 and 0.04 ± 0.02% by the DIP0733 mutant strain CAM-1 (Fig. 3b). As in the case of adhesion assays, transformation of the wild-type or CAM-1 with the vector pXMJ19 (empty vector control) had no influence on invasion rates (0.39 ± 0.15% and 0.08 ± 0.02% respectively). In contrast, transformation with the DIP0733 expression plasmid pXMJ19-DIP0733 resulted in increased invasion rates, which exceeded the wild-type rates by a factor of about four for the wild-type and about three for the mutant. As in the case of adherence, the internalization rate of the CAM-1 pXMJ19_DIP0733-cc strain was reduced (0.12 ± 0.05%). Moreover, the CAM-1 pXMJ19_Cg0896 + cc strain showed an invasion rate of about 0.16 ± 0.04% whereas the CAM-1 pXMJ19_Cg0896 strain had an invasion rate of only 0.01 ± 0.01%. The results obtained suggested a direct function of the DIP0733 protein in respect to the internalization of *C. diphtheriae* by epithelial cells.

Transepithelial resistance

Some pathogens can cause severe damage on cell membranes and the transepithelial resistance of cell monolayers is dramatically reduced due to the loss of cell integrity [17, 30]. In this study, *S.* Typhimurium NCTC 12023 was used as a positive control to test the influence of *C. diphtheriae* strains on transepithelial resistance (Fig. 4). The negative control without bacteria showed a gradual increase in the transepithelial resistance for about 4 h and later stayed constant up to 20 h, whereas the infection of Detroit562 monolayers with *S.* Typhimurium caused a fast breakdown of transepithelial resistance within 2 h. Compared to *S.* Typhimurium, the detrimental effects caused by *C. diphtheriae* were considerably lower. However, the cells infected with the wild-type CDC-E8392 showed a faster breakdown of transepithelial resistance within 6 h in comparison to the mutant CAM-1. Conversely, the cells infected with the mutant CAM-1 showed an increasing transepithelial resistance until about 6 h post infection, which later slighty reduced (Fig. 4a). Moreover, overexpression and

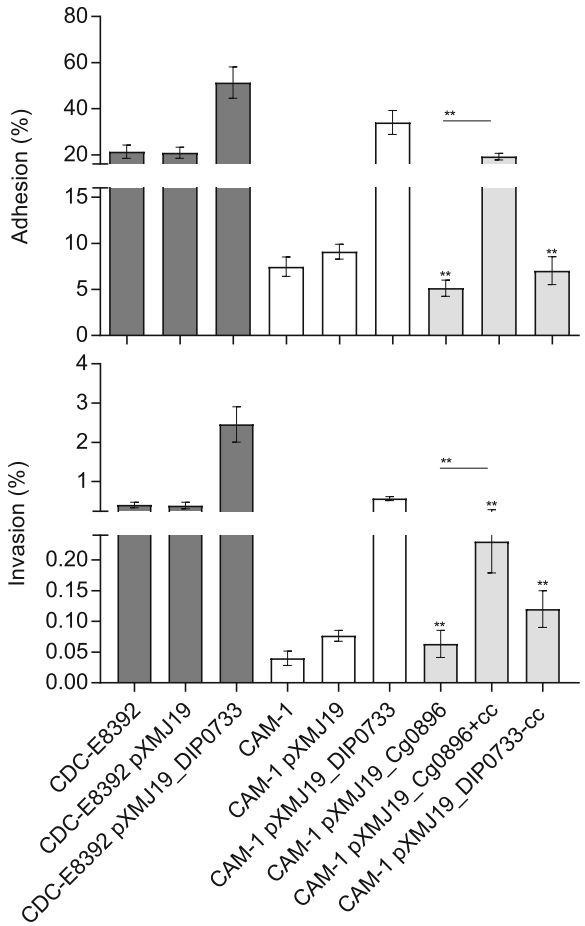

Fig. 3 Adhesion to and invasion of epithelial cells. Dark grey and white columns represent reproduced assays with strains previously showed by [14]. Grey columns represent the assays performed with new constructs for different truncated DIP0733 homologs (see Fig. 1). Statistically relevant differences between CAM-1 pXMJ19_DIP0733 and its respective truncated forms (light grey columns) were based on Unpaired Student's t-test. Values below 0.05, 0.01, 0.001 and 0.0001 are indicated by one, two, three and four asterisks, respectively. Adhesion and invasion are expressed as percentage of the inoculum, showing means and SD of at least three independent biological replicates

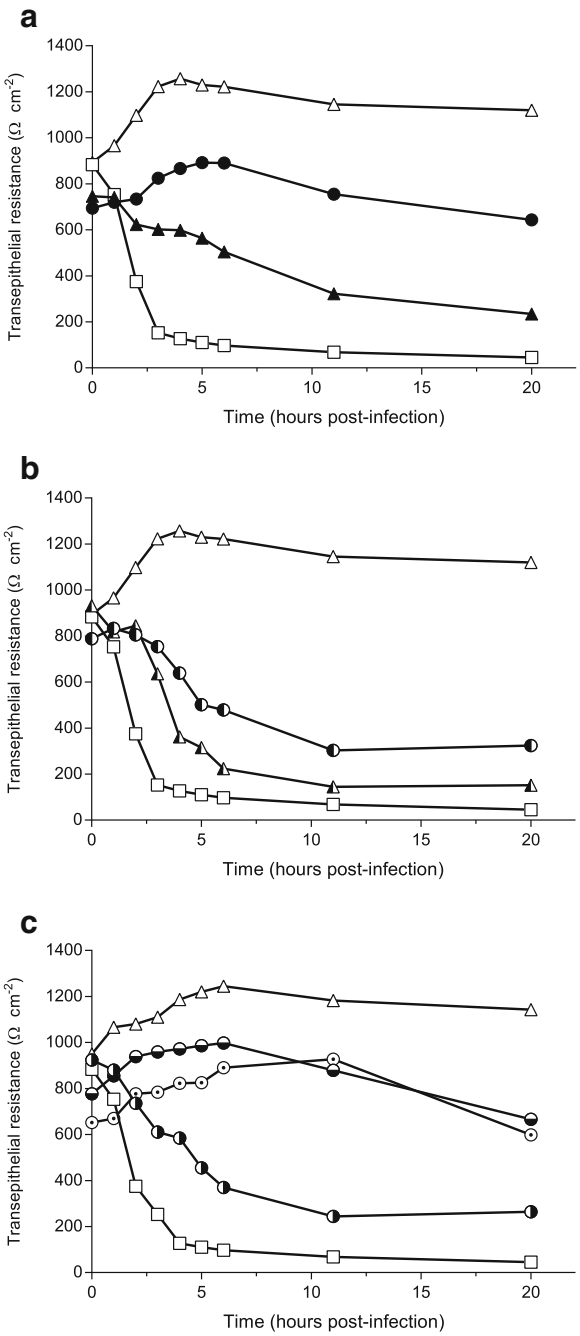

Fig. 4 Transepithelial resistance measurements. Polarized Detroit562 monolayers were grown on transwells and infected with *C. diphtheriae* strains CDC-E8392 (▲) and CAM-1 (●) (**a**); CDC-E8392 pXMJ19_DIP0733 (◭) and CAM-1 pXMJ19_DIP0733 (◐) (**b**); CAM-1 pXMJ19_Cg0896 (⊙), CAM-1 pXMJ19_DIP0733-cc (◒) and CAM-1 pXMJ19_Cg0896 + cc (◑) (**c**). For control, cells were incubated without (Δ) bacteria and (□) *S.* Typhimurium (**a**-**c**). Experiments were carried out independently in triplicate and typical results are shown

complementation strains induced a prominent detrimental effect of the cells within 10 h of infection. The breakdown of the transepithelial resistance by CDC-E8392 pXMJ19_DIP0733 was considerably faster than by the complementation strain CAM-1 pXMJ19_DIP0733, which reached a lower basal resistance of around 200 Ω cm^{-2} at just 6 h post infection (Fig. 4b). In comparison to the CAM-1 pXMJ19_DIP0733-cc strain, the transepithelial resistance of the infected cells with the CAM-1 pXMJ19_Cg0896 + cc was reduced dramatically (Fig. 4c). At 5 h post-infection, cells infected with the strain CAM-1 pXMJ19_Cg0896 + cc had already decreased the transepithelial resistance. On the other hand, cells infected with CAM-1 pXMJ19_DIP0733-cc remained with a high resistance of about 900–1000 Ω until 6 h and only after 11 h of infection was the transepithelial resistance of the cells reduced. The same tendency was observed for the

CAM-1 pXMJ19_Cg0896 strain. These data further supported the important role of the DIP0733 coiled-coil region in host cell interaction and cell damage.

C. elegans survival assay

Previous study of *C. elegans* as a model for bacterial infection [14] revealed a high ability of nematode colonization and killing by the *C. diphtheriae* strain CDC-E8392 in comparison to the DIP0733 disruption mutant CAM-1, and this result was confirmed by the survival assay of this present study ($p < 0.0001$) (Fig. 5a). About 70% of the nematodes survived in contact with the mutant strain CAM-1, while around 70% were killed by the CAM-1 pXMJ19_Cg0896 + cc strain within 5 days (Fig. 5). Interestingly, the survival curve represented by the worms infected with the strain CAM-1 pXMJ19_Cg0896 + cc showed no significant difference compared to the strain CDC-E8392 ($p = 0.576$), while a significant difference was observed when compared to the CAM-1 ($p < 0.0206$). The mutant strain expressing *C. glutamicum* DIP0733 homolog (CAM-1 pXMJ19_Cg0896) and the truncated mutant CAM-1 pXMJ19_DIP0733-cc were less virulent to the nematodes, depicting similar survival rates between 50 and 60% within 5 days post-infection (Fig. 5). Moreover, no significant difference ($p = 0.1651$ for CAM-1 pXMJ19_Cg0896 and $p = 0.0754$ for CAM-1 pXMJ19_DIP0733-cc, respectively) was observed for both survival curves analyses when compared with CAM-1.

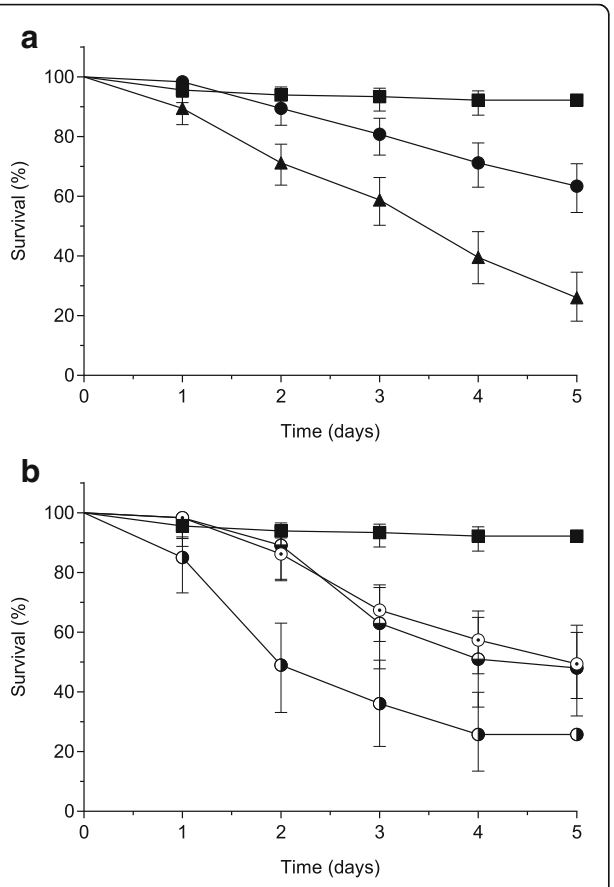

Fig. 5 Nematode survival assay. Nematode survival was followed after infection with *E. coli* OP50 (■), *C. diphtheriae* CDC-E8392 (▲) and CAM-1 (●) (**a**), CAM-1 pXMJ19_Cg0896 (⊙), CAM-1 pXMJ19_DIP0733-cc (◒) and CAM-1 pXMJ19_Cg0896 + cc (◑) (**b**). Data are the mean of at least three parallel experiments with 20 worms per plate and error bars represent 95% CI

Infection and monitoring of *G. mellonella*

G. mellonella larvae are well established as a reliable insect model host to study the pathogenicity of corynebacteria [15]. As a qualitative approach, the melanization process after 3 days of infection is shown in Fig. 6. During the 5 days post-infection, the wax larvae were monitored daily and their activity, melanization and survival were quantitatively scored according to the health index scoring system (Additional file 2: Table S1; Fig. 7). While the control wax moth larvae (injected with buffer) remained the typical beige color and were highly active over all days, injection of the non-pathogenic *C. glutamicum* ATCC 13032 led to the development of small black spots after 3 days (Fig. 6a, b and Fig. 7a). After the second day, the melanization process of the larvae became more pronounced in response to injection of toxigenic *C. diphtheriae* CDC-E8392, which led to less active brown larvae with black spots in contrast to the injection of DIP0733 disrupted mutant strain CAM-1 ($p < 0.0001$) (Fig. 7a). Larvae infected with CAM-1 pXMJ19 Cg0896 were active and light brown in colour with the presence of small black spots in the body after the third day of infection (Fig. 6g and Fig. 7a). In contrast, larvae infected with the CAM-1 pXMJ19_Cg0896 + cc strain showed a lower and decreasing health index score due to the strong melanization with black spots, and a reduced activity over time (Fig. 6h and Fig. 7b) Larvae infected with the CAM-1 pXMJ19_DIP0733-cc strain led to small black spots in the posterior part of the lower abdomen one day earlier than when infected with the CAM-1 strain ($p < 0.05$) (Fig. 6i and Fig. 7). However, after 3 days of infection, their health index score remained very similar to those larvae infected with CAM-1, its control strain CAM-1 pXMJ19 and the strain CAM-1 pXMJ19_Cg0896 (Fig. 7). *S.* Typhimurium was previously validated for pathogenic studies in *G. mellonella* [31] and therefore it was used as a positive control of infection with high degree of melanization, immobility and rapid death also in this study (Fig. 6c and Fig. 7a).

Discussion

The DIP0733 protein is a multi-functional virulence factor of *C. diphtheriae* that plays an important role in different interaction processes with host cells [13, 14]. Besides seven transmembrane helices, other annotated functional domains of DIP0733 have not been described

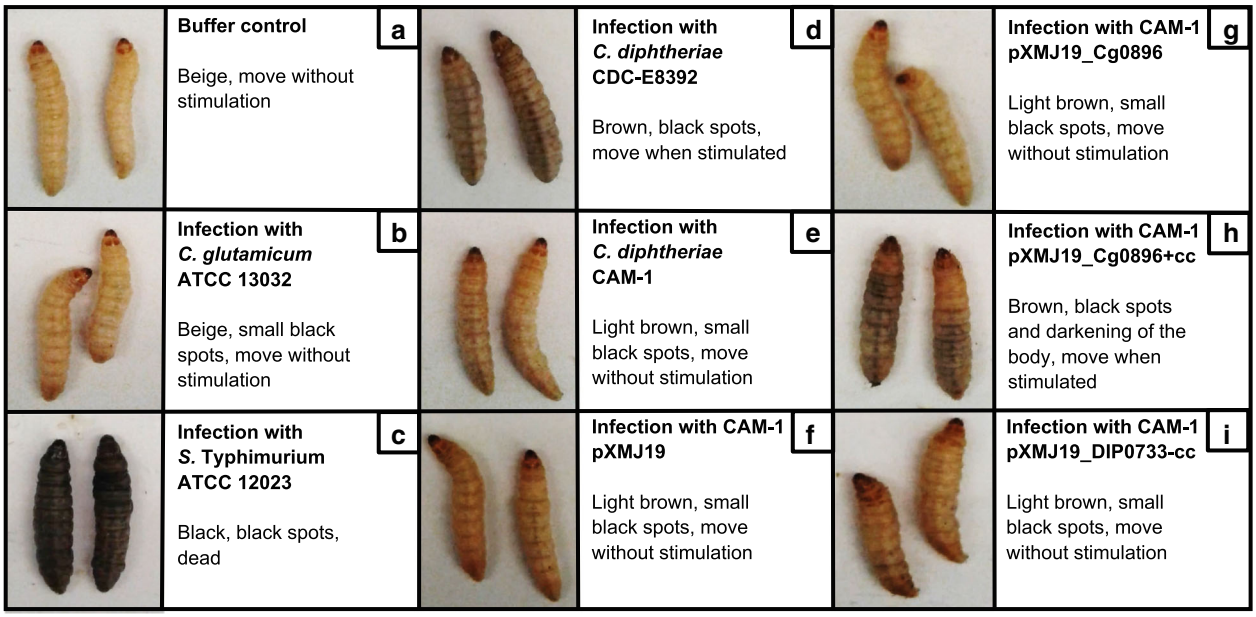

Fig. 6 *G. mellonella* infection assay. *G. mellonella* larvae were injected with 10 μM $MgSO_4$ buffer (**a**), non-pathogenic *C. glutamicum* ATCC 13032 (**b**), positive control for melanization *S.* Typhimurium ATCC12023 (**c**), *C. diphtheriae* strain CDC-E8392 (**d**), CAM-1 (**e**), CAM-1 pXMJ19 (**f**), and DIP0733 truncation mutants CAM-1 pXMJ19 Cg0896 (**g**), CAM-1 pXMJ19 Cg0896 + cc (**h**) and CAM-1 pXMJ19 DIP0733-cc (**i**)

until now. For a better understanding of the structure of DIP0733 and its function in the interaction with host cells, we investigated the SLiMs present among pathogenic and non-pathogenic homolog sequences. Our bioinformatic analysis showed that DIP0733 sequences from closely related pathogenic corynebacteria share higher similarities in SLiMs in contrast to non-pathogenic corynebacteria. While the role of SLiMs is well-characterized in eukaryotic intracellular signaling, in prokaryotic signaling it is less well-understood. Recently, the distribution of known and novel motifs in prokaryotic extracellular and virulence proteins across a range of bacterial species has been investigated [32]. Interestingly, many SLiMs present in virulence effector proteins were able to mimic eukaryotic motifs and facilitate the pathogen to control the intracellular processes of their hosts [32].

In this study, we investigated the role of the C-terminal coiled-coil domain of DIP0733 for pathogenicity of *C. diphtheriae*. Coiled-coil domains consist of two or more α-helical peptides that are enfolded around each other in a superhelical fashion [33]. They are ubiquitous folding motifs found in structural proteins and also play an important role in various intracellular regulation processes and membrane fusion [33]. In eukaryotes, this domain is present in

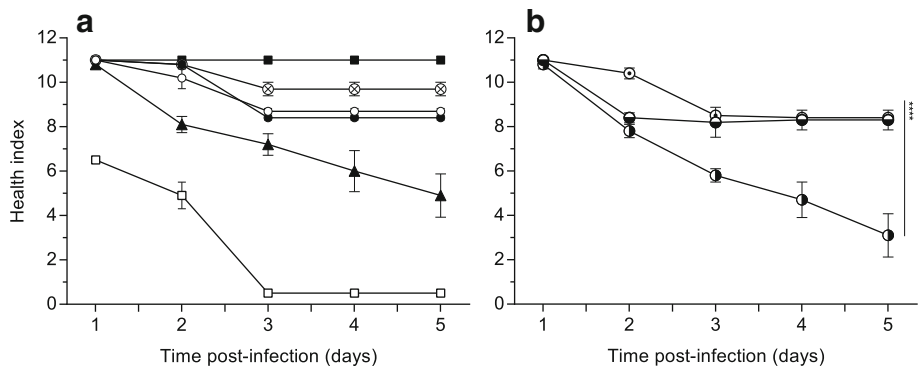

Fig. 7 *G. mellonella* health index score monitoring. *G. mellonella* were monitored post-infection and the activity, melanization and survival features were scored according to their health index. The wax worms were inoculated with buffer (10 μM $MgSO_4$), *S.* Typhimurium ATCC12023, non-pathogenic corynebacteria *C. glutamicum* ATCC 13032 (⊗), *C. diphtheriae* strain CDC-E8392 (▲), CAM-1 (●), CAM-1 pXMJ19 (o) (**a**), and the DIP0733 truncation mutants CAM-1 pXMJ19_Cg0896 (⊙), CAM-1 pXMJ19_Cg0896 + cc (◑) and CAM-1 pXMJ19_DIP0733-cc (◒) (**b**). Error bars represent mean ± SEM and 2-way ANOVA column statistics shows **** $p < 0.0001$

transcription factors as well as fibrous proteins like keratin, myosin, epidermin and fibrinogen [33]. In prokaryotes, important coiled-coil domains are found as a part of murein lipoprotein in *E. coli*, colicin E3 in *S.* Typhimurium and Pep M5 protein in group A streptococci [33, 34].

DIP0733 plays a role as a MSCRAMM (microbial surface component recognizing adhesive matrix molecule) helping *C. diphtheriae* to colonize human tissues or to evade host immune mechanisms of bacterial clearance [14]. At a biochemical level, our results indicate that the coiled-coil domain of DIP0733 is important for the binding to Type I collagen and fibrinogen. Another *C. diphtheriae* protein, DIP2093 was recently described to be involved in binding to Type I, but not to Type IV collagen [12]. This indicates that DIP0733 is not acting alone as a MSCRAMM in *C. diphtheriae*.

Some bacteria, including non-toxigenic corynebacteria, have a natural tendency to adhere to biotic and/or abiotic surfaces and to form biofilms [7]. However, the mechanisms for bacterial adhesion orchestrated by DIP0733 and its coiled-coil domain differ concerning the binding to both biotic and abiotic material. Furthermore, our data corroborates with a previous study [14] and provides the evidence that the DIP0733 protein is involved in these processes but is not exclusively responsible for it.

Moreover, DIP0733 is also involved in adhesion to, invasion into epithelial cells and cell death [13, 14]. On the other hand, a recent study showed that a corresponding mutant for the DIP0733 homolog in *C. ulcerans* (CULC22_00609) showed no effect on adhesion to and invasion into epithelial cells [35]. Remarkably, this data corroborates with our study, as the coiled-coil domain of DIP0733 was predicted to be present only in *C. diphtheriae* and *C. pseudotuberculosis* and absent in *C. ulcerans*. Moreover, our data indicated that the C-terminal coiled-coil region of DIP0733 is crucial for adherence and internalization of *C. diphtheriae* to HeLa cells. Equivalent results were supported by detrimental effects by the break-down of transepithelial resistance of Detroit 562 cell monolayers after infection with *C. diphtheriae* wild-type and DIP0733 homologs as well as its truncated mutant strains. Whilst a dramatic break-down of transepithelial resistance was not observed for most of the *C. diphtheriae* strains tested by Ott and co-workers, *C. diphtheriae* DSM43989 showed the most severe effect after 3 h of infection [17], which was similarly demonstrated by the CDC-E8392 wild-type strain in this study. Conversely, other strain specific proteins and cellular niche factors may be involved in this process as similar effects were described for *C. ulcerans* 809 [35].

As an in vivo approach, the pathogenicity of DIP0733 and its C-terminal coiled-coil domain was further investigated and confirmed using *C. elegans* and *G. mellonella* as invertebrate animal model systems. Previous study showed that the DIP0733 mutant CAM-1 exhibited significant attenuation in nematode colonization, proliferation inside the worms and killing of the host compared to the wild-type CDC-E8392 [14]. Remarkably, CAM-1 expressing the *C. glutamicum* DIP0733 hybrid variant with C-terminal coiled-coil region was able to kill the nematodes, as similarly demonstrated by the complementation strain CAM-1 pXMJ19_DIP0733 [14]. A corresponding tendency concerning the influence of DIP0733 and its coiled-coil domain on bacterial pathogenicity in *G. mellonella* was observed in our study. Some entomopathogenic strains are able to inhibit the phenol-oxydase activation and therefore evade the melanization pathway [36]. However, most of the *G. mellonella* infection assays using a variety of Gram-positive bacteria, including *Streptococcus*, *Enterococcus*, *Staphylococcus* and *Listeria* spspecies (for review, see [37]) and importantly, pathogenic species of *Corynebacterium,* including *C. diphtheriae,* presented different degrees of melanization as an evidence for bacterial pathogenicity towards invertebrate model systems [15]. Remarkably, our data indicates a key role of DIP0733 and its coiled-coil domain in the melanization process induced by the infection with *C. diphtheriae*. Synthesis and deposition of melanin in *G. mellonella* function to encapsulate pathogens at the wound site followed by hemolymph coagulation and opsonization, analogous to abscess formation in mammalian infections [37, 38].

Our data showed the importance of the coiled-coil domain of DIP0733 in *C. diphtheriae* pathogenicity. Whether the coiled-coil domain is responsible for the interaction either with the host cells or with the holding of possible protein oligomers itself still remains unclear. To address this point, the protein crystallization and its oligomerization status must be further investigated.

Conclusions

Taken together, DIP0733 is a multi-functional protein with an important C-terminal coiled-coil domain responsible for pathogenicity of *C. diphtheriae* in epithelial cells and invertebrate animal model systems.

Additional files

Additional file 1: Figure S1. DIP0733 sequences alignment and identity scores. The detailed Multiple Sequences Alignment (MSA) of DIP0733 homologs of *C. diphtheriae* CDC-E8392, *C. diphtheriae* INCA 402, *C. ulcerans* BR-AD22, *C. pseudotuberculosis* 258 and *C. glutamicum* ATCC 13032 was anlyzed using Sequence Viewer 8.0 (a). For MSA, DIP0733 (Accession id: CAE49255) was used as query sequence and the compositional substitution matrix adjustment method was executed on BLASTp (b). (PDF 1059 kb)

Additional file 2: Table S1. Health index scoring system for *Galleria mellonella* adapted from Loh and co-workers (2013) [24]. Post-infection, *G. mellonella* larvae were monitored and scored daily for their activity, melanization and survival. Healthy, uninfected wax moth larvae typically score between 10 and 11, while infected dead wax moth larvae score between 0 and 1.5. (DOCX 14 kb)

Abbreviations

CFU: Colony forming units; CLV: Cleavage sites; CSPD: Disodium 3-(4-methoxyspiro {1,2-dioxetane-3,2′-(5′-chloro)tricyclo [3.3.1.1^{3,7}]decan}-4-yl)phenyl phosphate; DEG: Degradation sites; DMEM: Dulbecco's modified Eagle's medium; DOC: Docking sites; ECM: Extracellular matrix; ELM: Eukaryotic linear motif; FBS: Fetal bovine serum; HI: Heart infusion; LB: Luria Bertani; LIG: Ligand binding sites; MOD: Post-translational modification sites; MSCRAMM: Microbial surface component recognizing adhesive matrix molecule; NGM: Nematode growth medium; PBS: Phosphate buffered saline; SLiMs: Short linear motifs; TRG: Targeting sites

Acknowledgements

We acknowledge the abstract content previously presented as e-poster at the 5th Joint Conference of the DGHM & VAAM. Biospektrum (2017) 23(Suppl 1): 1. https://doi.org/10.1007/s12268-017-0772-x. A sincere thank you to Dr. Georgia Isom for proofreading this manuscript.

Funding

ALMG and CAA were supported by the Coordination for the Improvement of Higher Education Personnel (CAPES). DW was supported by a PhD fellowship of the *Deutscher Akademischer Austauschdienst* (DAAD) and by the *Deutsche Forschungsgemeinschaft* in frame of SFB796 (MGK). CAA gratefully acknowledge the *Förderung von Frauen in Forschung und Lehre* (FFL) of the Friedrich-Alexander-Universität Erlangen-Nürnberg. The funding bodies had no role in the design of the study and collection, analysis and interpretation of data and in writing the manuscript.

Availability of data and materials

Strains, plasmids and data sets will be available upon request.

Authors' contributions

DW carried out extracellular matrix and plasma protein binding assays, adhesion and invasion experiments, transepithelial resistance assays and infection of *G. mellonella*. FS, CAA and HS performed cloning and bioinformatic analysis. CAA carried out the infection of *C. elegans* and the statistical analysis. AB was involved in writing of the manuscript and supervised the experiments of DW and FS. DW and ALMG were involved in writing of the manuscript. CAA was responsible for the draft and the final version of the manuscript. All authors read and approved the final manuscript.

Ethics approval and consent to participate

Not applicable.

Consent for publication

Not applicable.

Competing interests

The authors declare that they have no competing interests.

Publisher's Note

Author details

[1]Microbiology Division, Friedrich-Alexander-University Erlangen-Nuremberg, Erlangen, Germany. [2]Division of Bioinformatics, Institute of Biochemistry, Friedrich-Alexander-University Erlangen-Nuremberg, Erlangen, Germany. [3]Laboratory of Diphtheria and Corynebacteria of Clinical Relevance-LDCIC, Faculty of Medical Sciences, Rio de Janeiro State University, Rio de Janeiro, Brazil.

Received: 14 November 2017 Accepted: 23 August 2018
Published online: 04 September 2018

References

1. Burkovski A. Diphtheria and its etiological agents. In: *Corynebacterium diphtheriae* and related toxigenic species. 1st ed. Dordrecht: Springer; 2014. p. 1–14.
2. Hessling M, Feiertag J, Hoenes K. Pathogens provoking most deaths worldwide: a review. Biosci Biotech Res Comm. 2017;10:1–7.
3. Belchior E, Henry S, Badell E, Collet L, Benoit-Cattin T, de Montera A, et al. Diphtheria in Mayotte, 2007-2015. Emerg Infect Dis. 2017;23:1218–20.
4. Kolios AGA, Cozzio A, Zinkernagel AS, French LE, Kündig TM. Cutaneous *Corynebacterium* infection presenting with disseminated skin nodules and ulceration. Case Rep Dermatol. 2017;9:8–12.
5. Sahin A, Yildirim N, Gultekin S, Akgun Y, Kiremitci A, Schicht M, et al. Changes in the conjunctival bacterial flora of patients hospitalized in an intensive care unit. Arq Bras Oftalmol. 2017;80:21–4.
6. Santos LS, Sant'anna LO, Ramos JN, Ladeira EM, Stavracakis-Peixoto R, Borges LL, et al. Diphtheria outbreak in Maranhão, Brazil: microbiological, clinical and epidemiological aspects. Epidemiol Infect. 2015;143:791–8.
7. Gomes DL, Martins CA, Faria LM, Santos LS, Santos CS, Sabbadini PS, et al. *Corynebacterium diphtheriae* as an emerging pathogen in nephrostomy catheter-related infection: evaluation of traits associated with bacterial virulence. J Med Microbiol. 2009;58:1419–27.
8. Collier RJ. Understanding the mode of action of diphtheria toxin: a perspective on progress during the 20th century. Toxicon. 2001;39:1793–803.
9. Rogers EA, Das A, Ton-That H. Adhesion by pathogenic corynebacteria. Adv Exp Med Biol. 2011;715:91–103.
10. Readon-Robinson ME, Ton-That H. Assembly and function of *Corynebacterium diphtheriae* pili. In: Burkovski A, editor. *Corynebacterium diphtheriae* and related toxigenic species. Dordrecht: Springer; 2014. p. 123–41.
11. Ott L, Burkovski A. Toxigenic corynebacteria: adhesion, invasion and host response. In: Burkovski A, editor. *Corynebacterium diphtheriae* and related toxigenic species. Dordrecht: Springer; 2014. p. 143–70.
12. Peixoto RS, Antunes CA, Lourêdo LS, Viana V, Santos C, Silva JFR, et al. Functional characterization of the collagen-binding protein DIP2093 and its influence on host-pathogen interaction and arthritogenic potential of *Corynebacterium diphtheriae*. Microbiology. 2017;163:692–701.
13. Sabbadini PS, Assis MC, Trost E, Gomes DL, Moreira LO, Dos Santos CS, et al. *Corynebacterium diphtheriae* 67-72p hemagglutinin, characterized as the protein DIP0733, conttributes to invasion and induction of apoptosis in HEp-2 cells. Microb Pathog. 2012;52:165–76.
14. Antunes CA, Santos LS, Hacker E, Köhler S, Bösl K, Ott L, et al. Characterization of DIP0733, a multi-functional virulence factor of *Corynebacterium diphtheriae*. Microbiology. 2015;161:639–47.
15. Ott L, McKenzie A, Baltazar MT, Britting S, Bischof A, Burkovski A, et al. Evaluation of invertebrate infection models for pathogenic corynebacteria. FEMS Immunol Med Microbiol. 2012;65:413–21.
16. Sambrook J, Fritsch EF, Maniatis T. Molecular cloning: a laboratory manual. 2nd ed. New York: Cold Spring Harbor Laboratory Press; 1989.
17. Ott L, Höller M, Rheinlaender J, Schäffer TE, Hensel M, Burkovski A. Strain-specific differences in pili formation and the interaction of *Corynebacterium diphtheriae* with host cells. BMC Microbiol. 2010;10:257.
18. Birkenhauer E, Neethirajan S, Weese JS. Collagen and hyaluronan at wound sites influence early polymicrobial biofilm adhesive events. BMC Microbiol. 2014;14:191.
19. Peixoto RS, Hacker E, Antunes CA, Weerasekera D, Dias AA, Martins CA, et al. Pathogenic properties of a *Corynebacterium diphtheriae* strain isolated from a case of osteomyelitis. J Med Microbiol. 2016;65:1311–21.
20. de Bono M, Bargmann CI. Natural variation in a neuropeptide Y receptor homolog modifies social behavior and food response in *C. elegans*. Cell. 1998;94:679–89.
21. Browning DF, Wells TJ, França FL, Morris FC, Sevastsyanovich YR, Bryant JA, et al. Laboratory adapted *Escherichia coli* K-12 becomes a pathogen of *Caenorhabditis elegans* upon restoration of O antigen biosynthesis. Mol Microbiol. 2013;87:939–50.
22. Antunes CA, Clark L, Wanuske MT, Hacker E, Ott L, Simpson-Louredo L, et al. *Caenorhabditis elegans* star formation and negative chemotaxis induced by infection with corynebacteria. Microbiology. 2016;162:84–93.
23. Santos LS, Antunes CA, Santos CS, Pereira JA, Sabbadini PS, Luna M, et al. *Corynebacterium diphtheriae* putative tellurite-resistance protein (CDCE8392_0813) contributes to the intracellular survival in human epithelial cells and lethality of *Caenorhabditis elegans*. Mem Inst Oswaldo Cruz. 2015;110:662–8.
24. Loh JM, Adenwalla N, Wiles S, Proft T. *Galleria mellonella* larvae as an infection model for group a streptococcus. Virulence. 2013;4:419–28.
25. Gouw M, Sámano-Sánchez H, Van Roey K, Diella F, Gibson TJ, Dinkel H. Exploring short linear motifs using the ELM database and tools. Curr Protoc Bioinf. 2017;58:1–35.
26. Van Roey K, Dinkel H, Weatheritt RJ, Gibson TJ, Davey NE. The switches. ELM resource: a compendium of conditional regulatory interaction interfaces. Sci Signal. 2013;6:rs7.

27. Sabbadini PS, Genovez MR, Silva CF, Adelino TL, Santos CS, Pereira GA, et al. Fibrinogen binds to non-toxigenic and toxigenic *Corynebacterium diphtheriae* strains. Mem Inst Oswaldo Cruz. 2010;105:706–11.
28. Colombo AV, Hirata R Jr, Souza CM, Monteiro-Leal LH, Previato JO, Formiga LCD, et al. *Corynebacterium diphtheriae* surface proteins as adhesins to human erythrocytes. FEMS Microbiol. 2001;197:235–9.
29. Simpson-Louredo L, Ramos JN, Peixoto RS, Santos LS, Antunes CA, Ladeira EM, et al. *Corynebacterium ulcerans* isolates from humans and dogs: fibrinogen, fibronectin and collagen-binding, antimicrobial and PFGE profiles. Antonie Van Leeuwenhoek. 2014;105:343–52.
30. Gerlach RG, Claudio N, Rohde M, Jäckel D, Wagner C, Hensel M. Cooperation of *Salmonella* pathogenicity islands 1 and 4 is required to breach epithelial barriers. Cell Microbiol. 2008;10:2364–76.
31. Viegas SC, Mil-Homens D, Fialho AM, Arraiano CM. The virulence of *Salmonella enterica* serovar typhimurium in the insect model *Galleria mellonella* is impaired by mutations in RNase E and RNase III. Appl Environ Microbiol. 2013;79:6124–33.
32. Ruhanen H, Hurley D, Ghosh A, O'Brien KT, Johnston CR, Shields DC. Potential of known and short prokaryotic protein motifs as a basis for novel peptide-based antibacterial therapeutics: a computational survey. Front Microbiol. 2014;5:4.
33. Apostolovic B, Maarten D, Harm-Anton K. Coiled coils: attractive protein folding motifs for the fabrication of self-assembled, responsive and bioactive materials. Chem Soc Rev. 2010;39:3541–75.
34. Manjula BN, Fischetti VA. Sequence homology of group a streptococcal pep M5 protein with other coiled-coil proteins. Biochem Biophys Res Commun. 1986;140:684–90.
35. Hacker E, Ott L, Hasselt K, Mattos-Guaraldi AL, Tauch A, Burkovski A. Colonization of human epithelial cell lines by *Corynebacterium ulcerans* from human and animal sources. Microbiology. 2015;161:1582–91.
36. Crawford JM, Portmann C, Zhang X, Roeffaers MBJ, Clardy J. Small molecule perimeter defense in entomopathogenic bacteria. Proc Natl Acad Sci U S A. 2012;109:10821–6.
37. Tsai CJ, Loh JM, Proft T. *Galleria mellonella* infection models for the study of bacterial diseases and for antimicrobial drug testing. Virulence. 2016;7:214–29.
38. Tang H. Regulation and function of the melanization reaction in drosophila. Fly (Austin). 2009;3:105–11.
39. Grant SG, Jessee J, Bloom FR, Hanahan D. Differential plasmid rescue from transgenic mouse DNAs into *Escherichia coli* methylation-restriction mutants. Proc Natl Acad Sci U S A. 1990;87:4645–9.
40. Brenner S. The genetics of *Caenorhabditis elegans*. Genetics. 1974;77:71–94.
41. Trost E, Blom J, Soares SC, Huang IH, Al-Dilaimi A, Schröder J, et al. Pangenomic study of *Corynebacterium diphtheriae* that provides insights into the genomic diversity of pathogenic isolates from cases of classical diphtheria, endocarditis, and pneumonia. J Bacteriol. 2012;194:3199–215.
42. Abe S, Takayama K, Kinoshita S. Taxonomical studies on glutamic acid-producing bacteria. J Gen Appl Microbiol. 1967;13:279–301.
43. Peterson WD Jr, Stulberg CS, Swanborg NK, Robinson AR. Glucose-6-phosphate dehydrogenase isoenzymes in human cell cultures determined by sucrose-agar gel and cellulose acetate zymograms. Proc Soc Exp Biol Med. 1968;128:772–6.
44. Gey GO, Coffmann WD, Kubicek MT. Tissue culture studies of the proliferative capacity of cervical carcinoma and normal epithelium. Cancer Res. 1952;12:264–5.
45. Scherer WF, Syverton JT, Gey GO. Studies on the propagation *in vitro* of poliomyelitis viruses. IV. Viral multiplication in a stable strain of human malignant epithelial cells (strain HeLa) derived from an epidermoid carcinoma of the cervix. J Exp Med. 1953;97:695–710.
46. Jakoby M, Ngouoto-Nkili CE, Burkovski A. Construction and application of new *Corynebacterium glutamicum* vectors. Biotechnol Tech. 1999;13:437–41.

Pathogenic properties of a *Corynebacterium diphtheriae* strain isolated from a case of osteomyelitis

Renata Stavracakis Peixoto,[1,2,3] Elena Hacker,[1] Camila Azevedo Antunes,[1,3] Dulanthi Weerasekera,[1] Alexandre Alves de Souza de Oliveira Dias,[4] Carlos Alberto Martins,[5] Raphael Hirata Júnior,[3] Kátia Regina Netto dos Santos,[2] Andreas Burkovski[1] and Ana Luíza Mattos-Guaraldi[2,3]

Correspondence
Ana Luíza Mattos-Guaraldi
guaraldi@uerj.br

[1]Professur für Mikrobiologie, Friedrich-Alexander-Universität Erlangen-Nürnberg, Erlangen, Germany

[2]Department of Medical Microbiology, Institute of Microbiology, Rio de Janeiro Federal University (IMPPG/UFRJ), Rio de Janeiro, RJ, Brazil

[3]Laboratory of Diphtheria and Corynebacteria of Clinical Relevance-LDCIC, Faculty of Medical Sciences, Rio de Janeiro State University – UERJ, Rio de Janeiro, RJ, Brazil

[4]National Institute for Quality Control in Health (INCQS), Fundação Oswaldo Cruz–FIOCRUZ, Rio de Janeiro, RJ, Brazil

[5]Brazilian National Cancer Institute – Ministry of Health, INCA, Rio de Janeiro, RJ, Brazil

Received 2 June 2016
Accepted 7 October 2016

Corynebacterium diphtheriae is typically recognized as a colonizer of the upper respiratory tract (respiratory diphtheria) and the skin (cutaneous diphtheria). However, different strains of *Corynebacterium diphtheriae* can also cause invasive infections. In this study, the characterization of a non-toxigenic *Corynebacterium diphtheriae* strain (designated BR-INCA5015) isolated from osteomyelitis in the frontal bone of a patient with adenoid cystic carcinoma was performed. Pathogenic properties of the strain BR-INCA5015 were tested in a *Caenorhabditis elegans* survival assay showing strong colonization and killing by this strain. Survival rates of 3.8±2.7 %, 33.6±7.3 % and 0 % were observed for strains ATCC 27010^T, ATCC 27012 and BR-INCA5015, respectively, at day 7. BR-INCA5015 was able to colonize epithelial cells, showing elevated capacity to adhere to and survive within HeLa cells compared to other *Corynebacterium diphtheriae* isolates. Intracellular survival in macrophages (THP-1 and RAW 264.7) was significantly higher compared to control strains ATCC 27010^T (non-toxigenic) and ATCC 27012 (toxigenic). Furthermore, the ability of BR-INCA5015 to induce osteomyelitis was confirmed by *in vivo* assay using Swiss Webster mice.

INTRODUCTION

Corynebacterium diphtheriae is the classical aetiological agent of diphtheria (Hadfield *et al.*, 2000; Burkovski, 2013a, b). The infection causes localized inflammatory lesions of the upper respiratory tract, often with associated necrosis at distant sites, i.e. myocarditis and neuritis, attributable to the dissemination of the diphtheria toxin (Pennie *et al.*, 1996). Cases of cutaneous diphtheria, caused by toxigenic strains of *Corynebacterium*, occur when the organism is associated with wounds and lesions (often ulcerative) and are mainly found in tropical areas. The effects of diphtheria toxin are typically less detrimental in this form compared to respiratory diphtheria (Hadfield *et al.*, 2000; Burkovski, 2013a).

The introduction of mass immunization against diphtheria in the 1950s resulted in a lower incidence of this disease in most industrialized countries (Saragea *et al.*, 1979; Galazka, 2000; von Hunolstein *et al.*, 2003). Although the circulation of toxigenic strains declined in all countries with good vaccination coverage, non-toxigenic *Corynebacterium diphtheriae* strains have been increasingly related to cases of invasive infections, including septicaemia (Isaac-Renton *et al.*, 1981; Huber-

Abbreviations: ECM, extracellular matrix; FBS, foetal bovine serum.

Schneider *et al.*, 1994; Zasada *et al.*, 2005; Farfour *et al.*, 2012), endocarditis (Tiley *et al.*, 1993; Mortier *et al.*, 1994; Lehnert *et al.*, 1995; Mattos-Guaraldi & Formiga, 1998; Belko *et al.*, 2000; Zasada *et al.*, 2005; Hirata *et al.*, 2008; Muttaiyah *et al.*, 2011), splenic abscesses (Alexander, 1984), arthritis (Guran *et al.*, 1979; Afghani & Stutman, 1993; Mortier *et al.*, 1994; Puliti *et al.*, 2006; Dias *et al.*, 2011; Peixoto *et al.*, 2014) and osteomyelitis (Poilane *et al.*, 1995; Stavracakis-Peixoto *et al.*, 2011). A poor health status may predispose individuals to become infected by different *Corynebacterium* species (Mattos-Guaraldi *et al.*, 2001, 2003; Martins *et al.,* 2009; Rizvi *et al.,* 2011, 2013).

Cases of arthritis/osteomyelitis due to infections by other corynebacterial species have also been reported (Morrey *et al.*, 1977; von Graevenitz *et al.*, 1998; Wong *et al.*, 2010; Rizvi *et al.*, 2011; Verma & Kravitz, 2016). Patients with cancer are more susceptible to the appearance of cases of osteomyelitis obtained by haematogenic contamination, an infectious focus or lesions adjacent to the bone (Brady *et al.*, 2008). A case of osteomyelitis due to a non-toxigenic *Corynebacterium diphtheriae* biovar mitis (BR-INCA5015) strain in the frontal bone of a patient with adenoid cystic carcinoma was reported (Stavracakis-Peixoto *et al.*, 2011).

Since there are still only a low number of investigations of pathogenic potential of non-toxigenic strains of *Corynebacterium diphtheriae*, BR-INCA5015 strain obtained after the microsurgical removal of the frontal bone due to osteomyelitis was characterized in more detail in this study.

METHODS

Case presentation. A 41-year-old woman residing in a poor area of the city of Rio de Janeiro, Brazil, was admitted to the National Cancer Institute (Instituto Nacional do Cancer – INCA) in 2006, with a tumour in the right nostril. The patient underwent surgery, and to correct a surgical dehiscence, the patient was again operated on, in 2008. *Corynebacterium diphtheriae* BR-INCA5015 and meticillin-sensitive *Staphylococcus aureus* strains were found during primary culture obtained after the microsurgical removal of the frontal bone due to osteomyelitis (Stavracakis-Peixoto *et al.*, 2011). The corresponding strain was characterized in more detail in this study.

Bacterial strains and culture conditions. *Corynebacterium diphtheriae* and *Escherichia coli* strains used in this study are listed in Table 1. *Corynebacterium diphtheriae* strains were grown in heart infusion (HI) (Becton and Dickinson) broth at 37 °C and stored in HI medium with 20 % glycerol at −80 °C (Antunes *et al.*, 2015). *E. coli* OP50 was grown in Luria–Bertani (Becton and Dickinson) medium at 37 °C (Sambrook *et al.*, 1989; Antunes *et al.*, 2015; Santos *et al.*, 2015a).

Nematode infection model. The assays were performed as previously described with some adaptations for *Corynebacterium diphtheriae* and analysed by the Kaplan–Meier survival method (de Bono & Bargmann, 1998; Browning *et al.*, 2013; Antunes *et al.*, 2015; Santos *et al.*, 2015a). Briefly, *Caenorhabditis elegans* N2 was maintained on plates containing nematode growth medium agar for approximately 6 to 7 days at 20 °C and used in infection assays with *Corynebacterium diphtheriae* strains. Twenty L4 stage larval worms were infected with 20 µl of each bacterial strain (OD_{600} 1.0) on nematode growth medium plates at 20 °C for 24 h. The worms were assessed daily following infection, and the dead nematodes were counted and removed every 24 h for 7 days. For each strain, approximately 60 nematodes were used, and the assays were performed three times. *E. coli* OP50 was used as a control in these experiments.

Extracellular matrix (ECM) binding assays. The ECM protein binding assay was performed based on a modified protocol previously described (Gomes *et al.*, 2009; Birkenhauer *et al.*, 2014). Briefly, standard 96-well polystyrene microtitre plates (Greiner CELLSTAR) were coated with collagen types I and IV (Sigma) dissolved in PBS (50 µg ml^{-1}). To each well, a total of 200 µl of solution was added. Plates were then covered and allowed to incubate at 4 °C for 24 h. Coating solutions were gently removed after this time, and the wells were rinsed twice with PBS. The density of the inoculum was adjusted to an OD_{600} of 0.2, and 200 µl was inoculated in triplicate into the coated wells. Uninfected wells were used as control. Microtitre plates were incubated for 24 h at 37 °C under static conditions in order to allow biofilm formation. For quantification of biofilms, after 24 h incubation, microbial solutions were discarded, and the wells were washed three times with 200 µl PBS in order to remove unattached cells. Biofilms were heat fixed at 65 °C for 60 min and subsequently stained with 0.1 % (w/v) crystal violet (Sigma-Aldrich) for 15 min at room temperature. Crystal violet solution was removed, and the plates were rinsed by submersion in a container of tap water. Plates were then allowed to dry for 60 min at 35 °C. After this, crystal violet from stained biofilms was re-solubilized in 200 µl of 95 % ethanol, and absorbance was measured at 620 nm.

Human epithelial carcinoma (HeLa) cell interaction assays. The cellular interaction assays were performed using epithelial cells derived from human cervical carcinoma according to previously described protocols (Antunes *et al.*, 2015; Hacker *et al.*, 2015). Briefly, HeLa cells were cultured in Dulbecco's modified Eagle's medium (DMEM), high glucose with L-glutamine (PAA Laboratories) supplemented with 100 µg ml^{-1} gentamicin and 12 µg ml^{-1} ciprofloxacin and 10 % heat-inactivated foetal bovine serum (FBS) (Life Technologies) in a 5 % CO_2 incubator at 37 °C. Cells were passaged at a ratio of 1 : 10 twice per week. HeLa cells were seeded in 24-well plates without antibiotics (Nunc) at a density of 1×10^5 cells per well 24 h prior to infection. Bacteria were harvested by centrifugation, and cell density was adjusted to OD_{600} 1.0. A master mix of the inoculum with an m.o.i. of 50 was prepared in DMEM, and 500 µl per well was used to infect the cells. The plates were centrifuged for 5 min at 300 ***g*** to synchronize infection and subsequently incubated for 90 min. The cells were washed with PBS three times, detached with 500 µl Accutase per well (5 min, 37 °C, 5 % CO_2, 95 % humidity) and lysed by addition of 12.5 µl 10 % Tween 20 under the same conditions. Serial dilutions were made in pre-chilled 1× PBS and plated on Columbia agar with sheep blood (Oxoid) to determine the number of c.f.u.

For analysis of internalization, the cells were washed three times with PBS to remove planktonic and loosely attached bacteria. Subsequently, the cells were incubated for 2 h in DMEM (500 µl per well) containing 100 µg ml^{-1} gentamicin to kill the remaining extracellular bacteria. After incubation, the cell layers were washed three times with PBS, detached by adding 500 µl Accutase per well (5 min, 37 °C, 5 % CO_2, 95 % humidity) and lysed by addition of 12.5 µl 10 % Tween 20 to liberate the intracellular bacteria. Serial dilutions of the inocula and the lysates were plated out on Columbia agar with sheep blood (Oxoid) to determine the number of c.f.u. The percentage adhesion/invasion efficiency was calculated by the ratio of bacteria used for infection (c.f.u. inoculum plate) and bacteria in the lysate (c.f.u. lysate plate) multiplied by 100.

Human (THP-1) and murine (RAW 264.7) macrophage interaction assays. The macrophage interactions were performed based on protocols previously described (Hacker *et al.*, 2016). Human THP-1 cells were cultured in 10 % FBS-supplemented Roswell Park Memorial Institute medium 1640 (RPMI 1640; containing 100 U ml^{-1} penicillin and 100 mg ml^{-1} streptomycin) and 10 % FBS. Murine RAW 264.7 cells were cultivated in DMEM, high glucose with L-glutamine and sodium pyruvate (PAA Laboratories), supplemented with 120 mg ml^{-1} penicillin,

Table 1. Micro-organisms, human/murine cell lines and plasmids used in this study

Micro-organism	Description	Reference/source
Corynebacterium diphtheriae		
BR-INCA5015	*Biovar mitis, *tox* gene negative, previously isolated from the infected frontal bone of a cancer patient	Stavracakis-Peixoto *et al.* (2011)
ATCC 27010^T	*Biovar mitis, *tox* gene negative, type strain of the species *Corynebacterium diphtheriae* from the American Type Culture Collection	Dias *et al.* (2011)
ATCC 27012	*Biovar mitis, *tox* gene positive (positive diphtheria toxin expression), a well-used strain as reference. This strain is often used to demonstrate (significant amounts of) toxin production and can be used as a positive control for the ELEK test	Dias *et al.* (2011)
E. coli		
OP50	Uracil-auxotrophic *E. coli* B	Brenner (1974)
Cell line		
THP-1	Human leukaemia monocytic cells	Tsuchiya *et al.* (1980)
RAW 264.7	Murine leukaemic macrophages	Raschke *et al.* (1978)
HeLa	Human epithelial cervical carcinoma cells	Gey *et al.* (1952), Scherer *et al.* (1953)
Plasmid		
pEPR1-p45gfp	*P45*, *gfpuv*, *rep*, *per*, T1, T2, KM^R	Knoppová *et al.* (2007)

*A multiplex PCR for detection of *Corynebacterium diphtheriae* infection and differentiation between toxigenic and non-toxigenic strains was performed based on previously described techniques (Pimenta *et al.*, 2008). According to the API-Coryne System (API code 1010324; bioMérieux), BR-INCA5015 was *Corynebacterium diphtheriae* biovar mitis, as also observed by conventional phenotypic tests (Murray *et al.*, 2002; Stavracakis-Peixoto *et al.*, 2011).

120 mg ml^{-1} streptomycin and 10 % FBS. Before infection, THP-1 and RAW 264.7 cells were cultured in antibiotic-free medium containing 10 % FBS for 24 h, and THP-1 cells were differentiated into macrophage-like cells using 10 ng ml^{-1} phorbol 12-myristate 13-acetate. Bacteria were harvested by centrifugation, and cell density was adjusted to OD_{600} 1.0. A master mix of the inoculum with an m.o.i. of 25 was prepared in the respective medium, and the cells were infected with the inoculum or left uninfected. The plates were centrifuged for 5 min at 500 r.p.m. to synchronize infection. After incubation for 30 min, the medium was aspirated, and cells were treated first with medium containing 100 µg ml^{-1} gentamicin for 1 h. Then, medium with a lower gentamicin concentration (10 µg ml^{-1}) was added, and cells were incubated for 1, 7 or 23 h. At each time point of incubation, the supernatant was removed, and cells were lysed with 500 µl 0.1 % (v/v) Triton X-100. Serial dilutions of the inoculum and the lysates were plated out on Columbia agar with sheep blood (Oxoid) to determine the number of c.f.u. The intracellular viability was calculated by the ratio of bacteria used for infection (c.f.u. inoculum plate) and bacteria in the lysate (c.f.u. lysate plate) multiplied by 100.

Fluorescence microscopy. Fluorescence microscopy assays were performed by methods previously described (dos Santos *et al.*, 2010; Hacker *et al.*, 2016). Briefly, 1 day prior to infection, HeLa and RAW 264.7 cells were seeded at a density of 0.5×10^5 and 1×10^5 cells, respectively, on sterile coverslips in 24-well plates. *Corynebacterium diphtheriae* strains transformed with plasmids encoding *gfp* cultivated in HI medium with kanamycin were harvested by centrifugation, and cell density was adjusted in PBS to an OD_{600} 1.0 to infect macrophages as described above. After different time points, the medium was aspirated, and cells were fixed by addition of 500 µl 4 % paraformaldehyde in PBS and incubated for 20 min at 37 °C. Until further staining, cells were stored in PBS at 4 °C. For subsequent analysis by microscopy, coverslips were incubated with 30 µl of Alexa Fluor 647 phalloidin diluted 1 : 200 in Image-iT FX Signal Enhancer (Molecular Probes, Life Technologies) for 45 min in the dark to stain the cytoskeleton of the cells. After washing twice with PBS, the coverslips were dried and embedded on glass slides in ProLong Gold antifade mountant with DAPI (Molecular Probes, Life Technologies), and samples were stored in the dark at 4 °C. Micrographs were taken with the confocal laser scanning microscope Leica SP5 II (Leica Microsystems) and analysed with the LAS software suite.

Statistical analysis. Each experiment was conducted at least in triplicate (independent biological replicates), and statistical analyses were performed with the appropriate tests using GraphPad Prism 5.0 (GraphPad). $P<0.05$ was considered significant.

Animal experiments using mice model. Conventional Swiss Webster mice, sex matched, 18 to 22 g, from Cecal/Fiocruz were used. The study was performed in compliance with guidelines outlined in the International Guiding Principles for Biomedical Research Involving Animals as issued by the Council for the International Organizations of Medical Sciences and with the Brazilian government's ethical guidelines for research involving animals (Fiocruz Ethic Committee for Animal Experiments – CEUA/FIOCRUZ – L-034/07).

The possibility of developing osteomyelitis was analysed by the methods described previously (Dias *et al.*, 2011). Mice were infected intravenously through a tail vein with 0.5 ml of bacterial suspension prepared in sterile saline at OD_{570} 0.2. Control mice were injected with 0.5 ml of sterile saline. The experiments were performed in triplicate, and the mice were examined daily for 30 days by independent observers to assess the presence of joint inflammation and scarring macroscopically.

Histopathological studies. Histopathological procedures to evaluate the features of the disease were based on methods previously described (Dias *et al.*, 2011). Briefly, mice were inoculated intravenously with *Corynebacterium diphtheriae* BR-INCA5015 or sterile saline as control. Mice were sacrificed after 15 days. Paws (one per mouse) were removed aseptically, fixed in 10 % v/v formalin for 24 h and then decalcified using 10 % EDTA in PBS (0.1 M, pH 7.2) for 7 days. Subsequently, the

specimens were dehydrated, embedded in paraffin, sectioned at 5 to 7 μm and stained with haematoxylin and eosin. At this point, the specimens were decalcified in 5 % trichloroacetic acid (v/v) for 7 days and then dehydrated, embedded in paraffin, sectioned at 3 to 4 μm and stained with haematoxylin and eosin. Joints were examined for synovitis (defined as synovial membrane thickness of more than two cell layers), extent of infiltrate (presence of inflammatory cells in the subcutaneous and/or periarticular tissues), exudate (presence of inflammatory cells in the articular cavity), cartilage damage, bone erosion and loss of joint architecture.

RESULTS

Interaction with *Caenorhabditis elegans*

The nematode experiments indicated a high ability of nematode colonization and killing by the isolated *Corynebacterium diphtheriae* BR-INCA5015 osteomyelitis-related strain. Most (90 %) of the nematodes were already killed by the BR-INCA5015 strain after 3 days. However, the survival rates during infection of nematodes were much higher for the homologous strains toxigenic ATCC 27012 when comparing to the non-toxigenic ATCC 27010^T. Therefore, the BR-INCA5015 strain was more harmful to *Caenorhabditis elegans* compared to the homologous toxigenic ATCC 27012 and non-toxigenic ATCC 27010^T strains (Fig. 1).

Collagen binding activities of *Corynebacterium diphtheriae* strains

Compared to the control strains ATCC 27010^T (A_{620} 0.53 ±0.01) and ATCC 27012 (A_{620} 0.72±0.03), the binding level of the *Corynebacterium diphtheriae* BR-INCA5015 to type I collagen was significantly higher (A_{620} 1.57±0.04) (Fig. 2a). In the case of type IV collagen, only slight differences were observed between the strains: BR-INCA5015 (A_{620} 0.77 ±0.03), ATCC 27012 (A_{620} 0.87±0.06) and ATCC 27010^T (A_{620} 0.61±0.01) (Fig. 2b).

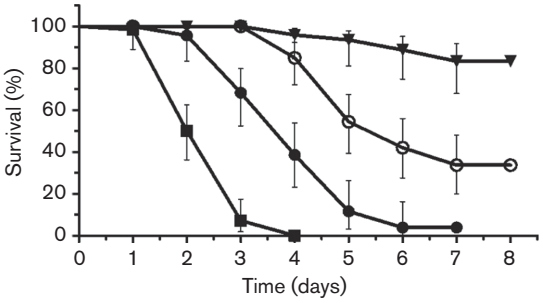

Fig. 1. *Caenorhabditis elegans* N2 nematode survival assay: infection with *E. coli* OP50 (▼), *Corynebacterium diphtheriae* BR-INCA5015 osteomyelitis-related strain (■), non-toxigenic ATCC 27010^T (●) and toxigenic ATCC 27012 (○) strains. Data shown represent the mean of three independent experiments; error bars represent SD.

Adhesion and invasion properties to HeLa epithelial cells

Although all three *Corynebacterium diphtheriae* strains tested were able to adhere to the HeLa epithelial cell line, after 90 min of infection, the *Corynebacterium diphtheriae* BR-INCA5015 osteomyelitis-related strain reached almost double the adhesion rate (9.59±0.91 %), compared to ATCC 27010^T and ATCC 27012 (5.64±0.61 % and 4.07 ±0.45 %, respectively) strains (Fig. 3).

Data of intracellular viability of *Corynebacterium diphtheriae* strains in HeLa cells using gentamicin protection assays (Fig. 4) showed that BR-INCA5015 expressed the highest internalization rates (0.46±0.06 %) 2 h post-infection, while invasion rates of 0.1±0.01 % and 0.03±0.007 % were observed for ATCC 27010^{T}and ATCC 27012, respectively (Fig. 4a). The ability to survive in the HeLa intracellular environment was also higher for strain BR-INCA5015 (0.23±0.05 %) compared to the controls ATCC 27010^T (0.002±0.0005 %) and ATCC 27012 (0.0003±0.0001 %) when evaluated 24 h after infection (Fig. 4b). Obviously, the *Corynebacterium diphtheriae* BR-INCA5015 osteomyelitis-related strain is highly active in colonization of HeLa cells.

Intracellular survival of *Corynebacterium diphtheriae* BR-INCA5015 osteomyelitis-related strain within human THP-1 and murine RAW 264.7 macrophage cell lines

In THP-1 macrophages, an internalization rate of 0.03 ±0.005 % was observed for *Corynebacterium diphtheriae* BR-INCA5015 osteomyelitis-related strain at 2 h post-infection, while ATCC 27010^T and ATCC 27012 reached only 0.01 ±0.002 % and 0.0003±0.0001 %, respectively. Analysis at 8 h post-infection indicated 0.06±0.02 % of viable BR-INCA5015 strain and 0.002±0.0006 % and 0.0005±0.0002 % for the ATCC 27010^T and ATCC 27012 strains, respectively. Viable bacteria were also recovered 24 h post-infection for all the three strains tested, and the percentages were 0.00013 ±0.00004 % for the BR-INCA5015 strain, 0.00001 ±0.000004 % for the ATCC 27010^T strain and 0.00002 ±0.00001 % for the ATCC 27012 strain (Fig. 5a–c).

In order to exclude cytotoxic effects due to diphtheria toxin, experiments using murine RAW 264.7 macrophage line lacking the toxin receptor were done. An uptake rate of 0.4 ±0.08 % was detected for BR-INCA5015 strain, while ATCC 27010^T and ATCC 27012 strains reached only 0.12 ±0.03 % and 0.15±0.04 % at 2 h post-infection. The number of viable bacteria decreased over time for all strains. After 8 h infection, the percentage of viable bacteria recovered for BR-INCA5015 strain was 0.25±0.07 % and, for the controls ATCC 27010^T and ATCC 27012, was 0.05±0.01 % and 0.07 ±0.03 %, respectively. Viable bacteria were recovered at 24 h post-infection for all the strains tested, and significant differences in the percentage of c.f.u were observed between BR-INCA5015 strain (0.01±0.002 %) and the controls

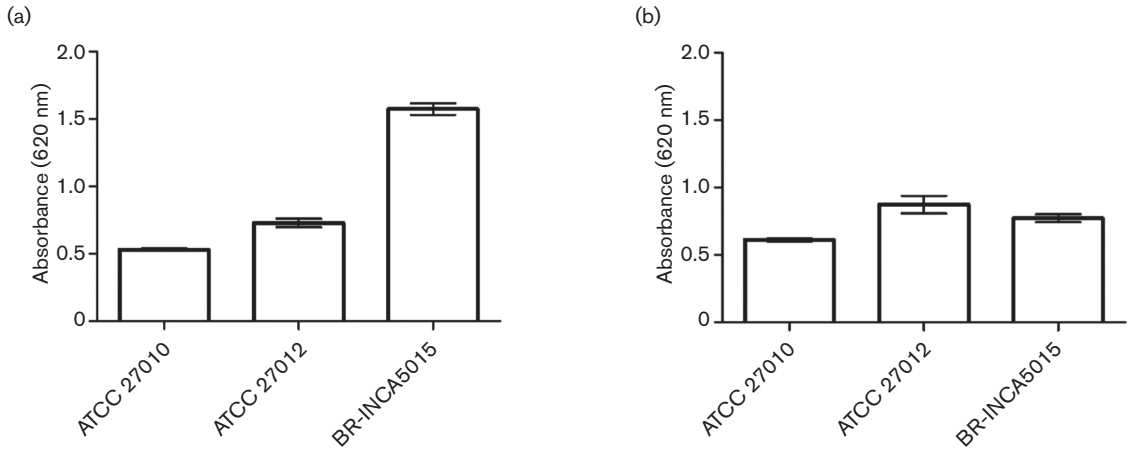

Fig. 2. Semi-quantitative analysis of *Corynebacterium diphtheriae* BR-INCA5015 osteomyelitis-related strain binding properties to I (a) and IV (b) collagen types. Data shown are mean±SD values of at least three independent biological replicates.

ATCC 27012 (0.004±0.002 %) and ATCC 27010^T (0.003 ±0.0007 %) (Fig. 5d–f).

Fluorescence microscopy assays

Fluorescence microscopy was used as an additional method to examine the interaction of *Corynebacterium diphtheriae* BR-INCA5015 osteomyelitis-related strain and control strains with RAW 264.7 macrophages and HeLa epithelial cell lines. All the strains were marked by GFP expression, nuclei were stained with DAPI and cytoskeleton was stained with Alexa Fluor 647 phalloidin. *Z*-stack micrographs were taken using the confocal laser scanning microscope Leica SP5 II and analysed with the LAS software suite to prove that the bacteria were located inside the cell (Fig. 6). In experiments using RAW 264.7 macrophages, the number of fluorescent bacteria declined within 24 h post-infection. However, a higher number of bacteria located inside the macrophage were observed in the BR-INCA5015 strain in all time points (Fig. 6a–c) compared to both ATCC 27010^T (Fig. 6d–f) and ATCC 27012 (Fig. 6g–i) strains. Similar results were obtained with THP-1 macrophages indicating that these findings are not limited to a single macrophage cell line or exclusively to murine macrophages (data not shown). Fluorescence microscopy images revealed adhesion to the surface of HeLa cells and internalized bacteria for all *Corynebacterium diphtheriae* strains tested. A higher number of bacterial cells associated and/or internalized within HeLa cells were observed in the *Corynebacterium diphtheriae* BR-INCA5015 strain (Fig. 6j, m) compared to those in the ATCC 27010^T (Fig. 6k, n) and ATCC 27012 (Fig. 6l, o) strains.

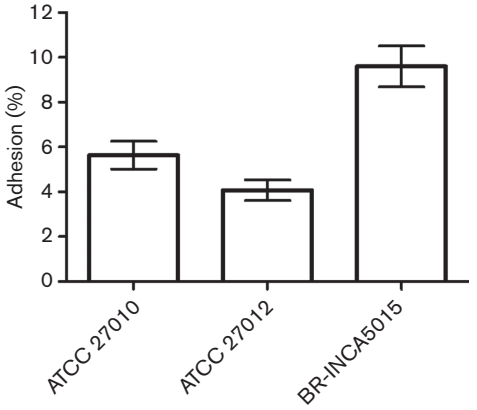

Fig. 3. Quantitative analysis of *Corynebacterium diphtheriae* adhesion rates to HeLa cells. Epithelial cells were infected with *Corynebacterium diphtheriae* BR-INCA5015 osteomyelitis-related strain, non-toxigenic ATCC 27010^T and toxigenic ATCC 27012 at m.o.i. of 50 for 90 min. After incubation, the cells were washed three times, detached and lysed, and dilutions of the lysate were plated on agar plates to determine the bacteria adherence percentage of the inoculum. Data shown are mean±SD values of at least three independent biological replicates.

Arthritogenic activity and histopathological findings

The ability to cause haematogenic and bone infection of *Corynebacterium diphtheriae* BR-INCA5015 osteomyelitis-related strain was demonstrated by an *in vivo* model system using mice. Upon injection of the bacteria into the tail vein and haematogenic spread, clinical signs of arthritis were evident starting 5 days post-infection (Fig. 7). The most frequently affected joints were ankle and wrist (Fig. 7a). Nodes on the tail and testicles were also observed as illustrated in Fig. 7(b, c). Histopathological studies of joints of mice infected with *Corynebacterium diphtheriae* BR-INCA5015 confirmed the clinical signs of arthritis and osteomyelitis. Three affected paws were examined. Micrographs in Fig. 7 (d, e) illustrate the histopathological features of arthritis and osteomyelitis in mice caused by *Corynebacterium*

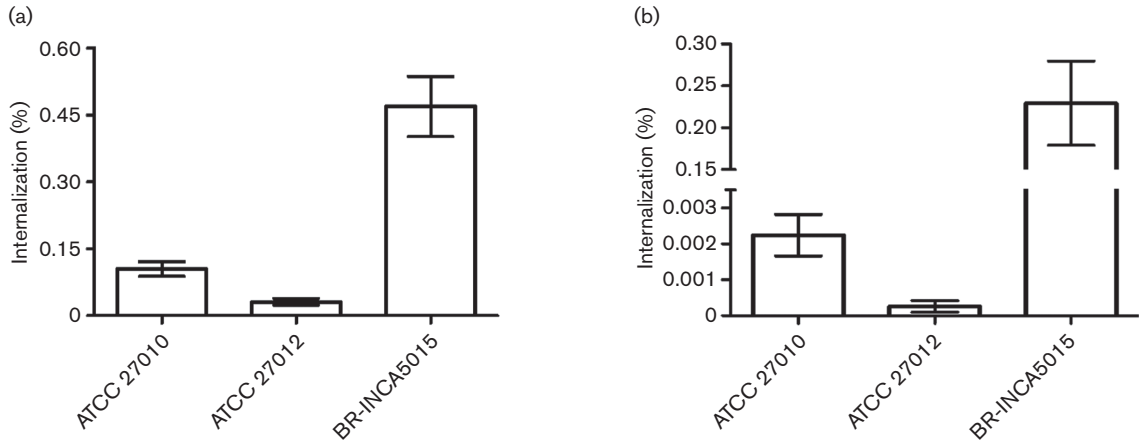

Fig. 4. Invasion of epithelial cells. HeLa cells were infected for 90 min with *Corynebacterium diphtheriae* strains, treated for 2 h with 100 μg ml^{-1} gentamicin in DMEM, washed with PBS, detached with trypsin solution, lysed with Tween 20 and plated on agar plates to determine the bacteria invasion percentage of the inoculum; (a) 2 h post-infection and (b) 24 h post-infection. Data shown are mean±SD values of at least three independent biological replicates.

diphtheriae BR-INCA5015, while control paws were completely symptom free (Fig. 7f).

DISCUSSION

The occurrence of diphtheria among immunized persons in addition to the increasing frequency of cases of invasive infections caused by *Corynebacterium diphtheriae* points to the importance of other virulence factors besides diphtheria toxin production (Hirata *et al.*, 2002; Mattos-Guaraldi *et al.*, 2003; Sabbadini *et al.*, 2010; Burkovski, 2013a; Santos *et al.*, 2015b). Non-toxigenic *Corynebacterium diphtheriae* strains, formerly considered as extracellular colonizers, have also been associated with cases of bacteraemia, catheter-related infection, endocarditis, septic arthritis and osteomyelitis (Guran *et al.*, 1979; Poilane *et al.*, 1995; Wilson, 1995; Mattos-Guaraldi & Formiga, 1998; Mattos-Guaraldi *et al.,* 2003; Puliti *et al.,* 2006; Hirata *et al.,* 2008; Gomes *et al.,* 2009; Dias *et al.,* 2011; Stavracakis-Peixoto *et al.,* 2011; Peixoto *et al.*, 2014).

Previous studies indicated a great variability in the pathogenicity islands of *Corynebacterium diphtheriae*, which may reflect bacterial lifestyle and physiological versatility (D′Afonseca *et al.,* 2011). Common adhesive properties and potential adhesins including pili (Gaspar & Ton-That, 2006; Ott *et al.*, 2010), haemagglutinins, hydrophobins, exposed sugar residues and enzymes with *trans*-sialidase activity to *Corynebacterium diphtheriae* strains were described (Mattos-Guaraldi *et al.*, 2000).

Adherence to and internalization by epithelial and endothelial cells were also highlighted as critical steps during blood barrier disruption and systemic dissemination of both non-toxigenic and toxigenic *Corynebacterium diphtheriae* strains (Hirata *et al.*, 2002; Peixoto *et al.*, 2014). Lately, the non-fimbrial DIP0733 protein was described as a multi-functional virulence factor involved in adhesion, invasion of epithelial cells and induction of apoptosis of a *Corynebacterium diphtheriae* strain. Furthermore, based on its fibrinogen-binding activity, DIP0733 seemed to play a role in avoiding recognition of *Corynebacterium diphtheriae* by the immune system (Colombo *et al.*, 2001; Sabbadini *et al.*, 2010, 2012; Antunes *et al.,* 2015). However, *Corynebacterium diphtheriae* isolates may behave differently when they meet host surfaces, with regard to the cells that they efficiently infect and the kind of inflammatory response that they trigger.

In this study, virulence properties that contribute to the ability of *Corynebacterium diphtheriae* strain BR-INCA5015 to cause bone diseases and disorders were verified.

Besides guinea pigs already employed by Loeffler, wax moth larvae (*Galleria mellonella*) and *Caenorhabditis elegans* nematodes were established as model systems for the investigation of *Corynebacterium diphtheriae* pathogenicity and virulence factors (Ott *et al.*, 2012; Broadway *et al.,* 2013; Santos *et al.,* 2015a; Antunes *et al.,* 2015, 2016). *Caenorhabditis elegans* is one of the major invertebrate model systems in biology based on advantageous properties such as short lifespan, transparency, genetic tractability and ease of culture using an *E. coli* diet. In its natural habitat, compost and rotting plant material, this nematode lives on bacteria. However, while *Caenorhabditis elegans* is a predator of bacteria, it can also be infected by nematopathogenic coryneform bacteria such *Microbacterium* and *Leucobacter* species. Depending on the nematode pathogen, aggregates of worms, termed wormstars, can be formed, or severe rectal swelling, so-called Dar formation, can be induced. *Caenorhabditis elegans* can also be infected by *Corynebacterium diphtheriae.* Earlier studies showed that *Corynebacterium*

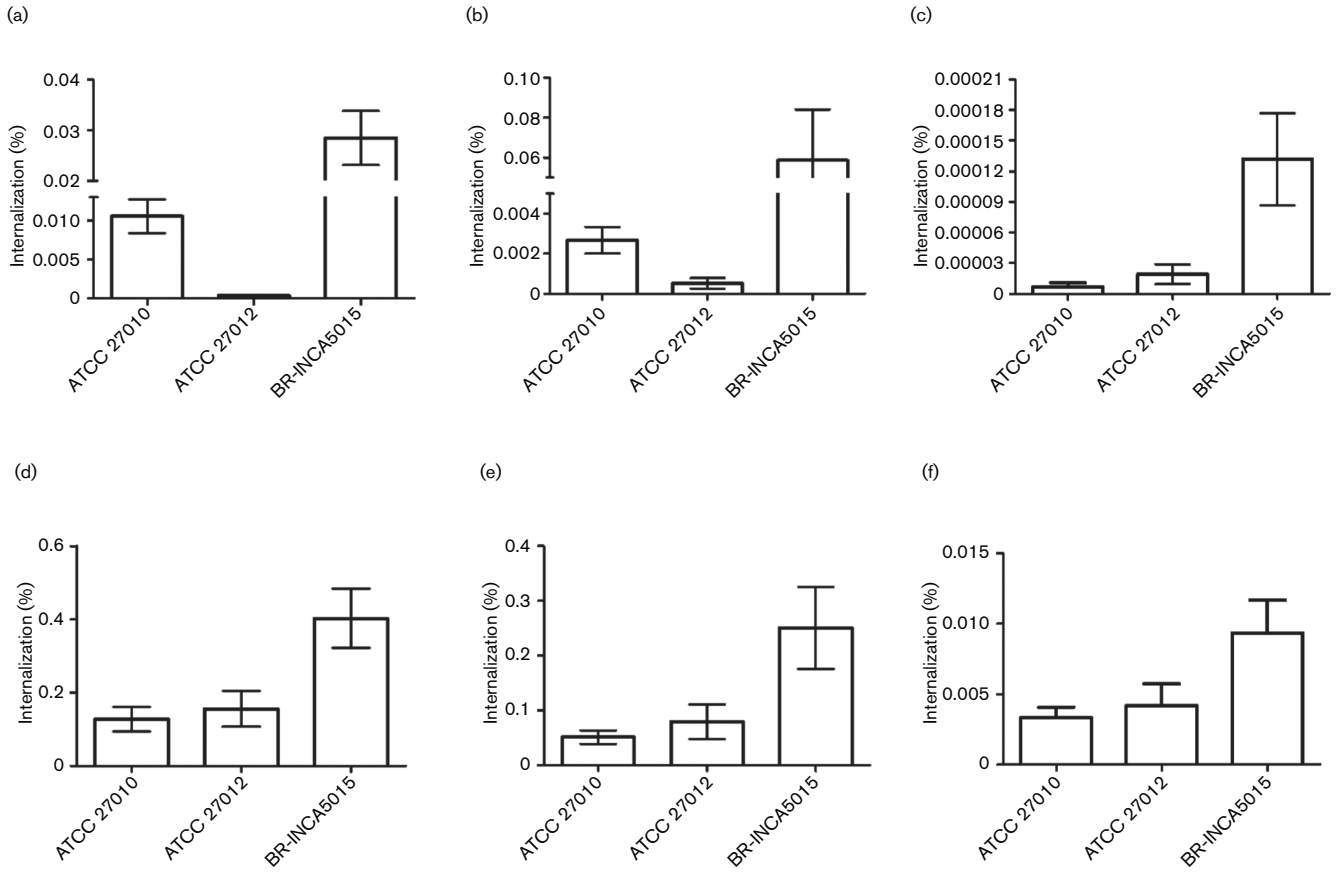

Fig. 5. Intracellular survival within differentiated human THP-1 cells using phorbol 12-myristate 13-acetate (a–c) and murine RAW 264.7 macrophage cells (d–f) of *Corynebacterium diphtheriae* BR-INCA5015 osteomyelitis-related strain, homologous non-toxigenic ATCC 27010^T control strain and toxigenic ATCC 27012 control strain. Percentage of viable bacteria at (a and d) 2 h, (b and e) 8 h and (c and f) 24 h post-infection was determined based on the inoculum. Data shown are mean±SD values of at least three independent biological replicates.

diphtheriae were found to induce star formation slowly in worms, as well as a severe tail swelling phenotype (Santos *et al.*, 2015a; Antunes *et al.*, 2015, 2016). In the present study, results of nematode survival assays indicated that the *Corynebacterium diphtheriae* BR-INCA5015 strain, isolated from osteomyelitis in the frontal bone of a patient with adenoid cystic carcinoma, expressed a high ability of host colonization and killing of *Caenorhabditis elegans*, as previously demonstrated for the toxigenic *Corynebacterium diphtheriae* CDC-E8392 strain (Santos *et al.*, 2015a; Antunes *et al.*, 2015, 2016). Interestingly, the osteomyelitis-related BR-INCA5015 strain was more harmful to *Caenorhabditis elegans* compared to the homologous toxigenic ATCC 27012 and non-toxigenic ATCC 27010^T strains tested.

When the first case of isolation of a non-toxigenic *Corynebacterium diphtheriae* biovar mitis of the non-sucrose-fermenting biotype (BR-INCA5015 strain) from osteomyelitis in the frontal bone of a patient with adenoid cystic carcinoma was reported, DNase, catalase and nitrate-reductase activities which possibly contribute to the invasive potential and survival of BR-INCA5015 strain within host tissues were observed (Peixoto *et al.*, 2011).

Similar to many other micro-organisms, *Corynebacterium diphtheriae* was formerly found to exploit the ECM and/or plasma proteins to colonize human tissues or to evade immune mechanism for clearance of bacteria (dos Santos *et al.*, 2010; Sabaddini *et al.*, 2010; Antunes *et al.*, 2015; Santos *et al.*, 2015a). The present data showed the ability of *Corynebacterium diphtheriae* strains to bind to collagen types I and IV. Type I collagen is the organic matrix molecule of mammalian bone and the most abundant in the human body (Balzer *et al.*, 1997; Maynes, 2012). Interestingly, the binding levels of the *Corynebacterium diphtheriae* BR-INCA5015 osteomyelitis-related strain were significantly higher for the type I collagen compared to those of the ATCC 27010^T and ATCC 27012 control strains.

The adhesion to and intracellular survival of *Corynebacterium diphtheriae* in epithelial cells have been demonstrated for different human cells, including epithelial cell lines like HeLa, HEp-2 (Hirata *et al.*, 2002; Stavracakis Peixoto *et al.*, 2014;

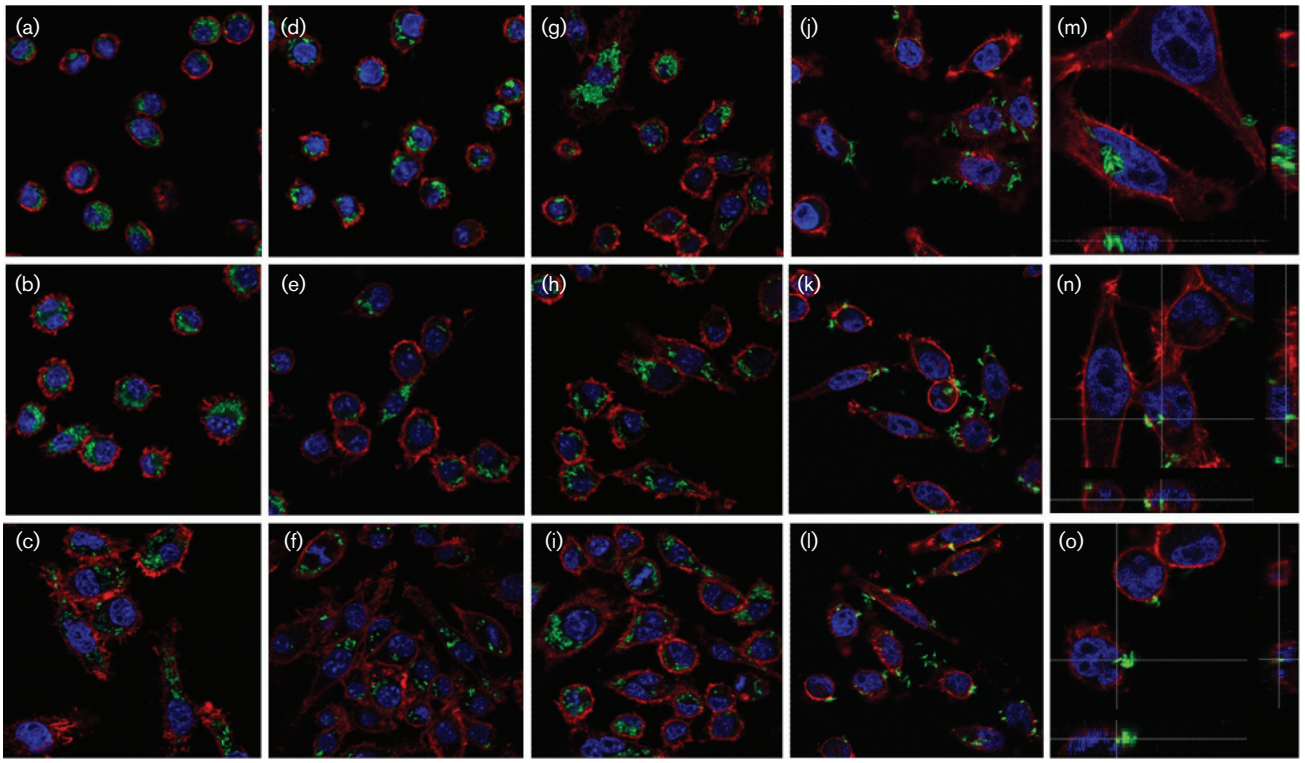

Fig. 6. Micrographic data of fluorescence microscopy assays of RAW 264.7 macrophage (30 min) and HeLa (90 min) cell line interaction with *Corynebacterium diphtheriae* BR-INCA5015 osteomyelitis-related strain prEPRIp45*gfp*, ATCC 27010^T prEPRIp45*gfp* strain and ATCC 27012 prEPRIp45*gfp* strain (m.o.i. of 25). Extracellular bacteria were killed by the addition of gentamicin and fixed at different periods of incubation. Nuclei were stained with DAPI, and cytoskeleton was stained with Alexa Fluor 647 phalloidin. *Z*-stack micrographs were taken using the confocal laser scanning microscope Leica SP5 II and analysed with the LAS software suite to prove that bacteria are located inside of the cell. Fluorescence microscopy images of RAW 264.7 cells 2, 8 and 24 h post-infection: BR-INCA5015 (a–c); ATCC 27010^T (d–f) and ATCC 27012 (g–i), respectively. Adhesion of *Corynebacterium diphtheriae* to epithelial cells (HeLa): BR-INCA5015 (j), ATCC 27010^T (k) and ATCC 27012 (l). Invasion of *Corynebacterium diphtheriae* into epithelial cells (HeLa): BR-INCA5015 (m), ATCC 27010^T (n) and ATCC 271012 (o).

Antunes *et al.*, 2015; Santos *et al.*, 2015a) and Detroit 562 (Ott *et al.*, 2012; Bertuccini *et al.*, 2004), human umbilical vein endothelial cells (Peixoto *et al.*, 2014) and U-937 and THP-1 macrophages (dos Santos *et al.*, 2010; Antunes *et al.*, 2015).

Corynebacterium diphtheriae BR-INCA5015 osteomyelitis-related strain expressed a higher ability to adhere to and survive within human (HeLa) epithelial cells compared to the other *Corynebacterium diphtheriae* strains currently tested.

For a successful dissemination in the case of a systemic infection, micro-organisms have also to cope successfully with macrophages. Human macrophages in the absence of opsonins may not be promptly effective at killing *Corynebacterium diphtheriae*. Those strains exhibit strategies to survive within macrophages and to exert apoptosis and necrosis in human phagocytic cells, independent of the *tox* gene (dos Santos *et al.*, 2010). Endorsing the aforementioned, intracellular survival of the non-toxigenic *Corynebacterium diphtheriae* BR-INCA5015 osteomyelitis-related strain within both human (THP-1) and murine (RAW 264.7) macrophages was significantly higher compared to both non-toxigenic ATCC 27010^T and toxigenic ATCC 27012 control strains. Interaction of the BR-INCA5015 strain with macrophages and epithelial cells was morphologically observed by fluorescence microscopy.

In an attempt to validate the ability of *Corynebacterium diphtheriae* BR-INCA5015 to promote haematogenic and bone infections *in vivo*, a murine experimental model was used. Histopathological studies of joints of mice infected with *Corynebacterium diphtheriae* BR-INCA5015 confirmed the clinical signs of arthritis and osteomyelitis. Interestingly, Dias *et al.* (2011) showed that the non-toxigenic ATCC 27010^T induced low arthritis index rates and the toxigenic strain ATCC 27012 had no ability to induce signs of arthritis in mice.

In conclusion, non-toxigenic *Corynebacterium diphtheriae* should not be merely regarded as contaminants, since they can be directly or indirectly related to the establishment and/or maintenance of invasive infectious processes. Data also endorsed the ability of some *Corynebacterium*

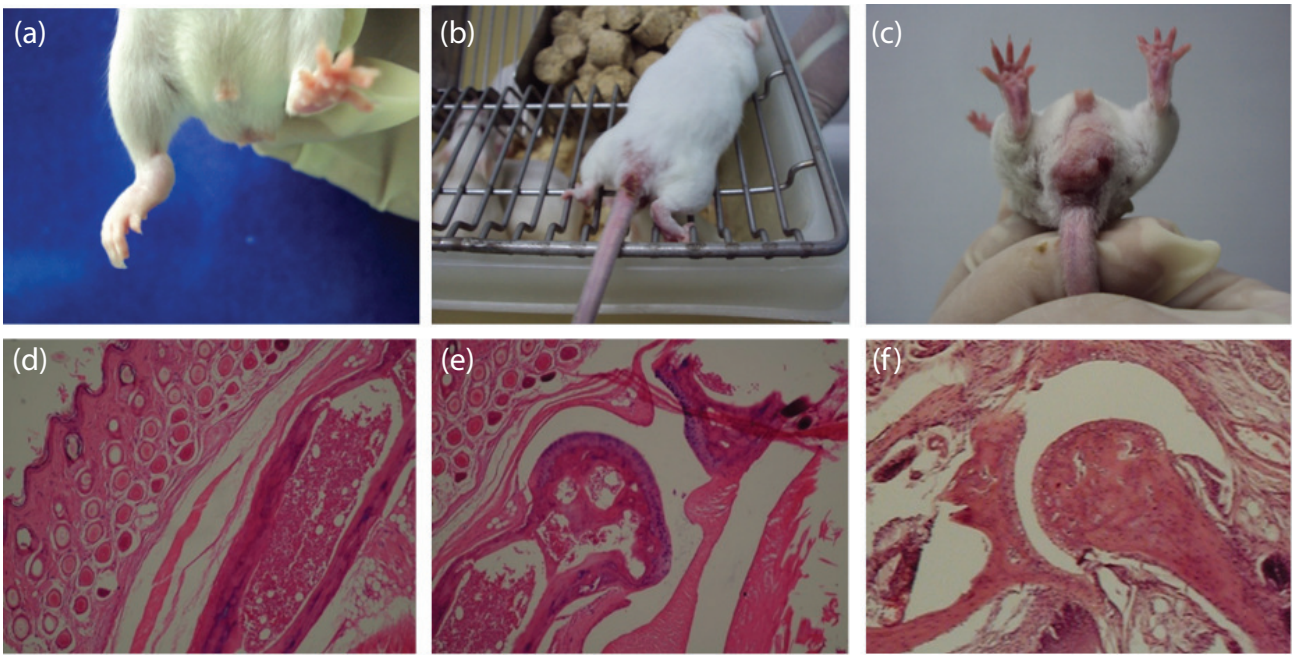

Fig. 7. Haematogenic and bone infection by *Corynebacterium diphtheriae* BR-INCA5015 osteomyelitis-related strain demonstrated by an *in vivo* model system using mice. Clinical signs of arthritis were present in mice on day 15 after intravenous infection with BR-INCA5015 strain. Photographs showing arthritic hind paws and tail with nodose. Arthritis on the right forepaws (a), excoriation in the tail (region of insertion) (b) and abrasions in the testicles, with increased volume indicating orchitis (c). Joint with arthritis of mice infected with BR-INCA5015 exhibiting capsular distension. (d, e) Intense leukocyte inflammatory infiltrate and osteochondral deformation. (f) Histopathological features of a normal joint. Magnification ×100.

diphtheriae strains, such as BR-INCA5015, to induce osteomyelitis. In all aspects evaluated in this study, BR-INCA5015 osteomyelitis-related strain expressed more severe virulent properties than the *Corynebacterium diphtheriae* control strains, clearly independently of the presence of *tox* gene or diphtheria toxin production.

ACKNOWLEDGEMENTS

This work was supported by a grant from the Coordination for the Improvement of Higher Education Personnel, Foundation for Support of Research in the State of Rio de Janeiro, SR-2/UERJ and the Brazilian National Council for Scientific and Technological Development including Science Without Borders Project.

REFERENCES

Afghani, B. & Stutman, H. R. (1993). Bacterial arthritis caused by *Corynebacterium diphtheriae*. *Pediatr Infect Dis J* **12**, 881–882.

Alexander, D. (1984). Splenic abscess caused by *Corynebacterium diphtheriae*. *Clin Pediatr* **23**, 591–592.

Antunes, C. A., Sanches dos Santos, L., Hacker, E., Köhler, S., Bösl, K., Ott, L., de Luna, M., Hirata, R., Azevedo, V. A. & other authors (2015). Characterization of DIP0733, a multi-functional virulence factor of *Corynebacterium diphtheriae*. *Microbiology* **161**, 639–647.

Antunes, C. A., Clark, L., Wanuske, M. T., Hacker, E., Ott, L., Simpson-Louredo, L., de Luna, M., Hirata, R., Mattos-Guaraldi, A. L. & other authors (2016). *Caenorhabditis elegans* star formation and negative chemotaxis induced by infection with corynebacteria. *Microbiology* **162**, 84–93.

Balzer, A., Gleixner, G., Grupe, G., Schmidt, H. L., Schramm, S. & Turban-just, S. (1997). In vitro decomposition of bone collagen by soil bacteria: the implications for stable isotope analysis in archaeometry. *Archaeometry* **39**, 415–429.

Belko, J., Wessel, D. L. & Malley, R. (2000). Endocarditis caused by *Corynebacterium diphtheriae*: case report and review of the literature. *Pediatr Infect Dis J* **19**, 159–163.

Bertuccini, L., Baldassarri, L. & von Hunolstein, C. (2004). Internalization of non-toxigenic *Corynebacterium diphtheriae* by cultured human respiratory epithelial cells. *Microb Pathog* **37**, 111–118.

Birkenhauer, E., Neethirajan, S. & Weese, J. S. (2014). Collagen and hyaluronan at wound sites influence early polymicrobial biofilm adhesive events. *BMC Microbiol* **14**, 191.

Brady, R. A., Leid, J. G., Calhoun, J. H., Costerton, J. W. & Shirtliff, M. E. (2008). Osteomyelitis and the role of biofilms in chronic infection. *FEMS Immunol Med Microbiol* **52**, 13–22.

Brenner, S. (1974). The genetics of *Caenorhabditis elegans*. *Genetics* **77**, 71–94.

Broadway, M. M., Rogers, E. A., Chang, C., Huang, I. H., Dwivedi, P., Yildirim, S., Schmitt, M. P., Das, A. & Ton-That, H. (2013). Pilus gene pool variation and the virulence of *Corynebacterium diphtheriae* clinical isolates during infection of a nematode. *J Bacteriol* **195**, 3774–3783.

Browning, D. F., Wells, T. J., França, F. L., Morris, F. C., Sevastsyanovich, Y. R., Bryant, J. A., Johnson, M. D., Lund, P. A., Cunningham, A. F. & other authors (2013). Laboratory adapted *Escherichia coli* K-12 becomes a pathogen of *Caenorhabditis elegans* upon restoration of O antigen biosynthesis. *Mol Microbiol* **87**, 939–950.

Burkovski, A. (2013a). Diphtheria. In *The Prokaryotes*, 4th edn, vol. 5, pp. 237–246. Edited by E. Rosenberg, E. F. DeLong, F. Thompson, S. Lory & E. Stackebrandt. New York: Springer.

Burkovski, A. (2013b). Diphtheria and its etiological agents. In *Corynebacterium diphtheriae and Related Toxigenic Species*, pp. 1–14. Edited by A. Burkovski. Dordrecht: Springer.

Colombo, A. V., Hirata, R., de Souza, C. M., Monteiro-Leal, L. H., Previato, J. O., Formiga, L. C., Andrade, A. F. & Mattos-Guaraldi, A. L. (2001). *Corynebacterium diphtheriae* surface proteins as adhesins to human erythrocytes. *FEMS Microbiol Lett* **197**, 235–239.

D'Afonseca, V., Soares, S. C., Ali, A., Santos, A. R., Pinto, A. C., Magalhães, A. A. C., Faria, C. J., Barbosa, E., Guimarães, L. C. & other authors (2011). Reannotation of the *Corynebacterium diphtheriae* NCTC13129 genome as a new approach to studying gene targets connected to virulence and pathogenicity in diphtheria. *Open Acess Bioinformatics* **4**, 1–13.

de Bono, M. & Bargmann, C. I. (1998). Natural variation in a neuropeptide Y receptor homolog modifies social behavior and food response in *C. elegans*. *Cell* **94**, 679–689.

Dias, A. A., Silva, F. C., Jr, Santos, L. S., Ribeiro-Carvalho, M. M., Sabbadini, P. S., Santos, C. S., Filardy, A. A., Myioshi, A., Azevedo, V. A. & other authors (2011). Strain-dependent arthritogenic potential of the zoonotic pathogen *Corynebacterium ulcerans*. *Vet Microbiol* **153**, 323–331.

dos Santos, C. S., dos Santos, L. S., de Souza, M. C., dos Santos Dourado, F., de Souza de Oliveira Dias, A. A., Sabbadini, P. S., Pereira, G. A., Cabral, M. C., Hirata, R., Jr & de Mattos-Guaraldi, A. L. (2010). Non-opsonic phagocytosis of homologous non-toxigenic and toxigenic *Corynebacterium diphtheriae* strains by human U-937 macrophages. *Microbiol Immunol* **54**, 1–10.

Farfour, E., Badell, E., Zasada, A., Hotzel, H., Tomaso, H., Guillot, S. & Guiso, N. (2012). Characterization and comparison of invasive *Corynebacterium diphtheriae* isolates from France and Poland. *J Clin Microbiol* **50**, 173–175.

Galazka, A. (2000). The changing epidemiology of diphtheria in the vaccine era. *J Infect Dis* **181**, S2–S9.

Gaspar, A. H. & Ton-That, H. (2006). Assembly of distinct pilus structures on the surface of *Corynebacterium diphtheriae*. *J Bacteriol* **188**, 1526–1533.

Gey, G. O., Coffmann, W. D. & Kubicek, M. T. (1952). Tissue culture studies of the proliferative capacity of cervical carcinoma and normal epithelium. *Cancer Res* **12**, 264–265.

Gomes, D. L., Martins, C. A., Faria, L. M., Santos, L. S., Santos, C. S., Sabbadini, P. S., Souza, M. C., Alves, G. B., Rosa, A. C. & other authors (2009). *Corynebacterium diphtheriae* as an emerging pathogen in nephrostomy catheter-related infection: evaluation of traits associated with bacterial virulence. *J Med Microbiol* **58**, 1419–1427.

Guran, P., Mollaret, H. H., Chatelain, R., Gropman, M., Prigent, F. & Beal, G. (1979). Arthrite purulent á bacille diphtérique atoxinogéne. *Arch Fr Pediatr* **36**, 926–929 (in French).

Hacker, E., Ott, L., Hasselt, K., Mattos-Guaraldi, A. L., Tauch, A. & Burkovski, A. (2015). Colonization of human epithelial cell lines by *Corynebacterium ulcerans* from human and animal sources. *Microbiology* **161**, 1582–1591.

Hacker, E., Ott, L., Schulze-Luehrmann, J., Lührmann, A., Wiesmann, V., Wittenberg, T. & Burkovski, A. (2016). The killing of macrophages by *Corynebacterium ulcerans*. *Virulence* **7**, 45–55.

Hadfield, T. L., McEvoy, P., Polotsky, Y., Tzinserling, V. A. & Yakovlev, A. A. (2000). The pathology of diphtheria. *J Infect Dis* **181**, S116–S120.

Hirata, R., Napoleão, F., Monteiro-Leal, L. H., Andrade, A. F., Nagao, P. E., Formiga, L. C., Fonseca, L. S. & Mattos-Guaraldi, A. L. (2002). Intracellular viability of toxigenic *Corynebacterium diphtheriae* strains in HEp-2 cells. *FEMS Microbiol Lett* **215**, 115–119.

Hirata, R., Pereira, G. A., Filardy, A. A., Gomes, D. L., Damasco, P. V., Rosa, A. C., Nagao, P. E., Pimenta, F. P. & Mattos-Guaraldi, A. L. (2008). Potential pathogenic role of aggregative-adhering *Corynebacterium diphtheriae* of different clonal groups in endocarditis. *Braz J Med Biol Res* **41**, 986–991.

Huber-Schneider, C., Gubler, J. & Knoblauch, M. (1994). [Endocarditis due to *Corynebacterium diphtheriae* caused by contact with intravenous drugs: report of 5 cases]. *Schweiz Med Wochenschr* **124**, 2173–2180 (in German with English abstract).

Isaac-Renton, J. L., Boyko, W. J., Chan, R. & Crichton, E. (1981). *Corynebacterium diphtheriae* septicemia. *Am J Clin Pathol* **75**, 631–634.

Knoppová, M., Phensaijai, M., Veselý, M., Zemanová, M., Nesvera, J. & Pátek, M. (2007). Plasmid vectors for testing in vivo promoter activities in *Corynebacterium glutamicum* and *Rhodococcus erythropolis*. *Curr Microbiol* **55**, 234–239.

Lehnert, F., Mortier, E., Mousseaux, E., Ollitrault, J., Goldstein, F., Carpentier, A., Acar, J. F. & Pauly-Laubry, C. (1995). *Corynebacterium diphtheriae* endocarditis complicated by septic arthritis and cerebral abscess. *Arch Mal Coeur Vaiss* **88**, 899–901.

Martins, C., Faria, L., Souza, M., Camello, T., Velasco, E., Hirata, R., Thuler, L. & Mattos-Guaraldi, A. (2009). Microbiological and host features associated with corynebacteriosis in cancer patients: a five-year study. *Mem Inst Oswaldo Cruz* **104**, 905–913.

Mattos-Guaraldi, A. L. & Formiga, L. C. (1998). Bacteriological properties of a sucrose-fermenting *Corynebacterium diphtheriae* strain isolated from a case of endocarditis. *Curr Microbiol* **37**, 156–158.

Mattos-Guaraldi, A. L., Duarte Formiga, L. C. & Pereira, G. A. (2000). Cell surface components and adhesion in *Corynebacterium diphtheriae*. *Microbes Infect* **2**, 1507–1512.

Mattos-Guaraldi, A. L., Formiga, L. C. D., Marques, E. A., Pereira, G., Moreira, L. O., Pimenta, F. P., Camelo, T. C. F. & Oliveira, E. (2001). Diphtheria in a vaccinated adult in Rio de Janeiro, Brazil. *Braz J Microbiol* **32**, 236–239.

Mattos-Guaraldi, A. L., Moreira, L. O., Damasco, P. V. & Hirata, R., Jr. (2003). Diphtheria remains a threat to health in the developing world—an overview. *Mem Inst Oswaldo Cruz* **98**, 987–993.

Maynes, R. (2012). *Structure and Function of Collagen Types*. Burlington, VT: Elsevier.

Morrey, B. F., Fitzgerald, R. H., Kelly, P. J., Dobyns, J. H. & Washington, J. A. (1977). Diphtheroid osteomyelitis. *J Bone Joint Surg Am* **59**, 527–530.

Mortier, E., Lehnert, F., Goldstein, F., Kitzis, M. D., Ollitrault, J., Pauly-Laubry, C., Carpentier, A. & Acar, J. (1994). *Corynebacterium diphtheriae* endocarditis complicated by arthritis and cerebral abscess. *Ann Med Interne* **145**, 510–511.

Murray, P. R., Rosenthal, K. S., Kobayashi, G. S. & Pfaller, M. A. (2002). *Medical Microbiology*, 4th edn. St Louis, MO: Mosby.

Muttaiyah, S., Best, E. J., Freeman, J. T., Taylor, S. L., Morris, A. J. & Roberts, S. A. (2011). *Corynebacterium diphtheriae* endocarditis: a case series and review of the treatment approach. *Int J Infect Dis* **15**, 584–588.

Ott, L., Höller, M., Rheinlaender, J., Schäffer, T. E., Hensel, M. & Burkovski, A. (2010). Strain-specific differences in pili formation and the interaction of *Corynebacterium* diphtheriae with host cells. *BMC Microbiol* **10**, 257.

Ott, L., McKenzie, A., Baltazar, M. T., Britting, S., Bischof, A., Burkovski, A. & Hoskisson, P. A. (2012). Evaluation of invertebrate infection models for pathogenic corynebacteria. *FEMS Immunol Med Microbiol* **65**, 413–421.

Peixoto, R. S., Pereira, G. A., Sanches dos Santos, L., Rocha-de-Souza, C. M., Gomes, D. L., Silva Dos Santos, C., Werneck, L. M., Dias, A. A., Hirata, R. & other authors (2014). Invasion of endothelial cells and arthritogenic potential of endocarditis-associated *Corynebacterium diphtheriae*. *Microbiology* **160**, 537–546.

Pennie, R. A., Malik, A. S. & Wilcox, L. (1996). Misidentification of toxigenic *Corynebacterium diphtheriae* as a *Corynebacterium* species with low virulence in a child with endocarditis. *J Clin Microbiol* **34**, 1275–1276.

Pimenta, F. P., Souza, M. C., Pereira, G. A., Hirata, R., Jr., Camello, T. C. & Mattos-Guaraldi, A. L. (2008). DNase test as a novel approach for the routine screening of *Corynebacterium diphtheriae*. *Lett Appl Microbiol* **46**, 307–311.

Poilane, I., Fawaz, F., Nathanson, M., Cruaud, P., Martin, T., Collignon, A. & Gaudelus, J. (1995). *Corynebacterium diphtheriae* osteomyelitis in an immunocompetent child: a case report. *Eur J Pediatr* **154**, 381–383.

Puliti, M., von Hunolstein, C., Marangi, M., Bistoni, F. & Tissi, L. (2006). Experimental model of infection with non-toxigenic strains of *Corynebacterium diphtheriae* and development of septic arthritis. *J Med Microbiol* **55**, 229–235.

Raschke, W. C., Baird, S., Ralph, P. & Nakoinz, I. (1978). Functional macrophage cell lines transformed by Abelson leukemia virus. *Cell* **15**, 261–267.

Rizvi, M., Khan, F., Raza, A., Shukla, I. & Sabir, A. B. (2011). Emergence of coryneforms in osteomyelitis and orthopaedic surgical site infections. *Australas Med J* **4**, 412–417.

Rizvi, M., Rizvi, M. W., Shaheen, A., Sultan, A., Khan, F., Shukla, I. & Malik, A. (2013). Emergence of coryneform bacteria as pathogens in nosocomial surgical site infections in a tertiary care hospital of North India. *J Infect Public Health* **6**, 283–288.

Sabbadini, P. S., Genovez, M. R., Silva, C. F., Adelino, T. L., Santos, C. S., Pereira, G. A., Nagao, P. E., Dias, A. A., Mattos-Guaraldi, A. L. & Hirata, R., Jr. (2010). Fibrinogen binds to nontoxigenic and toxigenic *Corynebacterium diphtheriae* strains. *Mem Inst Oswaldo Cruz* **105**, 706–711.

Sabbadini, P. S., Assis, M. C., Trost, E., Gomes, D. L., Moreira, L. O., Dos Santos, C. S., Pereira, G. A., Nagao, P. E., Azevedo, V. A. & other authors (2012). *Corynebacterium diphtheriae* 67-72p hemagglutinin, characterized as the protein DIP0733, contributes to invasion and induction of apoptosis in HEp-2 cells. *Microb Pathog* **52**, 165–176.

Sambrook, J., Fritsch, E. F. & Maniatis, T. (1989). *Molecular Cloning: a Laboratory Manual*, 2nd edn. Cold Spring Harbor, NY: Cold Spring Harbor Laboratory Press.

Santos, L. S., Antunes, C. A., Santos, C. S., Pereira, J. A. A., Sabbadini, P. S., Luna, M., Azevedo, V., Hirata, R., Jr., Burkovski, A. & other authors (2015a). *Corynebacterium diphtheriae* putative tellurite-resistance protein (CDCE8392_0813) contributes to the intracellular survival in human epithelial cells and lethality of *Caenorhabditis elegans*. *Mem Inst Oswaldo Cruz* **110**, 662–668.

Santos, L. S., Sant'anna, L. O., Ramos, J. N., Ladeira, E. M., Stavracakis-Peixoto, R., Borges, L. L., Santos, C. S., Napoleão, F., Camello, T. C. & other authors (2015b). Diphtheria outbreak in Maranhão, Brazil: microbiological, clinical and epidemiological aspects. *Epidemiol Infect* **143**, 791–798.

Saragea, A., Maximescu, P. & Meiter, E. (1979). Microbiological methods used in clinical and epidemiological investigations. *Methods Microbiol* **13**, 62–176.

Scherer, W. F., Syverton, J. T. & Gey, G. O. (1953). Studies on the propagation in vitro of poliomyelitis viruses. IV. Viral multiplication in a stable strain of human malignant epithelial cells (strain HeLa) derived from an epidermoid carcinoma of the cervix. *J Exp Med* **97**, 695–710.

Stavracakis-Peixoto, R., Siqueira, G. C. O., Luca, F. M., Sant´ anna, L. O., Santos, L. S., Rama, D. L. R., Souza, M. C., Sabbadini, P. S., Hirata, R. & other authors (2011). Aspectos fenotípicos e do potencial patogênico de amostra de *Corynebacterium diphtheriae* isolada de processo de osteomielite em paciente com neoplasia. *Rev Bras Anal Clin* **43**, 230–236 (in Portuguese).

Tiley, S. M., Kociuba, K. R., Heron, L. G. & Munro, R. (1993). Infective endocarditis due to nontoxigenic *Corynebacterium diphtheriae*: report of seven cases and review. *Clin Infect Dis* **16**, 271–275.

Tsuchiya, S., Yamabe, M., Yamaguchi, Y., Kobayashi, Y., Konno, T. & Tada, K. (1980). Establishment and characterization of a human acute monocytic leukemia cell line (THP-1). *Int J Cancer* **26**, 171–176.

Verma, R. & Kravitz, G. R. (2016). *Corynebacterium striatum* empyema and osteomyelitis in a patient with advanced rheumatoid arthritis. *BMJ Case Rep* **2016**, bcr2016214691.

von Graevenitz, A., Frommelt, L., Pünter-Streit, V. & Funke, G. (1998). Diversity of coryneforms found in infections following prosthetic joint insertion and open fractures. *Infection* **26**, 36–38.

von Hunolstein, C., Alfarone, G., Scopetti, F., Pataracchia, M., La Valle, R., Franchi, F., Pacciani, L., Manera, A., Giammanco, A. & other authors (2003). Molecular epidemiology and characteristics of *Corynebacterium diphtheriae* and *Corynebacterium ulcerans* strains isolated in Italy during the 1990s. *J Med Microbiol* **52**, 181–188.

Wilson, A. P. (1995). Treatment of infection caused by toxigenic and non-toxigenic strains of *Corynebacterium diphtheriae*. *J Antimicrob Chemother* **35**, 717–720.

Wong, J. S., Seaward, L. M., Ho, C. P., Anderson, T. P., Lau, E. O., Amodeo, M. R., Metcalf, S. C., Pithie, A. D. & Murdoch, D. R. (2010). *Corynebacterium accolens*-associated pelvic osteomyelitis. *J Clin Microbiol* **48**, 654–655.

Zasada, A. A., Zaleska, M., Podlasin, R. B. & Seferyńska, I. (2005). The first case of septicaemia and endocarditis due to non-toxigenic *Corynebacterium diphtheriae* in Poland. *Ann Clin Microbiol Antimicrob* **4**, 8.